EVALUATION OF METALLURGICAL RECOVERY FACTORS FOR DIAMONDS RECOVERED FROM KIMBERLITES

Stephen John Coward

School of Civil, Environmental and Mining Engineering

The University of Adelaide

This dissertation is submitted for the degree of Doctor of Philosophy

April 2020

ABSTRACT

Extraction and recovery of diamonds requires that the host rock, kimberlite, is fragmented to liberate and recover the contained diamonds. Optimal recovery requires trade-offs to be made between maximising liberation, minimising diamond breakage or loss and cost of recovery.

Effective fragmentation and recovery are not only dependent on the comminution and recovery techniques used but are also a function of the interactions between the diamond characteristics, the host rock properties and the technology used to crush the kimberlite and recover the diamonds. Prior approaches have been limited by a disregard for these relationships and how they change in response to variable kimberlite and diamond characteristics and their impact on diamond recovery. Incorrect recovery estimation impacts negatively on the evaluation, design and operation of diamond mining projects.

This research develops and demonstrates methods to collect and spatially estimate relevant orebody characteristics that impact on diamond liberation and subsequent recovery. These characteristics are used in an integrated value chain model to quantify the variability and uncertainty of diamond recovery. The use of this technique is demonstrated in two case studies.

The benefits of this approach include improved evaluation of diamond projects, development of better design and operational strategies and will improve not only the resilience of individual diamond projects, but also the performance and economics of the diamond mining industry.

Key words – diamond, diamond size distribution, diamond recovery, kimberlite, Value chain model, process simulation, Liberation, comminution

STATEMENT OF ORIGINALITY

Submitted by Stephen Coward to the University of Adelaide as a thesis for the degree of Doctor of Philosophy December 2019.

I certify that this work contains no material which has been accepted for the award of any other degree or diploma in my name, in any university or other tertiary institution and, to the best of my knowledge and belief, contains no material previously published or written by another person, except where due reference has been made in the text. In addition, I certify that no part of this work will, in the future, be used in a submission in my name, for any other degree or diploma in any university or other tertiary institution without the prior approval of the University of Adelaide and where applicable, any partner institution responsible for the joint-award of this degree.

I give permission for the digital version of my thesis to be made available on the web, via the University's digital research repository, the Library Search and also through web search engines, unless permission has been granted by the University to restrict access for a period of time.

I acknowledge the support I have received for my research through the provision of an Australian Government Research Training Program Scholarship.

2019-12-12

Stephen Coward Date

ACKNOWLEDGEMENTS

I am sincerely grateful to my family, friends and colleagues who have made this research possible and have helped in so many ways to develop and produce this thesis.

This research has taken place over a substantial period and has involved many collaborators who have helped to shape both the thinking behind the research and inform various avenues to resolve the research questions.

There are several groups of people who were particularly influential in the various phases of this research including the following:

Research Supervision at the University of Leeds and the University of Adelaide:

Professor Peter Alan Dowd who as principal supervisor has provided incredible patience and guidance throughout the process.

Minrad Extended Team;

Wynand Kleingeld, who was the initiator of the Wells research unit, and other members of the team including Niall Young, Johan Ferreira, Rob Pearce, Chris Prins, Ina Dohm, and Tessa Dodkin.

Matthew Field, who's collaboration, understanding and insights in the field of kimberlite geology provided a solid foundation for the design and execution of the sampling campaign that provided data for this research.

Grant Nicholas who played a material role in the formulation of the initial scope of the integrated model .

Special mention must be made of Chris Prins contribution and assistance with the finalisation of the thesis.

QG Team:

John Vann and Scott Jackson.

École nationale supérieure des mines de Paris:

Allan Galli, Margaret Armstrong, and Christian Lantuéjoul.

Academics:

Roussos Dimitrakopoulos, Kim Esbensen, David Vose.

Two anonymous reviewers who helped improve the content substantially.

Acknowledgement is also given to De Beers South Africa, Debswana, De Beers Marine (Pty) Ltd, De Beers Marine: Namibia, De Beers Canada Inc (Exploration) and Namdeb Diamond Corporation (Pty) Limited for support and making data and images available.

I would like to express my gratitude to several sponsoring companies including De Beers Family of Companies, , “Limn” sponsored by Dave Wiseman, Isatis sponsored by Geovariance, IoGas sponsored by Imdex.

Quantitative Geosciences and Interlaced for the opportunity, generous time, financial assistance and intellectual stimulation without which this research would not have been completed.

GLOSSARY

Term Used	Description or Definition
ASTM	American Standards for Testing and Materials.
Brownfield	Deposits where there is already a history of mining activity.
BTS	Brazilian Tensile strength.
Cpht	Carats per hundred tonnes.
HMA	Heavy Mineral Analysis.
HPGR	High Pressure Grinding Roll, A type of comminution device that is used to reduce the size of kimberlite rocks.
Intrinsic Hypothesis	Weak stationarity of the increments of a random function (Olea,1991).
Isotopic data	Refers to the availability of spatial sampling data where the same suite of variables has been measured at all sampled locations.
kWh/t	Kilowatt hours per ton.
LDD	Large Diameter Drilling.
Macro diamonds (MIDA)	A reference to diamonds that are above 0.5 mm in diameter.
Micro diamonds (MICRO)	Refers to diamonds that are less than 0.5mm in diameter.
NI-43-101	A Canadian Securities Exchange code for the reporting of mineral resources and reserves.
Ordinary Kriging	A linear estimation algorithm for a regionalised variable that satisfies the intrinsic hypothesis (Olea,1991).
QA/QC	Quality Assurance/Quality Control.
ROC	Required Operating Capability.
Rock	Material of the earth that may or may not be mineralised that is incorporated in block models and encountered whilst mining.
REP	Resource Extension Project.
TKB	Tuffasitic Kimberlite Breccia.
SEDAR	System for Electronic Document Analysis and Retrieval, the electronic filing system for the disclosure documents of scrip issuers across Canada.

Term Used	Description or Definition
Stationarity	First order stationarity assumes the mean of a variable is constant between samples independent of location; Second order stationarity is the assumption that the covariance between two points is the same for a given distance and direction regardless of the two points that are chosen.
Test Response variable	a variable that is a function of both the rock and a test that is performed on a rock - e.g. rate of dissolution.
Test Variables	parameters and characteristics of a test being performed that have an impact on the outcome of a rock test - e.g. the rate of loading during compressive strength tests.
t_{10}	Percentage passing one-tenth of a particle's original size for a given energy input.
UCS	Uniaxial compressive strength.
Unit Process response variable	A variable that represents the performance of a full-scale mineral process, e.g. the size distribution of rock produced by a crusher.
Waste	Rock material that may or may not contain mineral of interest, but that is deemed to have insufficient value to be selected for treatment.
Young's Modulus	Within the limits of elasticity, the ratio of the linear stress to the linear strain is termed the modulus of elasticity or Young's Modulus and may be written as E =(Stress/Strain). It is this property that determines how much a specimen will deform under load and is used to estimate the strength of rock.

Contents

1 INTRODUCTION 22

1.1 CURRENT APPROACHES USED TO EVALUATE DIAMOND MINING PROJECTS 23
1.2 SPECIFIC CHALLENGES FACED IN EVALUATING DIAMOND-MINING PROJECTS 25
1.3 DIAMOND PROJECT EVALUATION PRACTICE 31
1.4 USE OF THE METALLURGICAL RECOVERY FACTOR IN PROJECT EVALUATION 33
1.5 IMPACT OF RECOVERY PROCESS DESIGN AND OPERATION ON METALLURGICAL RECOVERY. 33
1.6 IMPACTS OF KIMBERLITE PROPERTIES ON TREATMENT PROCESS EFFICIENCY 35
1.7 IMPACT OF DIAMOND PROPERTIES ON THE RECOVERY FACTOR 37
1.8 THE SOURCES OF UNCERTAINTY IN ESTIMATING THE RECOVERY FACTOR 38
1.9 RESEARCH MODEL 41
1.10 THESIS STRUCTURE 43

2 LITERATURE REVIEW 44

2.1 PHYSICAL CHARACTERISTICS OF KIMBERLITES AND DIAMONDS 45
2.2 ROCK PROPERTY SAMPLING AND CHARACTERISTIC MEASUREMENTS 51
2.3 CHALLENGES OF SPATIALLY ESTIMATING PHYSICAL ROCK CHARACTERISTICS 57
2.4 MINERAL PROCESS MODELS AND SIMULATION PRACTICES 61
2.5 APPROACHES TO EVALUATING UNCERTAINTY AND VARIABILITY IN DIAMOND RECOVERY .. 67
2.6 SUMMARY OF PRACTICES AND LIMITATIONS IDENTIFIED IN THIS REVIEW 71

3 PROBLEM STATEMENT 73

3.1 INTRODUCTION 73
3.2 CURRENT LIMITATIONS IN THE DERIVATION AND USES OF THE METALLURGICAL DIAMOND RECOVERY FACTOR. 73
3.3 THE PROBLEM STATEMENT AND RESEARCH QUESTION 74

4 OREBODY SAMPLING AND COLLECTION OF ROCK CHARACTERISTIC DATA 76

4.1 INTRODUCTION 76
4.2 EXPERIMENTAL DESIGN 81
4.3 DATA COLLECTION PROCESS 93
4.4 DATA ACQUIRED 94
4.5 OBSERVATIONS ARISING FROM THE DATA COLLECTION 103
4.6 CONCLUSIONS ARISING FROM DATA COLLECTION 104

5 MODELLING PHYSICAL CHARACTERISTICS OF OREBODIES 106

5.1 INTRODUCTION 106
5.2 ESTIMATION OPTIONS CONSIDERED AND COMPARED 109
5.3 SELECTION AND PREPARATION OF PHYSICAL CHARACTERISTIC DATA FOR ESTIMATION 111
5.4 USING MULTIVARIATE TECHNIQUES IN ESTIMATION 112
5.5 ESTIMATION AND SIMULATION METHODS 116
5.6 GENERIC APPROACH AND CONSIDERATIONS FOR GENERATION OF SUITABLE SPATIAL MODELS 138

6 PROCESS SIMULATION AND ROCK CHARACTERISTICS 141

6.1 INTRODUCTION 141
6.2 MODELLING OF MINING PROCESSES 146
6.3 MODELLING OF DIAMOND TREATMENT PLANT PROCESS 148
6.4 UNIT PROCESS MODELS 153
6.5 ESTABLISHING RELATIONSHIPS BETWEEN COMMINUTION AND DIAMOND RECOVERY 170
6.6 PROCESS SIMULATION AND SENSITIVITY TESTING 191
6.7 LIMITATIONS OF PROCESSING MODELS 191
6.8 CONCLUSION 192

7 VALUE CHAIN MODELS - CASE STUDY 1 193

7.1 INTRODUCTION 193
7.2 BENEFITS AND LIMITATIONS OF THE METHODOLOGY 201

8 VALUE CHAIN MODEL - CASE STUDY 2 203

8.1 INTRODUCTION 203
8.2 THE VALUE CHAIN COMPONENTS 206
8.3 CONSIDERATIONS FOR DEVELOPMENT AND SIMULATION OF INTEGRATED VALUE CHAIN MODELS 211
8.4 CASE STUDY FINDINGS 213
8.5 GENERIC FINDINGS FROM THE IEM RELEVANT TO THE DERIVATION OF THE METALLURGICAL RECOVERY FACTOR 216

9 DISCUSSION 219

9.1 INTRODUCTION 219
9.2 A TAXONOMY FOR VARIABLES USED IN RECOVERY FACTOR DETERMINATION 219
9.3 INCREASING THE QUALITY OF SPATIAL ESTIMATES -USING PROXY MEASUREMENTS, SCALE-UP AND TESTING FOR ADDITIVITY OR NON-LINEARITY 224
9.4 DIAMOND METALLURGICAL RECOVERY FACTORS – EXPLORING UNCERTAINTY AND VARIABILITY BY EFFECTIVE USE OF VALUE CHAIN MODELS 225
9.5 CONCLUSION 226

10 SUMMARY AND CONCLUSIONS 227

10.1 INTRODUCTION 227
10.2 CONCLUDING THEMES 228
10.3 SPECIFIC CONTRIBUTIONS OF THIS RESEARCH 231
10.4 THE LIMITS OF THIS RESEARCH 232
10.5 RECOMMENDED AREAS FOR ADDITIONAL RESEARCH 233

11 REFERENCES 235

12 APPENDICES 246

APPENDIX 1 -EXPERIMENTAL DESIGN AND DATA FROM OREBODY SAMPLING 247

APPENDIX 2 -OREBODY CHARACTERISTIC ESTIMATES 251

LIST OF TABLES

TABLE 1: SELECTION OF SEVERAL DIAMOND MINES SHOWING THE MINE GRADE RECOVERED IN CPHT, AVERAGE DIAMOND VALUE IN $/CT AND THE AVERAGE REVENUE IN $/TONNE (PETRA DIAMONDS, 2019; ANGLO AMERICAN, 2018; DE BEERS GROUP SERVICES 2018) 26

TABLE 2: ANALYSIS OF DIAMONDS SIZED BY SCREENING (ADAPTED AFTER FERREIRA 2013) 27

TABLE 3: A DESCRIPTION OF THE COMPONENTS OF VOLCANICLASTIC KIMBERLITES 50

TABLE 4: RELATIONSHIPS BETWEEN ORE PROPERTY AND THE IMPACT ON MINERAL PROCESSING. 63

TABLE 5: A LIST OF PREFERRED VALUATION METHODOLOGIES USED IN SOUTH AFRICA (SILVA AND MINNITT, 2005) 68

TABLE 6: FORMULAE FOR ESTIMATING ELASTIC MODULI OF SOLIDS USING MEASURED ACOUSTIC VELOCITIES IN ROCK SPECIMENS. 89

TABLE 7: SUMMARY OF THE NUMBER OF EACH TYPE OF SAMPLE COLLECTED. 94

TABLE 8: SUMMARY STATISTICS OF ANALYSIS CARRIED OUT ON PETROLOGICAL SLAB SAMPLES. . 95

TABLE 9: SUMMARY STATISTICS FOR THE UNIAXIAL COMPRESSIVE STRENGTH (UCS) AND BRAZILIAN TENSILE STRENGTH (BTS) TEST WORK. 96

TABLE 10: SUMMARY STATISTICS OF DROP WEIGHT RESULTS OBTAINED FROM CORES. 97

TABLE 11: SUMMARY OF DOWNHOLE GEOPHYSICAL READINGS TAKEN FROM EACH HOLE DRILLED 101

TABLE 12: DESCRIPTIVE STATISTICS OF THE DOWNHOLE FORMATION TESTER RESULTS. 102

TABLE 13: SUMMARY STATISTICS FOR DROP WEIGHT TEST DATA SHOWING SAMPLE AND POLYGONAL STATISTICS. 117

TABLE 14:TABLE AND GRAPHICS OF THE MODELLED VARIOGRAMS FOR P-WAVE VELOCITY, T_{10} SPECIMEN DENSITY AND T_{10}_E1. 123

TABLE 15: SUMMARY STATISTICS FOR DATA AND FIRST PASS ESTIMATES. 124

TABLE 16: SUMMARY STATISTICS COMPARING ESTIMATED AND SIMULATED VALUES FOR P-WAVE VELOCITY AND DROP WEIGHT RESULTS AT THE 5M BLOCK SCALE. 129

TABLE 17: OPTIONS FOR USE OF SPATIAL DATA TO ESTIMATE PROCESS RESPONSE VARIABLES. 134

TABLE 18: SUMMARY STATISTICS FOR THE ESTIMATION AND CALCULATION OF BLOCK SCALE PROPERTIES FOR PATHWAY 1. 135

TABLE 19: SUMMARY STATISTICS FOR THE ESTIMATION AND CALCULATION OF BLOCK SCALE PROPERTIES FOR PATHWAY 2 135

TABLE 20: SUMMARY STATISTICS FOR THE ESTIMATION AND CALCULATION OF BLOCK SCALE PROPERTIES FOR PATHWAY 3. 136

TABLE 21: SUMMARY STATISTICS FOR THE ESTIMATION AND CALCULATION OF BLOCK SCALE PROPERTIES FOR PATHWAY 4. 136

TABLE 22: SUMMARY STATISTICS FOR THE ESTIMATION AND CALCULATION OF BLOCK SCALE PROPERTIES FOR PATHWAY 5. 136

TABLE 23: A TABULAR DEMONSTRATION OF A WHITTEN SELECTION AND BREAKAGE MODEL.. 163

TABLE 24: CALCULATION OF LOCKED DIAMOND CONTENT 175

TABLE 25: CALCULATION OF LOCK UP WITH CONSTRAINT PLACED ON THE MAXIMUM SIZE OF CONTAINED DIAMOND. 176

TABLE 26: LISTING OF DIAMOND SCREEN SIEVE CLASSES AND ASSOCIATED SIEVE APERTURES, AVERAGE STONE SIZE PER CLASS AND CRITICAL STONE SIZE PER CLASS 180

TABLE 27: DESCRIPTION OF METHOD USED TO CONVERT THE SAMPLED TAILINGS DISTRIBUTION TO A TOTAL KIMBERLITIC DISTRIBUTION. 185

TABLE 28: FITTING OF THE LOGNORMAL MODEL TO THE RECOVERED SIZE DISTRIBUTION. 186

TABLE 29: PROCESS PARAMETERS REQUIRED FOR THE GRANULOMETRY MODEL. 187

TABLE 30: CALCULATION OF THE MAXIMUM LOCKED DIAMOND SIZE IN KIMBERLITE PARTICLES IN EACH SIEVE CLASS. 187

TABLE 31: ALLOCATION OF THE LOCKED POTENTIAL IN EACH SIZE CLASS ACCORDING TO THE PROBABILITIES DERIVED FROM THE RECOVERED DIAMOND SIZE DISTRIBUTION.....188

TABLE 32: CALCULATION OF THE LOCKED CARAT POTENTIAL PER DIAMOND SIEVE CLASS. 189

TABLE 33: CALCULATION OF THE LIBERATED AND LOCKED POTENTIAL REVENUE. 190

TABLE 34: SUMMARY OF THE CHARACTERISTICS OF THREE SAMPLING CAMPAIGNS AND THAT USED TO DEFINE THE 'VIRTUAL OREBODY(V-BOD) 196

TABLE 35: THE DESCRIPTIVE STATISTICS FOR THE V-BOD AND EACH SCENARIO FOR GRADE, DYKE THICKNESS AND THE GEOMETRICAL VARIABILITY OF THE DYKE SURFACE (V1).....198

TABLE 36: SCHEMATIC DEPICTION OF TERMINOLOGY USED TO DESCRIBE ASPECTS OF THE INTEGRATED EVALUATION MODEL.....204

TABLE 37: SUMMARY OF MAJOR CAPITAL ITEMS PLANNED FOR EACH PHASE. 208

TABLE 38: AVERAGE EXPECTED DMS YIELDS FOR EACH PHASE. 208

TABLE 39: LIST OF MODEL SETTINGS USED FOR THE FINANCIAL MODEL. 210

TABLE 40: SUMMARY STATISTICS OF SPATIALLY SIMULATED GRADE, DENSITY AND DMS YIELD VALUES. 213

TABLE 41: SUMMARY STATISTICS OF $/TONNE DEPLETED BY LOBE BASED ON SIMULATED STONE VALUES. 215

TABLE 42: A LIST OF GUIDING PRINCIPLES FOR ROCK CHARACTERISTIC SAMPLING. 223

List of Figures

Figure 1: A schematic overview of a mining value chain, and a breakdown of the metallurgical recovery factor. Adapted after (Appleyard, 2001). 24

Figure 2: Plot of diamond stone counts per size class. 29

Figure 3: Variation of the average stone size estimated from small samples. 30

Figure 4: Typical relationship between diamond size and cut diamond retail value (adapted from Rappaport, 2009). 30

Figure 5: Comparison of the proportion of carats and proportion of revenue represented by different diamond size ranges, for the diamond parcel described in table 2. 32

Figure 6: A schematic representation of the research areas covered in this thesis. 41

Figure 7: Melt viscosity as a function of temperature at 1 bar for natural melts spanning the compositional range Rhyolite to komatiite. All compositions are volatile free. The temperature range is illustrative of typical eruption temperatures for each composition – adapted from (Sperra, 2000) and (Sparks et al., 2009). 47

Figure 8: A schematic view of a kimberlite pipe after Hawthorne (1975). 48

Figure 9: A schematic representation of the materials that could be found in a 'typical' kimberlite pipe, adapted after (Field and Smith, 1999). 49

Figure 10: A hierarchical depiction of the relationship of sources of error arising from sampling, Adapted after Gy (2004). 54

Figure 11: Results of a number of rock tests on a range of rock types after Copur et al. (2003). 56

Figure 12: Schematic of the process used to create a framework to quantify the impact of changes to sampling , estimating and simulating Kimberlites on process models. 59

Figure 13: Geological map of Venetia K2 (after Brown 2008) showing the location of the Geomet drill holes (orange cross). 82

FIGURE 14: A VIEW OF THE LAYOUT OF THE CORE HOLES DEPICTING THE LOCATION OF THE SUBSAMPLES. 82

FIGURE 15:LISTING OF SUBSAMPLES TAKEN FROM CORES THAT WERE FULLY SAMPLED..... 83

FIGURE 16: SCHEMATIC REPRESENTATION OF PREPARATION AND ANALYSIS OF PETROLOGICAL SAMPLES. (GSC=GEOSCIENCE CENTRE LABORATORY, UCT=UNIVERSITY OF CAPE TOWN, UOB=UNIVERSITY OF BRISTOL, SGS=TESTING LABORATORY IN JOHANNESBURG, EDINBURGH =EDINBURGH UNIVERSITY). 90

FIGURE 17: PREPARATION AND ANALYSIS OF GEOMETALLURGICAL SAMPLES..... 91

FIGURE 18: PREPARATION AND TESTING OF GEOTECHNICAL SAMPLES..... 92

FIGURE 19: XY PROJECTION OF THE LAYOUT OF THE CORE SAMPLES..... 93

FIGURE 20: HISTOGRAM OF THE DENSITY OF SAMPLES SUBJECTED TO DROP WEIGHT TESTING.... 97

FIGURE 21: COMPARISON OF HISTOGRAMS OF DROP WEIGHT RESULTS FOR ALL SAMPLES TESTED AT THREE DIFFERENT INPUT ENERGIES (TOP FIGURE IS LOWEST ENERGY; BOTTOM PANEL IS HIGHEST ENERGY). 98

FIGURE 22: HISTOGRAM AND BASE MAP OF SAMPLE DENSITY FOR THE VKBR DOMAIN. 99

FIGURE 23: A HISTOGRAM AND CROSS SECTION OF THE DENSITIES OF THE SAMPLES TAKEN FROM THE VK FACIES DOMAIN 99

FIGURE 24: COMPARATIVE HISTOGRAMS OF DROP WEIGHT RESPONSES AT THREE DIFFERENT INPUT ENERGY LEVELS FOR THE VKBR FACIES (LHS) AND THE VK FACIES (RHS).....100

FIGURE 25:HISTOGRAM OF "SHORT SPACED DENSITY" SHOWING HIGH READINGS.....101

FIGURE 26: A PLOT SHOWING THE THREE READINGS GENERATED BY THE FORMATION HARDNESS TOOL FOR HOLE DDH357. 102

FIGURE 27: HISTOGRAM (LHS) AND SEMI-VARIOGRAM (RHS) OF MM OF DEFLECTION ('DIFFERENCE')MEASURED BY THE DOWNHOLE FORMATION TESTING DEVICE. 103

FIGURE 28: SCHEMATIC SHOWING PATHWAYS OF GENERATING SPATIAL MODELS OF ROCK CHARACTERISTICS. 108

FIGURE 29: A PLOT SHOWING THE IMPACT OF THE SIZE OF THE INTERVAL USED ON THE TOTAL VARIANCE OF THE BULK MODULUS MEASUREMENT. 112

FIGURE 30: A PLOT SHOWING THE LINEAR MODEL DEVELOPED BETWEEN THE FORMATION HARDNESS TOOL READINGS AND THE UCS VALUES. 113

FIGURE 31: A BOX AND WHISKER PLOT SHOWING THE SAMPLE VALUE USED TO CALIBRATE THE PLS MODELS ON THE LEFT OF THE PLOT, AND THE ESTIMATE OF UCS DOWN THE HOLE ON THE RIGHT. THE HEIGHTS OF THE BARS INDICATE 'GOODNESS OF FIT' OF THE PARTIAL LEAST SQUARES MODEL DERIVED FROM MULTIPLE VERSIONS OF THE MODEL USING DIFFERENT COMBINATIONS OF SAMPLE AND HOLD OUT DATA. 114

FIGURE 32: A PLOT OF MEASURED UCS VALUES, AND MODELS FOR THE SAMPLES BASED ON THE DOWNHOLE ACOUSTIC SIGNAL AND CUTTER PENETRATION DEPTH. 115

FIGURE 33:PCA MODEL OF UCS DOWNHOLE BASED ON A PRINCIPAL COMPONENT ANALYSIS (PCA) MODEL USING P- WAVE VELOCITY, S WAVE VELOCITY AND LONG DENSITY, USING ONE PRINCIPAL COMPONENT (UPPER PANEL) AND TWO PRINCIPAL COMPONENTS (LOWER PANEL). 116

FIGURE 34: A 3D REPRESENTATION OF A POLYGONAL ESTIMATE OF DROP WEIGHT VALUES IN THE 0.7M X0.7M X 0.7M GRID. 118

FIGURE 35: AN EXPERIMENTAL AND FITTED MODEL FOR THE VARIOGRAM FOR THE UCS DATA. 119

FIGURE 36: N-S CROSS SECTION OF AREA ESTIMATED SHOWING HIGH UCS ESTIMATES IN HOTTER COLOURS AND LOWER VALUES IN COOLER COLOURS (LHS) AND A HISTOGRAM OF THE BLOCK UCS VALUES ESTIMATED. 119

FIGURE 37: HISTOGRAMS OF THE ORIGINAL T_{10} VALUES (LEFT) AND THE TRANSFORMED VARIABLE "MASS LESS 5MM IN G/TONNE" (RIGHT). 124

FIGURE 38: 3 DIMENSIONAL PROJECTIONS OF THE KRIGING OF DROP WEIGHT VALUES (LEFT) AND THE TRANSFORMED VARIABLE "MASS LESS 5MM IN G/TONNE" (RIGHT). 125

FIGURE 39: CROSS SECTIONS OF THE OREBODY AND HISTOGRAMS FOR THE THREE VARIABLES ESTIMATED INDEPENDENTLY INTO A 0.7M X0.7M X 0.7M GRID AND ACCUMULATED INTO A 5M X 5M X 5M GRID. 126

FIGURE 40: HISTOGRAMS SHOWING TRANSFORM OF DATA FROM RAW DATA TO GAUSSIAN VARIABLES. 127

FIGURE 41: VARIOGRAM MODELS (TOP LEFT AND BOTTOM RIGHT)AND CROSS VARIOGRAM MODELS (BOTTOM LEFT) FOR THE GAUSSIAN TRANSFORMS OF P-WAVE AND DROP WEIGHT TEST DATA. 127

FIGURE 42: PERSPECTIVE PLOTS SHOWING A CROSS-SECTION THROUGH THE TEST AREA FOR 5M X 5M X 5M BLOCKS FOR SIMULATED AND KRIGED P-WAVE VELOCITY (UPPER IMAGES) AND DROP WEIGHT TEST DATA(LOWER IMAGES). 128

FIGURE 43: SCHEMATIC OF THE OPTIONAL ROUTES TO USE POINT SCALE SAMPLE DATA TO PREDICT THROUGHPUT.....130

FIGURE 44: A RELATIONSHIP BETWEEN INPUT ENERGY AND DEGREE OF FRACTURE, EXPRESSED AS PERCENTAGE PASSING 1/10TH OF ORIGINAL PARTICLE SIZE (BLUE DIAMONDS), SHOWING A FITTED BREAKAGE FUNCTION IN BLACK. 131

FIGURE 45: PLOT SHOWING BROAD CORRELATION BETWEEN AVERAGE LONG RUN ENERGY CONSUMPTION IN SEMI AUTOGENOUS GRINDING (SAG) MILLS AND AVERAGE OREBODY A*B VALUES (DANIEL, LANE AND MCLEAN, 2010). 132

FIGURE 46: RELATIONSHIP BETWEEN POWER CONSUMPTION AND THROUGHPUT FOR A TARGET GRIND SIZE. 133

FIGURE 47: HISTOGRAMS OF THE VARIABLES THAT ARE CALCULATED AND ESTIMATED IN PATHWAY 1.....137

FIGURE 48: HISTOGRAMS OF THE VARIABLES THAT ARE CALCULATED AND ESTIMATED IN PATHWAY 3, DATA HAS BEEN GROUPED BY PREDICTED THROUGHPUT QUARTILES.....137

FIGURE 49: PLOT SHOWING THE VARIABILITY IN WEEKLY THROUGHPUT AND A TABLE WITH SUMMARY STATISTICS FOR EACH OF THE VARIABLES CALCULATED THROUGH EACH PATHWAY. 138

FIGURE 50: A SCHEMATIC DEPICTION OF APPROACHES TO ESTIMATING THE RECOVERY FACTOR FOR DIFFERENT PROJECT MATURITIES.....143

FIGURE 51: A PLOT OF THE SPECIFIC INPUT ENERGY AND CUMULATIVE PROBABILITY OF FAILURE FOR A FEW SELECTED MINERALS, SIZE PARAMETER SET TO 5MM (ADAPTED AFTER KING 2001). 158

FIGURE 52: A PLOT OF THE MEDIAN FRACTURE ENERGY FOR MINERAL PARTICLES OF DIFFERENT SIZES. 159

FIGURE 53: A PLOT OF ENERGY INPUT VS PRODUCT SIZE USING THE T_{10} APPROACH AND A ROSIN RAMMLER BREAKAGE FUNCTION MODIFIED AFTER KING (2001). 167

FIGURE 54: A DENSIMETRIC DISTRIBUTION PLOTTED FOR FOUR SAMPLES DERIVED FROM KIMBERLITE, CRUSHED TO 100% PASSING 12MM AND GROUPED BY DENSITY CLASSES.... 169

FIGURE 55: A PLOT OF THE LOG OF DIAMOND WEIGHT VS LOG OF THE NUMBER OF STONES IN EACH CLASS PER HUNDRED TONNES PER UNIT INTERVAL. 171

FIGURE 56: A PLOT OF THE LOGARITHM OF DIAMOND SIZE VS STONE FREQUENCY IN STONES PER HUNDRED TONNES PER UNIT INTERVAL. 172

FIGURE 57: PLOT SHOWING THE ACTUAL AND MODELLED LOG NORMAL DIAMOND SIZE DISTRIBUTION. 182

FIGURE 58: COMPARISON OF THE THICKNESS AND V1 BASE MAPS FOR THE KRIGED AND SIMULATED OUTPUTS OF EACH SCENARIO WITH THAT OF THE V-BOD. GRADE WAS HELD CONSTANT FOR EACH SCENARIO. 197

FIGURE 59: A DIAGRAM DEPICTING THE IMPLEMENTATION OF THE MINING CONSTRAINT LOGIC. 199

FIGURE 60: A DEPICTION OF LIBERATION AS A FUNCTION OF THE CONCENTRATION OF KIMBERLITE IN THE HEADFEED. 200

FIGURE 61: A VIEW OF THE THREE LOBES OF THE DEPOSIT LOOKING FROM THE WEST TO THE EAST (SOUTH LOBE IN DARK BLUE) ADAPTED AFTER CAMPBELL (2009). 207

FIGURE 62: SCHEMATIC OF PROCESS FLOWS USED FOR PROCESS MODEL. 209

FIGURE 63: PLOT SHOWING A SIMULATION OF THE SIZE OF 20 000 DIAMONDS DRAWN. 210

FIGURE 64: SCHEMATIC OF THE INTEGRATED EVALUATION MODEL ARCHITECTURE (ADAPTED AFTER BURBECK, 1992) 211

FIGURE 65: SUMMARY OF TONNAGE TREATED 214

FIGURE 66: SUMMARY PLOT OF CUMULATIVE DISCOUNTED CASHFLOW FOR THE AK PROJECT, P50 CASE SHOWN IN GREEN,P80 AND P20 CASE SHOWN IN RED, INDIVIDUAL CASES SHOWN IN GREY. 216

FIGURE 67: GRADE SIZE PLOT SHOWING THE IMPACT OF APPLYING A STRICT SIZE CUT-OFF TO A TOTAL CONTENT CURVE. 217

FIGURE 68: A SCHEMATIC REPRESENTING THE PRIMARY RESPONSE FRAMEWORK FOR GEOMETALLURGICAL VARIABLES. 220

FIGURE 69: A DATA TYPOLOGY ADAPTED AFTER KEENEY AND WALTERS (2008). 221

FIGURE 70: A LANDSCAPE FOR SAMPLE TYPE CLASSIFICATION IN TERMS OF BOTH SPATIAL CONTINUITY AND PRIMARY RESPONSE DIMENSIONS. 222

FIGURE 71: SCHEMATIC SHOWING THE LOCATION OF SAMPLES FROM K2 PIPE. 247

FIGURE 72: A VIEW OF THE LAYOUT OF THE CORE HOLES DEPICTING THE LOCATION OF THE SUBSAMPLES 248

FIGURE 73:LISTING OF SUBSAMPLES TAKEN FROM CORES THAT WERE FULLY SAMPLED 249

FIGURE 74: DEPICTION OF THE SUBSAMPLES TAKEN FROM CORES THAT WERE PARTIALLY SAMPLED. 250

FIGURE 75:A VIEW FROM THE SOUTH-WEST OF VENETIA K2 SAMPLED AREA - SHOWING DOWNHOLE DENSITY 251

FIGURE 76:A VIEW FROM THE SOUTH-WEST OF VENETIA K2 SAMPLED AREA - SHOWING DOWNHOLE DENSITY AND P WAVE VELOCITY. 252

FIGURE 77:A VIEW FROM THE SOUTH-WEST OF VENETIA K2 SAMPLED AREA - UCS SAMPLE VALUES AS SCALED SPHERES AND ESTIMATED BLOCK DENSITY IN TRANSPARENT BLOCKS. 252

FIGURE 78:A VIEW FROM THE SOUTH-WEST OF VENETIA K2 SAMPLED AREA - T_{10} SAMPLE VALUES AS SPHERES AND ESTIMATED T_{10} IN TRANSPARENT BLOCKS. 253

LIST OF APPENDICES

APPENDIX 1 -EXPERIMENTAL DESIGN AND DATA FROM OREBODY SAMPLING 247

APPENDIX 2 -OREBODY CHARACTERISTIC ESTIMATES 251

1 INTRODUCTION

The specific limitations of traditional recovery factor estimation processes addressed in this thesis are those that arise from the difficulty of incorporating variable and uncertain rock properties in the derivation of the metallurgical recovery factor. Failure to explicitly include the impacts of rock properties in traditional project evaluation can result in sub-optimal mine design, incorrect process configuration (design, operating strategy) and potentially biased production and cashflow forecasts.

The metallurgical recovery factor is introduced in the context of the diamond mining industry and its impact on diamond mining project evaluation. The connection between the unique characteristics of diamonds (their particulate nature, low concentration and logarithmic relationship between size and value), their host deposits (kimberlite), and the diamond recovery processes is explained.

The consequence of using global estimates for rock and diamond characteristics, based on few and spatially sparse data combined with the vast differences between the scale of measurements from small samples and the scale of estimation of these properties is described.

The primary response framework (Coward et al., 2009) is introduced to clarify the taxonomy for variables that are used in this research. This conceptual framework provides a basis for developing quantitative models of the relationships between variables that drive uncertainty in the recovery of diamonds. These models are used to propagate variability, and uncertainty through the diamond recovery value chain. The specific uncertainties explored include those associated with data collection, characteristic estimation, and process response modelling.

The introduction concludes with a demonstration of the role that the metallurgical recovery factor plays in evaluating the economic potential of diamond mines.

1.1 Current approaches used to evaluate diamond mining projects

Evaluating the economic and technical viability of diamond mining projects requires several inputs and assumptions. The report required by Canadian National Instrument NI-43-101 (NI43-101, 2001) for standards of disclosure for minerals projects comprises a detailed list of information and technical data vouched for by a Competent (Qualified) Person. Many orebody inputs (e.g., grade, tonnage estimates) are derived from limited, and/or spatially sparse, data and are thus characterised by a high degree of uncertainty. One of these uncertain inputs is the metallurgical recovery factor that is used to calculate the quantity and quality of the diamonds that will be delivered by the project.

Current reviewed methods of estimating and using the metallurgical recovery factor do not explicitly account for the impact that variable and uncertain kimberlite characteristics have on the derivation and use of the factor. Assumptions of continuity of kimberlite characteristics in large parcels of mined material has potential to under- or over-estimate recoveries and in some cases, lead to material inaccuracy in the estimate of project value (Mackey and Nesset, 2003).

This research project focusses on the development of a methodology that will improve the evaluation process by incorporating both variability and uncertainty of diamond and kimberlite characteristics in the evaluation of diamond mining projects. The approach is centred on the development of a value chain model that facilitates the propagation of variable physical characteristics of kimberlite through the value chain from the orebody to final product. The value chain approach allows the modelled variability of kimberlite characteristics to interact with constraints in the mining and processing of kimberlite. The system model is used to quantify the influence of the characteristics on process throughput, process efficiency and diamond recovery. Historic methods have, for various reasons, not used this approach.

The approach makes it possible to determine, at various scales of resolution, the expected differences between the estimated in situ diamond population and the population of diamonds that will be recovered. Passing multiple simulated realisations of the deposit's kimberlite properties through the value chain allows the generation of a range of plausible estimates for the metallurgical recovery factor. This range can be used to derive confidence limits or probability threshold values for the metallurgical recovery factor over the life of the mining operation.

The potential value of a diamond project is driven, to a large degree, by the size of the deposit, the in situ diamond grade and the in situ diamond value from the in situ resource. Translation of the estimate of in situ grades of the orebody into an

expected cash flow model for valuation of the mining project requires valid methods to determine diamond recovery and loss . The metallurgical recovery factor is one of the modifying factors used in the development of the valuation model. Its value reflects the proportion of the total population of in situ diamonds that is expected to be recovered when the mine is operational. This expected carat recovery is then integrated with the other estimates into a financial model to estimate a mining project's value.

This evaluation process is a component of the mining value chain. A schematic of this process is show in Figure 1.

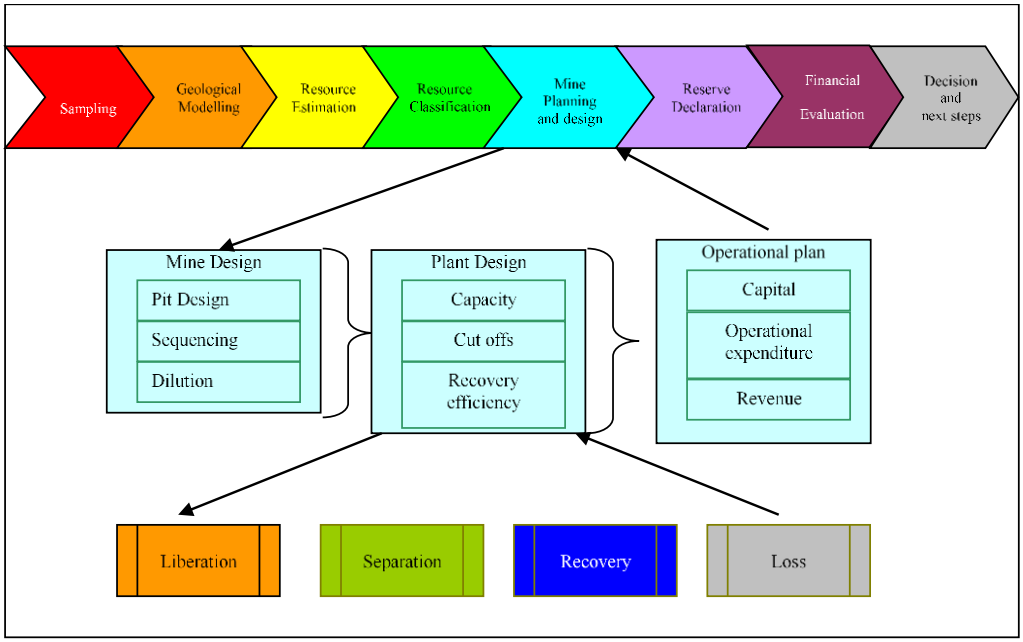

Figure 1: A schematic overview of a mining value chain, and a breakdown of the metallurgical recovery factor. Adapted after (Appleyard, 2001).

Development of a mining project begins with the discovery of a kimberlite that has the potential to contain diamonds. Once discovered, several sampling and measuring processes are initiated to gather data on the diamond content and information that is used to infer the size of the deposit. These activities include collection of geological information based on outcrops, core and trench samples. The uncertainty associated with the grade estimates of portions of the resource is used to classify the resource into inferred, indicated or measured categories as per the requirements of the prevailing codes for reporting exploration results, mineral resources and ore reserves, e.g. JORC (JORC, 2012) and SAMREC (SAMREC, 2016).

These resources are then subjected to a planning process that is usually divided into several phases. At each phase the number of options, or configurations considered, are reduced and ideally, as more information is acquired, confidence in the estimates of the primary parameters (Grade, Tonnage, Deposit shape) of the mineral project is increased. Once a mine plan and a proposed process plant design has been

completed, it is possible to estimate the expected tonnage and grade that will be produced by the project. This calculation includes assumptions about both mining and metallurgical process efficiencies. These efficiencies are used to estimate the reserves of the project that can be classified as either probable or proven as defined in the relevant classification code e.g., JORC (2012) code. The declared reserves are an essential input into the mine and process plant design and configuration.

The evaluation process is iterative in nature, and usually includes several phases of sampling, sample processing, resource estimation, mine and process design, reserve estimation and valuation. In each iteration, more information on the deposit is acquired, reducing uncertainty in the geological models, grade estimates, and other inputs used to evaluate the viability of the mining project.

At the end of each assessment stage a gating process is carried out to select the 'best next step' for the project. The next steps might include divesting from the project, halting the project, continuing the original plan, or increasing expenditure to expedite the project delivery. These decisions are informed by both the valuation of the project and, to some degree, the uncertainty of the valuation. (Brennan & Schwartz 1985; Bratvold & Begg 2002).

1.2 Specific challenges faced in evaluating diamond-mining projects

The evaluation of kimberlite diamond deposits faces several specific challenges, these include:

- A low proportion of kimberlite deposits contain diamonds;
- Kimberlites exhibit a range of geometries that result from multiple phases of volcanic intrusion;
- The concentration of diamond mineralisation is very low;
- The mineralisation is of a particulate nature; and
- Diamond value is a function of several characteristics that are difficult to sample in a representative way using small samples.

Low proportion of pipes are economic

Few of the kimberlites discovered to date contain sufficient diamonds to support a mining operation. There are approximately 5000 kimberlite pipes that have been discovered, of which around 50 have been mined at some stage, and about 15 are major producers (Kjaarsgaard, 1995). However, approximately 58% by value of diamonds mined are estimated to come from kimberlite pipes (De Beers Mineral

Resource Intelligence Unit, 2005). Although diamonds also occur in other deposit styles, such as alluvial and fluvial, this research is focused on kimberlitic deposits.

Kimberlite deposits exhibit a wide range of geometries

Kimberlites are the transport mechanism that brings diamonds from the diamond stability field in the earth's mantle into the crust in a medium that preserves the diamonds (Field & Scott Smith 1999).They are formed by a diverse range of natural volcanic events. Such events give rise to deposits that exhibit a wide range of geometries and thus require substantial geological investigation to understand the geometry of the phases of the deposit and the presence and dispersion of diamonds contained within each phase (Field et al. 2008).

Economic diamond concentrations are very low

The grades of diamond deposits are typically expressed as carats per hundred metric tonnes (CPHT). A carat is equivalent to 0.2g and thus this measurement equates to a weight-by-weight fraction of one part per 500 million. Table 1 gives a few examples of grades of mines that are, or were, operating at the time of publication.

Mine	Average production Grade in cpht.	Average Revenue $/ct.	$/tonne	Year
Jwaneng	**198**	**150**	**297**	**2016**
Venetia	**58**	**187**	**108**	**2013**
Finsch	**56**	**108**	**60**	**2018**
Orapa	**81**	**97**	**79**	**2016**
Premier Mine	**39**	**125**	**49**	**2018**
Koffiefontein	**6.4**	**525**	**34**	**2018**
Williamson	**7.6**	**270**	**21**	**2018**

Table 1: Selection of several diamond mines showing the mine grade recovered in cpht, average diamond value in $/ct and the average revenue in $/tonne (Petra Diamonds, 2019; Anglo American, 2018; De Beers Group services 2018)

Diamonds are particles with a wide distribution of sizes

Given the unique nature of diamond mineralisation, it is useful to consider the methods and variables used to describe diamond content and the methods used to analyse relationships between concentration and size. The variables include several forms of the diamond mass concentration and diamond stone size distribution.

Diamonds exist as individual particles embedded in a kimberlite matrix. Unlike assaying for metals where relatively small samples can be crushed and assayed to determine the average grade of the contained metal, the diamond sampling process requires the liberation and recovery of a mixed population of particles. The particles of interest (diamonds) range in size from 0.1µm to over 100mm. The abundance, by number, of small diamonds is higher than that of coarse diamonds. Table 2 gives an example of a parcel of diamonds that has been sieved and the weights retained on each sieve have been recorded.

Diamond Sieve	Lower Critical Size	Average Size	Unit interval Factor	Cts retained on each screen	Stone Count
#	Ct/Stone	Ct/stone		Ct	#
+15 CTS	14.8	17.118		0.00	0
+23	8.0360	10.9060	3.7704	0.00	0
+21	3.6910	4.8500	2.9595	0.00	0
+19	1.9180	2.4800	3.5175	0.00	0
+17	1.4230	1.5700	7.7134	0.00	0
+15	1.1950	1.2600	13.1862	1.75	1
+13	0.7030	0.8600	4.3400	3.22	4
+12	0.5230	0.5610	7.7849	2.57	5
+11	0.3170	0.3710	4.5989	0.92	2
+9	0.1790	0.2110	4.0289	0.92	4
+7	0.1170	0.1230	5.4151	3.38	27
+6	0.0792	0.0896	5.9011	0.90	10
+5	0.0485	0.0730	4.6952	0.90	12
+3	0.0256	0.0350	3.6036	0.60	17
+2	0.0138	0.0210	3.7263	0.43	20
+1	0.0054	0.0140	2.4541	0.02	2
-1	0.0020	0.0090	2.3182	19.00	2111

Table 2: Analysis of diamonds sized by screening (adapted after Ferreira 2013)

Diamond sieves are metal plates with round holes of a specific diameter punched in them. The diamond trading company nomenclature for the sieves is given in the first column of Table 2. Each aperture size can be related to a characteristic diamond weight that has a 50% probability of either passing through or being

retained on the screen of this aperture; this is referred to as the critical size for that screen aperture.

As the difference in the size of the orifices in the screen sequence varies between sieve sizes, the masses retained on each sieve need to be factored or standardised by the relative 'distance' of the interval between each sieve in order to compare relative abundance in each size fraction. This factor, known as the unit interval factor, can be derived from Equation 1

$$\boldsymbol{Unit\ Interval} = \mathbf{1} \Big/ \left[\log\left(\boldsymbol{Csz_{up}}\right) - \log\left(\boldsymbol{Csz_{low}}\right)\right] \qquad \textbf{Equation 1}$$

where Csz_{up} is the critical size in ct/stone of the previous sieve used in the sequence; and Csz_{low} is the critical size in ct/stone of the sieve on which the diamonds are retained. This unit interval is used to normalise the mass or number of stones retained per sieve class when plotting various charts of the diamond size distribution.

The diamonds retained in any sieve class can be reported as either a mass of diamond or a stone count. The average size of stone that is retained on a sieve size in the sequence is derived from sieving and counting stones retained on each sieve, and then dividing the total mass of the stones retained on the sieve by the stone count. This average can be used to generate an approximate estimate the number of stones retained in a sieve interval for other sieved parcels of diamonds.

The information in Table 2 is also depicted in Figure 2, which shows diamond weight class on the horizontal axis and diamond count on the vertical axis. The figure on the left demonstrates the relationship between size and stone abundance. In the plot on the right-hand side is calculated by taking the logarithm of the class average stone size and applying the unit interval correction to the stone count in each class.

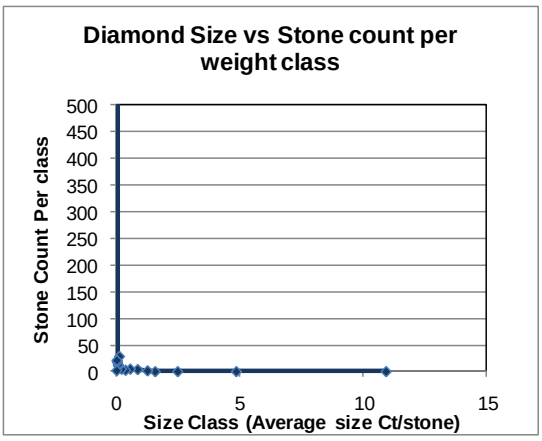

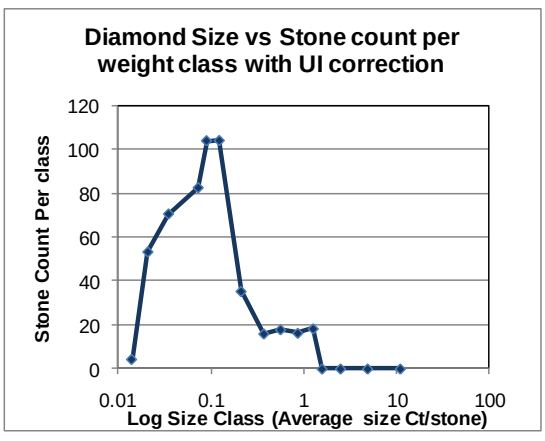

Figure 2: Plot of diamond stone counts per size class.

Diamond grade sampling is challenging

The purpose of the sampling process is to recover, as far as is possible, a good representation of the full size spectrum of diamonds contained within the target deposit. The relative abundance of smalls stones, and relative scarcity of large stones, suggests that small samples will be biased, containing a higher proportion of small stones and their average stone size will be below that of the true in situ value. Samples of sufficient support are required to so that both the sampled stone concentration as well as proportion of stones in each size class can be considered to be sampled in a representative manner. It is also important to note that not all the small diamonds will be recovered during the sample treatment process; those smaller than the bottom screen aperture will be lost, and a number will also remain 'locked' in the coarse discard stream. Figure 3 has been generated by simulating sampling of diamonds from the parcel shown in Table 1.

In each sampling iteration, the number of diamonds sampled is increased. The green line shows how the average stone size estimated from ten samples of the same number of stones increases with an increase in the size of the sample. The increasing size of the sample also reduces the range between the maximum and minimum estimate of the average stone size.

The graph also shows how the actual average stone size in the parcel is underestimated (biased) because of the under-representation of larger stones in the small samples. This demonstrates why large samples are required and even with very large samples there is always a probability that the recovered diamond size distribution may not be representative of the in situ size distribution. This is the reason that models of the relative abundance in each size fraction are often used to predict the diamond size distribution that will be recovered by a full-size production recovery process.

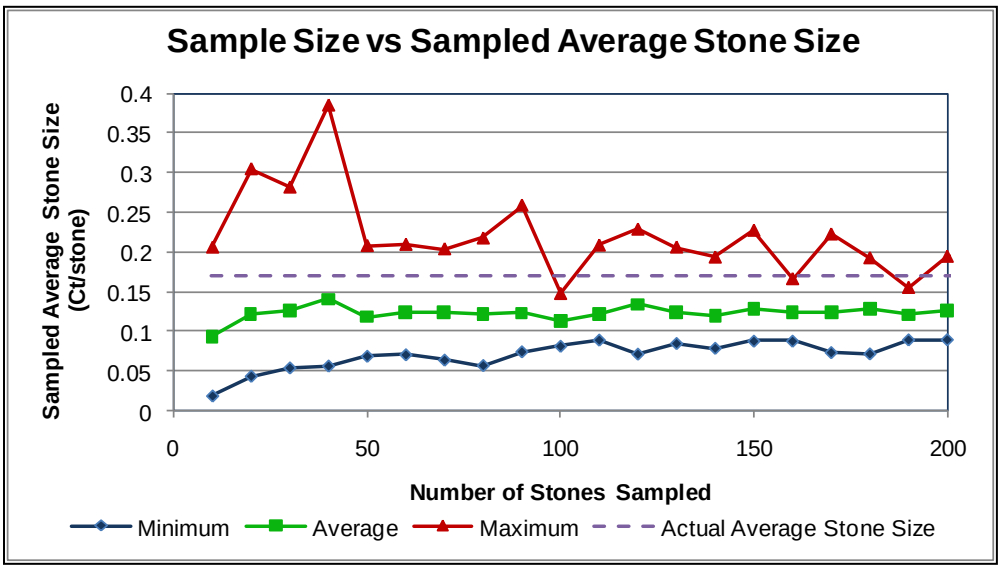

Figure 3: Variation of the average stone size estimated from small samples.

Relationship between diamond size and value

Diamond value is positively correlated with size. This relationship (see Figure 4) can be described using a logarithmic model for a given combination of shape, colour and quality. An accurate model of the in situ $/ct for each diamond size class in the population is required to estimate the in situ $/tonne.

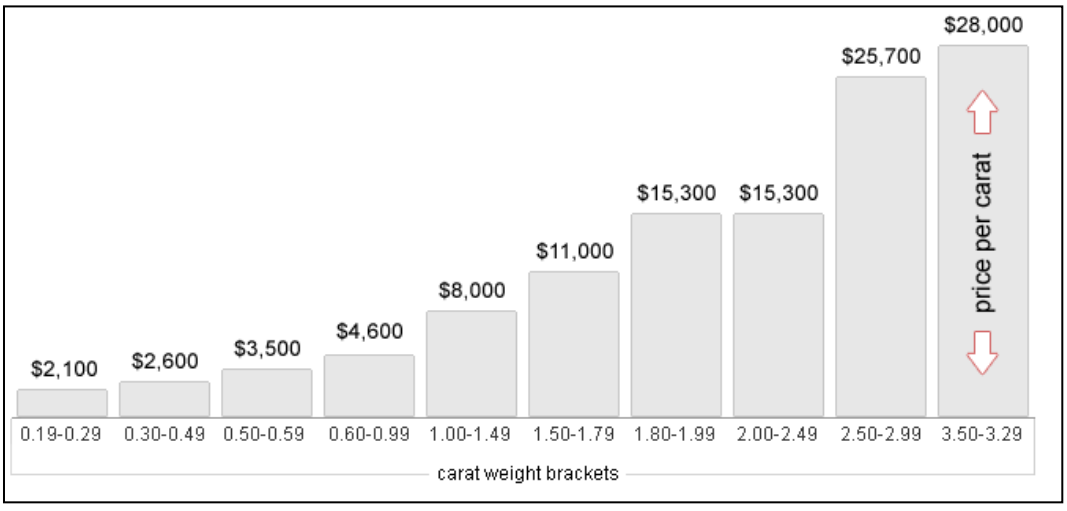

Figure 4: Typical relationship between diamond size and cut diamond retail value (adapted from Rappaport, 2009).

If the parcel in Table 2 was valued using a $/ct per sieve class like that depicted in Figure 4, its 'bench value' would be 140 $/ct. If the same parcel was sampled as

described above using samples containing 100 stones, the change in the sampled size distribution produces samples with bench values between 471 $/ct and 46 $/ct. The under-sampling, and low recovery, of large stones in small samples is a substantial source of uncertainty in the evaluation of kimberlite deposits. Methods that have been developed to address this are discussed further in the literature review section and their impact is described in case study 2.

1.3 Diamond project evaluation practice

Given the cost of diamond sampling and the low probability that a randomly selected kimberlite will have an economic diamond content, initial evaluation activities following discovery are used to limit expenditure to that which is sufficient to generate just enough data to decide whether the deposit is likely to contain diamonds in quantities that will support economic extraction.

The assessment of several geochemical and petrological characteristics of surface and core samples taken from the discovered deposit can be used to indicate the potential for diamond content (Cookenboo & Grutter 2010; Macnae 1995). Should the results indicate that the kimberlite is likely to be diamondiferous several cores are extracted from the deposit and are then dissolved to recover what are termed micro diamonds.

Micro diamonds are diamonds smaller than 0.5 mm in size that are recovered from core through a thermo-chemical dissolution process. Typically, samples of the order of 20 to 50kg are required. The analysis of micro diamond results is used to determine the size frequency relationships that exist in the lithologies within the deposit. This size vs stone frequency relationship is modelled and used to generate an estimate of the diamond potential in the deposit by extrapolating the size and stone frequency relationship from micro diamond sizes into larger diamond sizes. (Rombouts, 1995)

Should the potential diamond content be deemed sufficient for investment purposes then the next phase of evaluation is initiated, and usually aims to establish an estimate of the financial value of the diamonds in the deposit. The financial value of diamonds is influenced by several factors. These factors include diamond size, their quality (for example number of inclusions, flaws), their colour, and their shape. The valuation process starts with the definition of the size frequency of the diamonds. As the number of diamonds acquired increases, the assortment of the diamonds in the deposit begins to be revealed. The assortment refers to the shape, colour and quality of the diamonds in a deposit. To achieve reliable estimates of diamond values typically requires approximately three thousand to five thousand carats for assessment (Rombouts, 1995). Figure 5 based on the sample depicted in Table 2

shows a comparison between the relative proportion of carats and their proportional contribution to value.

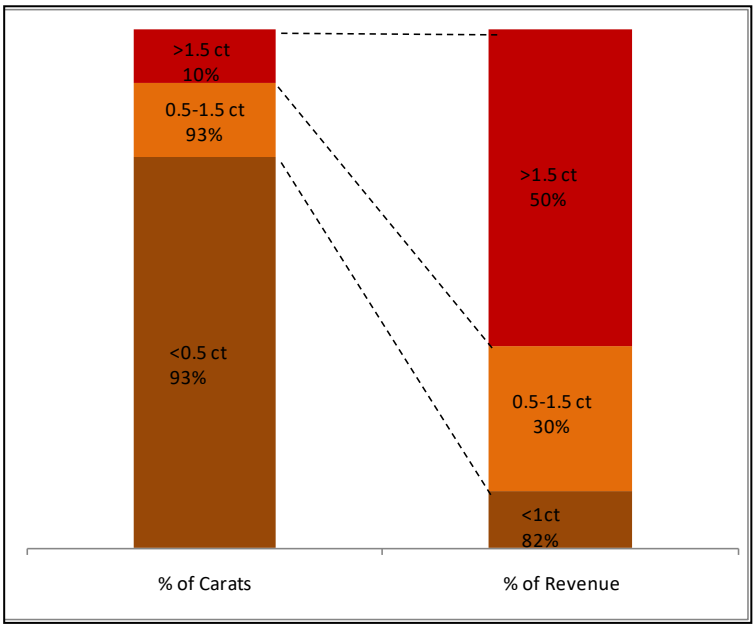

Figure 5: Comparison of the proportion of carats and proportion of revenue represented by different diamond size ranges, for the diamond parcel described in table 2.

To acquire a sufficient number of carats requires samples of the order of 10 to 100 tonnes each. The sample size and the numbers of samples required, however, depend on both the estimated average grade derived from micro diamonds as well as the geological heterogeneity of the deposit.

The assay, or sampling for macro diamonds is a process that requires large samples and produces results that, to some extent, depend on the efficiency of the recovery process. Any change in the efficiency of sample acquisition, sample crushing or density separation process will change the number of diamonds that are recovered from the samples.

Even with the time, cost and logistical complexity associated with the collection and treatment of large samples, it is possible, with sufficient core and large diameter drilling, to estimate the in situ macro diamond grade with reasonable confidence. It has been demonstrated that diamond grades are spatially correlated variables that can be estimated using spatial estimation techniques such as kriging. (Kleingeld, 1996; Rombouts, 1995).

1.4 Use of the metallurgical recovery factor in project evaluation

The metallurgical recovery factor is an expression that is used to convert the estimated in situ grade into an expected recovered grade. At an early stage of the project, the factor is expressed as a proportion of the recovered diamond grade divided by the estimated in situ diamond grade, in either a mass proportion (CPHT) or stone proportion (SPHT). In the absence of detailed spatial data, the recovery factor is derived heuristically (e.g., by comparison to analogous deposits of similar size and composition) and assumed to be a constant that is applied globally across the entire deposit.

As the project matures, and more information on the project is acquired, it becomes possible to improve the methods used to derive the recovery factor and increase the spatial resolution of the recovery factor, both into smaller areas of the deposit and/or to shorter periods of production that are associated with the mining and treatment of specific areas of the deposit. The form of the factor can also be adapted to express the expected recovery per diamond size fraction. The recovery factor does not depend on a single variable tied directly to a regionalised variable, but is the result of the complex interaction of the:

- mining and metallurgical processes used in diamond liberation, separation and recovery;
- mined country rock and kimberlite characteristics; and
- characteristics of the diamonds in the deposit.

These relationships are briefly described in the following sections.

1.5 Impact of recovery process design and operation on metallurgical recovery.

The recovery process aims, as far as is possible, to preserve the in situ diamond size distribution between the predetermined upper and lower size limits of the process. To do this the ore is crushed in stages with several cycles of diamond removal from the crushed products. The process flow sheet can be considered as having three primary objectives;

1 - Comminution of the kimberlite to liberate the diamonds,

2 - Separation of the diamonds from the gangue using density, and

3 - Recovery of the diamonds from the dense concentrate.

To achieve this efficiently several different size streams are generated by screening and each size stream is then subjected to slightly different processes that are tailored to the size distribution that is to be treated.

The selection of design parameters for the treatment of a given kimberlite deposit is based on a combination of deposit scale, assumptions about the kimberlite characteristics and long run performance of the selected unit processes. During the early stages of the project the recoverable diamond size envelope is determined, which defines the top and bottom cut-off size of diamond that will be recovered. As the project progresses several trade-offs studies are undertaken with the aim of optimising the balance between increased recovery and increased capital and operating cost of selected treatment processes.

If the host rock is crushed very finely a larger number of diamonds will be released but there will also be an increased probability of diamond damage and or breakage. The range of recovered diamond size and the sequence of crushing and separation that is used are very important considerations in the design and management of the operation. The configuration of these processes also has a material impact on the proportion and size distribution of diamonds that are liberated, recovered and lost through lock up and damage.

Blasting, which is the first phase of comminution, is a process used to extract the rock and reduce its size for delivery to the recovery plant. This changes the properties of the rocks to some extent and causes some diamond damage. Studies have, however, shown this to be negligible beyond more than five blast hole diameters (Wilmott, 2004).

In-pit and primary crushing usually produce a product with a top size that is in the range of 250 to 125mm. This reduces the feed to a manageable size for entry to the plant. The next stage of comminution reduces the material to a nominal cut size of 32mm usually through a combination of cone and impact crushers.

The material is then washed, and fines removed in preparation for dense media separation. In the Dense Media Separation (DMS) process the diamond particles, having a density of 3.5 g/cm^3, are separated from the particles of kimberlite, most of which have a density of less than that of diamond. Several machines are used to do this, but by far the most common is the hydrocyclone. This unit processes a mixture of water and ferrosilicon (the dense media) into which the crushed ore is mixed. This mixture is pumped into a hydro-cyclone and the dense particles pass to the spigot or underflow whilst the less dense particles migrate to the vortex finder and hence into the overflow.

The tailings from this process may contain diamonds in two forms:

1- Diamonds that have been incorrectly classified due to operational errors

2- Diamonds that have been correctly classified but have floated out of the separation process because the combined density of the particle consisting of diamond and kimberlite is less than the effective cut-point in the dense media separation process.

This stream may be re-crushed to liberate these so-called 'locked' diamonds and to recover any errant 'free' diamonds.

The undersize material and coarse oversize material from the process are usually disposed in so-called 'slimes dams' or 'processed kimberlite dumps.' Due to changing market conditions, and improving technology, over time these dumps may become economic to exploit.

1.6 Impacts of kimberlite properties on treatment process efficiency.

The impact that rock properties have on the process depends on the interaction of the rock properties with the process. This interaction is controlled by the following variables:

- Variables associated with the process design and configuration;
- Variables associated with the process operation,
- Variables associated with gangue that is mined with the kimberlite.

Kimberlites have been described, from a processing point of view, as a relatively soft clay-rich rock, however due to the process of emplacement they may contain differing amounts of several rock types that are mixed into the kimberlite (Boychuk et al. 2012). The process of mixing, and the contents of the resulting mixtures means that kimberlites comprise a wide range of rock types that have numerous and variable physical characteristics.

Impacts of kimberlite properties on comminution

Kimberlite contains clay minerals (montmorillonite, smectite etc.) and, when exposed to moisture, these clays swell and can materially change the strength of the rock that is processed (Boshoff et al., 2006). Moderate clay content reduces the strength of the rock and makes it more amenable to crushing, increasing crusher

throughput and reducing the average size of the particles produced. Excessive clay content can cause the particles to become sticky, cause agglomeration in the crushing chamber and reduce throughput due to clogging of crushers, feed and discharge chutes.

Fine grained fresh or hypabyssal kimberlites exhibit high rock strengths (e.g., Cullinan Mines Hypabyssal kimberlite has been measured to have a uniaxial compressive strength of 150Mpa). At this hardness, the energy required to crush this material can exceed the installed power of the comminution circuit. This can lead either to a reduction in the overall grind of the material or, for a given grind, require a reduction in the plant throughput.

Hardness variability can be difficult to deal with as the mass balance in the comminution circuit can vary to an extent where one part of the circuit is overloaded, which reduces overall throughput. Although this can be dealt with by increasing stockpile sizes, this is not always a feasible option, and during overload periods these reduced throughputs may not be detected if they are of short duration.

Impact of kimberlite properties on separation

The primary variable that controls separation is the apparent density distribution of the rock for a given rock size distribution. Species denser than the effective cut-point will sink along with the diamonds and species that are less dense will float and either be discarded or re-crushed to release more diamonds. To measure the proportion of material that is above the density cut point for a given lithology the samples are crushed to a nominal size. These are then put through a sequence of density separations in a static bath containing fluids of differing density. This distribution of density is used to predict the mass flows across the process. It also predicts the number of diamonds that are expected to be recovered from re-crushing the floats from the first pass DMS process. Depending on the mineralogy of the kimberlite there may be sizes of clasts that, when liberated, make a substantial difference to the density distribution. An example of this is the modal sizes of garnets that are dense and report to recovery.

Clay and fines content of the kimberlite may compromise the DMS operation by causing turbulence in the cyclone. Surges of high density or incorrectly sized material may cause overloading of the cyclone and reduce the rate of settling in the cyclone. Flat particles generated from brittle rock types also hinder the efficiency of the separation process. (Plitt, 1976)

Impact of kimberlite properties on final recovery processes

Final recovery processes use several diamond properties to reduce the mass of the concentrate from the DMS and upgrade the final product that is dispatched from the mine to diamond trading companies. The most common of these processes is the use of x-ray fluorescence to separate the diamonds from the concentrate. Kimberlite can, however, contain several minerals that fluoresce in a similar way, which can compromise recovery efficiency. Magnetic separation is also used to reduce the magnetite and other magnetic and paramagnetic particles from the recovered concentrates. One of the final processes used on mine sites is hand sorting where trained pickers are used to separate gangue from a rich diamond concentrate. Prior to valuation recovered diamonds are washed in various acids to remove any coatings that may impair downstream diamond grading and classification.

1.7 Impact of diamond properties on the recovery factor

The nature of diamonds makes them amenable to what is a relatively simplistic physical recovery process. The main challenge in the process is to liberate and recover as many diamonds as possible and yet preserve their size and quality distribution to maximise the revenue derived from the recovered diamonds. The effectiveness of the process in achieving this aim will determine what proportion of the total population of in situ diamonds will be recovered. A variety of recovery factors can be used to describe the relationship between the in situ diamond characteristics and the characteristics of the recovered diamonds.

The shape of the size distribution of diamonds will display some variation between deposits but can in most cases be modelled with a log-normal distribution. (Kleingeld et al, 1996). The crushing and screening process are normally designed to recover a portion of this size distribution that yields the highest proportion of the revenue. The diamonds above the top cut-size are crushed, and those below the bottom cut-off size are discarded as tailings. Premier Mine has one of the largest top cut-sizes at 65mm, more commonly however this is set to 25 to 32mm. As most of the screening is carried out on screens with square or rectangular openings, there is always some degree of misclassification. This misclassification impacts on both the mass flow of material and the shape of the recovered diamond distribution.

The selection of these cut sizes for a given mine is based on the average size distribution across the deposit. This is integrated with the revenue distribution to arrive at an expected $/tonne that will be recovered. This value, less the cost of treating the material, will determine the contribution that will be derived from each tonne of ore. This value is used to design the ultimate pit, the sequence and schedule

for mining. This highlights how the estimation of the metallurgical recovery factor impacts on strategic decisions in mine design and evaluation.

Diamonds are formed in the deep mantle, and during the emplacement process may be subjected to several cycles of heating, cooling and mechanical stresses. This may build up to a point where the diamonds become stressed and will be damaged in the comminution process. Little quantitative work has been undertaken to estimate the proportion of diamonds that are exceptionally stressed in situ, although as the diamond cutting and polishing industry has shown, stresses in recovered diamonds can impact on the yield that can be obtained when cutting and polishing the stones (Rombouts, 1995).

Several shape and size distribution classification systems have been developed for diamond populations (Caers and Rombouts, 1996). Their cubic crystal form is a face-centred cubic lattice but there are many crystal habits to which diamonds conform. The shape distribution has an impact on the way in which diamonds liberate from kimberlite, the way in which they settle in the DMS process and the trajectories exhibited in both magnetic and X-Ray processes. Surface features also impact on the way in which diamonds liberate. Incompletely liberated diamonds, sometimes referred to as 'comets', may float out of the dense media separation process as the adhering kimberlite is less dense than the diamond so that the aggregate particle density is less than that of the dense medium. These composite particles may also be lost in the X-ray recovery section as the kimberlite may shield the diamond from the incident X-rays and prevent the diamond from luminescing sufficiently to be detected. The fine ferrosilicon media used in the DMS may adhere or enter cracks in the diamonds, and as this media is magnetic, diamonds contaminated in this way will be lost in magnetic separation units that are used in final diamond recovery plants.

Although the colour distribution of diamonds, caused by several impurities, does not always impact on the diamonds X-ray induced fluorescence, the presence of impurities in the diamond may give rise to fluorescence characteristics that impair the effectiveness of X-ray recovery machines. The fluorescence characteristics that impair recovery include the total brightness that the stone will achieve (total luminescence), the time to achieve this brightness (rise time), and the duration of residual luminescence.

1.8 The sources of uncertainty in estimating the recovery factor

Kimberlites contain heterogeneous mixtures of rocks. When mined, the properties of the daily feed to the treatment plant will vary substantially as the feed will contain a mixture of rocks from different locations. It would be costly and very time

consuming to generate the number of samples that would be required to be representative of the full range of kimberlite characteristics within each lithology or facies. The response of the process to each individual rock type may also be different to the process response to a mixture of rock types. One approach used to overcome these limitations is to make up composite samples of kimberlite material sourced from separate lithologies and mixed in predetermined proportions. The proportions are based on the expected mixtures that will arise during mining operations. Results from tests carried out on these mixtures, or composite samples, are used to design the process and estimate the process capability (Lewis, 2001; Ashley and Callow, 2000). The assumptions implicit in this approach include:

- variations in rock properties are stable within a geological domain;
- a representative sample of all the rock and mineral combinations can be acquired;
- samples can be composited in such a way as to represent worst, best and average scenarios;
- response of composites at sample scale can be equated to responses of full-scale operation;
- there is complete knowledge of the proportion and the range of mineralisation;
- blending achieved during sampling will closely mimic that of mining; and
- historically derived scale-up factors can be used to scale-up the results of tests to estimate process response of a full-size unit process.

The approach does not deal explicitly with expected variation of the recovery factor. It can be demonstrated that there is a squared relationship between the uncertainty in the estimate of the recovery factor and the uncertainty in the recoverable grade. (Lantuéjoul, 1990). Hence, if the uncertainty in the recovery factor is halved, uncertainty in the recoverable grade will be quartered. Under-estimation of the magnitude of the uncertainty in recovery can prevent projects from reaching their full potential and, in extreme cases, lead to cessation of operations shortly after starting up. Conversely, by improving the protocols and methodology to estimate this factor and reduce the uncertainty, it is possible to increase substantially the value that can be attributed to reserves. (Benicelli et al, 2000)

Acquiring data of rock characteristics with enough spatial coverage and support to generate unbiased estimates is problematic. Even if sufficient data are obtained from a high number of samples with large supports to generate unbiased rock property estimates, the use of these estimates to predict process response at production scale requires adaption of existing methods of modelling process performance. One approach to address scale-up explicitly, termed ‘Comminution Economic Evaluation Tool’ (CEET) developed by MinnoveEX, now owned by SGS, is

a system developed for short-term optimisation. CEET addresses the scale-up issue by adapting the parameters of the prediction model so that the outputs of the model match actual production outputs (Ameluxen et al., 2001). This approach provides a good way to modify the inputs into the model by conditioning the models with data once the plant and mine are running, but it is not suitable for prospective operations, and has limited forecasting power.

Current practice in De Beers makes use of a combination of core samples and bulk sampling. This includes the measurement and testing of a range of rock characteristics, as described in the literature review. Diamond liberation and lock-up is predicted based on a combination of rock size reduction measured during bulk sampling and process models based on average kimberlite characteristics. This approach has several shortcomings including:

- sample selection is based on geological domains that have been derived from grade continuity and not necessarily processing characteristics;
- samples are consumed during testwork and hence usually must be drilled specifically for estimating a single ore property ('it's not possible to break the same rock twice');
- test methodologies aim to ensure that the parameters of the process are kept within strict tolerances and, therefore, do not capture the impact that the material being tested has on the characteristics of the process;
- as kimberlite contains clays that rapidly alter the physical characteristics of the rock if it is exposed to moisture, some test results may be compromised by sample degradation. In addition, if there is a variable time between blasting and treating, the measured laboratory response will not be a valid input for predicting the operational process response;
- using small-scale tests based on composite samples is problematic. Measured results from mixtures are only applicable to the specific mixture that is tested. If the proportions are changed the results may vary in a non- linear fashion. Resulting data cannot be used to model relationships between primary rock characteristics and specific process responses for individual lithologies. It is often possible mathematically to mix results from tests on specific rock types, but invariably impossible to un-mix results derived from composite sample treatment;
- timing of data - bulk samples are often only taken at the feasibility stage and hence pilot plant process information is not available at early stages in new projects requiring the recovery factor to be made

on data derived from core samples that have been used to model and predict the in situ diamond distribution.

1.9 Research model

Although work has been done to improve the methods used for sampling, ranging from drilling techniques to improved laboratory practices, the underlying problem of integrating the data acquired from sampling and estimation of rock properties with the process design over the life of the mine has not yet been addressed.

Against the discussed background information, the research led to a methodology for recovery factor estimation that utilises an integrated value chain of the operation as shown schematically in Figure 6.

A sampling strategy that collects and integrates both destructive and non-destructive data from core sampling was designed and executed. The data from this sampling experiment are used to estimate and simulate the physical rock characteristics into an orebody model.

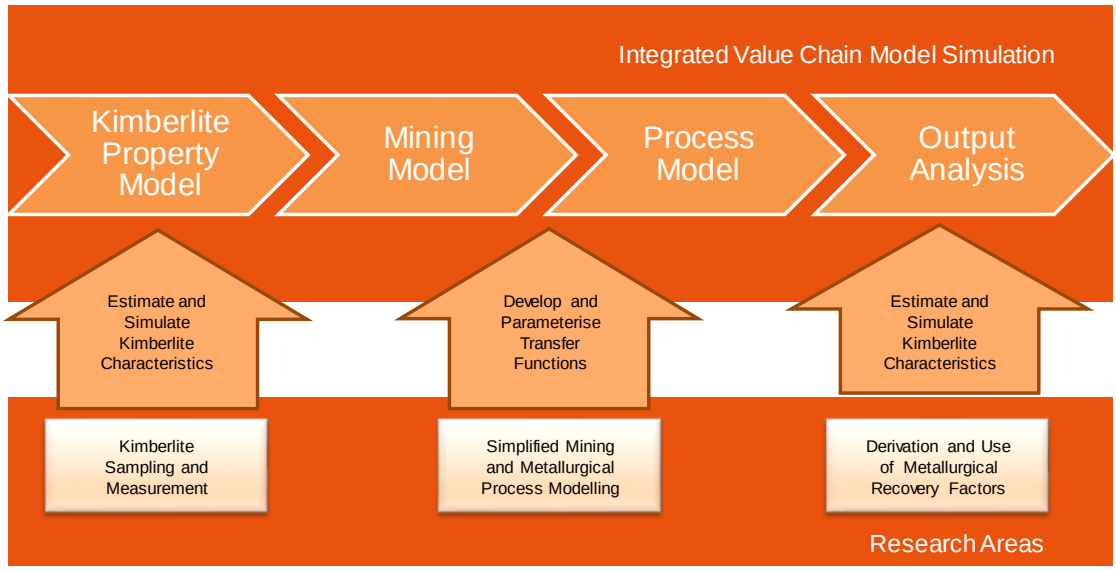

Figure 6: A schematic representation of the research areas covered in this thesis.

This orebody model is depleted and treated using simulated mining and metallurgical processes to evaluate the impact that the spatially varying rock properties have on the treatment plant processes. A quantitative diamond recovery model that responds to the rock characteristic variability and includes uncertainty was developed. The process model is used to simulate the operation and produces data that can be used to estimate both the expected diamond recovery and the

uncertainty in metallurgical recovery for different periods of the mine's operation, at different scales of resolution.

The relationship between the sources of the variances in the integrated model can be formulated as in Equation 2:

$$\sigma_{rf}^2 = F(\sigma_r^2)G(\sigma_p^2)H(Cov.\sigma_r^2\sigma_p^2) \qquad \text{Equation } \mathbf{2}$$

Where:

σ_{rf}^2 : Variance of the recovery factor

σ_r^2 : Variance of the rock properties

σ_p^2 : Variance of the recovery process efficiency

$(Cov.\sigma_r^2\sigma_p^2)$: Covariance between the rock and process properties

F, *G*, *H* are functions that are derived from either sampling and modelling or observed relationships between the rock characteristics and the specific process that is being considered. They must be calibrated for each specific facies of the kimberlite bodies, and to the specific unit processes.

The building of the integrated value chain model required the following objectives to be met:

- Development of an understanding of the relationships between geological descriptions of kimberlite characteristics (e.g., texture, grain size) and sampling instrument responses and destructive test responses;
- Review of several non-destructive geophysical measuring techniques that could potentially augment the destructive data that are collected;
- Model the relationship between measured (or estimated) rock characteristics and processes of comminution, separation and recovery;
- Develop or apply an appropriate methodology to create a spatial representation of rock properties,
- Develop or apply a methodology to simulate the mining and metallurgical processes that will respond appropriately to the estimated and simulated rock characteristics; and

- Develop an integrated model of the mine operation to quantify the impact of the spatial and temporal correlations of rock characteristics on the metallurgical recovery factor.

1.10 Thesis structure

The literature review (Chapter 2) that follows addresses the nature of the kimberlite, sampling theory, and sampling methods developed in this research to augment limited destructive data with geophysical data. Spatial estimation and simulation techniques used to generate models of the physical characteristics of the orebodies being mined is followed by a review of mining and metallurgical process simulation techniques. The literature review concludes with a statement of the research problem (Chapter 3).

The first area of investigative research (Chapter 4) covers data acquisition and describes the design and execution of a rock property sampling experiment that was conducted to generate data required for this research project.

The data gathered are used to explore techniques for using non-destructive data to augment the costly destructive data and estimate spatial kimberlite rock characteristics. (Chapters 5)

A second area of research (Chapter 6) compares several methods of adapting traditional mineral process models so that they can be used with spatial orebody models to derive the metallurgical recovery factor and assess the impact of incorporating stochastic uncertainty in process models.

The integrated model has been developed and applied to several projects during this research process. Two case studies are presented to demonstrate the implications of model outcomes on real diamond projects (Chapters 7 and 8).

A brief discussion follows to describe how the outcomes of this research can be applied in an industrial framework (Chapter 9). The thesis concludes in Chapter 9 with several recommendations for further research.

The research was conducted in the context of this background to improve the estimation of rock and diamond characteristics, model the complex interaction of these with the recovery processes, and predict process responses at the scale of diamond operations. The findings of this research provide an important milestone in the development of methods to improve the derivation and use of the metallurgical recovery factor. This will result in improved evaluation, design and operation of diamond mining projects.

2 LITERATURE REVIEW

To understand the magnitude of the challenges faced in deriving metallurgical recovery factors, current methods of sampling, measuring and spatially estimating rock characteristics in kimberlite diamond deposits are investigated. The limitations and constraints in using this data in models of the diamond extraction process are described. The aim is to identify clearly how it might be possible to improve the derivation and use of metallurgical recovery factors by integrating spatial models of rock characteristics with metallurgical simulation models.

The review begins with the description of the current understanding of kimberlite emplacement processes and the consequent composition of kimberlitic diamond deposits that these give rise to. It is shown that kimberlites exhibit a wide range of rock characteristics and that this heterogeneity must be considered when sampling for, and estimating, the characteristics required to derive metallurgical recovery factors.

The current state of the art in sample acquisition, sample measurement tools, quality assurance and control techniques reviewed. Non-linear relationships between primary rock characteristics and process response variables are explored, as is the impact that so-called "non-additivity" has on spatial estimation, and up-scaling (from laboratory test to block-scale response predictions) of the estimated or predicted variables. If incorrectly addressed, this important aspect of recovery factor estimation can lead to significant undetectable bias in estimates. Using the correct samples, measurement tools and sampling strategies can assist by determining the nature of these relationships that can then be accounted for in the subsequent estimation or simulation of the spatial characteristics of interest.

A description of mathematical modelling of mineral processing practices is provided with explicit focus on comminution and dense media separation (DMS) processes. Their use in recovery evaluation and limitations, both technically and conceptually are discussed. The aim is to identify ways in which models of these two processes, which play an important role in diamond recovery, can be used in a value chain model that explicitly connects, at a block scale, with estimated and simulated orebody models.

The review demonstrates that current practical approaches used to propagate rock characteristic variability through the mining value chain have been hampered by

both availability of suitable software tools and limited processing capacity. This review describes the evolution of optimisation models used in mining projects. It demonstrates how a single optimised solution may not result in robust project design if there is any orebody or processing uncertainty. The review concludes with a description of a conceptual framework for an Integrated Evaluation Model. This model aims to provide more robust estimates of the metallurgical recovery factor using an integrated mining project value chain simulation.

The benefits of this approach are described as are the philosophical and practical challenges presented by adopting a systems approach to a complex stochastic problem.

2.1 Physical characteristics of kimberlites and diamonds

Kimberlites are pipe-like bodies that carry diamonds, formed deep in the earth's mantle, to the surface of the earth's crust (Field, Stiefenhofer et al., 2008).

The objective of reviewing the literature on kimberlites is to gain an understanding of the range of physical properties that this rock type exhibits and to understand the implications of these on sampling, property measurement, estimation and process modelling and simulation.

The research is focussed on one mineral in one geological setting. However, when considered in the spectrum of rocks, kimberlite is an extreme end-member. There are numerous processes that give rise to these bodies both during and after emplacement. Not only do kimberlites exhibit a diverse range of geometries, the post emplacement processes, such as weathering and alteration, add further complication to the rock and mineral assemblage. This makes the design and implementation of sampling campaigns capable of achieving representative results particularly challenging.

Important aspects of kimberlite geology that impact on the sampling measurement and estimation of the physical characteristics of the rocks to be mined and treated include:

- The origins of Kimberlite bodies and the nature of diamond mineralisation.
- Clear definition of the rock property measurement problem by describing the range of rock types that need to be considered and implications for rock property measurement.
- An investigation of the range and variation of physical properties within a given geological domain and between domains. This leads into a discussion on the implications for defining zones within which estimates are to be made.

- Identification of the factors that govern rock strength and how these are dealt with in other rock types. This includes measurements of rock texture, fracture frequency and measures of weathering and alteration in similar rock types.
- A comparison and contrast of geological classification systems, their objectives and the implications this has for both sampling for rock property and estimating rock properties at a larger scale.
- Understanding the implications of the great differences in the scale of measurement and the scale of estimation. This includes an assessment of the challenges that these large differences present for change of support modelling especially when the models must deal with non-additive, highly skewed data.
- The scale on which this research requires estimates of rock characteristics and the implication for mineral processing and diamond recovery modelling and simulation.
- Identifying and modelling relationships between qualitative and quantitative measurements of rock characteristics

An overview of kimberlite geology

Kimberlites are the host rock of numerous diamond deposits. They are a suite of rocks that show great diversity in morphology, composition and hence mechanical properties. They usually form pipe-shaped deposits of volcanogenic origin that are mixed with country rock fragments and exhibit variable degrees of alteration. The differences in kimberlite composition between pipes and even within the same pipe can be substantial, these differences are exhibited from microscopic to macroscopic deposit scale. Due to the economic significance of these deposits, classification and nomenclature used to describe them continues to receive considerable attention. Kimberlites were formally named after their type location, "Kimberley", in 1887 by Henry Carvill Lewis at a meeting of the British Association for the Advancement of Science in Manchester. He described them as “porphyritic mica-bearing peridotite and suggested that they be recognised as a type of volcanic breccia.” (Lewis referenced in (Mitchell, 1996)

The concept of petrologic clans was introduced by Reginald Daly in 1914 (Mitchell, 1996) and is predicated on the assumption that it is possible to classify rock types into several suites by interpreting the composition of the magmas that led to the rock formation. To a large degree, the original descriptive schemes have been adapted by several authors. These include Skinner and Clement (1979) who developed a system based on the modal mineralogy of the groundmass, based on the belief that the ubiquitous presence of olivine was insufficient grounds for classification. Since then several schemes have been proposed and these are reviewed in more detail in this section.

The challenges faced by any generic description system include the requirement to describe the following characteristics across a diverse range of scales and emplacement settings:

- location, extent and geometry of the deposit;
- the geometry and location of the contained lithologies and smaller scale structures, such as faults and fractures;
- content of the rock (elemental, mineral composition and rock types);
- genesis and spatial relationships; and
- alteration since emplacement.

Kimberlite occurrences, distribution and architecture

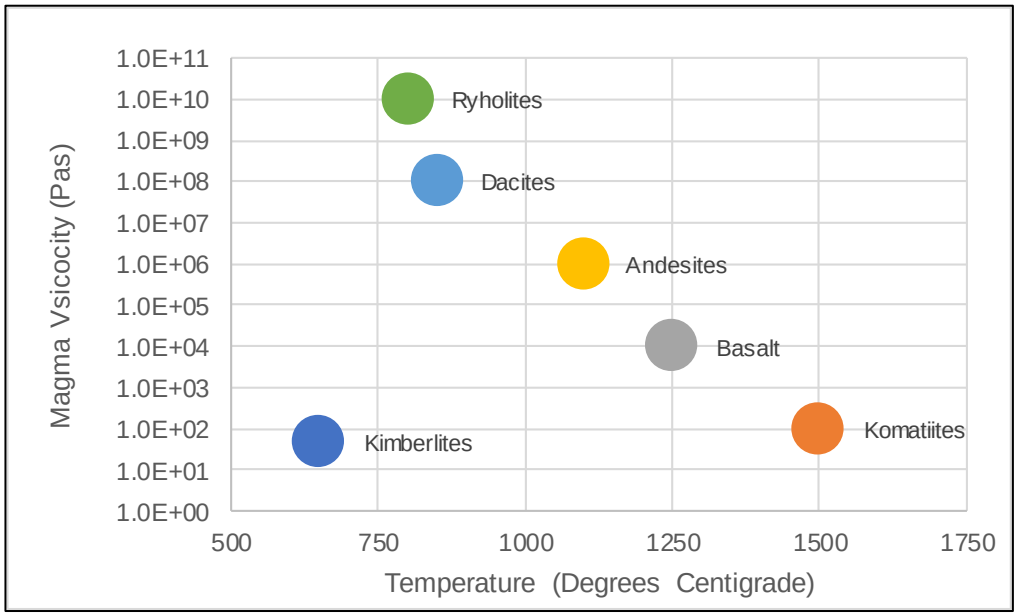

Figure 7: Melt viscosity as a function of temperature at 1 bar for natural melts spanning the compositional range Rhyolite to komatiite. All compositions are volatile free. The temperature range is illustrative of typical eruption temperatures for each composition – adapted from (Sperra, 2000) and (Sparks et al., 2009).

In the range of styles of volcanism, kimberlites can be viewed as an end member (see Figure 7). They form at low temperatures from ultra-basic, low viscosity magmas that range in age from early Proterozoic to early tertiary. This low viscosity and low temperature of emplacement has consequences for the expected pipe geometry and the geometry of internal contacts in these deposits. They are very commonly preserved as downward tapering pipes and craters that have been infilled with clastogenic mixtures of kimberlite and country rock clasts (Sparks et al., 2005).

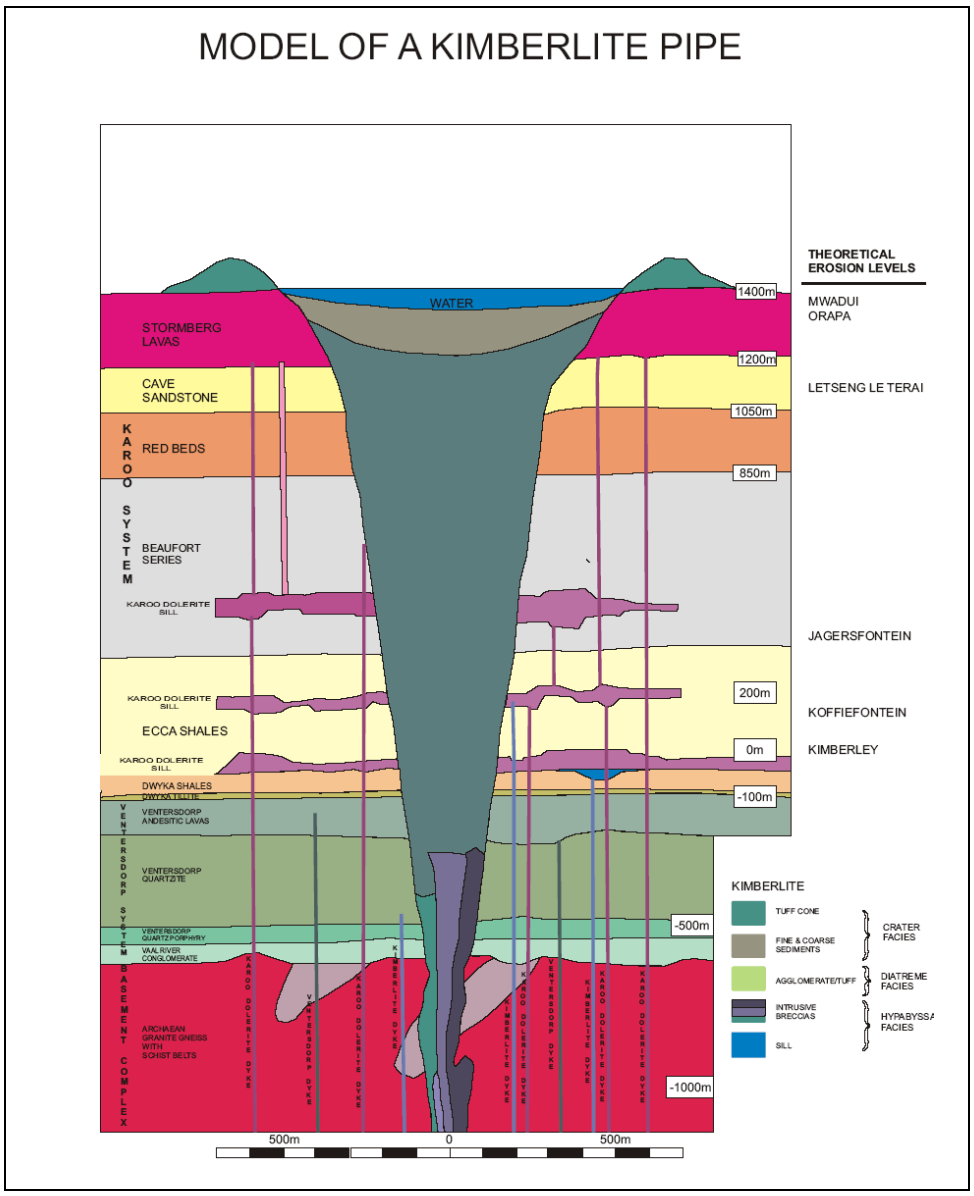

Figure 8: A schematic view of a kimberlite pipe after Hawthorne (1975).

The shape and size of the deposit is related to the nature of the rocks into which the pipes have intruded. A schematic cross section of a typical kimberlite pipe geometry is presented in Figure 8. At least three types of kimberlite pipes have been identified:

- Deep (up to 2 km), steep-sided pipes which comprise three distinctive zones (crater, diatreme, root)
- Shallow pipes (<500m) which comprise only a crater zone and are in-filled exclusively with volcaniclastic kimberlite, mainly pyroclastic material, and;
- Small (<600-700m deep), steep-sided pipes filled predominantly with re-sedimented material and less common pyroclastic kimberlite or, in a few instances, with hypabyssal kimberlite (Field and Smith, 1999).

Even though most of the deposits seen today have been eroded to an extent where the products of the emplacement volcanism are not present, some of these products,

such as fine ash and pyroclastic surge deposits, can be found within the body of the pipes.

Kimberlites also occur as sills and dykes, and similar kimberlite pipes can contain highly variable grades (e.g. Marsfontein, South Africa). However, even if one only considers the pipe-like bodies, the range of rock types that can be identified is substantial. A breakdown of the proportional contents that might be found in a kimberlite deposit is shown in Figure 9.

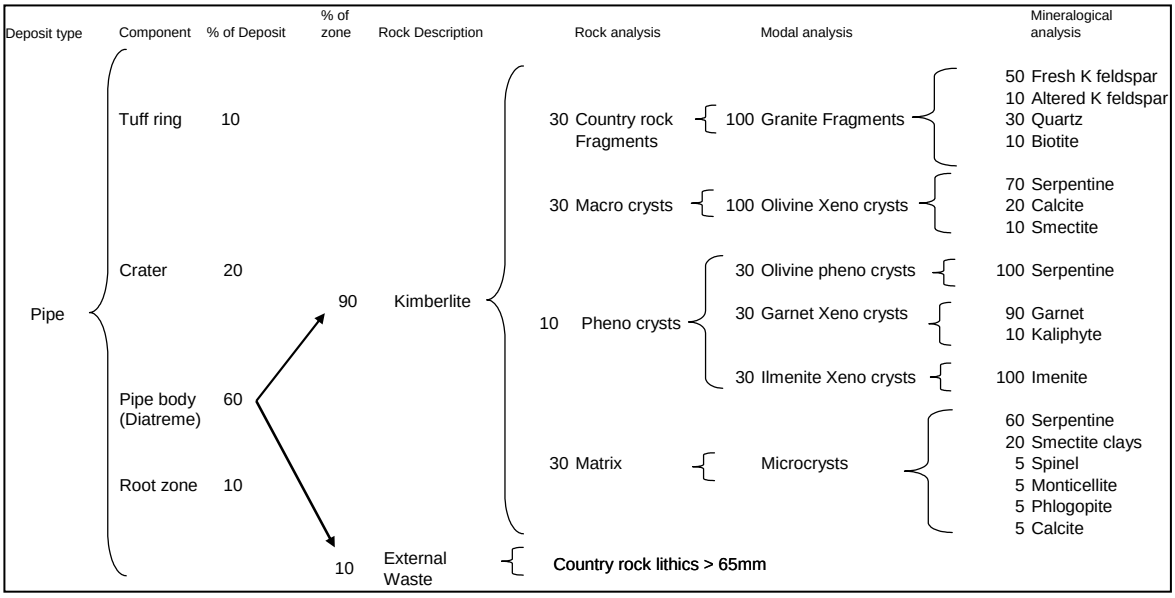

Figure 9: A schematic representation of the materials that could be found in a 'typical' kimberlite pipe, adapted after (Field and Smith, 1999).

Work by Sparks (2006) on several of the southern African pipes, has suggested that the rock types in the diatreme could be classified as four basic types:

- Massive volcaniclastic kimberlite (MVK)
- Layered volcaniclastic kimberlite (LVK)
- Marginal wall rock breccias (MWRB)
- Hypabyssal kimberlite (HK)

The massive volcaniclastic kimberlite (MVK), and layered volcaniclastic kimberlite (LVK) can be considered as having similar components. The primary components of this type of rock are listed in Table 3.

The kimberlite minerals are dominated by various forms of olivine (phenocrysts, macro-crysts and xenocrysts). A distinction can however be made between group one and group two kimberlites, with group one kimberlites containing olivine micro

phenocrysts (groundmass perovskite, spinel, and monticellite or calcite) and group two kimberlites, which have phlogopite as a major mineral.

Component	Examples
Juvenile components derived from the magma	Lapilli, phenocrysts and groundmass minerals
Minerals, xenocrysts	Xenocrysts related to the breakup of mantle nodules or basement crystalline rocks
A mega-cryst suite	Crysts including olivine ilmenite and garnet
Xenoliths of deep origin	Peridotite and eclogite
Country rock accidental lithics	Can be correlated with the geology of the basement and host country rock

Table 3: A description of the components of volcaniclastic kimberlites.

Layered volcaniclastic rocks can be distinguished from the massive type by visual inspection of the large-scale rock fabric. There are many sub-facies in this category reflecting the wide variety of scales and kinds of layering. Within these layers the gradation of size, nature of clasts, and degree of sorting varies widely. These textures are best preserved in kimberlites where the crater facies are preserved but are also evident in deep parts of narrow pipes. Some of these varieties can be ascribed to primary pyroclastic processes and some to redistribution of primary constituents from reworking by normal sedimentary agents such as water, wind and gravity. Terms such as pyroclastic or re-sedimented kimberlite may then become applicable if the origin is not in doubt (Sparks, 2006).

Marginal wall rock breccias are the third prominent rock type. They range from breccias composed entirely of wall rock to breccias with variable amounts of kimberlite matrix of the MVK type. The latter vary from net veining of in situ wall rock to clast-supported breccias to matrix-supported varieties.

The fourth type, hypabyssal kimberlites (HK), are those that have not been involved in an eruptive process, and hence appear to be uniform in texture and coherent (Skinner and Marsh, 2003). The country rock lithic clasts are usually strongly altered due to the reaction between the fresh kimberlite magma and the rock into which it intrudes. These rocks can be found in all parts of the pipe and are characterised by abundant macro crysts and groundmass containing typical kimberlitic minerals (E.g. monticellite, spinel, perovskite, calcite, and serpentine).

Understanding the makeup of each of these types of rocks is important both from a sampling perspective, and to understand relationships between rock type and physical properties.

2.2 Rock property sampling and characteristic measurements

Estimates of the physical characteristics of rocks within a kimberlite pipe are often based on samples of the rock that are many orders of magnitude smaller than the pipe itself. There are several processes used to obtain samples of the kimberlite, including coring, chip sampling and bulk samples acquired from trenches or shafts. The perceived cost of sample acquisition, especially in the case of early in the life of projects where capital is rationed, is one of the main constraints on sample size, sample count and the spatial distribution of samples within the kimberlite body. These constrains often compromise or limit the representativity of the samples acquired. Technical challenges of acquiring the rock mass required for testing have also been documented (Hoek, 1997). The challenge is proportional to the variability and scale of the orebody, and because kimberlite orebodies are complex, proportional and representative sampling is challenging.

The objective of taking samples is to measure a portion of the total population and acquire data that can be used to generate unbiased estimates of identified characteristics of values at un-sampled locations. Sampling optimisation is the process of identifying the set of tools and processes that will enable one to estimate with least bias, imprecision, uncertainty and at lowest cost, the values, and properties at un-sampled locations. This suggests that any value-optimising business will try to balance the cost of sampling with the value of the information obtained. The difficulty has always been to value the potential additional information that will be acquired by the sampling before the sampling takes place. Sampling technologies and practices reviewed are focused on the method of sampling and measuring the characteristics of the in situ kimberlite that impact on process performance in such a way as to facilitate the spatial estimation of the characteristics that have been measured on the samples.

Metallurgical test work, as described by Lewis (2001), requires representative samples from each defined lithology, or geological zone, which are prepared and put through a laboratory scale test that resembles some aspects of operational scale processes. The aim of these tests is to measure the rock's response to the applied process (such as the bond work index (Bond, 1943)). The data acquire in this way requires upscaling to predict operational scale performance. The scaling factor, or factors, is commonly derived from experience of historical scale up that has been required for other rock types or mine locations. The aim of this research was to develop techniques to measure and/or sample the primary properties of the rock, and its constituents, to be able to predict the relationship between the primary rock properties and the expected process responses.

This research has found, for kimberlites, that it is possible to sample the primary properties of the rock, estimate and simulate these at block scale and then to use these estimates to predict the operational scale process response.

Geostatistical techniques, such as ordinary kriging, can be used to generate estimates for variables at unsampled locations (Armstrong, 1998). It is imperative that sources of variation or error in the sampling as well as any bias is minimised. Lower error in the input data would imply that the spatial models built on this data would also have lower error. It is also possible to improve spatially estimated models with integrated data acquired from different measurement techniques and/or tools (Dowd, 1997).

It is important to understand and quantify the impacts that the nature of the variable measured has on selection and execution of geostatistical estimation methods. The 'strange' behaviour of several response variables suggest that it is important to validate assumptions that underpin the geostatistical estimation or simulation method used. This includes, for instance being able to validate the relationship between change of support and variable additivity (Carrasco et Al., 2008).The implications here are that the design of sampling and testing programs for physical rock characteristics should include collection of information that will allow the testing of assumptions that are important to identify and select a validate the estimation method. This is expanded on in section 2.3.

This research presents an experiment in which a combination of physical tests were carried out with a description of each sample's morphology, mineralogical content and a number of non-destructive geophysical measurements. This sampling framework has provided a data set that can be used to explore the some of the challenges associated with the measurement and estimation/simulation of these variables. Many of the rock characteristic variables required in the value chain simulation exhibit characteristics that may hinder the generation of valid block scale spatial models. These include:

- **Scale** - the scale of the sample and the scale of the estimate may be very different. Although the sample data are considered to be "Point" values they are in reality some statistic (e.g. an average) of a phenomenon collected or measured over some support. This support (the size shape and orientation of the sample) and the way the test integrates the measure over the support will influence the characteristics of the data produced (means and variances). When making predictions, either at sample support scale or far larger scales the combination of support attributes of the sample and estimated volume needs to be carefully considered. Change of support calculations require a model of the relationships between distributions at

different supports. Deriving these models for complex distributions, non-additive variables and variables that are ratios can be problematic;

- **Additivity** - if the variables are not additive then linear weighted combinations of sample values will not produce unbiased estimates,
- **Skew distributions** - If the distribution of a variable has a high coefficient of variation, is dispersed, and is skewed it is likely that a large number of samples will be required to characterise the variable. Also, for this type of distribution not only will the variance reduce as we take more and or larger samples, but the mean of the sampled variable will shift. This has consequences for change of support calculations;
- **Non-linear relationships** - If the relationship between the rock characteristics and the measured response is non-linear, averages of the responses will produce biased estimates. in some cases if the range of variables is small the bias resulting from non-linearity may not have a material effect;
- **Short Ranges** - if the variable at a given support has a short range, close spaced sampling will be required. If this is not possible then the spatial structure of covariance will not be able to be modelled, and will mean that limited spatial estimation methods can be considered with resulting low confidence in the spatial model; and
- **Large Scale Phenomena** - is certain cases the specified sample support for a test may not be able to capture a phenomena that operates at a larger scale e.g.., trying to measure the abundance of large clasts in a rock type where the sample dimensions are close to the size of the large clast, or 2m fractures in 1m rocks.

These challenges reinforce the notion that where possible the preferred approach is to spatially estimate or simulate so-called "Primary" additive variables wherever possible (Coward, 2008). Many rock "response" variables are not additive, this suggests that the variability and scale relationships are not simple, and hence their spatial estimation and simulation will require rigorous demonstration that these variables do indeed meet with the requisite assumptions of the estimation and simulation techniques used.

Implications of the Theory of Sampling

The development of the Theory of Sampling (TOS) in a mineral context is attributed to Pierre Gy, whose first paper on the subject was published in 1950. Although most of the test work presented here was carried out on in situ materials that are not necessarily 'broken ore,' the concept of discrete materials relates clearly to scale. "All matter is, at an atomic level, discrete and continuity is in essence a mathematical concept" (Gy,2004). This is of critical importance when making measurements of rock properties on kimberlite cores which may only be

representative of one of the many components that make up kimberlite (e.g., a country rock clast that contains no kimberlite matrix material) rather than of the 'mixture' of components that will drive recovery. In extreme cases, it is easy to identify flaws in sampling protocols, but it becomes more difficult when the heterogeneous nature of kimberlite creates subtle biases and errors.

A taxonomy of sources of error is central to the concepts that underpin the theory of sampling. These are then used to determine a way to relate the mass of the sample to the expected error in the estimate. The Discrete Selection Model formalised and published in 1975 has recently been updated (Gy, 2004) and the relationship between sources of error can now be depicted as in Figure 10.

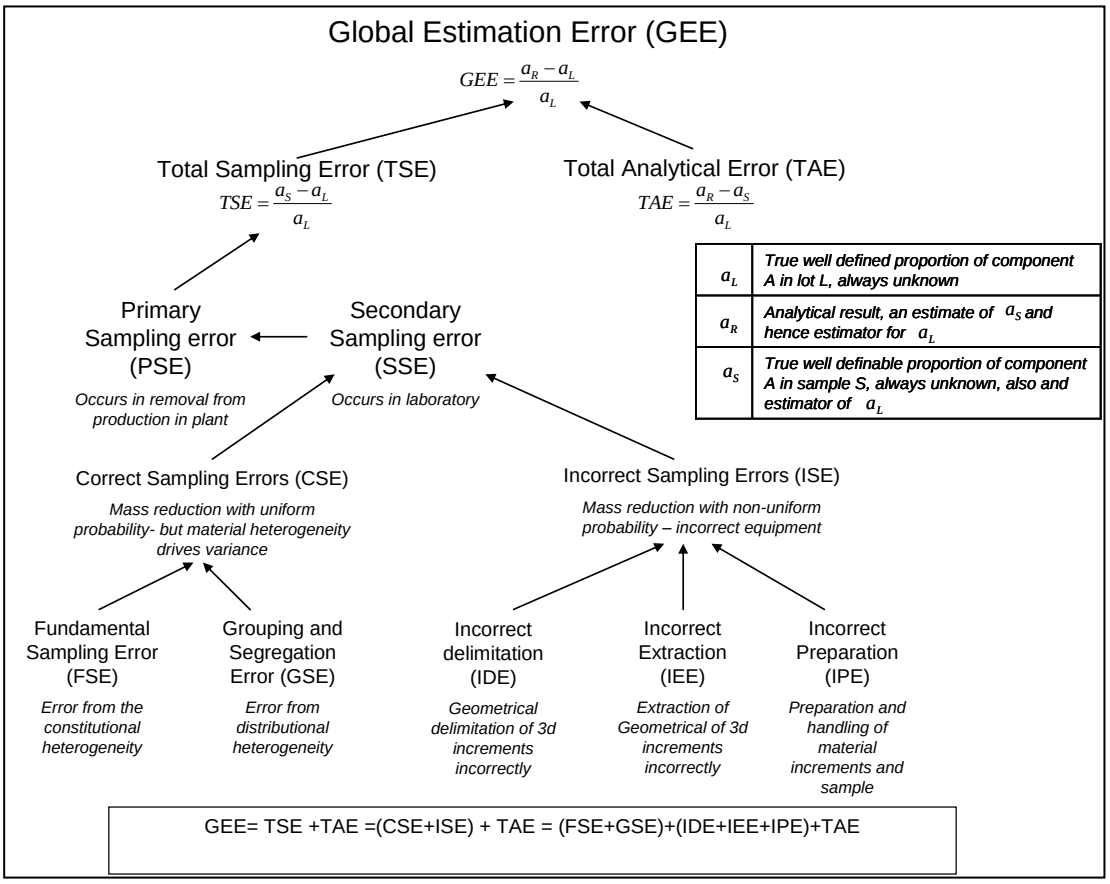

Figure 10: A hierarchical depiction of the relationship of sources of error arising from sampling, Adapted after Gy (2004).

The dominant error is taken to be the fundamental error, although the others should be minimised as far as possible. The primary cost driver in processing samples is likely to be size, thus using this approach to sample design aims to minimise the size without increasing the fundamental error to such an extent that the information obtained is of negligible use in estimation. To this end Gy proposed the formula for deriving the Fundamental Sampling Error. A simplified version is presented in Equation :

$$\sigma^2(FSE) = \frac{C \cdot d^3}{M_s} \qquad \text{Equation 3}$$

Where

C is the sampling constant, consisting of four sub-constants,

d is the top particle size (upper 95% average grain diameter)

M_s is the sample mass

Gy proposed several simplifications of this calculation, with associated assumptions concerning the constants that might apply. Gy's work identifies errors associated with particle size as being the most important. Most of the experimental sampling in this research has been on in situ material. At some clast size the heterogeneous nature of the material being tested will dominate the variance of the results obtained. One potential approach is to determine the end member response of the country rock clasts and that for pure kimberlite. It would then be possible to define the maximum acceptable size of clast for a specific variance in the measurement taken. This methodology is a version of the method suggested by Royle (1986).

Errors will arise from many sources; hence effort should be focussed on identifying and eliminating sources of error when sampling. Where the errors cannot be eliminated, the estimate of the magnitude of the relative errors must be considered in any consequent data analysis that is carried out.

The properties selected and identified in section 1.4 include those that can be used to model and predict kimberlite comminution, diamond liberation and effectiveness of separation processes. They can be broadly described as either primary or response variables as defined by Coward (2009).

Early project stage sampling

From early stage exploration through to the beginning of production, the dominant source of material characterisation data is from downhole logging, core and chip samples that are subjected to several non-destructive and destructive tests.

Work carried out by Copur and Billgin et al. (2003) on a range of rocks yielded the data that is depicted in the plot in Figure 11. Although the range of rocks tested are not kimberlites the work demonstrates how it is possible to collect different types of data to explore the existence of a relationship between the primary variables (e.g.,

various textural measures, measures of rock content) and response variables . The nature of these relationships is clear for some rock types and not for others. This suggests that for some rock types the variance of rock responses within the 'rock type domain' may well be greater than the variance of rock characteristics between 'rock type domains'.

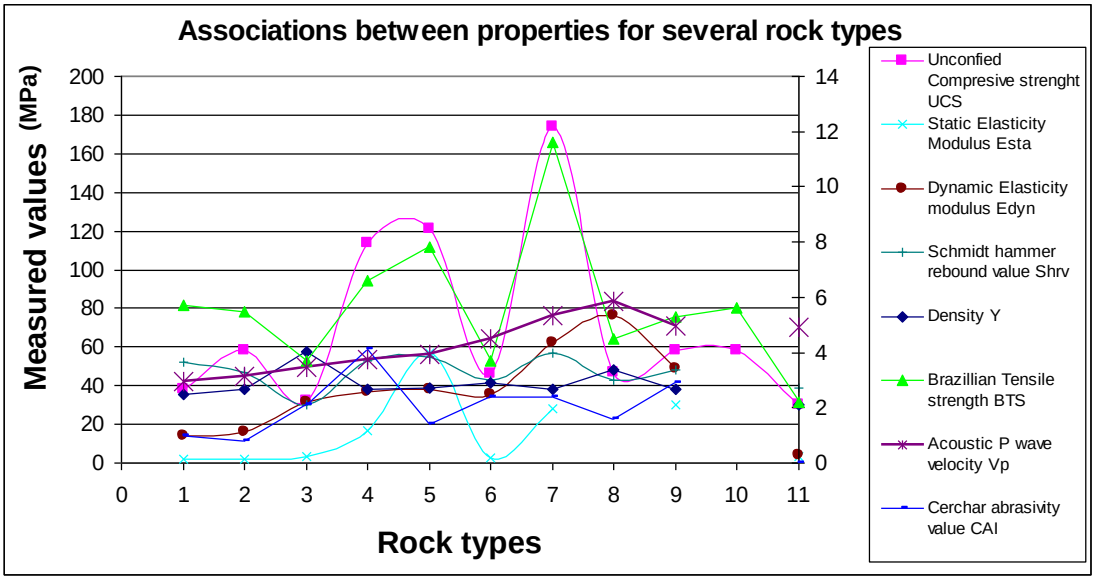

Figure 11: Results of a number of rock tests on a range of rock types after Copur et al. (2003).

The use of downhole measures and laboratory scale tests relevant to this research, such as acoustic velocity is described more fully in section 4.2. The outcomes of early stage sampling are used in desktop studies to validate additional exploration of the target.

Feasibility and production stage sampling.

To create a sufficiently robust business case to justify the funds required design and build diamond mines requires reduction of the uncertainty in the value of diamonds in the intended recovery size envelope. as these often have a large impact on the mine's revenue. To acquire a parcel of diamonds that is representative of the diamond size distribution, especially diamonds > +10ct size fraction, often requires bulk samples of the order of several thousands of tonnes. During the treatment of these bulk samples, several process parameters and performance characteristics are recorded. This data is gathered to describe the kimberlite's impact on five areas of the diamond recovery process including:

1. Comminution, with measures of rock hardness/competence and amenability to various forms of comminution;
2. Dense media separation, with measures of dense particle abundance in specific size ranges;

3. Fines, ultra-fines and their impact on water handling, with measurements of modal mineralogy in appropriate size fractions, especially of smectite clay minerals, and extractable sodium percentages in process water-clay slurries;
4. X-ray luminescent intensity of gangue minerals in DMS concentrates with the potential to increase diamond-by-weight percentages in the final recovered product; and
5. Magnetic properties of concentrates from DMS that have the potential to be stripped from concentrates before final recovery thus reducing quantities of material being processed through final recovery.

Each of these aspects may include qualitative descriptions of the characteristics of the kimberlite fed to each process, the sampled size distribution and measures of the rock characteristics such as density where appropriate.

These data can be used for process design, informs the geological model and improves the models of the relationships between primary and response variables. The data is however usually restricted in spatial coverage as the bulk samples are likely to be selected from single accessible locations in each major kimberlite domain

2.3 Challenges of spatially estimating physical rock characteristics

Data obtained from measuring the physical characteristics of samples can be used to estimate the characteristics of the un-sampled portions of the orebody. These variables, unlike grades, may exhibit various behaviours that make their estimation at block scale somewhat challenging.

There are several ways to generate spatial models of variables at different scales, the methods considered here include:

- Averages of the samples
- Polygonal estimates
- Geostatistical estimation techniques such as ordinary Kriging
- Spatial Simulation using geostatistical techniques

Using sample averages to estimate rock properties

It is possible to process the data rapidly by using the average of relevant sample values as the estimate for the variable of interest. This however does not consider the spatial correlation of either the samples or the locations and volumes that are to

be estimated. However, if the rock is very homogenous and the sampling has been carried out in a very regular grid, then this may be an appropriate approach.

Although this approach is computationally efficient it does not consider the spatial location of samples, does not account for the differences of the scale of the sample vs the scale of the estimate, and does not provide a means to assess the quality of the estimate made.

Polygonal estimates

This approach utilises the generation of a volume that the sample is deemed to represent. The region of interest is divided into shapes that fill the volume, in a way that ensures that each volume has at least one sample in it.

This approach may be appropriate when there are sufficient samples regularly located throughout the region of interest. It is computationally efficient and does not require any modelling of functions.

Kriging

Kriging is a term used for a family of estimators whose origins were attributed to Danie Krige by George Matheron (1963). Matheron (1963) named the process used to generate estimates "Kriging" as a tribute to the work of Danie Krige. Ordinary kriging is a linear estimation algorithm for a regionalised variable that satisfies the intrinsic hypothesis.

The benefits of this approach are that the estimate of the variable of interest at unsampled locations is unbiased, and that the error of the estimate at sampled locations is calculated during the estimation procedure.

Spatial simulation

The evaluation of the metallurgical recovery factor requires an understanding of both the average, expected, and variable nature of the rock characteristics on the recovery factor. One approach to overcome some of the limitations of block scale estimates is to generate a sufficient number of equally plausible realisations of the orebody characteristics and then to use these as inputs to a process simulation. The set of simulations represents the uncertainty in the ore characteristics and each individual realisation can be used to explore the impact of block to block variability on process performance.

These rich spatial models can be created using one of several spatial simulation techniques (Dowd, 1994). Spatial simulations aim to reproduce the histogram of the data and the spatial co-variance of the data.

Selection of a combination of methodologies is required to develop spatial models of several characteristics of the kimberlite deposits that can be used in the simulation of the operation of kimberlite mines. The process flow that this research has followed is similar to that used by (Dowd and Dare-Bryan, 2004) and is depicted in Figure 12. Both estimated and simulated orebody models can be generated from the original real sample data.

One of the realisations of the simulation set (based on real data) is selected at random and deemed to be the "Real deposit. This model can be sampled using different sample grids to generate data that represents the results of sample experiments that have different geometric layouts and sizes.

These 'virtual samples' from the 'virtual orebody' can be used to generate new estimated orebody models and condition a new set spatial simulations of the kimberlite deposit.

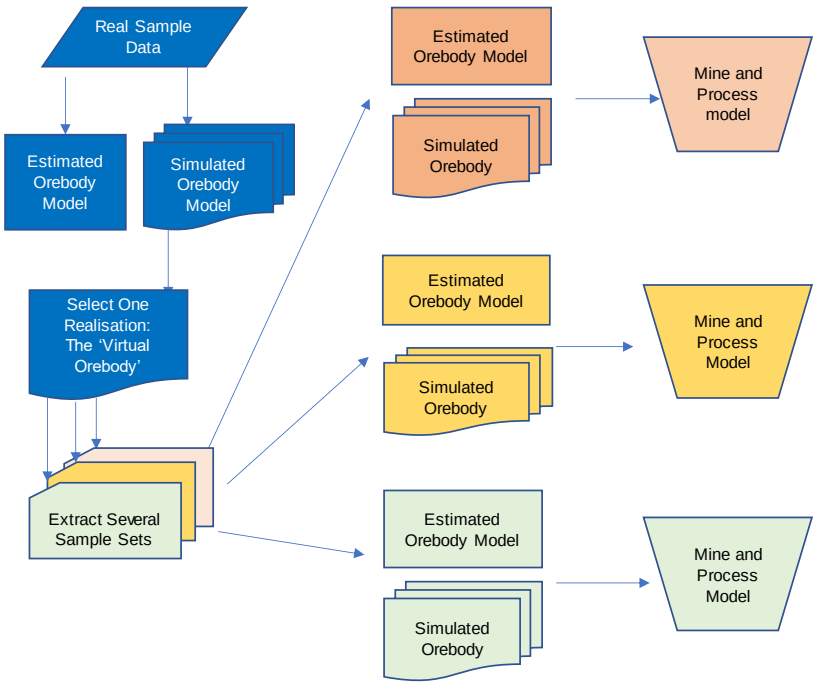

Figure 12: Schematic of the process used to create a framework to quantify the impact of changes to sampling , estimating and simulating Kimberlites on process models.

The 'Virtual orebody,' (i.e. the one selected realisation taken from a simulation set based on real sampling data) can be taken to represent so-called 'perfect knowledge case' against which various comparisons can be made (e.g., the impact of sample spacing, simulation method used, crushing process model etc.). The method has a few limitations and is computationally demanding but allows for a myriad of possible comparisons. The framework or platform is used to compare several aspects of the methods and techniques presented in this research, including a comparison between estimates of expected recovery based on limited information with that which would have been realised had the 'virtual orebody' been treated.

The techniques that can used to generate spatial simulations include turning bands, sequential indicator and sequential gaussian simulation. Each has their own benefits and drawbacks; a brief description 'turning bands' which has been used in this research is described.

Turning bands simulation was developed in the early 1970's (Dowd, 2004). This method of simulation uses a one-dimensional random function that is set up along lines that have an even spatial density. The simulations from these lines are then projected out onto a grid that is set up around the lines. Some of the limitations of this approach include the generation of artefacts if insufficient lines are used. The method deals with anisotropy indirectly, usually through grid expansion and shrinking, and the method requires a separate kriging step to condition the simulation.

Implications

The method used to generate spatial estimates and simulations of rock characteristics has consequences for the use of these models in value chain simulation. Estimates derived using linear methods such as ordinary kriging are likely to underestimate the variability of orebody variables such as grade that will be observed during operation. Simulated realisations of variables of interest at block scale will better reflect the variability of the characteristics of the blocks as they are processed. It is however important to consider that the scale of measuring rock characteristics (typically the size of core) is many orders of magnitude smaller than the size at which the process will respond to the change in the specific characteristics.

The approach described in this thesis suggests that matching the support of the sample, the location and spread of samples in the pipe to be evaluated and the scale of the spatial estimate is a very important aspect that will determine the effective use of this important input into value chain modelling.

2.4 Mineral process models and simulation practices

Mineral processing, such as crushing and dense media separation, can be modelled using several mathematical techniques. King (2000) provides a demonstrated taxonomy of systems together with a classification of these with benefits and short comings. The emerging use of so-called “expert systems” integrated with dynamic simulation for use for a) calibrating process simulation models and b) for improving operational decision making.

The processes used to recover diamonds from kimberlite can be divided into mining and treatment processes. There are several levels of process modelling and simulation, from 'black box simulations', that merely transform an input to an output through a simplistic mathematical function, to complex systems, that address the interaction of individual particles and elements in very small-time increments.

The objective in this research is to identify current practices in mining and treatment simulation that can be validly used in a value chain model to analyse the metallurgical recovery factor. The models that have been considered for use in this value chain modelling need to meet with the following criteria:

- The models respond appropriately to estimated and simulated rock characteristics; and
- The models can be used in a system simulation that can be run in a realistic time frame.

The primary objective of the integrated evaluation model is to create a value chain, comprising linked models, that can be used to simulate the operation of the mine and treatment plant system. The mining model translates the estimate of in situ rock characteristics into a sequential ore stream. The ore stream characteristics are used to drive process models which are used to calculate the plant throughput and efficiency and derive an estimate for diamond production based on the characteristics of the incoming ore stream.

Models of mining processes

Kimberlite pipes are mined using open pit and underground methods.

The design, or planning, of an open pit mine has three primary components:

1. Determination of the geometry of the ultimate pit shell;
2. The feasible extraction sequence of the blocks; and
3. The scheduling of block extraction for mining.

Several algorithms have been developed to optimise the process of mine design, including the Lersch Grossman approach developed from graph theory (Lerchs and Grossman, 1965). The aim of the optimiser is to achieve the maximum present value by offsetting estimates of cost to mine the block against the value recovered from the block. The estimate of block value is usually derived by multiplying the contained mineral in the block by the price that will be obtained for the mineral minus the cost of extracting, processing and delivering the valuable content of the block. The associated present value can be obtained by developing and applying a feasible production schedule.

Underground methods used to mine kimberlites include block caving and room and pillar methods. These methods are subject to many geometric and ground condition constraints. The processes used to derive the geometry and sequence of the operation are beyond the scope of this research.

For the models considered here it is assumed that an optimal mine plan has been designed for the simulated deposit based on the kriged estimate of recovered value. Re-running the mine design for each realisation would not only be time consuming but is not appropriate given that the simulations are designed to maximise the variance at block scale. There is however ongoing work to incorporate uncertainty in the derivation and optimisation of the ultimate pit shell, block sequence and schedule (Dowd and Dare-Bryan, 2004, Lamghari and Dimitrakopoulos, 2016.).

Mining is the first stage of the process where ore breakage occurs. The processes used include a combination of primary drilling and blasting. An approach aimed at optimising selectivity during the drill and blast cycle has particular relevance to this research (Dowd and Dare-Bryan, 2004). The method is centred on the creation of an in situ model that represents “perfect knowledge at all scales” through simulation. This simulation is then sampled on a user-defined grid to provide the limited information that would normally be available for planning. This information can then be used to design the blast and muck pile clearing pattern. It is then possible to evaluate how well the plan is likely to perform by comparing what was selected and trammed to the plant given the mixing caused by blasting, against the expectation derived from simply using the estimated block characteristics of the planned mining blocks.

Although the approach has been designed to optimise selectivity, the simulation approach used to create estimates at relatively small scales, far smaller than the smallest selective mining unit (SMU), demonstrates that rock properties can be simulated into blocks of an appropriate scale. The key limitation is the minimum size of the block that can be simulated in the blast process. The minimum dimensions are driven by the resolution of sampling, and the processing power to simulate this process.

Methods aimed at optimising the size distribution of material fed to a mineral processing plant have been developed into a multi-organisational project 'Mine to Mill' and several of the developments in blast modelling have relevance to this research (Napier-Munn et al., 1999). Central to this approach is the balancing of the cost of fragmentation achieved through blasting and the cost of fragmentation in the process plant. The study has led to the development of non-contact visual technologies that can be used to monitor fragmentation in the mine and in the processing plant.

Mineral processing modelling

A research survey carried out across the De Beers group of South African mines, obtained from senior process managers their views of which ore properties would influence process design, cost and efficiency, identified the following variables:

- Brittleness, strength and plasticity – impacts crushability and resulting ore size distribution hence mass balance, other derived measures such as nip angle were also mentioned.
- Clay type and content – impact on mass balance, water consumption and treatment requirements, also impacts on the Dense Media Separation (DMS) process.
- Ore Density distribution – the relationship between changes in size distribution and the change in density distribution of the ore stream impact both mass balance and yield from the DMS process. This also affects the efficiency of DMS when the enclosed minerals have a narrow size distribution.
- Nature of dense species, which will sink in the DMS, in the ore and their impact on recovery processes –includes luminescence distribution, magnetic susceptibility, and porosity.
- Diamond characteristics – including the size distribution shapes and luminescence distribution.

Process Function	Material Property	Impact on Process
Liberation	Bulk Fabric, micro fractures, Faults	Determines blasting characteristics
	Hardness	Change in power consumption, and size distribution
	Brittleness	Change in size distribution, better fragmentation
	Clay content	Higher clay requires more water, slower settling rates
	Friability	Dust creation, scrub ability
Separation	Density distribution	Impacts on separation, and yield
	Shape of rock particles	Impacts on effective cut point
	Size distribution	Screening efficiencies and separation efficiency
Recovery	Gangue Magnetic Susceptibility	Impacts of magnetic separator yield
	Gangue X-Ray Luminescence	Impacts on X-Ray through put and efficiency
	Diamond Magnetic Susceptibility	Impacts on Magnetic separator efficiency
	Diamond X-Ray Luminescence	Impacts on X-Ray through put and efficiency

Table 4: Relationships between ore property and the impact on mineral processing.

In a review of current plant design practice, a listing of typical plant specification variables was obtained (Lilford, 2003). Several of these specifications are based on data obtained from samples taken from the orebody to be treated. Although there are numerous input variables(e.g., rock hardness, UCS etc.), the design criteria are often based on the maximum, average and minimum values of these variables. These are obtained from a set of samples deemed to be 'representative' of the orebody. It is suggested that the relationship between the sample values, their size and the design criteria affected is an area for further investigation.

In 2000 an analysis of operational cost databases indicated that the highest individual costs on average for the suite of De Beers operations were; manpower, electrical power, and ferrosilicon (Shipiki-Kali, 2000). Most of the electrical power was consumed by comminution devices. Subsequent analysis of the cost data for 2003 indicates that the major cost drivers have not changed. This finding implies that the data obtained from sampling for kimberlite characteristics may also be useful for improving the estimates of power consumed for comminution and in reducing the uncertainty in the prediction of operational cost.

Modelling comminution

The modelling of comminution has received much attention by several authors (Agricola, 1556; Bond, 1943; Witten, 1972; Napier-Munn et al., 1999). To model comminution requires a generalised formulation for the mechanisms that drive the reduction in the size of rocks. When rocks are crushed the mechanisms of size reduction include:

- Attrition;
- Chipping;
- Impact fracture of rock particles; and
- Breakage of contained mineral particles.

King (2001) proposed a generalised model based on assigning weights to several probabilistic breakage models. The weights and breakage models are calibrated to suit both the material being crushed and the device that is used. An example of a breakage model for a mill is given below to show the composition of the breakage functions. Essentially this is comprised of the summation of the proportion of material arriving and leaving each size fraction per unit time across all size fractions.

Specific attrition rates are ore specific. Techniques developed by the Julius Kruttschnitt Mineral Research Institute show that this can be determined by treating a sample for 10 minutes in a tumble mill and the progeny screened (Napier-Munn and Morell et al., 1999).

An attrition breakage function can be obtained from assessing the slope of the graph depicting the cumulative size distribution of the finer fractions. The change in mass (m) in a size fraction per unit time is expressed in Equation 4 :

$$\frac{dm}{dt} = -3k\frac{m}{d_f^{1-\Delta}} \qquad \text{Equation } \mathbf{4}$$

Where

dm is the change in mass per unit time;

m is the mass in a size fraction;

$d_f^{1-\Delta}$ is the geometric mean of the feed size distribution; and

k is a material-specific constant

Integration of this equation with respect to time will determine the total comminution, or size reduction that will be achieved for a given unit process. Comminution modelling and its use in the value chain model is described more fully in section 6.3

Modelling dense media separation

This process uses the difference in density between kimberlite and diamond to separate the diamonds from gangue material. If the overall size distribution achieved by the comminution section can be calculated, then this 'Total Grind' can be used to estimate diamond liberation and recovery. The 'Diamond Liberation Granulometry Model,' estimates the lock up in different diamond classes and predicts what proportion of the recovered diamond distribution is lost in the tailings from the DMS circuit. These losses can be used to estimate the metallurgical recovery factor. The model can be used to calculate the proportion of each diamond size class that will be liberated given an estimate of the total grind size distribution of the kimberlite. As the model works across all diamond size classes it is also possible to use the model to assess the impact of changed liberation on the recovered diamond size distribution.

The model was developed by Kleingeld (1976) in an attempt to estimate the locked diamond content of cemented gravels that were discarded by coastal operations in southern Namibia.

The purpose of the model is to produce a reliable estimate of the diamonds that might plausibly be contained in the discarded rock stream based on the operating parameters of the plant and the size distribution of the recovered diamonds. Each size class of ore particles (for example the -10mm +8mm size fraction) has a potential to float out of the dense media during the separation process and report to waste. The particle class that is discarded can carry with it a size of diamond that can be determined through the density relationship between diamond, the rock that it is enclosed in, and the effective density cut point at which the separation is made.

The model requires the following inputs:

- the total grind achieved estimated from ore stream size distributions;
- the number of ore particles in each size fraction;
- the average ore density in each size distribution; and
- the recovered diamond distribution.

The probable locked diamond distribution is calculated by assessing the proportion of each particle class volume that could potentially be diamond, so that the combined particle density is equal to the medium density. This locked distribution can be added to the actual distribution to create a predicted total plant feed diamond distribution. The difference between the two gives the possible additional diamonds that could be recovered assuming that 100% liberation and recovery is achieved.

The model is applied during the sample phase to estimate the liberation during bulk sampling. Although the estimate of locked diamonds is not added to the modelling phase of the total content distribution, it is used as a qualitative guide to the difference in liberation that is likely to be achieved between the sampled grade and the expected production facility.

Currently it is not common practice to determine how the range of rock properties will vary in the short term and how this will impact on the efficiency and throughput of the process. In most cases, the global average rock properties are used to estimate the expected ore grind size distribution and diamond liberation.

The research reported in this thesis seeks to demonstrate that that the ‘Diamond Liberation Granulometry Model,’ can be adapted and used effectively to integrate total diamond content models with spatial models of kimberlite properties to evaluate diamond recovery.

2.5 Approaches to evaluating uncertainty and variability in diamond recovery

Published accounts of estimated diamond recovery factors often only report a single value for expected grade recovery (Farrow, 2015). A single point estimate of expected, or most likely, recovery of the contained diamond content does not give any indication of how uncertain or variable the diamond production will be over the life of the operation.

One important source of uncertainty arises from the design of sampling campaigns to define reserves. These campaigns are often constrained by the capital allocated to sampling the orebody. The optimal selection of the size, number and geometric location of samples to achieve a specified degree of confidence in the orebody grade cannot be determined with any degree of accuracy prior to executing the sampling campaign. There are some generic 'rules of thumb' that can be applied to the classification of resources and reserves (Parker, 2000) based on the expected variation in production that can be inferred from the quality of a completed resource estimate. The metrics used in classification range from search neighbourhood size, drill hole spacing, and/or kriging variance (Silva and Boisvert, 2014). It is however difficult to predict these prior to executing the sampling campaign and performing the estimate. Some inference can be made from early geological modelling or from other kimberlites with similar architectures to predict the resulting uncertainty in estimates of in situ volume, density, tonnage and grade, but it is far more difficult to predict the recovered values for these variables.

An alternative approach to sampling campaign design would begin with defining the tolerable financial uncertainty for a project and then use these limits to define the required degree of confidence in the variation in expected recoverable reserves. To do this however requires estimates for several technical factors and a methodology that can be used to calculate how the in situ values, which are spatial in nature, will be transformed into revenues over the life of the project.

The understanding of tolerable financial uncertainty is determined, to an extent, by a combination of listing code requirements such as JORC (2012) and SAMREC (2016), and the availability and structure of the finance that will be used to fund the project. The variance of the cash flows will be driven by the variance in the estimate of reserves, the ability to mine and extract the mineral commodity and the range of the prices that the mineral could realise. For illustrative purposes, research reported in this thesis has assumed that the commodity price and ability to market and sell the diamonds is given. In the remaining two areas that influence financial variability, the research evaluates several methods to model the uncertainty in the recovery factor and its variability. The approaches are described in chapter 6 and

demonstrated in chapters 7 and 8. This work shows how it is also possible to derive confidence limits for the project value based on predicted variability in project cashflow.

Calculating the expected return of a mineral deposit is a multistep iterative process. The output of this process is used to guide investment decisions. There are many valuation techniques that can be used to create a financial model for mineral deposits, but all require an estimate of future cash flows (Table 5)

Development stage	Preferred methodology	Approach
Mineral Rights	Market comparables or nominal rate	Cost of Sales comparables
Early exploration	Multiple of expenditure, R/Ha or $/oz market comparables	Cost of sales comparables
Advanced exploration	Discounted cash flow, option pricing	Income option pricing
Pre-feasibility studies	Discounted cash flow	Income
Feasibility studies	Discounted cash flow	Income
Development stage	Discounted cash flow	Income
Production stage	Discounted cash flow	Income
Salvage or closure	Appraised value or historical cost	Cost of sales comparables

Table 5: A list of preferred valuation methodologies used in South Africa (Silva and Minnitt, 2005) .

There are, however, moves within the industry to attempt to create guidelines for this process. This includes the international valuation standards committee as well as several other bodies around the world. Although it is a guideline and not prescriptive SAMVAL (2016) suggests:

“Proven and Probable Reserves valuation should be based on the application of appropriate, disclosed modifying factors, as applied in the Life of Mine plans of the operations or company, with historic cost reporting as an alternative.”

Although not prescriptive on the methods used it is suggested that the three bases for valuation should be income, sales comparison and cost. A brief description of the assumptions and limitations of methods used to value mining projects is presented

below. The review also demonstrates how to incorporate the metallurgical recovery factor into financial models and hence demonstrate the financial impact of the range and uncertainty of the recovery factor in financial terms.

Times pay back and duration of payback methods

One of the simplest methods of evaluating a mining investment is to calculate the number of times that a project will pay back the initial investment and the time that this is expected to take. The method is particularly useful at an early stage of evaluation when there are many scenarios to compare. The method can be expanded by discounting the cash flows at a certain interest rate to account for the relative values of cash flows received at different times.

Discounted cash flow methods

The principle of discounted cash flow assumes that cash flow today is worth more than the same cash flow tomorrow. The change in value is a function of both potential depreciation in value as well as a measure of uncertainty of the cash flow tomorrow. This necessitates the use of a discount rate. The selection of an appropriate discount rate is key to all discounted cash flow methodologies. The rate is sometimes referred to as the hurdle rate, or the opportunity cost of capital. The discounted value of a cash flow at some time in the future can be expressed as in Equation 5.

$$DCF = \frac{\sum cashflows_i}{(1+r)^i} \qquad \textbf{Equation 5}$$

Where

DCF is the discounted cash flow

r is the discount rate

i is the period number

The model described above can, and often is, used in deterministic fashion to assess the relationship between an input variable and the value of the project; This is known as sensitivity analysis. Sensitivity analysis may be a suitable technique for assessing relationships between input variables and output values for relatively simple valuation models.

By flexing one parameter at a time (termed 'independent sensitivity analysis') it is possible to calculate project value for a range of values for the input variables, for example it would be possible to show how the forecast discount rate for a project with a lot of debt has a substantial impact on the calculated project value. This is repeated for several of the input variables. The analysis then ranks the importance of the variables based on the 'sensitivity' of project value to proportional changes in the values of the input variables. The assumption is made that the variable that is most important (or presents the most risk to the project) is the one that results in the biggest change in project value for the smallest change in input variable,

As valuation models include more variables to improve the 'reality' of the model, independent sensitivity analysis is increasingly likely to incorrectly identify the variables that that are going to have the largest impact on project value. To mitigate this risk, it is possible to build in correlations between the input values e.g. as interest rates rise so do wages and perform a 'correlated sensitivity analysis'.

The 'sensitivity centric' approach to assessing project risk often gives a better indication of the structure of the model itself rather than providing a valid way of quantifying the relationships that exist between the orebody uncertainty and variability, project configuration and project outcomes. The main shortcoming in this approach is that the ranking does not account for the probability distribution of the range for each of the input variables.

A slightly more complex technique is to use input distributions, that may or may not be correlated, to generate the range of input variables used in the project model. The parameters used for the distributions are selected in a qualitative manner using expert opinion (Vose, 2002, Davis, 1995) as discussed further in section 9. In this approach the type of distributions for important variables, and the values of their parameters, are elicited from a panel of experts that can be weighted in several ways (Aspinall, 2018). The limitation of this approach includes the biases that arise during the process of eliciting expert opinion and potential biases that arise from underweighting of extreme events, and overweighting of recent events (Kahneman, 2011). The use and application of these approaches are reviewed in more detail in chapter 9.

Sensitivity analysis is carried out by drawing values for the input variables from the calibrated distributions, and rerunning the model, in the order of thousands of times. The distributions of outcomes can then be analysed to provide a far richer understanding of the variable relationships that exist in the project. This approach is sometimes referred to as 'monte carlo analysis'.

There are cases when two or more variables oscillate simultaneously, or are correlated in a complex relationship over time , for instance the relationships that

exist overtime between the grade of the material mined and the cost of processing that material. Prediction of the financial performance of complex systems require models of appropriate sophistication (Dowd, 2015). The 'integrated evaluation model' techniques described in this thesis have been developed to address the complexities in such cases. It has been demonstrated that for mining projects this method is likely to outperform sensitivity analysis (Nicholas et al., 2007). A more recent evolution of the approach termed "Scenario Based Project Evaluation" (Coward, et al., 2013) incorporates a more sophisticated approach to deal with future operating environments as suggested by Bradfield et al.(2005).

2.6 Summary of practices and limitations identified in this review

Kimberlites are formed through several high energy processes over a long geological timeframe (Field, 2009). This gives rise to deposits with a variety of geometries and the domains within the deposits vary greatly in shape and size. They contain many diverse minerals and exhibit a wide range of physical characteristics. Mineralisation and mineral assemblages mean that the variables of interest can have very different spatial covariances and that these can change over very small ranges.

This research describes how the variability and uncertainty of the estimates of mineral resource contents and physical characteristics can be used to improve the estimate of uncertainty in production output and express this uncertainty in financial metrics.

Simulation outputs of the mining and treatment processes includes an estimate of the tonnage that can be treated and number of diamonds and their size distribution that will be recovered. This output is used to generate a cash flow estimate that can be used to value the deposit in several ways (Dowd, 2002). Although this research is not focussed on developing new financial evaluation methods it is important that the complexity of the financial model and value indicators used have an appropriate degree of sophistication. The approach demonstrated here makes it possible to show how uncertainties in resource estimation and reserve evaluation can be expressed as risk in quantified financial terms. The aim here is to select several indicators of project performance, ranging from valuation of very simple production outputs(e.g., value of diamonds produced in a period) to more complex financial metrics (e.g., Internal Rate of Return) to demonstrate how the impact of implicit and explicit treatment of the recovery factor in the valuation process can be assessed.

The literature review clearly shows that the recovery factor has a material bearing on the value of diamond projects. Furthermore, technology now exists that will enable sufficient cost-effective samples to be taken from orebodies to enable

estimation and simulation of physical characteristics of the kimberlite that will drive mining and diamond extraction process efficiency. It is possible with some additional work to link these directly to mining and metallurgical process models and to use these to determine the range and variability in the metallurgical recovery factor. These data can be used in appropriately sophisticated financial models to express the impact that the range of metallurgical recovery will have on mining projects in financial terms.

The remainder of this thesis covers experimental data acquisition, mathematical modelling and value chain simulation to demonstrate and validate this approach.

3 PROBLEM STATEMENT

3.1 Introduction

The factors that influence the expected value of a kimberlite diamond mine include the proportion of the total contained diamond population that will be recovered, the diamond sales price and the cost of mining and recovering the diamonds. Diamond recovery and loss is a function of the effectiveness of the mining and metallurgical processes. This research addresses important shortcomings of current methods used to derive and quantify the range and uncertainty of metallurgical recovery.

Incorrect estimation of the metallurgical recovery factor impacts on decisions made throughout the life of diamond mines. It has potential to mislead investors and project owners, result in design of inappropriate processes, implementation of poor strategies and can ultimately result in failed projects.

The challenge of quantifying the range and uncertainty of diamond recovery impacts on the evaluation of mining projects from early discovery phases through to operating mines and into project closure. Errors in predicting the recovery of diamonds arise from the complex process required to acquire kimberlite orebody information, the low concentration of the mineralisation and the difficulty of sampling and estimating the physical characteristics of the kimberlite that impact on process rate, process efficiency and cost.

This research presents a framework to address the primary shortcomings of the traditional approach to deriving and using the metallurgical recovery factor. The framework facilitates quantitative assessment of strategies that aim to reduce diamond mining project risks that arise from uncertainty in the metallurgical recovery factor.

3.2 Current limitations in the derivation and uses of the metallurgical diamond recovery factor.

Large kimberlitic diamond deposits are often formed by multiple phases of intrusion and subsequent reworking. The resultant diamondiferous orebodies exhibit complex geometries, variable diamond concentrations (Field, 2008) and a wide range of physical rock characteristics.

Due to the range of rock types contained in these orebodies, the granular nature of the mineralisation and its very low concentration, sampling of the grade and size distribution of in situ macro-diamonds (diamonds >0.5mm) is time consuming and costly (Ferreira, 2013). The accuracy of grade sampling that is carried out is subject to biases that can arise during sample acquisition and treatment.

Bulk sample plants crush and separate diamonds using similar techniques to full size production scale diamond processing plants. The impact of the rock characteristics on the variability of recovery efficiency at sample scale is different to that at full production scale. The relationships at different scales exhibit non-linear relationships that are difficult to model and adapt for scale.

The technology selection, process configuration and operating philosophy of diamond process plants is often based on long-run averages of the expected feed characteristics and expected diamond characteristics (Morell, 2003; Daniel, 2010). In some cases, these designs are adapted to accommodate an 'operating envelope' of feed rock characteristics. There is however little indication in the literature reviewed of the use of short-term variability to improve the design and operation of processing plants.

Process simulation capability continues to develop and improve with advances in computing processing capacity, processing speed, and several advances in processing algorithms (King, 2001). Historically, however, they have been limited in several ways by the computing intensity required to generate realistic representations of the processing functions at a scale that is useful for understanding changes in processing and rock interaction over longer time scales.

Output from constrained simulations that have been constructed and executed to determine the 'single best design' cannot be used for risk mitigation evaluation , over and above the limited sensitivity analyses that have in some cases be used to assess the impact of uncertainty (Nicholas, 2007).

3.3 The problem statement and research question

Current known techniques for calculating the expected metallurgical recovery of diamonds for kimberlite diamond deposits are based on global assumptions and average values and do not explicitly incorporate the spatial variation of rock properties.

The problem stems from the following inadequacies:

- Limitations of existing methods used to measure and estimate the physical spatial characteristics of kimberlite;
- Mine production and metallurgical process modelling is not suited to incorporating multiple multivariate spatial estimates of the physical characteristics of kimberlites; and
- Project evaluation frameworks do not readily incorporate the change in project value that can be attributed to mitigating recovery factor variability and or uncertainty.

Through a combination of sampling, measurement, modelling, and simulation experiments and two case studies, this research develops and demonstrates a methodology to quantify the range of the metallurgical recovery factor for diamonds recovered from kimberlitic deposits. This methodology improves the estimate of the expected metallurgical recovery factor and provides an approach to derive confidence limits.

A sampling experiment has been conducted on the K2 kimberlite at Venetia mine in South Africa to generate a data set of measurements of rock characteristics. Measurements were taken on cores, and the holes from which they were retrieved to demonstrate methods to improve spatial data collection and show how these can be used to generate spatial estimates of rock characteristics.

In parallel with this work, a modelling and simulation framework has been developed to demonstrate how multivariate estimates and spatial simulations of the physical characteristics of an orebody can be used in a linked-up value chain model to derive a metallurgical recovery factor and create confidence limits for the range and variability in the metallurgical recovery factor over time.

A quantified view of the variability and uncertainty of metallurgical performance facilitates a quantitative evaluation of a range of risk mitigation strategies. These strategies include blending and stockpiling, selection of alternative grinding and crushing technologies, or adapting the processing configuration. The benefits are quantified in monetary terms using simplified discounted cashflow metrics.

4 OREBODY SAMPLING AND COLLECTION OF ROCK CHARACTERISTIC DATA

4.1 Introduction

The methodology used in this thesis to derive the metallurgical recovery requires a spatial estimate of country rock and kimberlite characteristics that impact on the diamond recovery process. The estimation of these characteristics is not trivial and requires the collection and testing of samples to derive appropriate spatial data of these characteristics. This chapter describes the design and execution of an experiment to gather data that was used to evaluate options for generating spatial estimates and simulations of the required kimberlite characteristics.

The nature of so-called 'non-grade' variables requires special consideration during sampling and subsequent spatial modelling. Failing to objectively consider the unique properties of these variables may seriously compromise the validity of the sample selection, sample treatment, data models and the subsequent decisions that are based on these models. In addition to addressing the vexed question of collecting an 'unbiased and representative' sample, the sampling and modelling approach must consider issues of scale, both geostatistical support and the relationship between bench-scale data and operational-scale mineral processing performance (Coward et al., 2009).

As identified in the literature review, the traditional approach to optimise process design and treatment strategies is often based on the assumption that the waste, ore and diamond characteristics are 'consistent' within a given kimberlite 'facies.' This has meant that the sampling designs are often aimed at generating samples that will be representative of the average characteristics of interest. These averages are then used to derive recovery factors for each of the facies within the deposit. (Ashley and Callow 2000). To create a sample that has these 'average characteristics' several large representative samples are taken from the orebody and then mixed to form what is called a 'composite sample.'

There are several short comings of using a 'compositing' approach to sampling, including:

- It is incorrectly assumed that an average of the results of measurements on a number of composite samples will give the best estimate of the rock characteristics that will be observed when the deposit is mined. As most rock characteristics are not additive this approach could lead to incorrect results.

- An incorrect assumption that it is possible to compile a single sample which has a suite of characteristics that are equivalent to those of an entire spatial domain / facie /geological type. This is not possible as it would require prior knowledge of the entire composition of the attributes throughout the domain/facie or geology.

- A further incorrect assumption postulates that mixing and treating number of different samples in equal mass proportions will result in the average response being observed. If the mixing is not effective, and characteristic being measured does not respond in a linear way to changes of rock composition, a proportional blend will not give the equivalent proportional change in the measured response. There are several reasons for this including the difference in serialisation of the material; i.e. the mixed sample will not have the same properties as the range of materials that are treated during operations, as the properties will change in relation to the sequence in which the ore blocks are mined.

- It is further assumed that it is possible to compile a range of composite mixtures that will cover the range of expected mixtures that will be treated over the life of the operation. It is also assumed that a physical blending of the samples is possible and the response to the blend can be modelled in some representative way. As an illustrative example, sampling is usually limited in number by the required minimum sample mass to run steady state tests (e.g., 100kg for a full drop weight characterisation test). To compile a set of composites that covers mixtures of two rock types in increments of 10% one would need over a tonne of material, three rock types would require several tonnes.

- The sample is not the estimate - A further shortcoming of the use of 'average' ore characteristics to determine recovery factors for a geological domain is that the average of the results of treating the 'average composite' samples, which are far smaller than the domain for which the predictions are being made, do not constitute an estimate of the 'average recovery' that can be expected for that domain, i.e. $F(E(x)) \neq E(F(x))$.Without having sufficient

> sampling (where 'sufficient' suggests a large enough number of representative samples of large enough support to enable the characterisation of both the histogram and semi-variogram model in a way that supports estimation) of the variables of interest it will not be possible to estimate the characteristics at the right scale to reasonably predict plant responses (efficiency throughput, balance etc.) at an operational scale. Using averaged results, or responses from treatment of small samples as an estimate or prediction of full-scale response is a flawed approach.

In the absence of project constraints (e.g., time, access, cost) sufficient samples of appropriate size, i.e. geostatistical support, would be acquired from all domains in the orebody so that both the average and variability of the characteristic variables can be spatially modelled with a known degree of uncertainty. In addition to collecting enough samples, the sampling programme will also consider the relationship between bench-scale testing and operational-scale performance, and the implications for the minimum mass of samples required for metallurgical tests. (Coward et al., 2009)

Mineral projects are constrained by both time and cost, which in turn limits the scope of sampling and testing programmes (e.g., limited access) that are designed to characterise the orebody. This often leads to a trade-off between the number and size of samples that are collected, measured and/or processed. Some tests and measures require less sample mass, and for these it is possible to acquire large numbers of samples e.g. point load tests (masses of several grams). The very small support used to acquire data from the sample can compromise the measurement's validity (i.e. the measurement does not correctly reflect the true value of the total sample) and impact on overall sample representivity. It is important to be able to quantify the impact of different numbers, sizes and types of samples on the scale-up from sample support to production support. In cases where a large sample is collected e.g., 100 tonne pit samples, the number of samples are limited, and so spatial coverage is usually insufficient for estimation. Thus, it is often the case that the support, spatial location and number of sample points are insufficient to characterise the spatial character of the rock property variables and hence rendering reliable spatial estimation difficult if not impossible.

This chapter describes the design and execution of a sampling campaign that aimed to address many of the limitations of traditional sampling approaches. Several different properties of kimberlite were measured using a range of methods and tools on cores derived from holes that were relatively closely spaced (~5m).

It should be noted that this work was carried out in collaboration with Dr. Matthew Field, who assisted with the design and management of the sampling campaign. The work was generously funded by De Beers, who also allowed on-site staff at Venetia

Mine to supervise core drilling and core collection and logistics. The author co-ordinated destructive tests on core samples at several laboratories. The author undertook several site and laboratory visits during the process of the sampling campaign. Rob Pierce assisted with project management and compilation the geological data base.

The experiment objectives included:

- Assessing the relationships between the primary kimberlite properties (geological description, contents) and the measured response variables (UCS, BTS, acoustic velocity);

- Describing and evaluating the nature and strength of associations between the different measurements on the core and down the hole;

- Identifying and using relationships between descriptive and measured primary properties to assess the quality of prediction of characteristics of the rock at sampled and un-sampled locations; and

- Defining the minimum range of descriptors and measurements that is required to be able to characterise the mean, variance, variogram and histogram of the variables of interest in the block of rock that has been sampled.

The sampling design used in this experiment aimed to test the assumption that, given sufficient geological controls (i.e. within a geologically homogenous, grade 'domain'), it would be possible to sample kimberlite cores, and augment data acquired from destructive rock testing with a range of geophysical measurements to facilitate geostatistical characterisation and hence estimation of rock characteristics. This required a data set to be generated from samples taken from a real deposit that was geologically well defined, with closely spaced (i.e. less than 5m apart) samples. Spatial intensity, or spatial coverage, can be defined as some function of the average distance between the samples. Sufficiency criteria can range from qualitative rules of thumb (Parker, 1978) for the mineralisation type to a quantitatively derived measure such as having observations that are within half the range of the semi-variogram. As no such data set was readily available for the variables that were to be sampled in this kimberlite, this sampling experiment was designed and executed based on the minimum feasible distance that could be achieved within the physical constraints of the drilling equipment and the most likely variogram range that would be expected for the variables considered.

The scope of the programme included the following activities:

- Describe and classify the geological characteristics of the entire sampled area;

- Design a layout of samples and core holes to acquire and test core from several closely spaced drill holes of 50 m in length;

- Define how each portion of core is to be sampled and describe protocols for core selection, preparation and treatment;

- Assess the operation of several downhole geophysical tools and potential to use data generated from these tools to improve spatial estimates of rock characteristics; and

- Investigate the correlations between different types of data acquired and assess potential for easily measured variables (e.g. downhole geophysics) to be used as reliable proxies for other test data that are more difficult or time consuming to acquire (e.g., destructive rock strength testing).

This chapter describes the sampling layout, gives an overview of the geology of the site selected, and describes the tests and tools used to generate the data. The independent variables include all the primary properties of the rocks and the dependant variables are the response variables. Process variables are those used to control the properties of the processes used to carry out the tests.

A programme was carried out on a block of in situ ore (50m x 50m x 50m) located at Venetia Mine in South Africa. Nineteen core holes were planned to be drilled and each core was subject to several phases of description and testing according to a pre-determined procedure.

The data set described in this chapter has been used in subsequent chapters to demonstrate the proposed methodology to determine the impact that the variable rock properties can have on diamond recovery.

This exploratory data analysis begins with an evaluation of the correlations between measures:

- Between different types of destructive data;
- Between destructive and non-destructive testing;
- Downhole measures and destructive tests; and
- Quantitative Geological descriptors and physical rock responses.

In the next chapter, the spatial behaviour and correlations established between these measurements are reviewed and their usefulness in generating spatial estimates of the in situ the rock characteristics is assessed.

4.2 Experimental design

The main aspects of the specific sampling campaign that was carried out included:

- Site selection, hole layout and sub sample design;
- Non-destructive downhole and core measurement tools used;
- Destructive test selected;
- Data collection quality assurance and quality control measures applied; and
- Assumptions made in the in the absence of controls.

Location, hole spacing and sample layout

Experience from grade estimation exercises in kimberlites shows that diamond grades commonly produce variograms with ranges of around 50m (Bush, 2010). It was possible that the rock property variables that this programme investigated would have a shorter range. Even if the range was larger than 50 m, the nugget effect of these variables has not been documented in the known literature. Relatively short 5m centred drill hole spacing was thus selected for the experiment.

Orientated core holes were drilled at 5m centres from the centre hole in a cross pattern to a depth of approximately 50m from the hole collar. This cross pattern has been established as a reasonably robust methodology for establishing short-distance component of variograms (Chiles et al., 1999). The reason for the close-spacing of these holes is that one of the most important aspects of the spatial relationships are the nugget effect (i.e. random component) and the range over which individual measurements are correlated. If the expected range is 50m, then it is essential that some data points are located between 0 and 50m.

The location of the cluster of holes was determined largely by the availability of suitable areas in the open pit that would allow for access and extraction of the cores. Mapping of the K2 open pit by Brown (2008) provided good geological control, and the pit was made available for experimental drilling from November to December 2004. The cluster of holes straddled the faulted contact between “fine-grained, homogenous volcaniclastic kimberlite” occupying the eastern part of the pipe, and the more varied lithologies lying to the west of the faulted boundary. This approach ensured that the data set would cover two distinct domains (Figure 13).

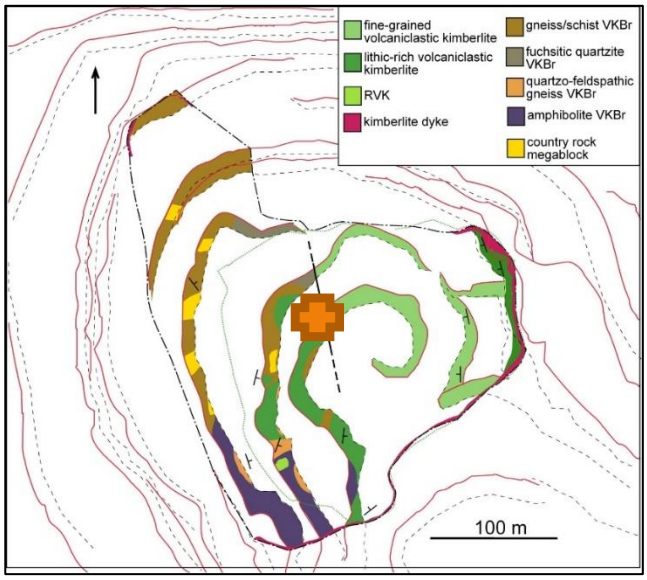

Figure 13: Geological map of Venetia K2 (after Brown 2008) showing the location of the Geomet drill holes (orange cross).

Two categories of drill holes were defined; The first are holes where all the material was sampled, and the second where only portions were sampled.

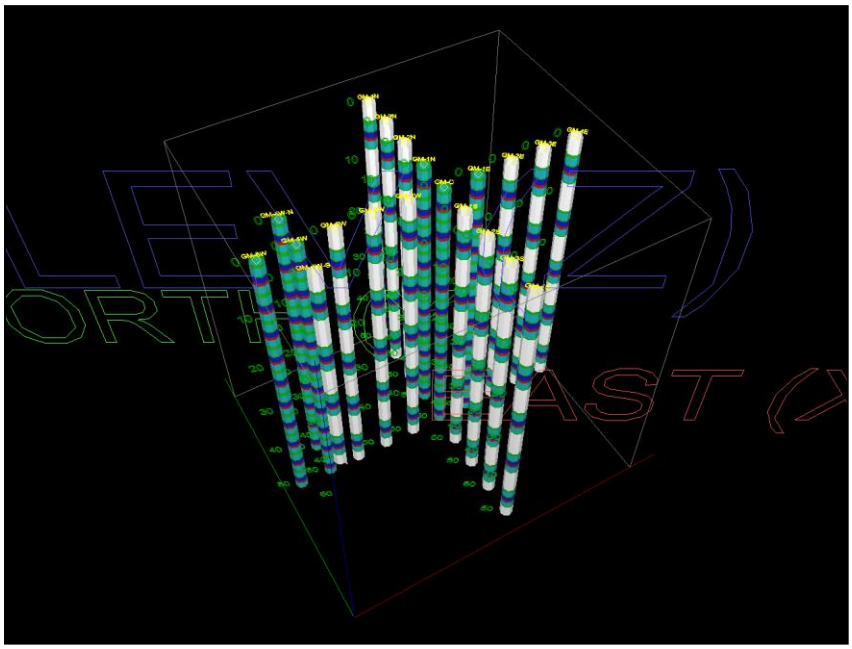

Figure 14: A view of the layout of the core holes depicting the location of the subsamples.

The sampling layout of the cores extracted is depicted in Figure 14. White intersections were not sampled but retained; all other coloured intersections were sampled. Details are of the subsamples are shown in Figure 15. It was important to assign a sample type to each of the lengths of core prior to recovery of the core to

minimise selection bias. This is of importance when selecting cores for destructive testing. Post drilling selection methods can result in only competent cores being selected for test work which introduces large biases in the resulting data.

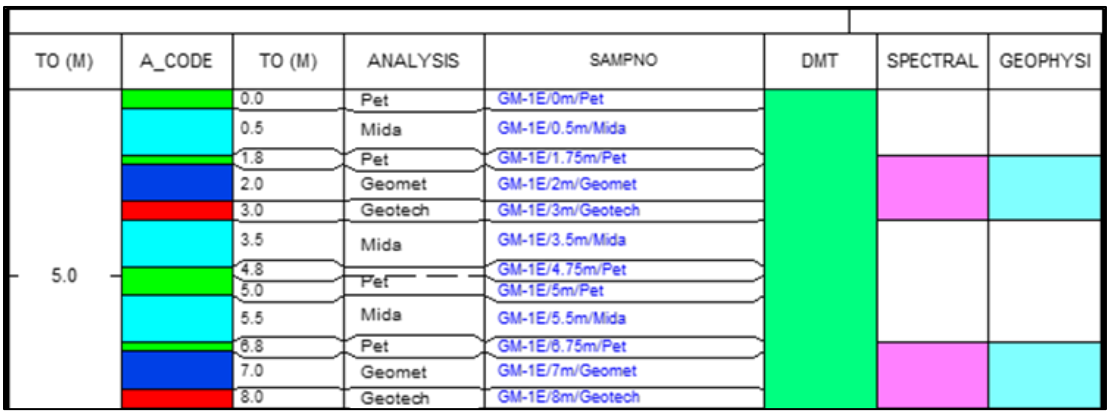

Figure 15:Listing of subsamples taken from cores that were fully sampled.

The layout ensured that the fully sampled holes would provide a duplicate set of samples for each mining bench, whilst the sub-sampled holes would provide a one sample set per bench.

Ideally, all the data would be collocated at the same point and all the data would be available at all points, and this data could then be termed 'isotopic.' As several of the sampling tests destroy the core it is not possible to generate truly isotopic data. The destructive tests were thus 'bracketed' with petrographic samples to test for short scale changes in geological characteristics. The petrographic data were used during analysis of the data to identify the bench sets where the assumption of geological continuity within the bench would be tenuous.

A 'sample set' consisted of:

- three small petrographic samples (Pet) spread through the interval to enable the geology of the section to be described;
- two microdiamond samples (Mida) to evaluate the diamond grade of the sampled interval;
- a geometallurgical sample (Geomet) that would be used to determine the physical rock characteristics; and
- a geotechnical sample (Geotech) that was used for destructive geotechnical testing.

Non-destructive core analysis

The core that was extracted was logged and subjected to a range of non-destructive description, analysis and destructive tests. This included:

- Descriptive logging by an onsite geologist, to identify lithological type, xenolith types, abundance and distribution;
- Images of the core were captured using a DMT (Deutsche Montan Technologie GmbH) core scanner. This unit generated high-quality visual spectrum light images of the core, creating a permanent record of the fresh core. The images were also used to obtain modal analyses of the particles that make up the rock, and to perform a structural analysis of the rock.
- Selected portions of the core were scanned using a Geotek core scanner. This recorded core-diameter, P-wave, gamma-ray attenuation, magnetic susceptibility, core-imaging, natural gamma and electrical resistivity.
- Selected portions of the core were also scanned with a near infrared spectral scanner to generate images in the near infrared wavelengths. These images can be analysed to infer the type and abundance of clay mineral minerals. Hydrous minerals such as phlogopite, serpentine and smectite clays make up most of the fine-grained matrix of kimberlites. These minerals play a role in determining a kimberlite's strength and slime content. As these minerals are often very fine-grained, they are not easy to detect, and conventional analysis by X-ray diffraction techniques is difficult, time-consuming and expensive. In recent years infra-red spectrometry has been used as an exploration tool in kimberlite exploration because it can detect the Mg-OH bonds present in these minerals. Development of this system into a core-scanning technique makes the acquisition relatively intensive spatial data of these mineral species possible.

Downhole data collected

The downhole geophysical data were collected to evaluate the potential for building relationships between several continuous measures and the discontinuous destructive tests that were carried out on the core. These relationships can be used to enhance the estimates of destructive test responses at unsampled locations. The nature of this data also lends itself to assessment of the representativity of the sub-samples that were taken from the core. As an example, the density distribution of the sub-samples can be readily compared to that of the density measures derived from the geophysical tools.

As these geophysical data are continuous, they can to some extent be used to assess the impact of support on the derived measurements. The true support of the tools

not only differs from tool to tool but will also vary between rock types that respond differently to the signals being used.

The downhole data were gathered using several tools, each of these tools and their rock-tool responses are briefly described below:

Downhole Calliper

This tool measures the size of the hole using three arms that trail behind the tool and rub up against the walls of the drilled-out cavity. The deflection of the arms is measured and the circumference of the hole at that location is calculated assuming that the hole is circular. Variations in the size of the hole are related to different properties of the lithology that has been drilled through and to some extent the drilling parameters. Using the calliper data, it is possible to calculate the volume of the core extracted. Comparing the calipered volume against the measured recovered core volume makes it possible to calculate in core recovery. Core recovery is correlated with both rock quality and drill rig operating parameters.

Resistivity

The direct contact resistivity tools work on having several point contacts with the wall rock that are used to pass a current through the wall of the hole. The rock resistivity is determined from the relationship between the voltage that is applied across the contacts and the current flow that is realised. Some tools induce a current in the wall using coils that are energised with high frequency alternating currents and induce a current in the wall rock. This induced current is inversely proportional to the resistivity of the rock being tested. Resistivity is deduced from the amplitude and relative phase of the secondary magnetic fields that are sensed by measuring coils. Direct contact tools provide high resolution logs but do not provide the penetration of the wall rock that can be achieved with inductive tools.

Natural gamma radiation

The natural gamma tool uses a sodium iodide scintillation detector to measure the natural gamma ray radiation emitted by the formation that it is passing through. The signal is processed into five distinct peaks that correspond to the radiation energy from three most common elements that contribute to naturally occurring radiation; potassium, thorium and uranium. The count rates in each of the five segments of the energy spectrum are used to determine the relative proportion of these components in the rock. In strata where relatively, low counts are obtained logging speed can be reduced to ensure that the number of emissions measured remains statistically

valid. The data can be expressed as total gamma ray, a uranium free gamma ray, and the concentration of uranium, potassium and thorium.

Long and short spaced density

There are several tools that measure density down the hole. In this case the instrument (or sonde) consisted of a gamma ray source that is contained in the downhole probe. The gamma rays are scattered by the wall rocks. The intensity of the returning gamma rays is a function of the electron density of the rock that in turn is related to the bulk density of the rock. The back scatter is detected at two distances from the source. The further the detector from the source the greater the support of the density measurement. Short spaced readings may in some cases may biased toward that of the drilling fluid if the hole surface is coated with drilling mud.

Formation hardness testing tool

This tool has been developed to measure the hardness of the wall rocks of boreholes. The unit consists of a calliper that measures the original hole diameter and has a cutter wheel that runs along the outside of the hole. The deflection of the cutter into the wall is recorded at small intervals and reported as a penetration reading in mm.

Acoustic velocity

The velocity and attenuation of acoustic signals in rocks is related to the nature of the material that is carrying the signal including its density, porosity, the fracture frequency and orientation as well as the clast size distribution. The strength and frequency of the input signal can be adapted, to improve the quality of the data obtained.

There are several ways in which acoustic velocities in rock can be measured. Most rely on transmitting an acoustic signal through a specimen of rock and measuring the speed and attenuation of the signal of both compression waves and shear waves.

An alternative approach for extracted core is to create a right cylinder of the rock and then input a signal of varying amplitude and frequency until the resonant frequency of the specimen is obtained.

If it is assumed that that rocks being measured are homogenous, linear elastic and propagate acoustically induced waves at the same velocity in all directions (isotropic) it is possible to create a mathematical relationship between measured shear wave and compression wave velocities and several of the physical moduli. This approach is particularly useful for characterising the physical characteristics of

the rocks considered and so the relationships between acoustic velocities and material characteristics are described here in more detail.

There are three broad categories of moduli:

1. Young's modulus;
2. The Bulk modulus; and
3. The Shear modulus.

Young's modulus is a measure of the elastic stiffness of a material. Named after the 18th Century British scientist Thomas Young. It describes how a solid deforms under load within its elastic limit. It is defined as the ratio of imposed pressure to relative deformation (strain) measured in a direction that is parallel to the direction of the imposed pressure. Strain is a measure of deformation normalised to the sample length or area (Equation 6). It can be derived from measuring the slope of the stress strain curve near the origin, or in the interval from the onset of the deforming pressure to a point before plastic deformation occurs. It is in this range that the deformation on the solid is directly proportional to the imposed force. This behaviour is described by Hooke's law, so named after the 17th century British Physicist, Robert Hooke.

$$\boldsymbol{e = \frac{\Delta L}{L}} \qquad \textbf{Equation 6}$$

Where

e is the calculated strain reported in dimensionless units;

ΔL is the measured change in length of the sample; and

L is the original length of the sample.

Young's modulus is described in Equation 7

$$\boldsymbol{E = \frac{Tensile\ Stress}{Tensile\ Strain} = \frac{F/A}{\Delta L/L}} \qquad \textbf{Equation 7}$$

where

G is the derived shear modulus in Pascals (Pa);

F is the applied force;

A is the area of the sample being tested;

Δx is the measured tangential displacement of the sample; and

L is the original length of the sample

The bulk modulus is the response of a solid to uniform multi-axial compression forces, it is described in Equation 8.

$$\boldsymbol{K = -V\frac{\Delta P}{\Delta V}} \qquad \textbf{Equation 8}$$

where

K is the derived Bulk modulus measured in Pa;

V is the volume of the sample;

ΔP is the change in pressure applied to the sample;

ΔV is the change in the volume observed for the given change in applied pressure.

The inverse of the bulk modulus gives the compressibility of the sample

The shear modulus, sometimes referred to as the modulus of rigidity, is the ability of a sample of material to resist deformation in a direction that is tangential to the main axis of the sample (Equation 9). It is reported in Pa and is measured by applying a bending force to a sample and measuring the deflection as the bending force is increased.

$$\boldsymbol{G = \frac{F/A}{\Delta x/L}} \qquad \textbf{Equation 9}$$

where

G is the derived shear modulus in Pa;

F is the applied force;

A is the area of the sample being tested;

Δx is the measured tangential displacement of the sample; and

L is the original length of the sample.

It is possible to estimate the above moduli using measures of the acoustic velocity in a solid. Alternative equations that can be used to estimate these quantities are given in Table 6. These equations have specific measurement requirements, and are based on assumption that the rocks being tested are linear elastic, homogenous and isotropic (Momayez et al.,1995).

Young's Modulus	Shear Modulus
$E = V_p^2 \rho \frac{(1-\upsilon)(1-2\upsilon)}{1-\upsilon}$	$G = \frac{E}{2(1+\upsilon)}$
$E = V_p^2 2\rho(1+\upsilon)$	$G = V_s^2 \rho$
$E = \frac{9Gk}{(G+3K)}$	
$E = 2G(1+\upsilon)$	

Table 6: Formulae for estimating elastic moduli of solids using measured acoustic velocities in rock specimens.

Where:

V_P = compression wave velocity

V_s = Shear wave velocity

ρ = density

E = Young's modulus of elasticity

G = shear modulus of elasticity

k = Bulk modulus of elasticity

υ = Poisons ratio

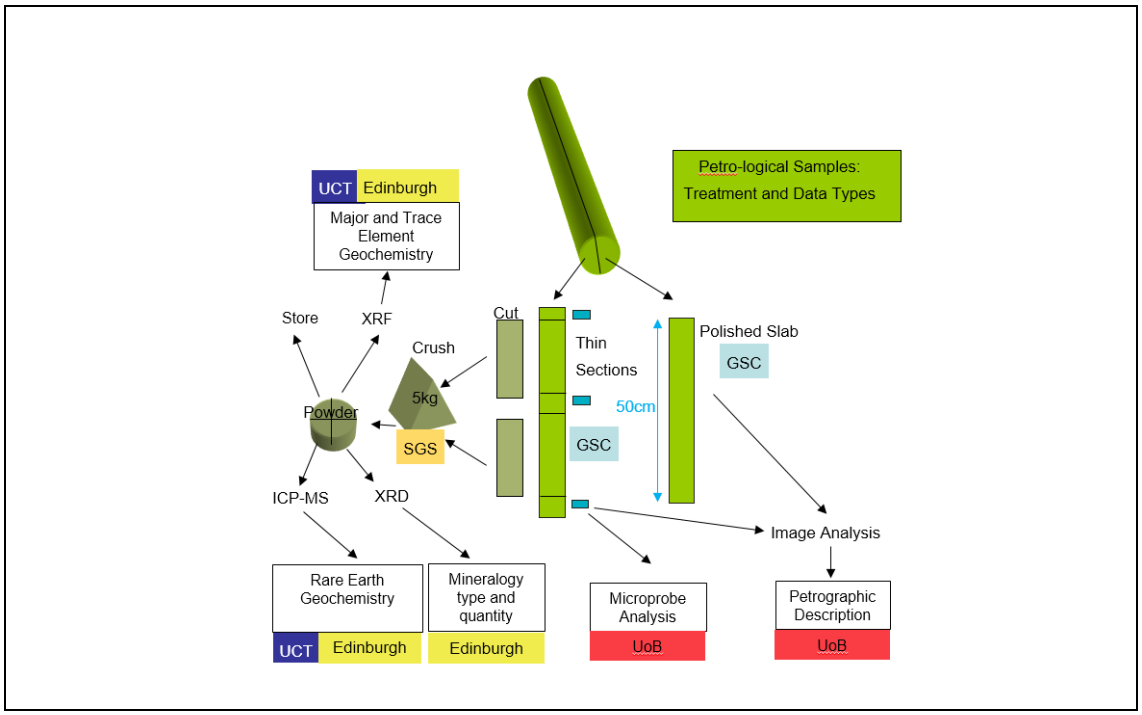

Figure 16: Schematic representation of preparation and analysis of petrological samples. (GSC=Geoscience Centre laboratory, UCT=University of Cape town, UOB=University of Bristol, SGS=Testing laboratory in Johannesburg, Edinburgh =Edinburgh University).

Prior work on kimberlites has included an analysis of Venetia kimberlite material. Measurement of the broadband acoustic properties of kimberlite used a wide range of input frequencies, and compared the response of core and quarried specimens (Sothcott *et al.*, 2005). Six samples were tested at ultrasonic frequencies, and one sample at range of sonic frequencies 3 kHz to 60 kHz.

The work showed that the ratio of compression wave velocity to shear wave velocity was lower for samples taken from the pit than for core samples. Further analysis indicates that this is a function of both weathering and potentially the introduction of micro-cracks introduced during the mining process. The author did, however, conclude that acoustic signal measurement could be used to discriminate between waste rock species and different lithotypes in the Venetia deposit.

Destructive core testing

Once all the non-destructive testing and core description was completed, the process of sampling the core to obtain further information commenced.

The following types of samples were taken from the cores:

Petrological: These samples were removed according the procedure shown above and were submitted to the De Beers Geoscience Centre Johannesburg for sample preparation according the scheme depicted in Figure 16.

Micro-diamond Samples: These samples were removed and submitted to the Kimberley Acid Laboratory as per De Beers' standard procedures. Diamonds were recovered down to 150 microns.

Geometallurgical samples:

These samples of 1 metre of core were sawn to length, dried and packed in cellophane and dispatched from site to SGS laboratories in Johannesburg.

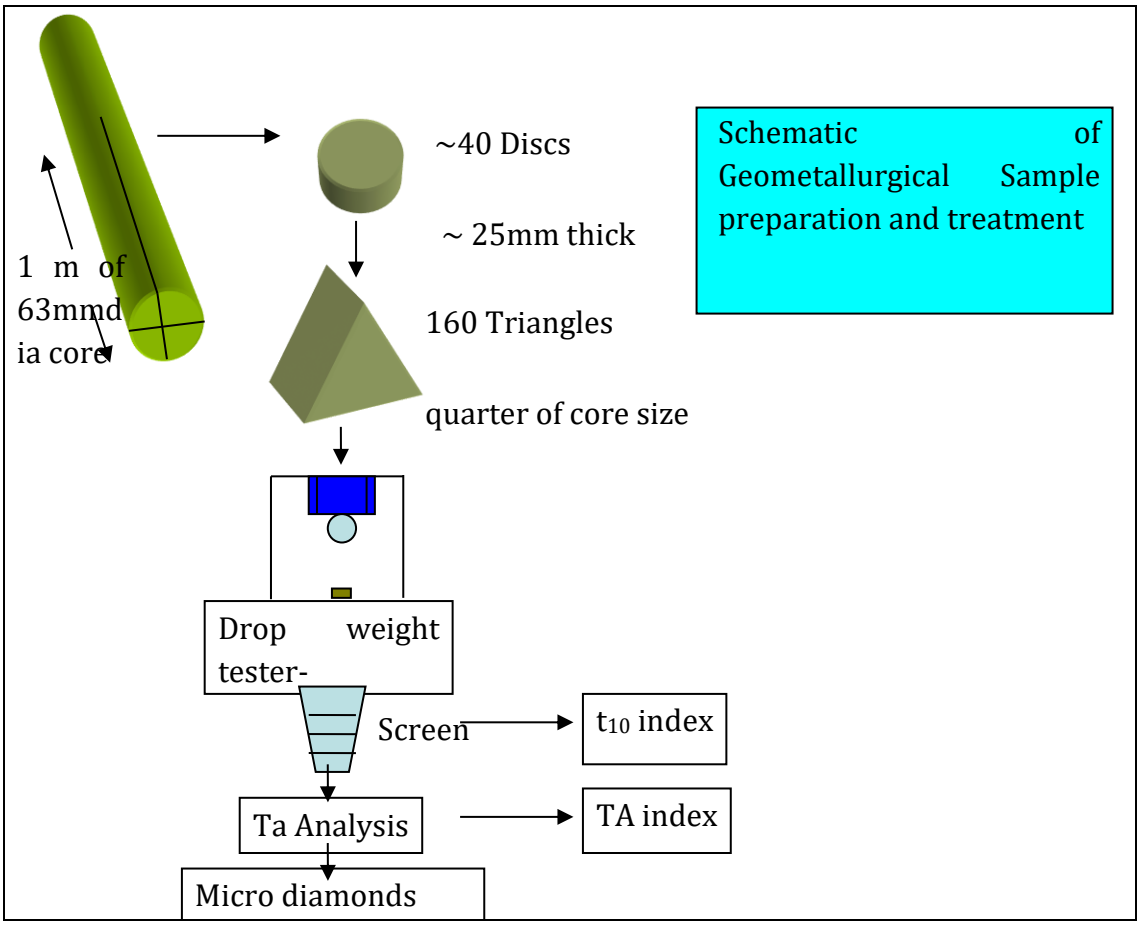

Figure 17: Preparation and analysis of Geometallurgical samples.

The method used for rock breakage testing follows the procedure described by Morell (Morell, 2003) and termed the SMC test. This test has been developed by the JKMRC in conjunction with several industry partners. The method has recently been refined by Dr S. Morrell to utilise a smaller support of core (Morell, 2003). Essentially the method aims to impart a fixed energy into several fragments sawn

from the core and the resultant degree of fragmentation is measured by sieving the progeny of the breakage test. It is then possible to relate the energy input to proportion of material that has been crushed to less than one tenth of the size of the original fragments. This is the so-called t_{10} and gives a measure of the samples' resistance to crushing.

At the laboratory in Johannesburg the cores were cut into quarters and then each quarter section was cut into 40mm lengths to form triangular sectors of quarter core for testing. Each of the triangles was then subjected to drop weight testing. The product of the controlled energy fracture was collected and sized. These data were then used to determine the energy breakage relationship for each sample (Figure 17).

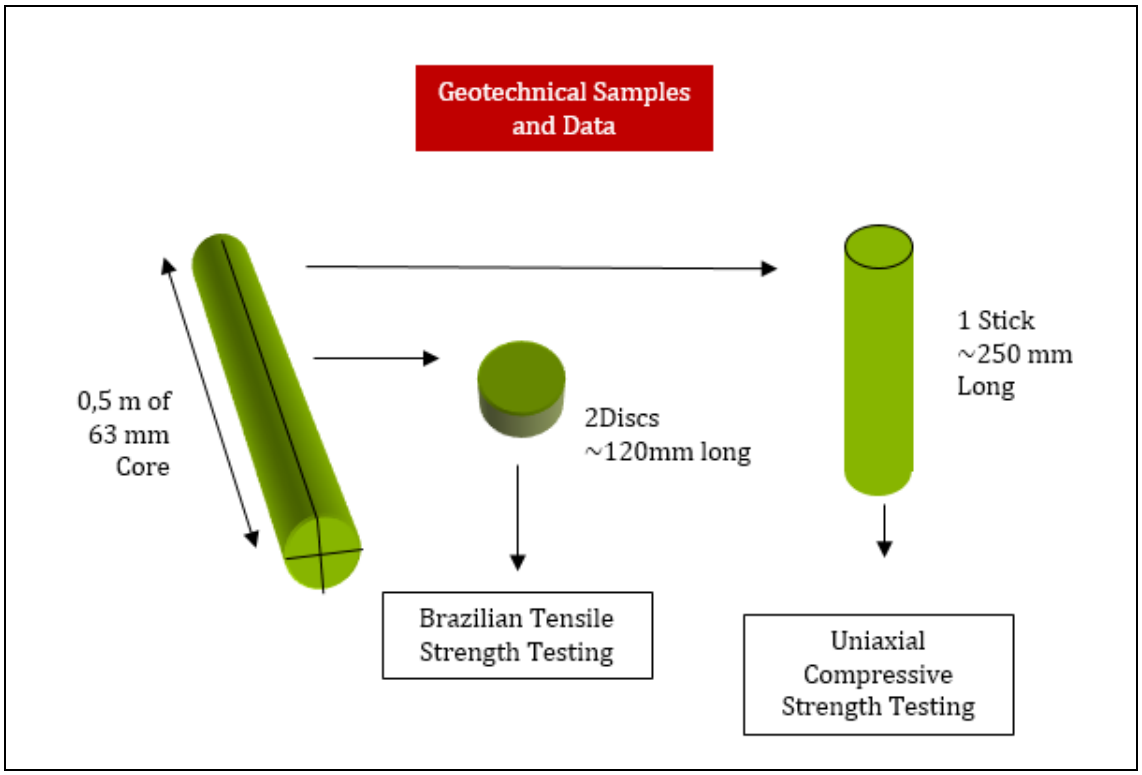

Figure 18: Preparation and testing of Geotechnical samples.

Geotechnical Samples: A half a metre of core was sawn using kerosene as the cutting fluid. The section of core was then cut into lengths of approximately 120mm for uniaxial compressive strength testing. The remainder of the core was cut into discs of 40 mm of core length for Brazilian tensile strength as described in the literature review section. This process is depicted in Figure 18.

4.3 Data collection process

The samples were extracted from Venetia, a kimberlite mine located in northern South Africa. 17 cores were extracted from the K2 pipe in the form of a cross with the samples located 5m apart. The samples were collected from the core as per the recipe described above.

The plan view layout of the core location is shown in Figure 19.

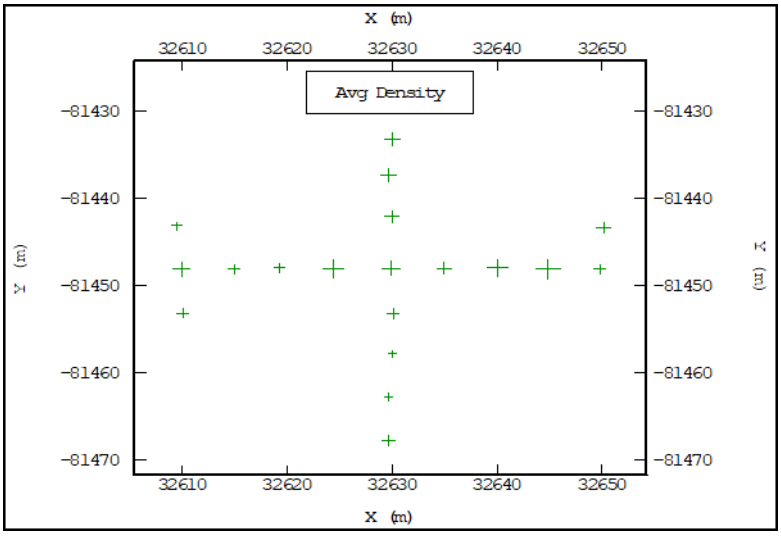

Figure 19: XY projection of the layout of the core samples.

The samples were collected in the middle of 2005 and subjected to destructive testing shortly afterwards. Rocklabs, a testing laboratory located in Pretoria carried out the UCS and BTS testing and SGS laboratories in Johannesburg carried out the drop weight tests.

Cores were drilled out, collected and scanned using a visual spectrum core scanner. The holes were subject to a suite of geophysical measures. The scanned core was then marked according to the original sub-sampling design, regardless of the 'suitability' of the selected interval, this was done to minimise selection bias. The sub-sampled lengths of core were also photographed to ensure that. where anomalies were detected later in the analysis, the photographic record would provide a means of further investigation.

The core was then cut into subsamples that were dispatched to several laboratories. As the data were returned, they were compiled into an access database. Substantial time was spent ensuring correct location of the data using several methods. This is important because to test associations between measures (e.g. Downhole geophysics and UCS) there must be a high resolution on the data location.

4.4 Data acquired

The data collected are described using descriptive statistics that include some measures of spatial dispersion and expected relationships in the data set. This section provides data for this thesis and thus needs to be detailed in a way that supports further analysis and identifies shortcomings in the data collection process that might in future be improved by adapting the data acquisition protocol.

The data comprise several types of tests, collected from several different laboratories, and have been stored in an access database titled Venetia K2.mdb. The numbers of samples collected during this programme are given in Table 7.

Sample Type	Number of Samples
Geomet	130
Geotech	130
MIDA	120
Petrological	627

Table 7: Summary of the number of each type of sample collected.

The aims of the descriptive statistics include:

- Describe the data that has been collected, identify any limitations in the data collection process;
- Data preparation – removing outliers e.g., impact of casing on geophysical readings;
- Evaluation of the relationship between geological characteristics and test responses;
- A comparison and contrasting of the results from the different destructive testing methods; and
- Identification and recommendation of changes improvements that can be made to improve the reliability of the results of this type of testing.

The types of data collected included:

- Petrological logging
- Microdiamond sampling
- Downhole and core geophysical measurements
- Destructive test measures

Results of Petrological Sampling

A total of 43 petrological samples were acquired. The core sections were cut into slabs and polished. The surfaces of the slabs were photographed at high resolution and the images. The variables that were generated during this phase included the grain size distribution and mineral abundance, the summary statistics of this data are displayed in Table 8.

	Total Area mm^2	Lithics Area mm^2	Olivines Area mm^2	Matrix Area mm^2	Lithics Area% mm^2	Olivines Area% %	Matrix Area % %	Lithic Grains count	Olivine Grains count
Minimum	7938	2242.3	0.0	0.0	16.99	0.00	0.00	1	0
Median	15067	5690.6	1564.5	7757.2	36.99	10.43	50.51	1837	896
Mean	14846	6190.8	1519.6	7136.1	42.17	10.09	47.74	1887	1057
Max	16770	13314.9	2825.2	10870.1	100.00	17.80	68.10	4259	3132
Std dev	1699	2488.1	662.4	2407.5	17.82	4.00	14.72	1076	696
Coeff Variation	0.11	0.40	0.44	0.34	0.42	0.40	0.31	0.57	0.66
Count	43	43	43	43	43.00	43.00	43.00	43	43

Table 8: Summary statistics of analysis carried out on petrological slab samples.

The petrological data show the average proportion of area of each sample that is made up of typical so-called ground mass minerals (matrix), olivine and lithics. The olivine gives an indication of the proportion of deep mantle minerals (including diamonds) that are in the sample, the matrix gives an indication of the state of the kimberlite during emplacement, and the lithics give some indication of the proportion of dilution in the kimberlite sample. For this data, although the matrix makes up about half of the area sampled, in some specimens this value drops to zero when the waste contamination rises to 100%. In this sample set, olivine constitutes on average 10% of the area but it ranges from 0 to 17% in the samples.

Destructive test methods

Three different tests were used to determine rock fracture properties:

- Brazilian hardness test
- Uniaxial compressive stress
- Drop weight fracture testing

A brief description of each testing methodology follows:

Brazilian hardness testing:

The specification for this test is given by the American Society for Testing and Materials (1988). It can be described as a compression to failure test where a core specimen, cut into a disc of predefined dimension, is placed under load to failure.

During the compression of the core the deformation of the sample translates the compressive force into a tensile force that leads to tensile failure.

Uniaxial compressive strength

This is also defined as an ASTM test. In this case a section of core is cut to a rectangular cylinder of predefined dimensions and loaded until failure. As the core is loaded the deformation of the core can be measured by means of strain gauges and several other derivatives of rock strength can be calculated.

	UCS Specimen Density	UCS Strength	BTS Specimen Density	BTS Strength
	g/cm^3	Mpa	g/cm^3	Mpa
Minimum	2.38	14.96	2.32	1.3
Median	2.52	31.11	2.52	5.1
Mean	2.56	44.66	2.56	6.2
Max	2.94	169.36	2.90	35.5
Std dev	0.13	39.49	0.14	4.0
Coeff. Variation	0.05	0.88	0.05	0.7
Count	137	137	135	136

Table 9: Summary statistics for the Uniaxial Compressive strength (UCS) and Brazilian Tensile Strength (BTS) test work.

Drop weight tests

A total of 130 core samples that were 63mm in diameter were submitted for testing. A total of 117 results were used for analysis. The method is described in Napier-Munn et al. (1999) and requires several specimens of known size to be crushed with a known energy input.

The 'no data' responses were a result of not being able to cut the core to the required size. This suggests that these samples either were mishandled or had weathered to an extent where cutting was made impractical. The infrared scans of these cores were reviewed to identify high proportions clay in the following samples: 01, 02, 09, 20, 2, 26, 36, 44, 66, 68, 69, 96, 111, and 115.

The t_{10} data were gathered at three different energies and included the density and size distribution of the product material after it was subject to drop weight testing. A total of 117 results were obtained, and summarised statistics are given in Table 10.

	Average Density	t_{10} at 1 Kwh/t	t_{10} at 0.5 Kwh/t	t_{10} at 0.25 Kwh/t
	g/cm^3	% passing	% passing	% passing
Minimum	0.0	0.0	0	0
Median	2.5	32.8	20.89	10.75
Mean	2.3	29.9	18.86	9.83
Max	2.8	41.5	27.04	15.29
Std dev	0.7	10.7	6.92	3.97
Coeff Variation	0.32	0.4	0.37	0.40
Count	118	117	117	117

Table 10: Summary statistics of drop weight results obtained from cores.

In Table 10 it is noted that the coefficient of variation of the t_{10} increases with decreasing energy. This large change in the range of the variability of the response variable may be the result of a few outliers in the data set.

It appears that at an energy input of 0.25 Kwh/t, at which only 10% of the material has been reduced to one-tenth of its original size, that the differences in the pre-existing fractures of the rock specimen used for drop weight measurements has more of an impact than the intrinsic rock fabric. Histograms of this data are presented below.

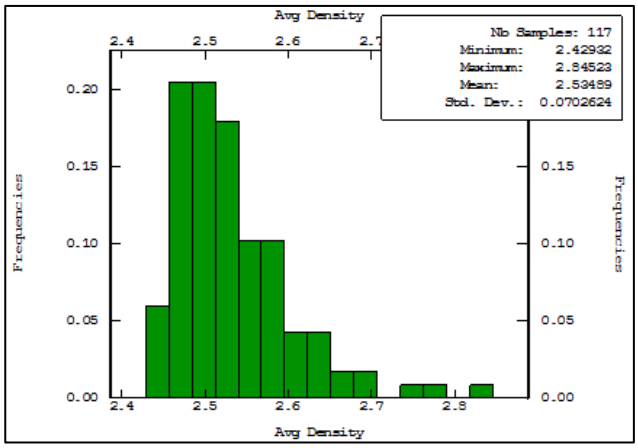

Figure 20: Histogram of the density of samples subjected to drop weight testing.

The t_{10} data range from 41 to 4% passing one-tenth of its original size at three different energy levels. There are some samples which were identified as waste rock that gave results that lie in the tails of country rock; these have been labelled as waste rock.

It is however known that there is a relationship between the lithology from which the sample comes, the density of the sample and the resulting susceptibility to fragmentation. The histograms in Figure 21 show the spread of this data. In this data, the increasing spread of responses is also indicated (the top panel in this figure is at a lower energy than the histogram in the lowest panel). This suggests that at higher energy input levels the range of resulting fracture is higher, and the

histogram is less skewed. This gives an important indication to the design of future experiments, suggesting that appropriate energy levels are required to fully characterise the rocks energy breakage relationship.

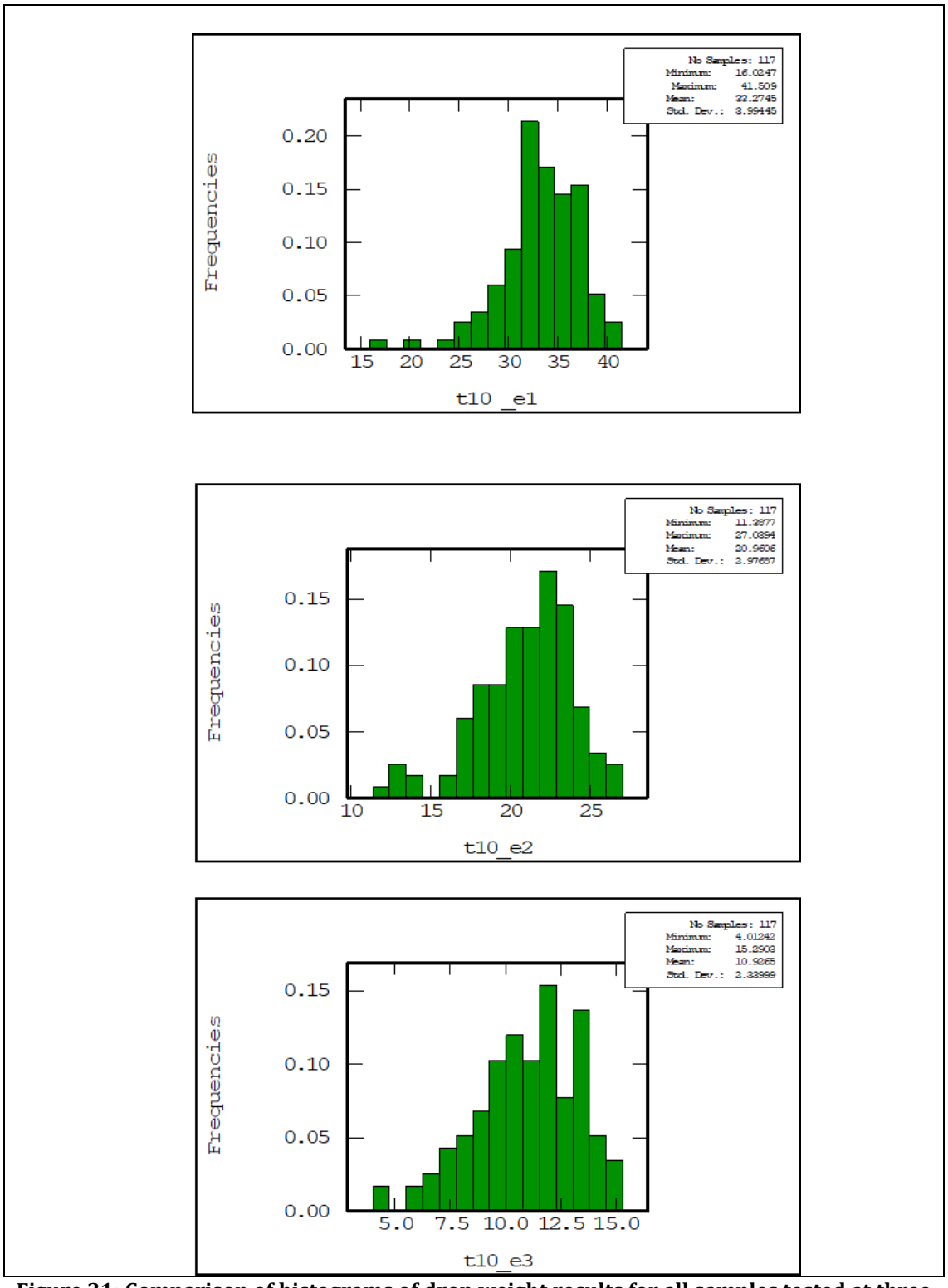

Figure 21: Comparison of histograms of drop weight results for all samples tested at three different input energies (top figure is lowest energy; bottom panel is highest energy).

The samples were taken from two different rock types, a breccia domain which includes many country rock fragments, and a more coherent volcaniclastic domain. The data can thus be grouped using the rock type criteria. Figure 22 and Figure 23 present a comparison of the location and histograms of density for the VKBR and VK domains respectively

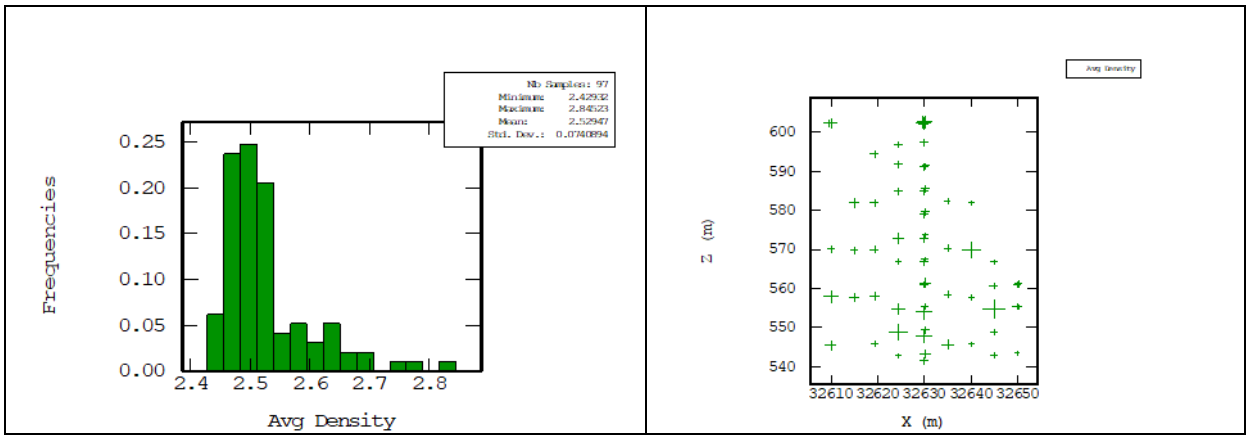

Figure 22: Histogram and base map of sample density for the VKBR domain.

From these figures it is apparent that the VK domain has a smaller variation of density and so we would expect to see a less variable measure of rock fracture for a given energy input as depicted in Figure 24.

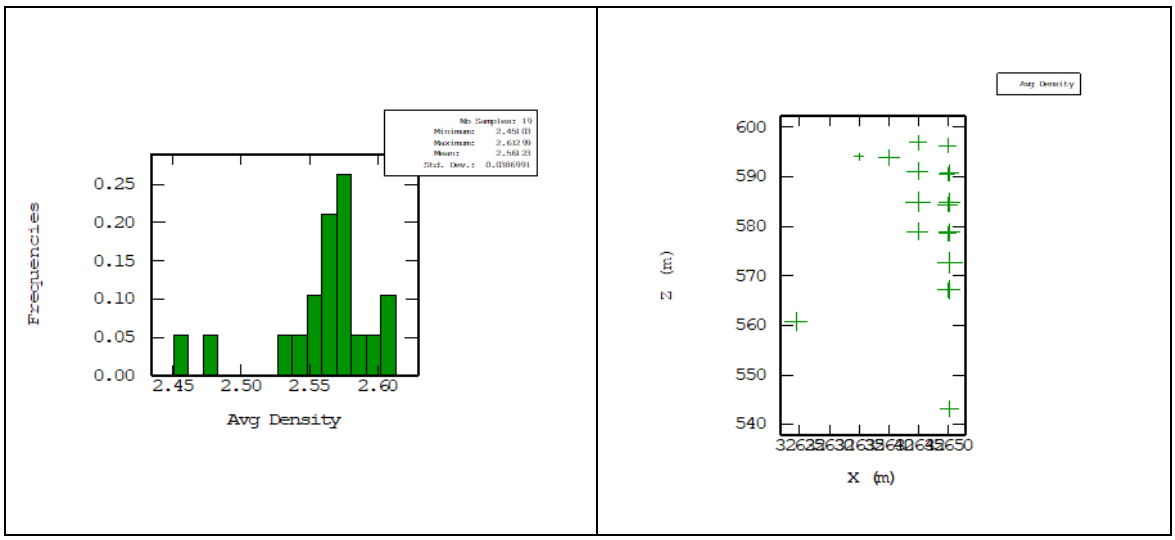

Figure 23: A histogram and cross section of the densities of the samples taken from the VK facies domain

As confirmed by the lower dispersion of the histograms depicted in Figure 24.

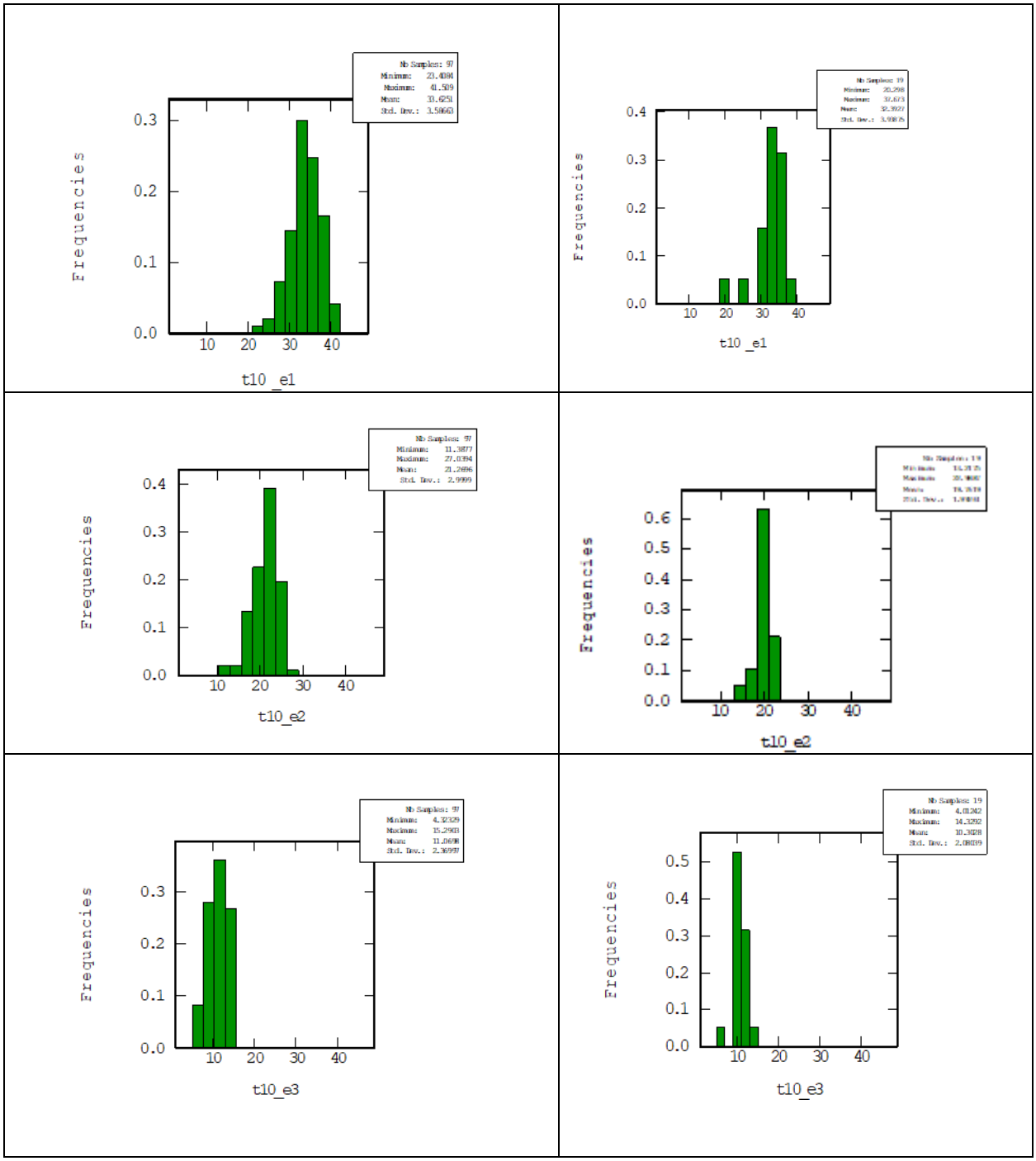

Figure 24: Comparative histograms of drop weight responses at three different input energy levels for the VKBR facies (LHS) and the VK facies (RHS).

This change in location and dispersion of the t_{10} variable with differing energy input suggests that during analysis modelling of this variable in a spatial context will not be trivial. Several approaches to dealing with the skewness and instability of the histogram will always require testing if this variable is to be used.

Descriptive statistics of downhole wireline geophysical data

The downhole data were acquired by running several tools down and up the drilled holes at a controlled rate. All data were then provided to the project and summarised in a database.

Table 11 below contains summary statistics of the results for all holes that were surveyed using the tools provided.

Summary Statistics- Data obtained from Wireline Geophysical measurments										
	Measured Depth	Clipered diameter	Short Spaced Density	Long Spaced Density	Magnetic Suceptability	Neutron Count	Natural Gamma	Resistivity	P Wave Velocity	S Wave Velocity
	m	mm	g/cm^3	g/cm^3	mm^2	#	Api units	Ohm/m2	m/s	m/s
Minimum	0.3	0.0	0	0	-11	0	0.0	0.0	0.0	0.0
Median	24.6	96.3	2.58	2.57	0.3	714.1	90.2	9.9	263.9	488.4
Mean	29.1	95.1	2.53	2.50	17.4	726.1	89.4	34.0	246.6	464.1
Max	69.3	123.2	3.71	3.54	831.0	1698.2	210.7	5013.2	323.4	617.7
Std dev	19.7	13.0	0.58	0.53	110	163	27.1	278.6	58.3	106.1
Coeff Variation	0.68	0.1	0.23	0.21	6.34	0.22	0.3	8.2	0.24	0.23
Count	9726	9726	9726	9726	9726	9726	9726	9726	9726	9726

Table 11: Summary of downhole geophysical readings taken from each hole drilled.

A brief analysis of this data indicates that there is an impact of the steel casing that was used around the collar. This can be seen in the histograms for density which shows several observations in the 3.5 g/cm^3 range (Figure 25). The main implication is that the observations from the cased portion of holes can be used to check the calibration of the density measures, and that it is important to discard this information from any further rock property interpretation.

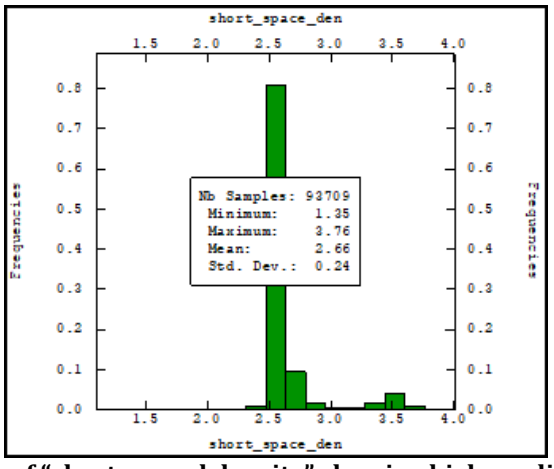

Figure 25:Histogram of "short spaced density" showing high readings.

Statistics of downhole formation hardness testing

The analysis of the data produced in this way aims to determine the following relationships:

- Penetration and lithological and petrological classification;
- Penetration and destructive tests; and
- Penetration and other geophysical measures

The tool was deployed down four holes DDH 357, 358, 359, 365 and 366. The basic descriptive statistics of the downhole formation data is contained in Table 12.

	Hole DDH357	Hole DDH358	Hole DDH359	Hole DDH365	Hole DDH366
Average	1.0	0.5	0.6	1.7	0.6
Maximum	17.8	4.9	15.7	14.7	11.5
Minimum	0.0	-0.6	-1.9	-0.4	-0.8
Standard Deviation	0.7	0.5	0.7	2.1	0.5
Coeff Variation	68.2	113.3	134.6	125.0	82.7
25 th percentile	0.7	0.2	0.3	0.4	0.4
75th percentile	1.0	0.6	0.6	1.8	0.8
Interquartile range	0.4	0.4	0.3	1.4	0.4

Table 12: Descriptive statistics of the downhole formation tester results.

A plot of the three readings for hole DDH357 is shown in Figure 26, a histogram and downhole variogram of the cutter penetration (the difference in location between the calliper and cutting wheel) is provided in Figure 27. The ranges of the data clearly demonstrate that the unit is indeed responding to the different lithology types and higher variances in penetration are seen in breccias. It is also interesting to note that the points of extreme deflection are associated with break out from the drilled cavity. This information can be used to quality control the downhole calipering of the holes.

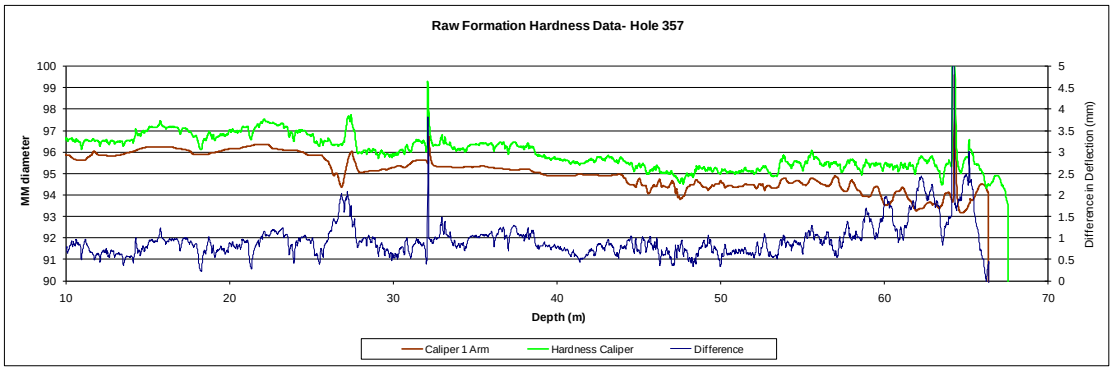

Figure 26: A plot showing the three readings generated by the formation hardness tool for hole DDH357.

As can be seen from the downhole semi-variogram (Figure 27)the range of the raw semi-variogram is of the order of 15 m, justifying the requirement for spacing of holes by approximately 7m.

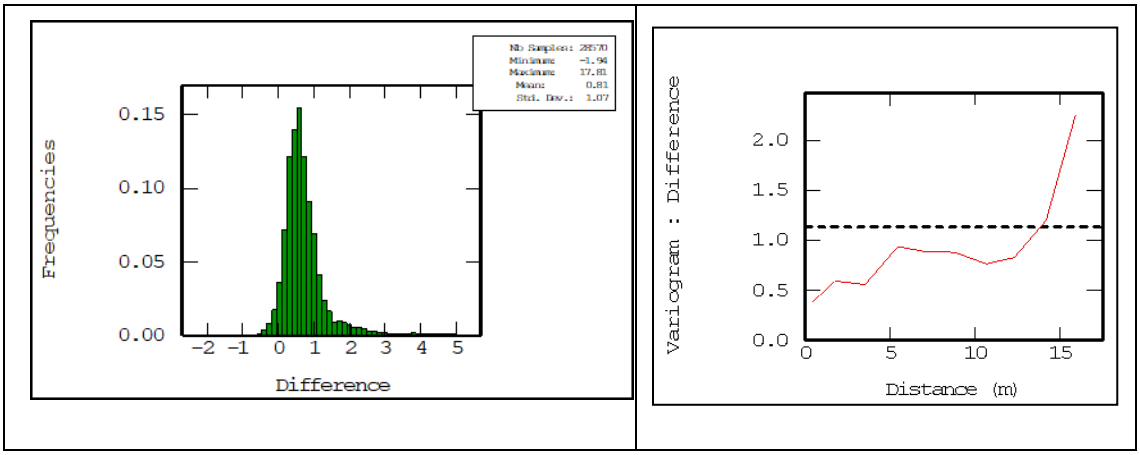

Figure 27: Histogram (LHS) and semi-variogram (RHS) of mm of deflection ('Difference')measured by the downhole formation testing device.

4.5 Observations arising from the data collection

The design and execution of this programme required substantial support from the mine and its operational staff for which the researcher is very grateful. Ensuring that the right equipment and access could be provided to the site required substantial planning and coordination. It is essential that in the execution of this type of study that frequent and on-going communication is facilitated.

Several of the test units, which although they were housed in an air-conditioned container, had occasional problems with operating temperature and dust. As this campaign aimed to get many different types of close spaced data from the samples generated the programme took several months to complete. The study does however demonstrate that it is possible to obtain collocated data of different types for the evaluation of kimberlitic deposits.

The petrographic data that have been gathered provide a basis for segmenting the geology of the test area based on the composition of the rock mass and the abundance of different types of rock fragments. The analysis shows that one of the limitations in the data collection was the misinterpretation of the location of the contact between the breccia and coherent volcaniclastic kimberlite. This led to the coherent volcaniclastic kimberlite being under-represented in the dataset.

The destructive data that have been gathered is co-located with multiple geophysical measures and hence provides a basis for investigating the potential to

use the geophysical data to augment the destructive test data and improve the estimation of the physical characteristics of the kimberlite properties in the test area.

The sampling programme required substantial supervision of the core extraction, core handling and tracking through the protocol. Use of core and hole imaging provided an excellent basis for quality control of the multiple processes that the core was exposed to. As the two images can be compared side by side it is possible to correctly allocate core loss and identify where cores have been incorrectly loaded into core trays. Ideally this analysis should be carried out between core collection and subsampling to prevent incorrect allocation of core to test destinations. The primary use of the images in this experiment was to ensure that the geophysical data that was collected was correctly matched with to the samples selected for destructive testing.

4.6 Conclusions arising from data collection

A data set was generated for this research by samples taken from, and measurements made on, two distinctly different rock types; a highly variable kimberlite breccia and a more spatially continuous volcaniclastic lithology. The data have been quality controlled and then captured and compiled into a substantial and accessible database to facilitate further analysis.

This experiment aimed to demonstrate that it is possible to overcome some of the challenges that are faced in the collection of samples and generation of data that can be used to generate spatial characteristics of kimberlite rocks. Due to constrained access to the orebody and limited sample mass that is typically acquired the sample design must try, as far as possible, to optimise:

- the spatial location of the cores,
- the sub-sampling of the core and assignment of appropriate measures and destructive tests on the core, and
- the use of the core hole that is drilled for additional data acquisition.

The next chapter expands on the statistics and reviews associations that exist between the measures made and demonstrates how these can be used to generate estimates of rock properties at un-sampled locations.

The work described here comprises a cost-effective method of generating unbiased samples that can be used to measure a range rock properties. The colocation of destructive and non-destructive measures facilitates the investigation of relationships that can be used to predict the destructive measures at unsampled

locations. The data gathered here and their use in the value chain model to predict the expected range of the metallurgical recovery factor is explored in the next chapter

The quantitative understanding of the spatial characteristics of geological, mineralogical, geochemical and geophysical variables and their impact on physical characterisation can be used to improve the design of future sampling campaigns.

The approach that has been demonstrated here is applicable in the exploration phase of new deposits and is also of significant use in assisting the sampling programme design when extension of the resource and reserves of existing operations is required.

5 MODELLING PHYSICAL CHARACTERISTICS OF OREBODIES

5.1 Introduction

A model of the in situ ore and waste-rock properties that impact on the mining and recovery of diamonds is required as an input into the value chain model that is used to estimate the expected overall diamond recovery.

The properties that are important can be usefully classified as two types of variables:

1 -Primary (in situ) variables: these are mostly characteristics that can be directly measured, for example measurements of grade, density, grain size; and

2 -Response variables: these are measurements of the result of doing something to the rock - for example recovery, throughput etc.

This framework is designed to assist with developing sampling approaches and identifying the most appropriate spatial modelling approach. The proposed framework can also help identify the risks associated with designing, sampling and modelling of both types of geometallurgical variables (Coward et al., 2009). The important aspect of the framework is that primary variables are, in general, far easier to sample, and estimate, whereas response variables require far more thorough consideration.

Current approaches reviewed to date that are used to model rock characteristics are limited in that they aim to produce BLUE (Best Linear Unbiased Estimates) of the characteristics. These properties of the estimate can be useful for several purposes e.g., when the estimate is being used in a long-term design optimisation process but may have some limitations when used in a value chain model as the estimates produced are smoother than the real in situ variability. The methodology demonstrated here suggests the use of estimates and simulations of the rock

characteristics, which allows the variability and uncertainty of the characteristics to be propagated through the value chain.

In this chapter the different methods of spatially estimating rock properties at an appropriate scale for inclusion into a spatial block model are explored and their impacts on the value chain model analysed. This leads to a recommended sequence and approach to generate orebody models that have properties that will have the required characteristics for use in the value chain model to derive the range of values for the metallurgical recovery factor.

The process of building appropriate robust spatial models of rock properties includes:

- Identifying and selecting the characteristics of the ore and waste rocks that have a material impact on the process rate and efficiency;
- Design and execution of a sampling programme to acquire enough mass and number of representative samples of material from each 'domain;'
- Selection and preparation of samples for laboratory-scale treatment test work;
- Quality control of numerous laboratory tests;
- Relating primary physical rock characteristics to test responses;
- Support and scale corrections for laboratory-scale test results to process scale response;
- Modelling of spatial behaviour of acquired data;
- Estimation and/or simulation of characteristics at block scale; and
- Evaluating the error, variability and uncertainty of the estimates made.

Figure 28 presents a schematic of an approach to developing models of required rock characteristics.

The process of building spatial models is centred on data that can be acquired in many ways, one useful distinction is that between 'direct' and 'indirect' data (Dowd and Pardo-Igúzquiza, 2006). 'Direct data' are data acquired from a sample taken from a known location. The sample data are acquired by subjecting the sample to a

controlled measurement or testing process. This is referred to as direct in that the result and the location, and to some extent the error, of the data can be directly associated with the sample that has been treated.

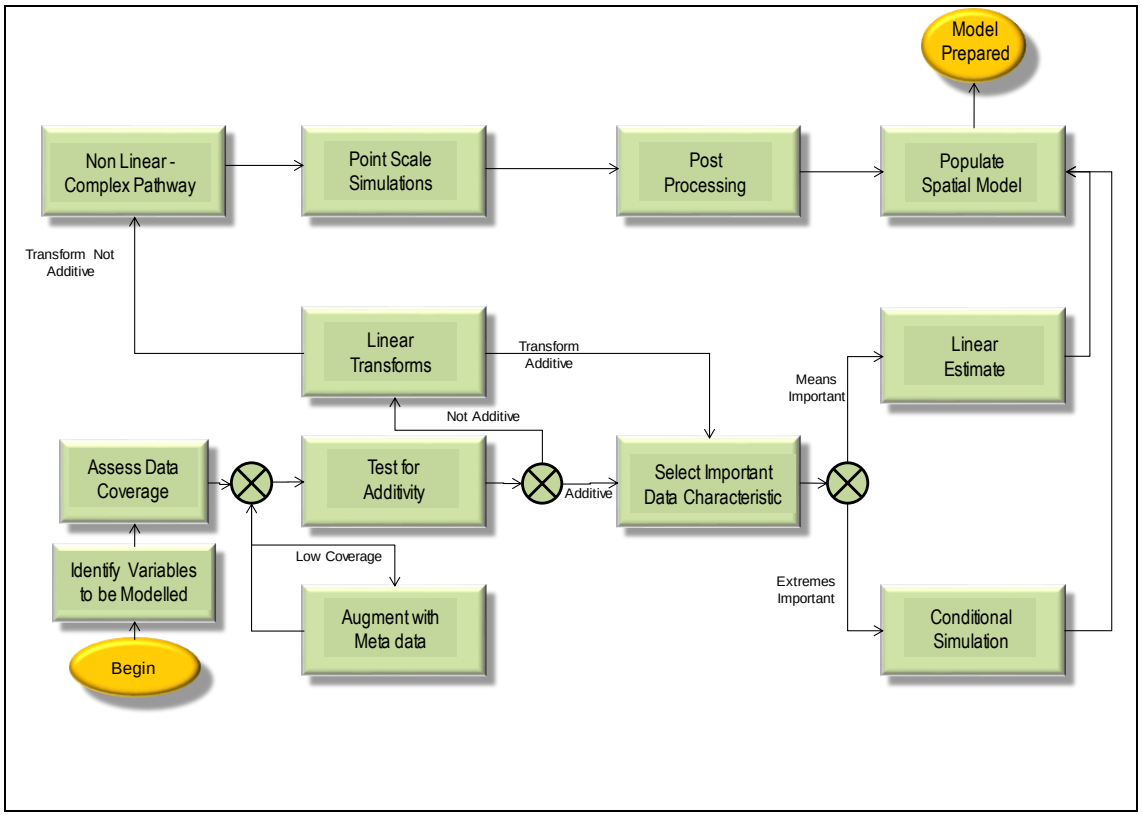

Figure 28: Schematic showing pathways of generating spatial models of rock characteristics.

The term 'indirect data,' on the other hand, refers to the acquisition of data where the input is acquired from a tool that measures the rock response to a geophysical input; the geophysical response is then used to inform the property of the rock that would have exhibited had it been exposed to direct testing and measurement, but in an indirect way though some form of mathematical model. The value of integrating these two data types is that the relationship between the direct and indirect data can be used to improve the estimate of the unknown quantity at un-sampled locations.

Importantly, direct data are usually sparse and need to be expanded in coverage and support. Indirect data can, however, be adapted to provide larger support, is far more exhaustive and usually needs some form of compression or summarisation.

In this chapter, methods to improve the quality of the rock characteristic estimates using relationships between the direct, indirect, non-destructive and destructive data are explored. These improvements include the reduction of the error of the estimate of rock characteristics derived from destructive tests at un-sampled

locations and the identification of potential sampling bias that might arise from sample selection.

The approach adopted can broadly be separated into two phases. The first is an exploratory data analysis phase in which relationships between the variables of interest are evaluated, followed by a second phase that evaluates different methods for spatially estimating values into the block model needs to be considered.

This chapter begins with a brief review of the data that have been collected from the experiment. These data are then used to a) improve the estimates of the rock characteristics at point scale 'down the hole' using a few multivariate techniques and b) to review the implications of different pathways that are available to generate block scale estimates of response variables.

5.2 Estimation options considered and compared

Previous work on the integration of different sources of data has included several methods that use spatial data to generate property estimates at block model scale (Dowd 1997, Dowd and Pardo-Igúzquiza, 2006). These can be grouped into two types:

1)Those designed to deal with large amounts of data in a reductionist way - these use a variety of multivariate statistical methods, including linear regression, principal components; and

2)Those used to understand and exploit the spatial nature of the data to generate spatial estimates of variables at a mining block scale. These methods also use spatial covariance models to integrate direct data and sensed data .

Multivariate modelling techniques include linear regression modelling, principal components analysis, and partial least squares models (Esbensen, 2002 and Wackernagel, 1995).

Spatial modelling approaches considered here include polygonal estimation and linear geostatistical methods. In Dowd and Pardo-Igúzquiza (2006) direct and indirect sample data are integrated using several methods. The performance of the various estimation methods was assessed by a range of statistics including mean error and mean squared error.

The methods used included ordinary kriging, standard linear regression, and estimation of a local mean, and simple kriging with estimation of a local mean,

kriging with external drift, co-kriging, and Bayesian integration. The outcome of this study indicated that if there is less than 10% direct data available, and the correlation between direct and indirect data is less than 0.3 then geostatistical methods are better as they give lower mean squared errors than linear regression. Co-kriging is best when the correlation co-coefficient is above 0.2. Above 0.3 external drift and or local means perform best (Dowd and Pardo-Igúzquiza, 2006).

Spatial variables assume values that change as some function of the support and locations at which they are measured. Most spatial estimation methods create some form of weighted average the measured values of a variable at a point, over a specific volume (e.g., the grade of a drill core is the average grade over a cylinder of rock). The variance of a spatially correlated variable usually decreases as the support on which the measurement is taken increases. There are several methods available for using point data acquired from some location in space to estimate the value of a spatial variable at an un-sampled location and these are briefly reviewed.

The simplest of these is to create a polygonal estimate where the values that have been measured in the sample are used to inform a volume around the sample. In this approach, no averaging is carried out, but neither is a specific change of support calculation, so that the estimate will have a variance that is a function of the sample layout, and hence volume estimated, and it is likely that the estimates generated in this way will have a lower variance than the real values.

Ordinary kriging is a minimum variance, linear, unbiased estimator (Journel and Huijbrechts, 1978). It has been applied successfully in many fields where the variable of interest has a spatial component and is widely used for grade estimation in mining. The estimate at any given location is a linear weighted combination of a selection of the sampled values.

When using a kriging approach for estimation, the spatial variability of the data is characterised in the form of a spatial covariance model or semi-variogram. Reliable estimation of the parameters of the spatial covariance model requires sufficient data that are representative of the domain within the orebody that is to be estimated. Domains are variable-specific and selecting and defining domains of stationarity for response variables requires consideration of both statistical and geological aspects of the variable to be modelled.

Rock characteristic variables may require sampling on various sample volumes and over a range of distances to provide an adequate quantification of spatial variability. Linear geostatistical estimation methods (e.g. ordinary kriging) require variables to be additive. Thus, if the variables are non-additive this process is not applicable but may be used if a data transform can be used to render the data sufficiently additive,

or if the range over which the variable is observed appears not to show too much non-linear behaviour.

In some cases, however it is the extreme values that are of interest in the orebody – e.g., for example extreme hardness that will damage crushing equipment. In this case geostatistical simulation methods are required. These can be used to honour the data at the sampled location and produce the variability at a scale suitable for the value chain model. Individually the simulations present a 'truer' reflection of variability in the ore characteristics, and when used as a set can give an indication of the range of values for the characteristic of interest. Methods described in the literature review will be demonstrated here.

5.3 Selection and preparation of physical characteristic data for estimation

The variables selected for modelling are useful for predicting process performance and diamond recovery. These broadly cover variables that will influence the fracturing of the rock in a process, and the efficiency of the separation of diamonds from their host rocks.

There are several destructive tests that can be used to measure the strength of rock specimens. In this work the focus has been on obtaining data that quantify the nature of the rock strength in tension and compression, and the fracture that results from energy input. The tests considered include uniaxial compressive strength (UCS), the Brazilian tensile strength (BTS) and t_{10}.

Some existing test standards have well-defined support, even though this may be inappropriate for all rock textures (ASTM, 1998). This is because the scale at which they are carried out may not be sufficient to measure the responses that are valid at the scale of the required estimates. This is arguably true of rock strength measurement in coarse grained rocks or in breccia lithotypes. To overcome this, it is suggested that several tests are conducted over a range of sizes larger and smaller than those laid down in the standards in use.

Several of the rock characterising tests (Bond Work Index, Drop weight test, UCS, BTS) have been developed to mimic at a small scale the processes that the rock will undergo during mining and treatment. The underlying philosophy has been that if one can obtain a representative sample it is possible to carry out small-scale tests with sufficient rigour and control to enable their results to be scaled up using some form of factorisation.

5.4 Using multivariate techniques in estimation

During the acquisition of rock characteristic data, it is possible to augment the primary point data with higher coverage, but potentially lower quality, geophysical data. As the support of the destructive and non-destructive tests may be vastly different, the raw data require some transformation to enable the two types of data to be used together.

Scaling of geophysical data

Downhole geophysical readings create a valuable data set as the readings are continuous and data acquired from different tools can be used in concert to improve the estimate of destructive results at un-sampled locations. The downhole geophysical wireline log readings are taken approximately every 10mm. At this scale, the tools are potentially responding to several very small features, and the readings may to some extent be smeared.

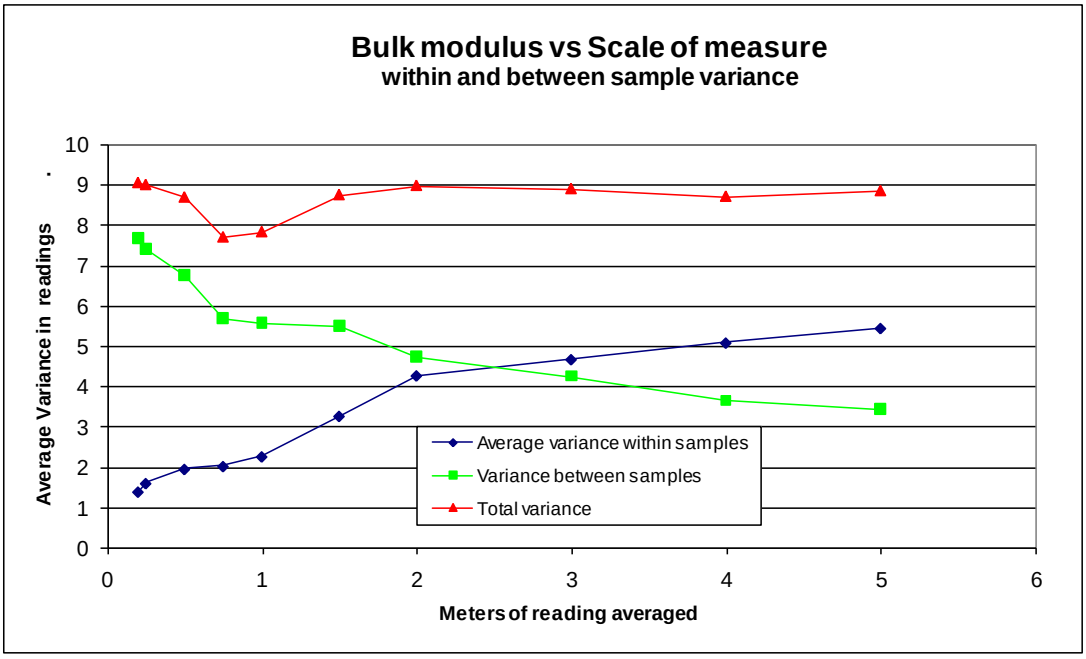

Figure 29: A plot showing the impact of the size of the interval used on the total variance of the bulk modulus measurement.

To improve the relationship between the wireline geophysical signals and the destructive tests the geophysical signals need to be accumulated. The data were accumulated over increasing intervals and the within and between interval variance calculated. The interval over which the sum of these variances is minimised is deemed to be the appropriate length for averaging the geophysical signal. In the case of acoustic data this was found to be about 70cm of readings (Figure 29).

This has the impact of reducing the signal variance and improving the correlations between the wireline geophysical log and the results of the destructive tests. It is strongly recommended that in the search for appropriate proxies this approach to upscaling be used to evaluate associations between destructive and non-destructive rock measurements.

Linear regression models

The correlations between all measured data were calculated. Some of the higher correlations were observed between acoustic velocity and various measures of rock hardness. Indeed, it is possible to translate acoustic velocities into various estimates of destructive rock properties using the formulae discussed in Momayez et al. (2004).

In this case it can be demonstrated that in the volcaniclastic facies there is a reasonable correlation between the formation hardness tool estimate and the measured UCS, as shown in Figure 30. In this plot, the correlation is relatively low, even though several outliers have been removed from the data. This is partially because of the breccia lithology being a very heterogeneous rock type.

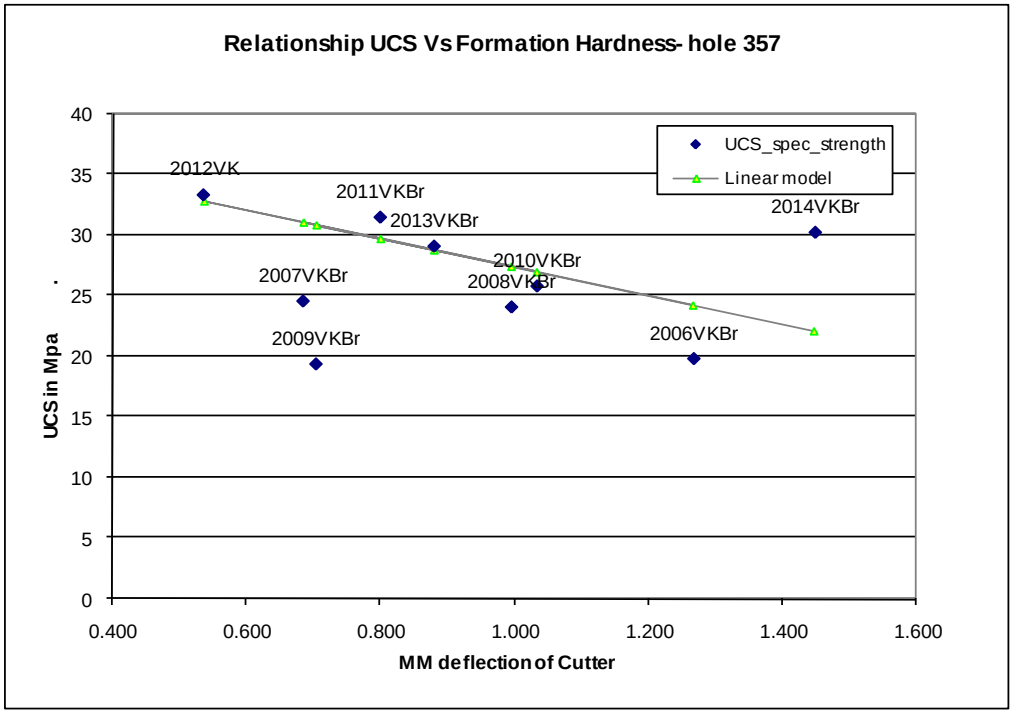

Figure 30: A plot showing the linear model developed between the formation hardness tool readings and the UCS values.

Even though the relationship is weak, it is possible to use these data in several ways, such as co kriging to improve the estimate of the destructive variable (UCS) using the downhole response (Cutter deflection).

Multivariate techniques for data augmentation

There are several multivariate techniques available to integrate data of different types. This creates an opportunity to augment sparse destructive data with more abundant geophysical data to improve the estimate of the response properties. (Dowd, 1997).

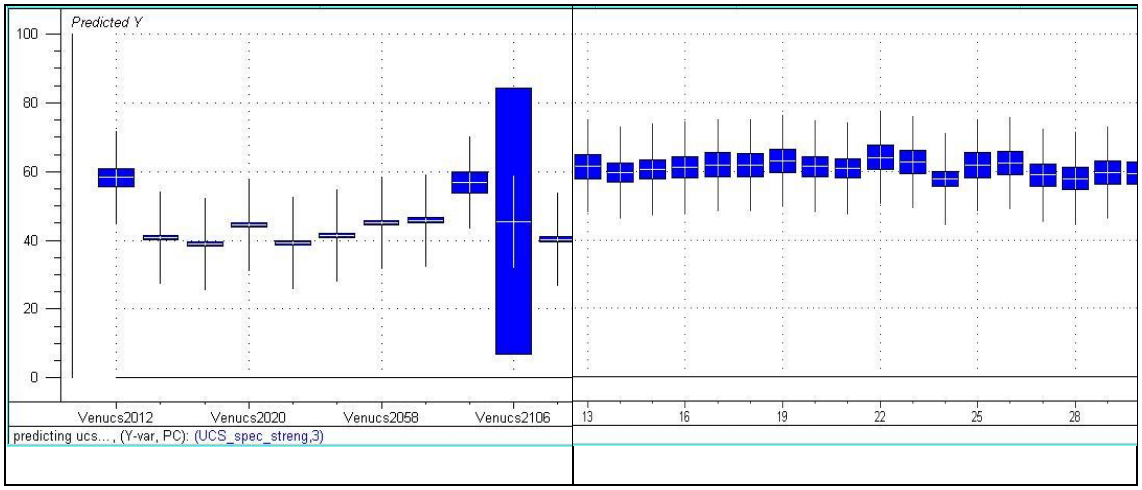

Figure 31: A box and whisker plot showing the sample value used to calibrate the PLS models on the left of the plot, and the estimate of UCS down the hole on the right. The heights of the bars indicate 'goodness of fit' of the partial least squares model derived from multiple versions of the model using different combinations of sample and hold out data.

The sampling experiment gathered abundant geophysical data that are correlated, albeit weakly with the spatially sparse destructive data. In this case a trial was made using a PLS model to estimate the UCS of core along its length. To do this, a calibration set of samples is required to define the relationship, which can then be used to estimate the values at un-sampled locations. In Figure 31, generated using Camo's Unscrambler software, the sample values are plotted next to an estimate of the values downhole 358. The very high bar on the left shows that there is one sample (Venucs 2016) for which the relationship between the model and the actual value is very weak and does not correspond with the model parameters.

There is also a way to incorporate directly the results of the acoustic velocity data into the downhole estimates. These can be plotted together to provide a means of visually reviewing the models as shown in Figure 32.

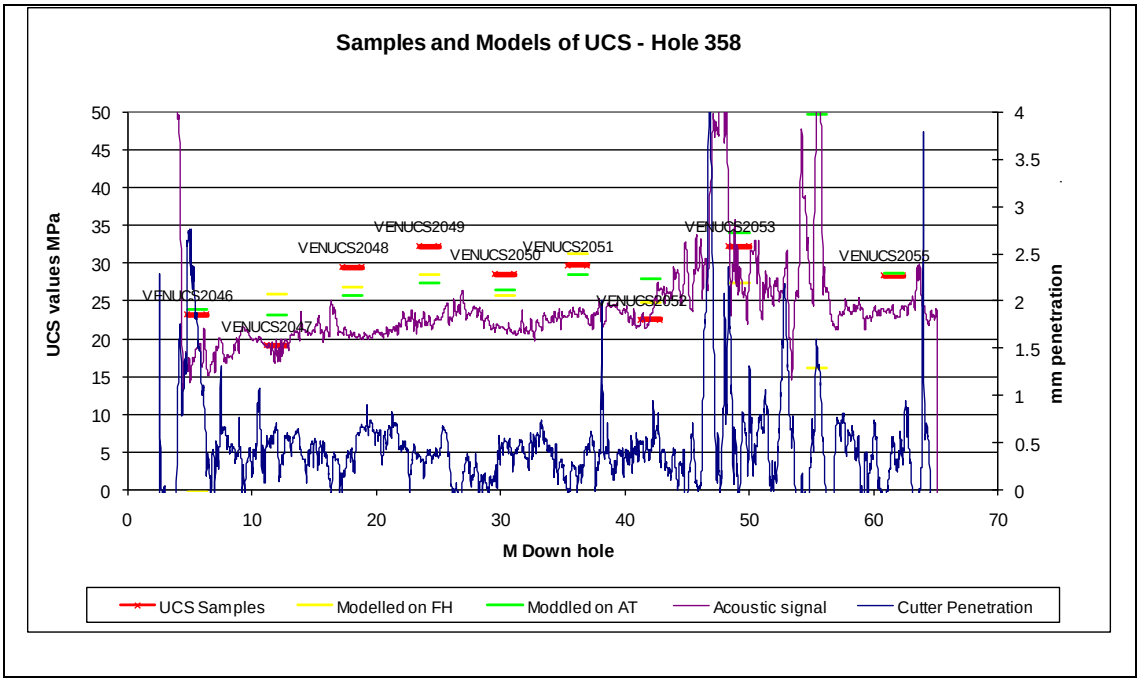

Figure 32: A plot of measured UCS values, and models for the samples based on the downhole acoustic signal and cutter penetration depth.

In Figure 33 the UCS values down the hole for the samples recovered from the VK facie have been calculated using a PCA model of P-wave acoustic velocity measurements, S wave acoustic velocity measurements and measured densities. The boxes show the range of values that would be calculated for redoing the PCA multiple times and leaving out approximately 10% of the data in draw – this gives a sense of the uncertainty or potential error that is in the PCA model.

Multivariate model validation and future work

Results of several methods have been presented, however rigorous testing of the assumptions and reliability of each approach is still required. The ideal way to do this is to generate simulations that can be 'virtually' sampled, and the samples used in the different ways demonstrated here. This would provide a method to compare and rank both the benefits and deficiencies of each method.

The second way in which these methods can be evaluated is to generate estimates and then evaluate the predictions based on the actual properties that are encountered when this part of the orebody is mined. The challenge in this approach is that the estimated ore will not be the only source of rock to be treated. There will, however, be an opportunity to carry out in-pit sampling as the mine deepens and

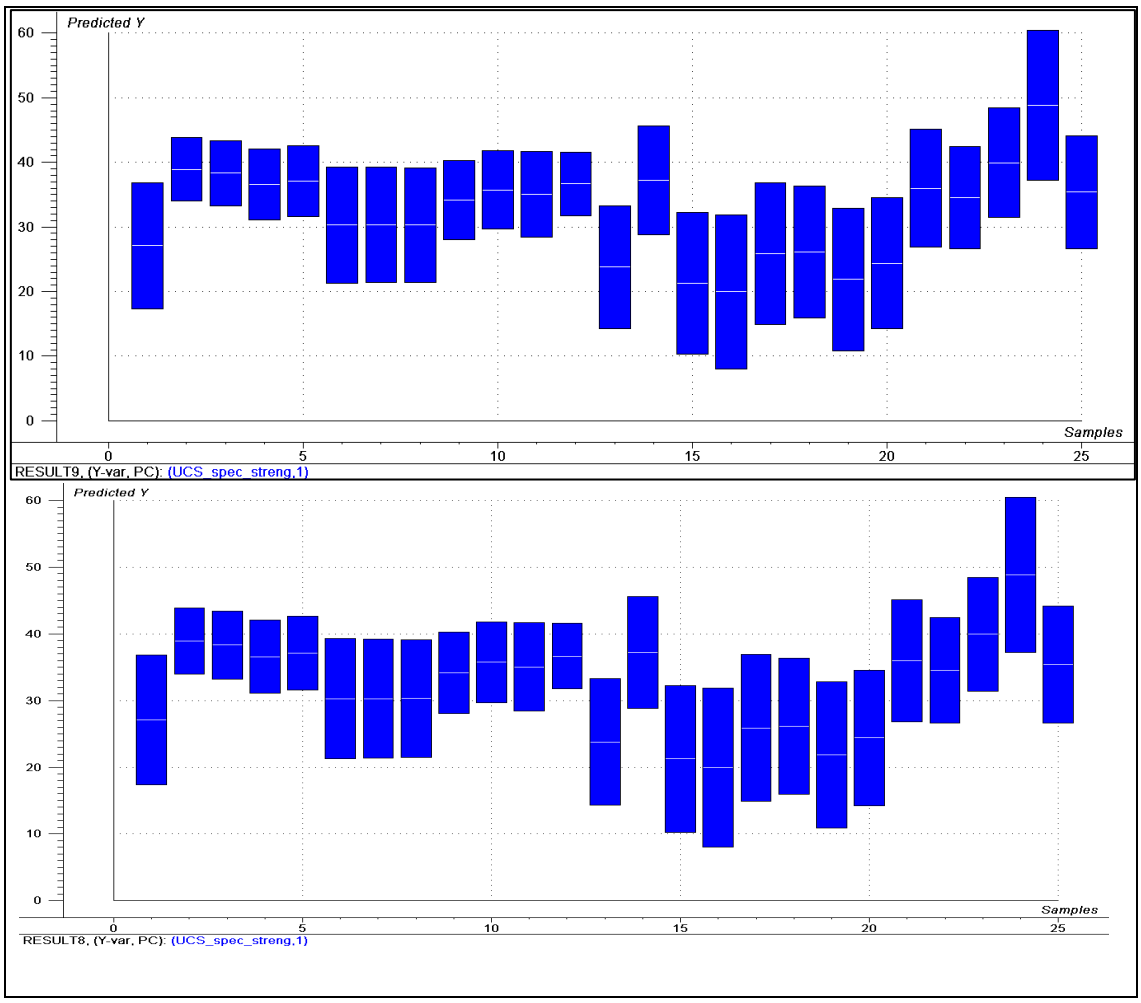

Figure 33:PCA model of UCS downhole based on a Principal Component Analysis (PCA) model using P- wave velocity, S wave velocity and long density, using one principal component (upper panel) and two principal components (lower panel).

5.5 Estimation and simulation methods

The benefits and limitations of a few approaches to estimating rock characteristics are explained and demonstrated.

Polygonal

For a highly heterogeneous domain in which the underlying spatial structure cannot be discerned it is reasonable to assign each sample attribute value as the best estimate of the attribute of a volume, of specified shape and size, centred on the sample. In this case downhole models would be used to generate estimates for samples of 70cm cores (as indicated by the prior work on upscaling). These can then be used to estimate the values into polygons measuring 0.7m*0.7m *0.7m. In this way, the sample statistics and the block statistics would be the same (which, of

course, is impossible). The sample and estimate statistics using this method on the experimental area are contained in Table 13.

Statistic	Sample Values	Polygonal Block Estimate values (0.7mx0.7mx0.7m grid)	Polygonal estimate averaged into 5m x 5m x 5m block model
Count	116	376 094	1330
Minimum	16.02	16.02	21.2
Mean	33.30	33.15	33.42
Maximum	41.51	41.51	41.51
Variance	16.03	16.09	13.61

Table 13: Summary Statistics for drop weight test data showing sample and polygonal statistics.

The underlying assumption with this approach is that the samples and modelled values are representative of the areas between holes. When drilling is not closely spaced this assumption may become very tenuous. The impact of sample layout on the estimate generated using this approach is demonstrated in Figure 34. Note how samples that are located far from other samples influence a far larger area than samples close together.

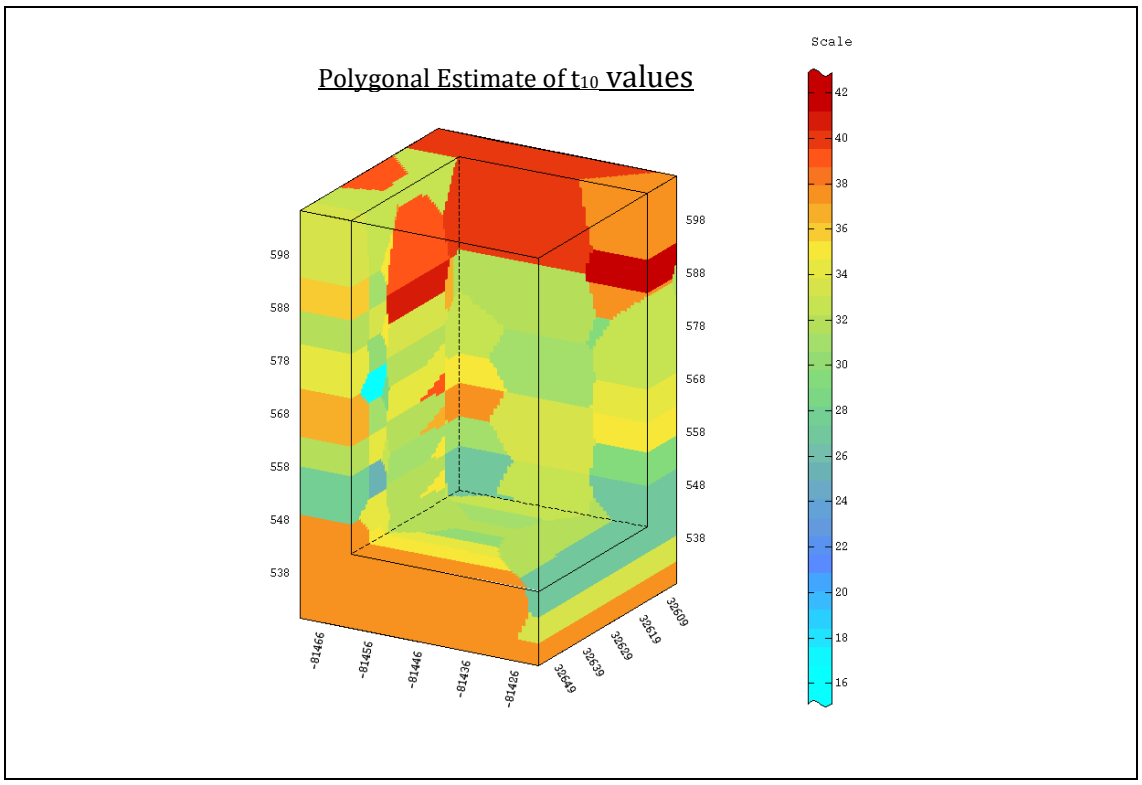

Figure 34: A 3d representation of a polygonal estimate of drop weight values in the 0.7m x0.7m x 0.7m grid.

Geostatistical estimation and simulation methods

The data were imported into Isatis, a geostatistical software package, and raw semi-variograms were calculated, modelled and interpreted. Initial analysis has detected ranges in the order of 6m to 15 m. This short range is thought to be due to the nature of the orebody sampled and the small specimen size.

Increasing the support by 'compositing down the hole' has not decreased the overall variance as the samples are not contiguous along the core. Further experimental work would be required to determine the impact on both the distribution of destructive rock property values and their ranges. One approach might be to acquire larger diameter core and thereby increase the sample support. This would, however. increase the cost and time taken for sampling.

The experimental and fitted semi-variograms for the UCS data are displayed in Figure 35.

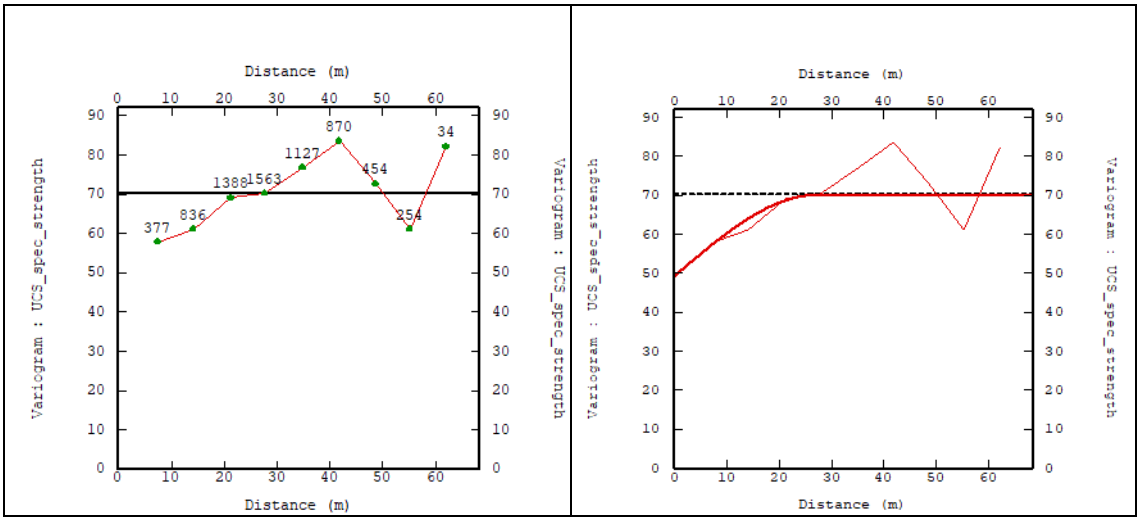

Figure 35: An experimental and fitted model for the variogram for the UCS data.

The fitted semi-variogram model comprises a nugget effect and two spherical structures with ranges of 25m and 27m. The kriging was carried out with an isotropic search radius of 27m and used a minimum of 5 samples and a maximum of 10. A cross-section of the area estimated is depicted in Figure 36, where hotter colours represent higher values and cooler colours represent lower values.

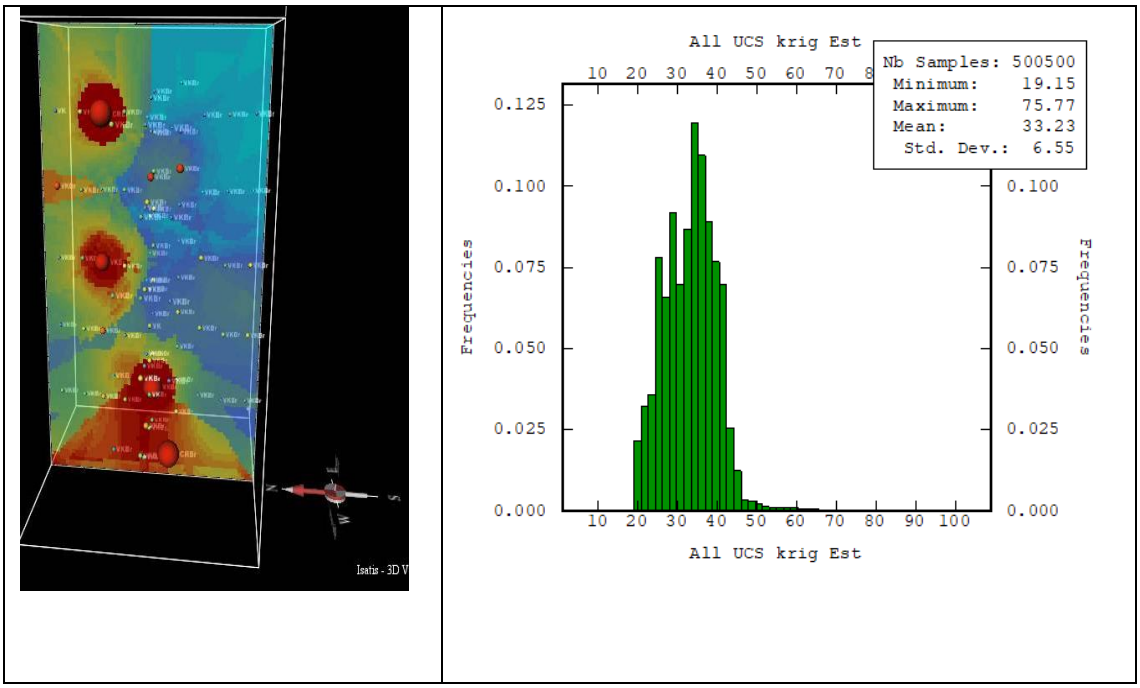

Figure 36: N-S cross section of area estimated showing high UCS estimates in hotter colours and lower values in cooler colours (LHS) and a histogram of the block UCS values estimated.

The statistics of the estimates as shown on the histogram indicate that the mean of the UCS is slightly lower than the mean of the samples but that the standard deviation of the block UCS has dropped from 27 to 6.5. It is also evident that the estimate in this specific case is influenced by a few very high values.

Fortunately, the data were collected with very well documented geological descriptions and it was possible to determine that these results had been influenced most strongly by their waste rock content. This suggests that when sampling for rock characteristics, especially in breccia kimberlite facies, there may be a requirement to carry out some form of indicator kriging to deal with the highly skewed nature of the so-called 'contaminating country rock fragments.' Alternatively, a separate estimate of the proportion of dilution of each major type might be used in generating the spatial model.

Comparison of estimation and simulation techniques for rock characteristics

Estimation of individual rock property variables using linear estimation techniques, such as ordinary kriging, will produce results that are unbiased provided a number of assumptions are met. One of these requires that the variables of interest are additive. The additivity property of a variable requires that the arithmetic mean of a variable at an unsampled location can be calculated, without bias by a linear weighted combination of the available data. There are some variables, including many of those that describe rock characteristics response variables, that are not strictly additive. The values at unsampled locations can technically be estimated at sample scale using linear methods, but these estimates will be biased in some way. This approach may in a few unique cases be acceptable when resulting bias in the estimate may not have a material impact on the use of the biased estimates. Unfortunately, it is not always possible to determine the magnitude and sign of the bias nor to reliably identify when the resulting bias may have material impact.

As an example of a non-additive response variable, t_{10} represents the mass proportion of a sample that is below a given size fraction following a controlled breakage test. In some cases (e.g. if the samples were all of the same support and density) it would be possible to transform this variable using data from the sample to the mass of the sample that is below a given size for a given energy input, a 'mass by mass' variable much like metal grades. In the post processing of these estimates it would be possible to predict fragmentation and mass flows by using the energy size relationship presented in Equation 13.

Carrasco, Chiles and Séguret (2008) present a mechanism to test the consequences of treating a non-additive variable as additive. In this model a comparison is made

between the 'illegitimate average of ratios' and the 'legitimate ratio of averages' as presented in Equation 10.

$$\boldsymbol{R = \frac{Z_r}{Z_h}} \qquad \textbf{Equation 10}$$

Using a similar notation, the variables in this case would represent :

$\boldsymbol{Z_h}$ as the in situ sampled t_{10} can be treated as the in situ ratio, or proportion, and can be incorrectly estimated using kriging from samples into blocks.

$\boldsymbol{Z_r}$ can be considered the size distribution that results from crushing at the treatment plant derived by correctly converting t_{10} into the mass proportion in a block of a given size; and

$\boldsymbol{R}$ is the response variable the ratio of the treated and mined t_{10}. represents the process response variable of tonnes to undersize of 2mm

In this way it is possible to calculate the **R** variable in two different ways and then determine the impact of the underlying bias that arises from averaging a non-additive variable. :

The difference between the two approaches will be 'immaterial' when:

$\boldsymbol{Z_h}$ is constant, or $\boldsymbol{Z_r}$ is a constant;

the ratio of $\boldsymbol{Z_r}$to $\boldsymbol{Z_h}$ is a constant;

or the range of the values of $\boldsymbol{Z_r}$, $\boldsymbol{Z_h}$ and the change in the ratio of $\boldsymbol{Z_r}$to $\boldsymbol{Z_h}$ is very small.

In the case here block size is assumed to be constant and so it is likely that the impact of the bias of incorrectly using a linear geostatistical technique would be almost immaterial. It is possible to krig and apply weights w_i to the samples to estimate the ratio of two variables ($Z_1(x)$ and $Z_2(x)$)where the data for both variables is available at all sample Equation 11.

$$\frac{\boldsymbol{Z_1^*(x)}}{\boldsymbol{Z_2^*(x)}} = \sum_{\boldsymbol{i=1}}^{\boldsymbol{n}} \boldsymbol{w_i} \frac{\boldsymbol{Z_1\,(x)}}{\boldsymbol{Z_2\,(x)}} \qquad \textbf{Equation 11}$$

The ratio of the two estimated variables will be unbiased if ;

- the weights sum to one ($\sum_{i=1}^{n} w_i = 1$);
- the same variogram is used for the estimation of $Z_1^*(x)$ and $Z_2^*(x)$; and
- first order stationarity holds , at least within the search neighbourhood.

As a further caution, even if it is possible to mathematically justify an assumed 'quasi-additivity', the use of linear estimation techniques may still result in material post processing errors, especially when the response of the process that will be determined from the estimate involves physical blending of different rock types. In the case of using t_{10} data to predict the fracture of mixtures of rock types may result in material error as the energy transfer between rocks of different strengths is, in many cases, non-linear and so the overall degree of fracture is related not only to the t_{10} values but the differences between the t_{10} values that are being mixed.

It is also important to distinguish between estimating sample-size volumes and estimating larger volumes. The variance of the latter must, of course, be less than the variance of the sample data. The estimates of the larger volumes will also have lower variance than the real sample volumes, but for larger volume data, we don't know the real variance.

Spatial simulation on the other hand will produce models of block values that have a higher variability than estimated kriged models which may be useful for assessing the impact of rock property variability on process performance. The assumptions of the data properties for spatial simulation are more onerous and require sufficient sampling to enable modelling of the histogram of the data and testing of geological domains to ensure that assumptions of stationarity hold.

A demonstration of the differences between methods of estimating and simulating the t_{10} for the study area is provided in this section. The approaches demonstrated include:

- A test for additivity of the t_{10} variable;
- Independent kriging of the t_{10} values based only on the t_{10} data;
- Co-kriging of t_{10} with acoustic velocity and density;
- Sample support scale modelling the t_{10} at locations in each hole that have not been sampled; and
- Simulation of t_{10} using a turning bands method.

The suggested methodology begins with an up scaling of all the collected data to a 70cm composite. In this way the support of the destructive data (t_{10}, and t_{10} sample density) and the geophysical data (P wave slow) is equalised. Variograms were modelled and the estimation parameters set (Table 14). Estimates were run on two different search neighbourhoods, the second far larger than the first, as the first pass estimation did not populate all blocks.

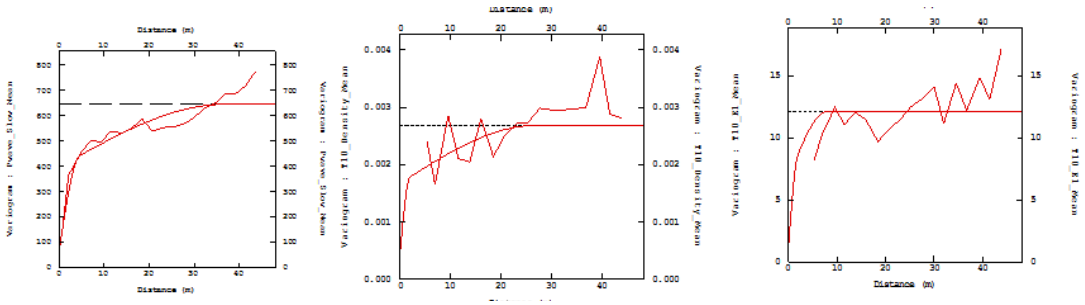

P-wave Velocity **Sample Density** **t_{10}_E1**

Variable	Nugget		Range (m)		Sill	
	C0	% of Sill	Structue 1	Structure 2	Structure 1 %	Structure 2 %
P_wave Velocity	0	0	2.93	6.48	54	46
Density	0.00046	17	2	6.72	45	38
Drop Weight t_{10}	3.98	33	1.1	6.1	39	28

Table 14:Table and graphics of the modelled variograms for P-wave Velocity, Specimen Density and drop weight data.

Table 15 gives the summary statistics for the variables selected for estimating and the statistics of the estimates generated into blocks of 0.7m x 0.7m x 0.7m

VARIABLE	Count	Minimum	Maximum	Mean	Std. Dev	Variance	CV
Pwave_Slow_Krig	427,004	162.52	308.89	249.36	19.71	388.49	1.56
Pwave_Slow_Mean	1,283	144.51	318.79	254.2	25.6	655.15	2.58
% Shift		12	-3	-2	-23	-41	-40
VARIABLE	Count	Minimum	Maximum	Mean	Std. Dev	Variance	CV
T10_Density_Krig	376,094	2.43	2.85	2.54	0.04	0	0
T10_Density_Mean	114	2.43	2.85	2.54	0.07	0	0
% Shift		0	0	0	-43		
VARIABLE	Count	Minimum	Maximum	Mean	Std. Dev	Variance	CV
T10_E1_Krig	376,094	16.02	41.51	33.34	2.71	7.33	0.22
T10_E1_mean	114	16.02	41.51	33.3	4.04	16.29	0.49
% Shift		0	0	0	-33	-55	-55

Table 15: Summary Statistics for Data and first pass estimates.

In all cases the average of the raw variables and the estimates differ by less than 3%, as expected the coefficient of variation of the kriged estimates is lower than that of the raw data. The number of blocks populated for 'T10_density' and t_{10}_e1 are far fewer than that for P-wave. This is a result of the range used for P-wave variable being far greater than that of the other two variables.

An analysis of the additivity of t_{10}

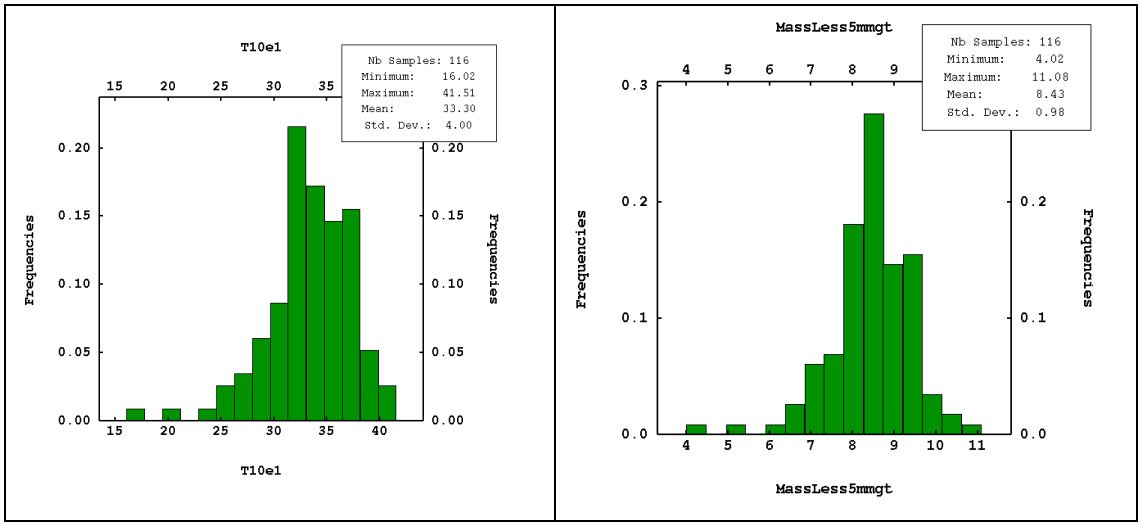

Figure 37: Histograms of the original t_{10} values (left) and the transformed variable "mass less 5mm in g/tonne" (Right).

The t_{10} transformation used is displayed in Equation 12. This transform converts the proportion of the sample passing one tenth of the original rock size to a 'grade' like variable which expresses the rocks amenability to crushing in the grams of rock that would be below a certain size for a given energy input.

$$\boldsymbol{MassLessThan5mm = (t_{10} * D1 * V_s) \times 100} \qquad \textbf{Equation 12}$$

Where:

t_{10} is the percentage by mass passing 1/10th of a particles original size for a given energy input;

$D1$ is the average density of the sample tested; and

V_s is the volume of the sample that was tested.

In this case the data comprise 116 values, at sample scale. The average of the sampled t_{10} value is 33.29, which is the average of the ratios. To calculate the ratios of the averages the average mass less than 5mm was divided by the average mass of the samples to give a value of 33.262. The difference between the average of the ratio and the ratio of the averages is 0.107% of the average of the original t_{10} values.

Ordinary kriging was carried out on both variables and the sample density to populate the test block grid (as described in section 4.4). The block models showing the variables estimated are shown in Figure 38. The average of the block estimates for t_{10} was 33.54, and the average of the mass less 5mm was 8.44 g/tonne.

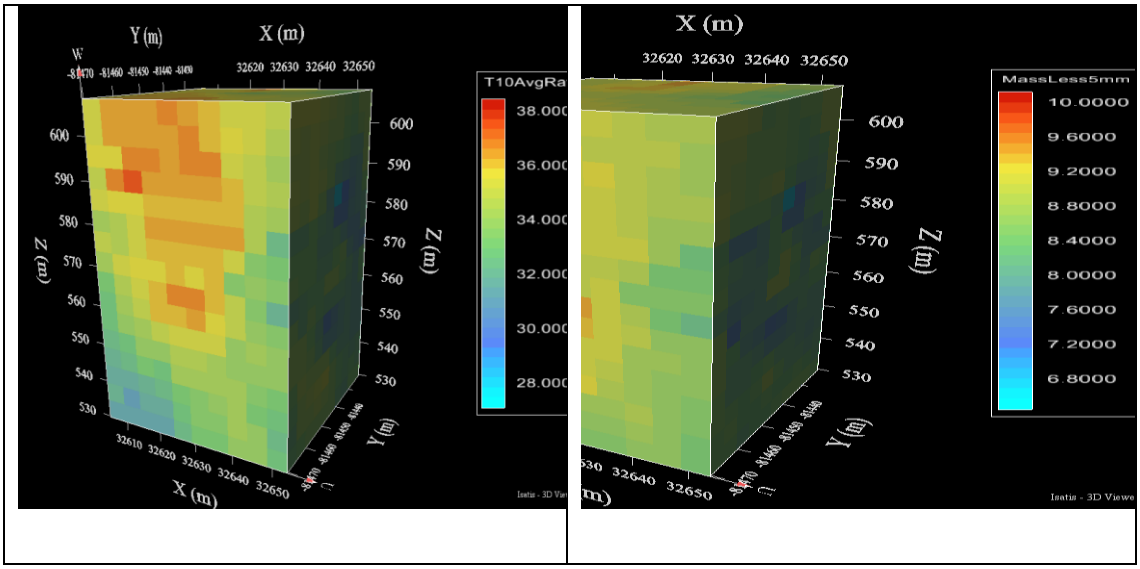

Figure 38: 3 dimensional projections of the kriging of drop weight values (left) and the transformed variable "Mass less 5mm in g/tonne" (Right).

The result of dividing the average undersize by the average mass of the block (the ratio of the averages) is 32.13, which is a difference of just over 5%. The magnitude of the difference is sensitive to the change in the density estimate which in turn affects the variation of the mass in each block.

This data set shows a range of values that is relatively narrowly dispersed - with a coefficient of variation for the t_{10} samples of 12% and density of 3%. At block scale the coefficients of variation reduce to ~5% for t_{10} and a density coefficient of the blocks of ~1.2%. This does not prove that the t_{10} variable is additive but gives some indication that for this specific set of data the risk of treating t_{10} as an additive variable may result in a 5% bias in the estimation.

Ordinary kriged estimates

Figure 39 shows cross-sections and histograms of the estimates for each variable when they are up scaled to mining blocks sizes of 5m x 5m x 5m. It is noticeable that there is now a considerably higher degree of smoothing.

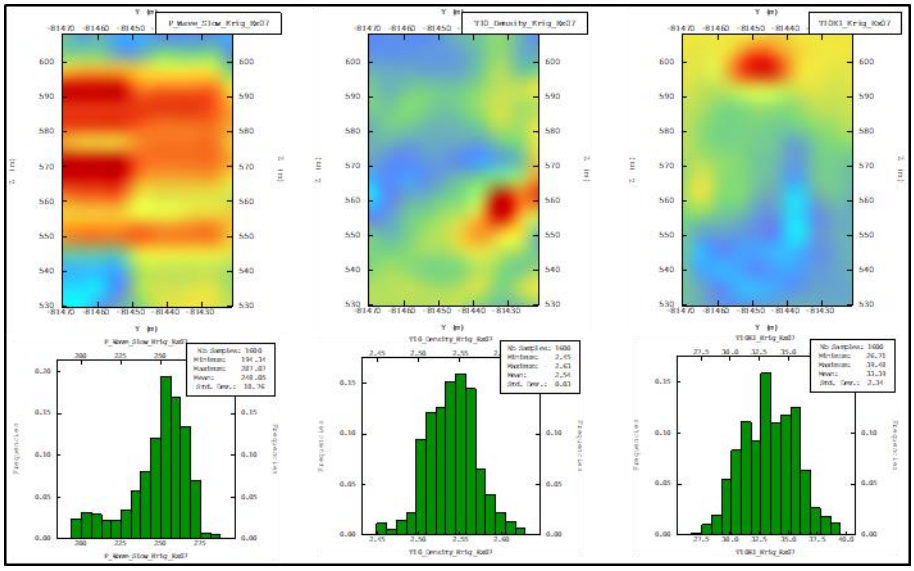

Figure 39: Cross sections of the orebody and histograms for the three variables estimated independently into a 0.7m x0.7m x 0.7m grid and accumulated into a 5m x 5m x 5m grid.

Simulation of rock characteristics

The same data were then used to generate a turning bands simulation of the same area of the deposit. To do this the data variables were converted to Gaussian variables using a Gaussian anamorphosis. The impact of the transformation is depicted in Figure 40.

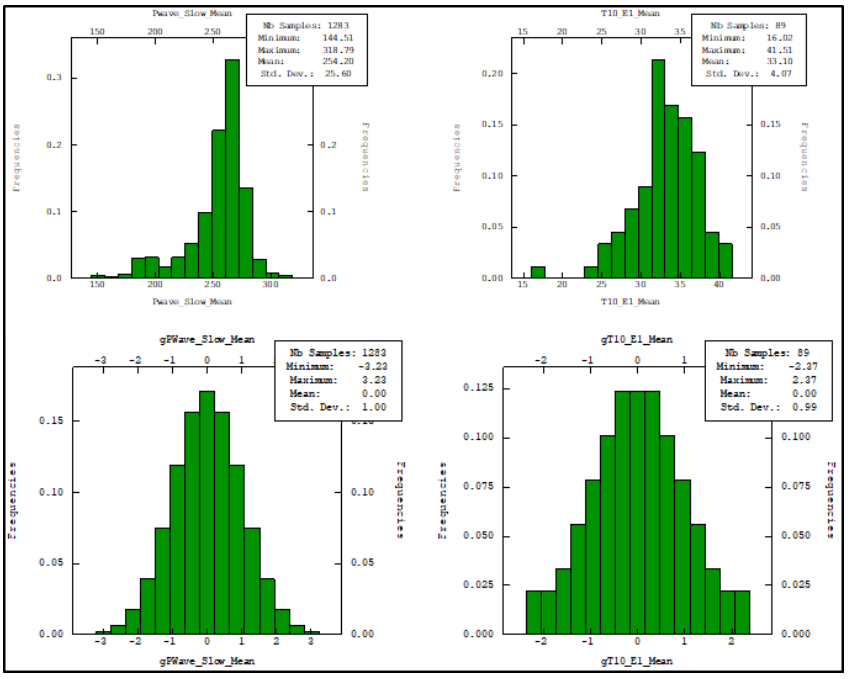

Figure 40: Histograms showing transform of data from raw data to Gaussian variables.

These Gaussian data were used to develop the semi-variogram models depicted in Figure 41. The three primary directions all seem to have similar ranges, with the structure of the P-wave variograms being far more stable than those of the variograms for the t_{10} data.

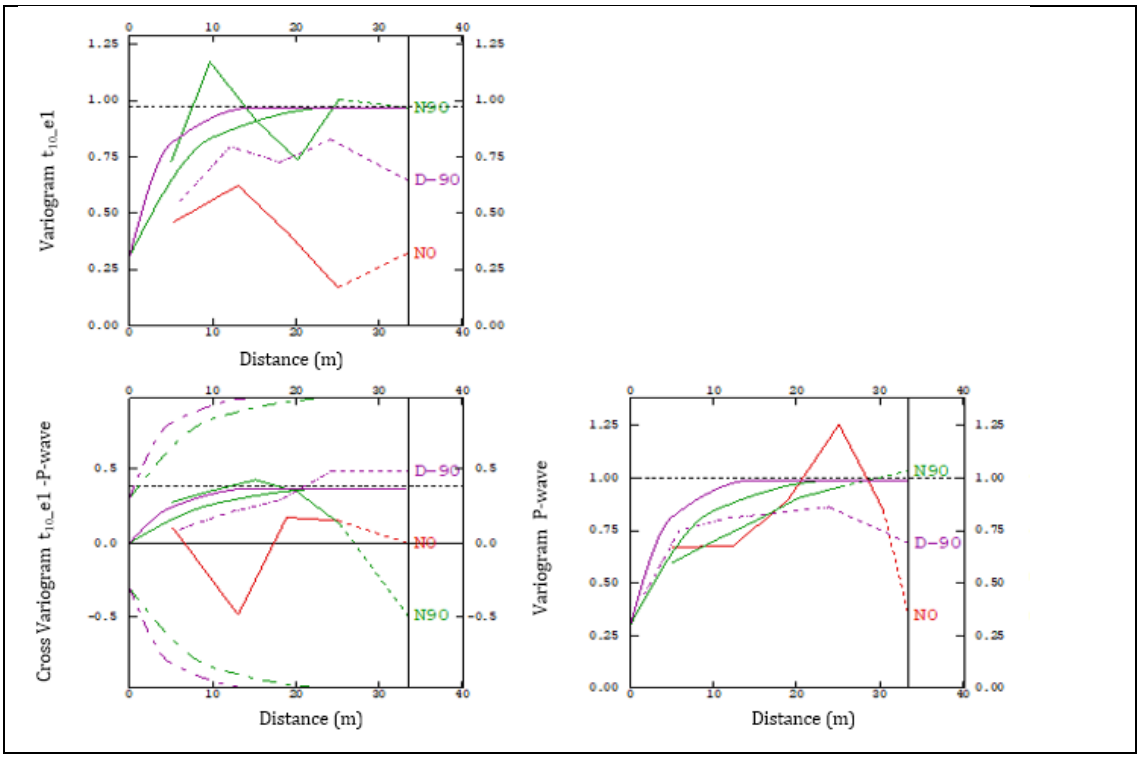

Figure 41: Variogram models (top left and bottom right)and cross variogram models (bottom left) for the Gaussian transforms of P-wave and drop weight test data.

These inputs were used to generate 50 spatial realisations of the variables at block scale. The simulated values were back transformed, and the simulations were validated by comparing the simulated histograms replication of the input data. Perspective views of cross-sections of these variables comparing the texture of the simulated values vs the kriged values are shown in Figure 42.

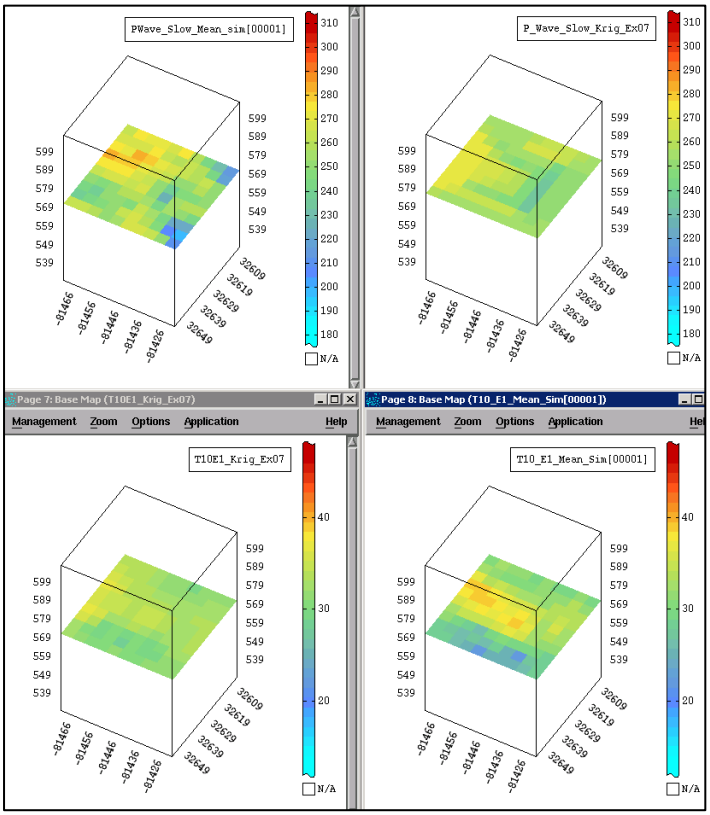

Figure 42: Perspective plots showing a cross-section through the test area for 5m x 5m x 5m blocks for simulated and kriged p-wave velocity (upper images) and drop weight test data(lower images).

The statistics for the block are given in Table 16 and show the differences in averages, std. deviation and extreme values. As expected, the estimates have a lower variance than the simulated values.

In this specific case, the differences between the simulated and estimated maximum and minimum values are relatively small. This is to some degree a function of the relatively closely spaced holes (5m) whereas in normal production models the drill spacing will be far larger and hence the difference in variance between the estimated and simulated values will be greater.

Estimate Type	Count	Minimum	Maximum	Mean	Variance
P-Wave Kriged	1600	194.34	287.07	248.05	351.95
P-Wave Simulated	1600	161.43	293.34	247.34	547.18
t_{10}_e1_Kriged	1600	26.71	39.48	33.39	5.46
t_{10}_e1_Simulated	1526	16.88	41.32	32.33	19.88

Table 16: Summary statistics comparing estimated and simulated values for P-wave velocity and drop weight results at the 5m block scale.

Implications of different estimation and simulation pathways

The objective of this analysis is to demonstrate how different transformations of the primary variables, and subsequent estimation of the transformed variables, may impact on prediction of response variables at operational scale.

If it is assumed that the purpose of the operating strategy for a crushing and grinding circuit is to achieve a given target grind size and allow throughput to vary, it is possible to predict throughput in each period for a given input rock hardness. To convert the measured in situ variable t_{10}, to a prediction of throughput requires several steps including:

- Measure the fracture response of a rock at three different energy inputs;
- Model an energy breakage relationship, and capture the “A” and “b” parameters of the fitted function;
- Use the product of the “A” and “b” parameters to predict the energy consumption;
- Given an assumed installed comminution power predict the throughput; and
- Assign a block mining sequence to evaluate the throughput achieved in different periods of operation.

The alternative pathways through these steps are depicted in Figure 43.

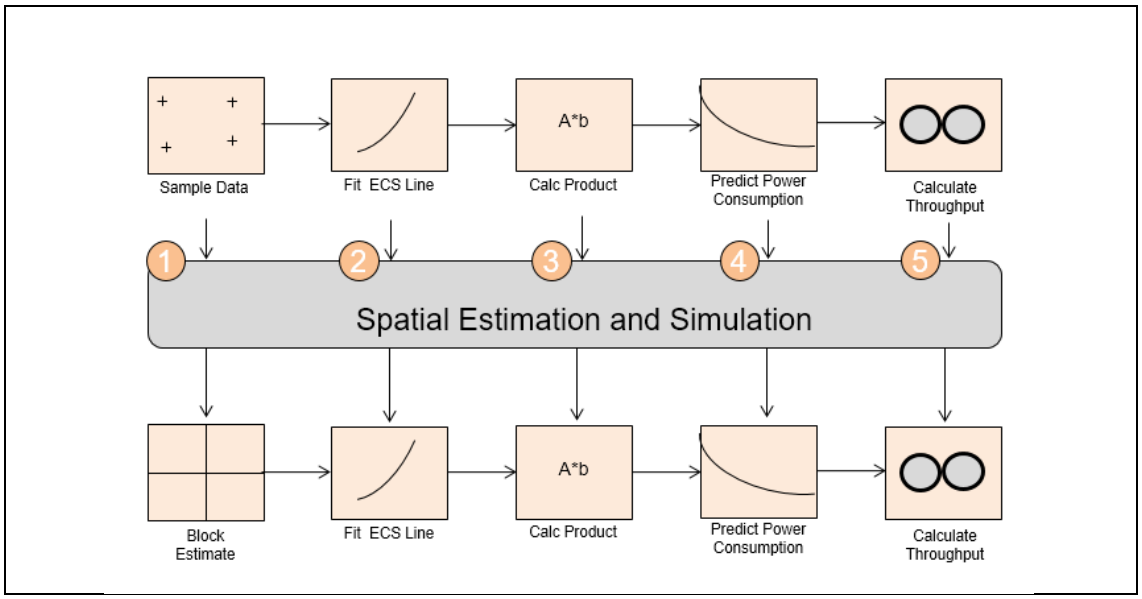

Figure 43: Schematic of the optional routes to use point scale sample data to predict throughput.

The mechanics of each of the calculation steps are briefly described below:

Fracture response to energy consumption

The procedure for sample testing requires that several fragments of rock are subject to a range of controlled, known input energies and the sizes of the resultant broken particles are measured and expressed as the percentage of material passing one tenth of the fragments' original size (the t_{10}) for a given energy input. The relationship between increasing energy input expressed as kWh/t and the increasing percentage of material passing one-tenth of its original size can be plotted. A so-called breakage function can be fitted through these points. Figure 44 shows a plot for the case where fragments of the sample have been exposed to three different energy levels, which have produced three different levels of fracture.

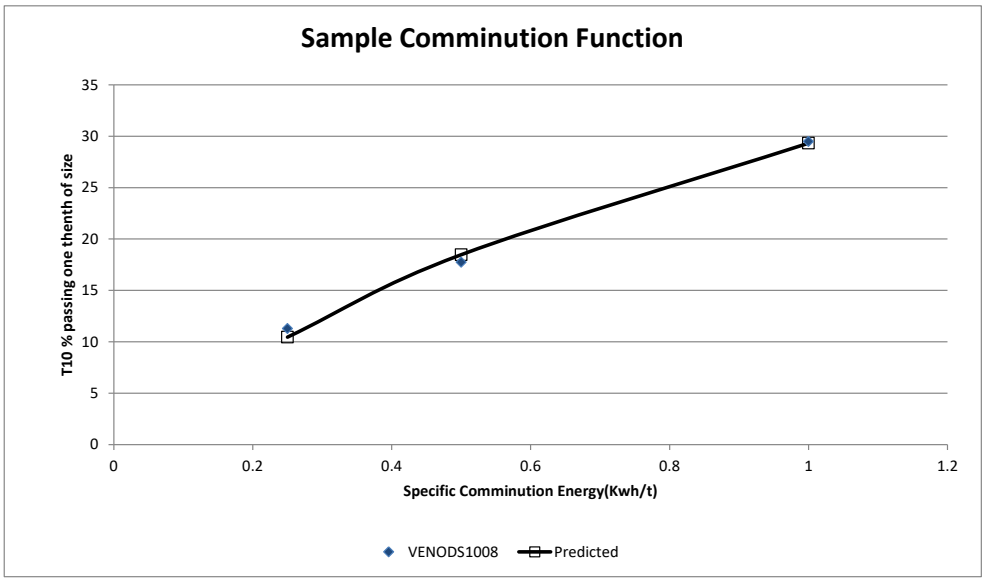

Figure 44: A Relationship between input energy and degree of fracture, expressed as percentage passing 1/10th of original particle size (blue diamonds), showing a fitted breakage function in black.

Equation 13 describes The function that can be fitted though the data:

$$t_{10} = A\left(1 - e^{-b \times E_c}\right) \qquad \textbf{Equation 13}$$

In this case the A value is 44 and the B value is 1.06, giving a A*b value of 47.65.

Using modelled breakage function parameters to estimate power consumption

Several authors (e.g., Bye et al., 2011) have used the product of the parameters fitted to the breakage function (A*b) value to relate the t_{10} value directly to milling energy consumption (although in reality the achieved throughput is a function of a host more variables there it has been demonstrated that there is some relationship and hence this could be a good variable to use to predict throughput for a target grind size). This raises the issue of the impact of selecting a 'controlling' or 'target operational response variable' for estimation and allowing others to fluctuate in response to operation with the objective of meeting a targeted response.

This behaviour arises from the interaction of ore characteristics and an operational strategy and not strictly only the properties of the ore being treated and hence could be misleading if estimated into the block model without careful and precise documentation of the assumptions and models used.

Ideally in the value chain modelling, all response variables should be determined 'at run time'– e.g., the value chain model constraints would include a policy that the process targets a grind size of p80 of 75 µm and allows the feed rate to fluctuate. A separate run of the value chain model might alternatively target 1000tph feed rate and let the grind size oscillate in full response to the input rock properties. In both cases the relationship between the primary variables and response variables will be very different, so the primary variables should be in the block model and the response and operating strategy should be calculated in the value chain model.

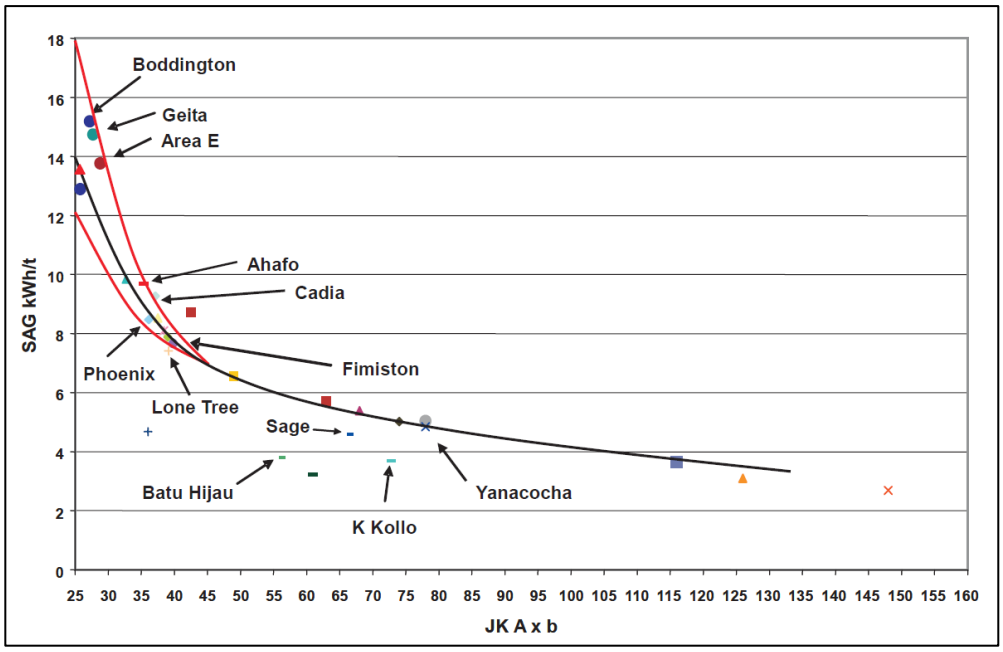

Figure 45: Plot showing broad correlation between average long run energy consumption in Semi Autogenous Grinding (SAG) mills and average orebody A*b values (Daniel, Lane and McLean, 2010).

Mapping Energy Consumption to Throughput

In this model, a simple inverse relationship is used where increased energy consumption of the rock breakage reduces throughput; this relationship is depicted in Figure 46 . This is based on prior performance data observed at the sample site.

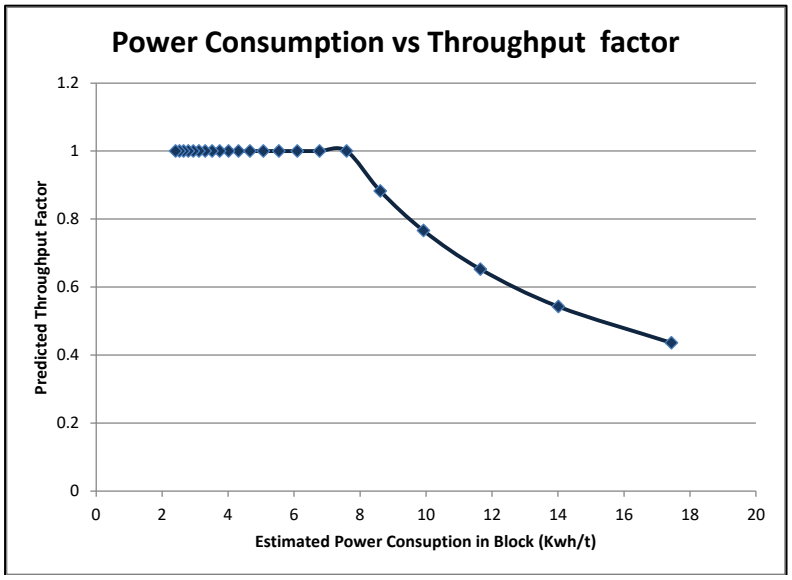

Figure 46: Relationship between power consumption and throughput for a target grind size.

Mine planning and block sequencing

The mine plan was simplified to a layer-by-layer plan to assign each block a mining sequence – the blocks then mined could be assigned a time to crush based on their t_{10}, which can then be cumulated into a daily, weekly and monthly throughput.

Several pathways are possible to convert the sample data into block estimates of throughput assuming that the process will be constrained to deliver a fixed size distribution. These options are briefly described in Table 17.

#	Point data derivation	Pre-estimation calculation	Spatial estimation	Post estimation calculation	Block scale prediction	Comments
1	Break sample sieve and determine % passing 1/10th of original particle size, for three energy levels. Generates three-point values at each sampled X, Y Z location	None	Co simulate or estimate three t_{10} values	In each block use three t_{10} to fit curve and derive A and b value, Multiply A by b- then used A*b through function to predict throughput	Throughput	t_{10}'s are a proportion by mass of the sample passing a given size. If the blocks are of the same size and density t10 can be considered additive
2	Break sample sieve and determine % passing 1/10th of original particle size, for three energy levels	Fit function to three points at each sample location, derive A and B value	Estimate A and B values	Use A*B in each block, put through a transfer function and derive throughput	Throughput	As A's and B's are parameters of curves tests for additivity and non-linearity would be required
3	Break sample, sieve and determine % passing 1/10th of original particle size, for three energy levels.	Fit function to three points at each sample location, derive A and B value, calculate A*b and estimate A*b, Calculate energy consumption and throughput in the block	Spatially estimate and or simulate product of A*b	Calculate energy consumption and throughput in the block	Throughput	
4	Break sample, sieve and determine % passing 1/10th of original particle size, for three energy levels.	Fit function to three points at each sample location, derive A and B value, calculate A*b, Calculate energy consumption	Estimate Energy Consumption	Calculate throughput in the block	Throughput	
5	Break sample, sieve and determine % passing 1/10th of original particle size, for three energy levels.	Fit function to three points at each sample location, derive A and B value, put A*B through transfer function, Calculate throughput at point	Spatially estimate and or simulate the throughput variable	None	Throughput	As throughput is a rate variable is subject to constraints and limited to some maximum and minimum. This approach may estimate infeasible throughput values
6	Break sample, sieve and determine % passing 1/10th of original particle size, for three energy levels, where there are no samples down the core used Geophysical relation to t_{10} to augment core values.	Use correlation between t_{10}s and Geophysical response to calculate t10's at un-sampled locations down core	Co simulate or estimate three t_{10} values	In each block use three t_{10}s to fit curve and derive A and b values, Multiply A*B- then use A*B through function to predict throughput	Throughput	t_{10} are a proportion by mass of the block, thus variable is additive
7	Break sample sieve and determine % passing 1/10th of original particle size, for three energy levels, where there are no samples down the core used Geophysical relation to T10s to augment core values	Use correlation between t_{10}s and Geophysical response to calculate t10's at un-sampled locations down core	Co simulate or estimate three t_{10} values	Run value chain model that incorporates a process simulator, treats groups of blocks, dynamic population balance models, predicts many aspect of process response	Throughput	Incorporates inter-block interaction and dynamic effects of operation

Table 17: Options for use of spatial data to estimate process response variables.

Outcomes from pathway one

In this pathway, the individual laboratory results achieved from crushing each sample are converted to three t_{10} values treated as point data. The three t_{10} values are spatially estimated using ordinary kriging.

Strictly speaking t_{10} is not an additive variable. It could however be transformed to a mass proportion variable and then kriged. It would be possible to do a back transform to t_{10} by recalculating, in each block, the proportion of the total mass of material that is less than 1/10th of its original size. In this synthetic example all of the blocks in the model have the same volume and density and thus the transform to a mass variable is not required. (See tests for Additivity in Section 5.5)

The resulting values of t_{10} in each block were analysed and a least squares curve was fitted. The A*b value for each of these curves is used deterministically to calculate power consumption and throughput. Summary statistics for the block estimates are shown in Table 18.

	t_{10}_e1	t_{10}_e2	t_{10}_e3	Model A	Model b	A*b	Predicted Power Consumption	Proportion of max throughput possible	Time to treatblock (Portion of day)	Days Treated
Minimum	7.58	16.63	26.71	35.45	0.06	34.98	5.46	0.65	0.31	0.31
Average	10.92	20.92	33.39	60.05	0.92	51.17	7.50	0.96	0.33	266.58
Maximum	13.79	24.01	39.48	562.93	1.75	65.84	11.65	1.00	0.48	522.60
Std. Deviation	1.15	1.35	2.34	23.70	0.24	5.35	0.99	0.07	0.03	150.54
Cof. Var. %	10.53	6.47	7.00	39.47	25.75	10.45	13.20	6.80	7.94	56.47

Table 18: Summary statistics for the estimation and calculation of block scale properties for pathway 1.

Pathway two

In this pathway, the t_{10} values at the point are plotted as described in Figure 44 and the A and b parameters fitted. The estimation process estimates the A and b values. Once the estimate is completed the A and b values in each block are multiplied together to generate the A*b product value which is used to calculate the resulting energy consumption and throughput (Table)

	t_{10}_e1	t_{10}_e2	t_{10}_e3	Model A	Model b	A*b	Predicted Power Consumption	Proportion of max throughput possible	Time to treatblock (Portion of day)	Days Treated
Minimum	7.58	16.63	26.71	44.53	0.43	42.64	2.64	0.83	0.31	0.31
Average	10.92	20.92	33.39	65.28	0.96	60.51	6.26	0.99	0.32	254.37
Maximum	13.79	24.01	39.48	250.46	2.05	120.73	9.19	1.00	0.38	505.09
Std. Deviation	1.15	1.35	2.34	20.20	0.18	10.95	1.16	0.03	0.01	145.46
Cof. Var. %	10.53	6.47	7.00	30.94	18.51	18.10	18.55	2.78	3.08	57.18

Table 19: Summary statistics for the estimation and calculation of block scale properties for pathway 2

Pathway three

In this pathway, the t_{10} data are used to derive a breakage function, the A and b values are multiplied, and this product is estimated. The statistics are summarised in Table 20.

	t_{10}_e1	t_{10}_e2	t_{10}_e3	Model A	Model b	A*b	Predicted Power Consumption	Proportion of max throughput possible	Time to treatblock (Portion of day)	Days Treated
Minimum	7.58	16.63	26.71	44.53	0.43	38.37	5.48	0.73	0.31	0.31
Average	10.92	20.92	33.39	65.28	0.96	51.93	7.36	0.97	0.32	263.96
Maximum	13.79	24.01	39.48	250.46	2.05	65.57	10.43	1.00	0.43	519.13
Std. Deviation	1.15	1.35	2.34	20.20	0.18	5.37	0.95	0.06	0.02	149.94
Cof. Var. %	10.53	6.47	7.00	30.94	18.51	10.34	12.84	5.96	6.68	56.81

Table 20: Summary statistics for the estimation and calculation of block scale properties for pathway 3.

Pathway four

This pathway generates estimates of power consumption values that are then converted to throughput by calculation. The summary statistics for the outputs of this process are given in Table 21.

	t_{10}_e1	t_{10}_e2	t_{10}_e3	Model A	Model b	A*b	Predicted Power Consumption	Proportion of max throughput possible	Time to treatblock (Portion of day)	Days Treated
Minimum	7.58	16.63	26.71	44.53	0.43	38.37	5.52	0.57	0.31	0.31
Average	10.92	20.92	33.39	65.28	0.96	51.93	7.57	0.95	0.33	269.98
Maximum	13.79	24.01	39.48	250.46	2.05	65.57	13.34	1.00	0.55	527.07
Std. Deviation	1.15	1.35	2.34	20.20	0.18	5.37	1.04	0.07	0.03	152.22
Cof. Var. %	10.53	6.47	7.00	30.94	18.51	10.34	13.69	7.32	8.45	56.38

Table 21: Summary statistics for the estimation and calculation of block scale properties for pathway 4.

Pathway five

In this pathway, the t_{10} data are used to derive A*b values and these are used to calculate the energy consumption and the throughput. The point scale calculated throughput values are then used to generate estimates of throughput at block scale. The statistics of the output are given in Table 22.

	t_{10}_e1	t_{10}_e2	t_{10}_e3	Model A	Model b	Axb	Predicted Power Consumption	Proportion of max throughput possible	Time to treatblock (Portion of day)	Days Treated
Minimum	7.58	16.63	26.71	44.53	0.43	38.37	5.52	0.71	0.31	0.34
Average	10.92	20.92	33.39	65.28	0.96	51.93	7.57	0.93	0.34	274.86
Maximum	13.79	24.01	39.48	250.46	2.05	65.57	13.34	1.00	0.44	538.14
Std. Deviation	1.15	1.35	2.34	20.20	0.18	5.37	1.04	0.06	0.02	155.66
Cof. Var. %	10.53	6.47	7.00	30.94	18.51	10.34	13.69	6.08	6.53	56.63

Table 22: Summary statistics for the estimation and calculation of block scale properties for pathway 5.

Although pathways 5 and 6 have been given in table 2 above the outputs of these pathways will be discussed in Chapter 6 as they require a dynamic process model to evaluate these approaches to estimation pathways.

Comparison of outcomes of different methods

The distribution data for each of the variables calculated and/or estimated are shown in Figure 47.

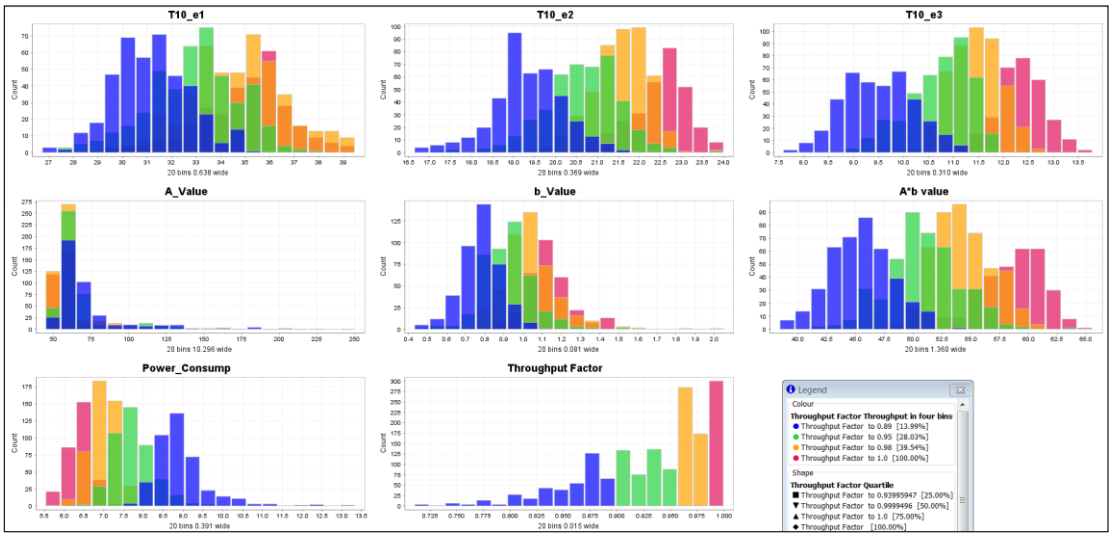

Figure 47: Histograms of the variables that are calculated and estimated in pathway 1.

In these histograms, the data have been grouped by the resulting throughput factor. This figure clearly shows the relationship between the variables used to derive the throughput indicator. These distributions can be contrasted with the histograms for pathway 3 depicted in Figure 48.

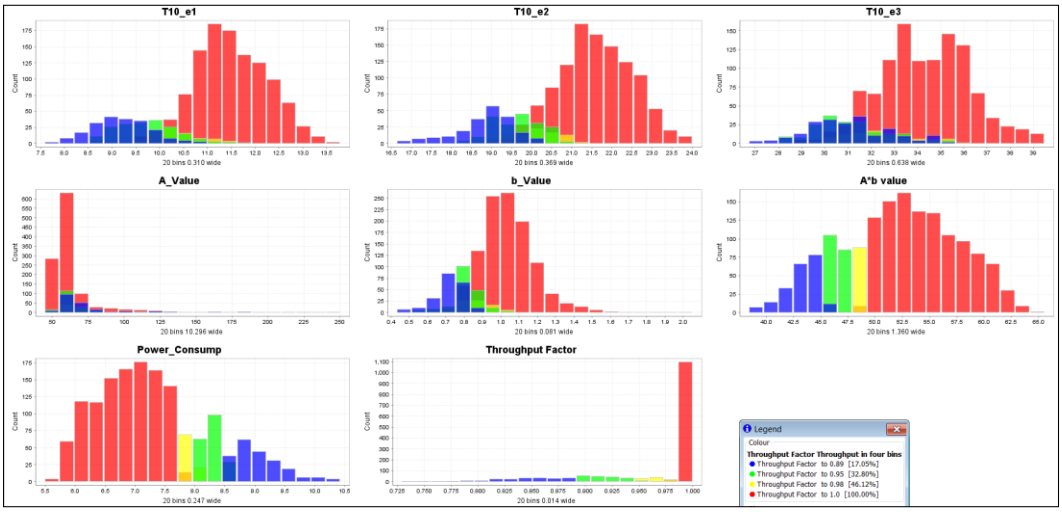

Figure 48: Histograms of the variables that are calculated and estimated in pathway 3, data has been grouped by predicted throughput quartiles.

In pathway three the estimation of the A*b variable results in a distribution of the A*b variable that is less dispersed than that for pathway 1. This ultimately results in a far higher estimate of the throughput factor.

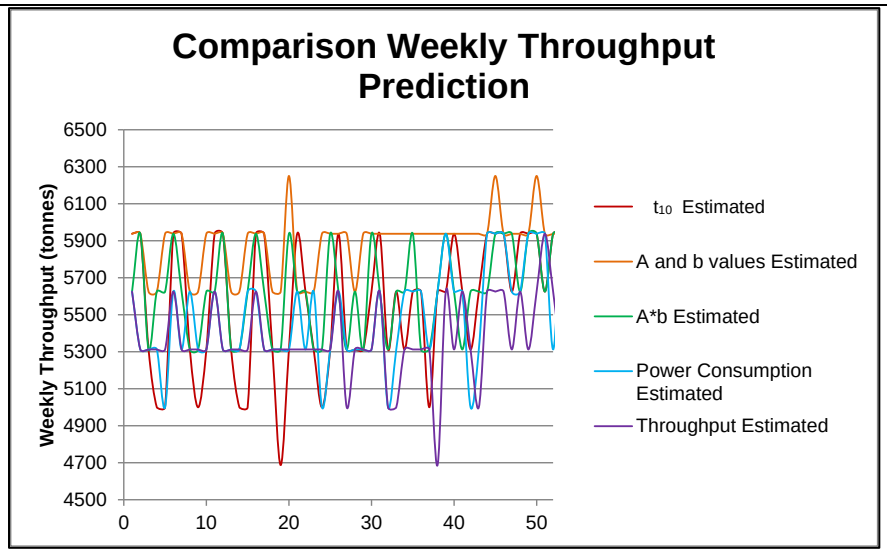

	t10 e1	t10e2	t10 e3	Model A	Model b	A*b	Power Consuption	Throughput Factor	Predicted Annual throughput
Sample Average	10.93	20.96	33.27						
Estimated Average	10.92	20.92	33.39	65.28	0.96	51.93	7.57	0.93	
Modelled Average1				60.05	0.92	51.17	7.50	0.96	338,750
Modelled Average2						60.51	6.26	0.99	354,688
Modelled Average3							7.36	0.97	341,250
Modelled Average4								0.95	333,438
Modelled Average5								1.00	326,875

Figure 49: Plot showing the variability in weekly throughput and a table with summary statistics for each of the variables calculated through each pathway.

The implications of this can be demonstrated by reviewing the different predictions that result from using the different approaches. Figure 49 shows how the average values differ, but perhaps more importantly also shows how the weekly predicted throughout would vary. In some weeks the difference exceeds 22% of the mean throughput prediction, and on a block-by-block scale this would be even more significant.

5.6 Generic approach and considerations for generation of suitable spatial models

Figure 28 depicts a pathway to generate a spatial model that depends on the sample data available, the variable being considered and the use of the estimate and ore

The spatial modelling of rock properties has potential to contribute substantially to the value of mining projects. To do this successfully requires integration of tools and techniques from several fields, including geology, mining, metallurgy and Geostatistics. There are several ways in which the modelling processes can be improved.

Improved data analysis at existing operations, which includes retrospective analysis of process response to orebody characteristics at an operational scale, will provide

an opportunity to develop a generic understanding of the important orebody properties that impact on different unit responses and that have systematic impacts on operational performance.

Development of an iterative and integrated approach to sampling, measurement and variable estimation is an important strategy to follow when trying to design and execute rock characteristic estimation programmes.

Geophysical tools can yield data that, although weakly correlated with destructive tests, can achieve a higher spatial coverage at a far lower cost than destructive tests. Using this additional data has potential to improve the estimates of spatial rock characteristics in the following ways:

- Identification of potential bias in sample layouts used for destructive testing;
- Including this weakly correlated data in the rock characteristic estimation process; and
- Identifying anomalous results.

The effective use of geophysical tools however requires that careful attention is given to the accurate location of the geophysical data and careful and repeated on-site calibration of the sondes used. Even a small deviation of the order of 0.5m can destroy the correlation required to make this data useful. As demonstrated here the acquisition of geophysical data from both the core and the hole that it is extracted from can be used to correct core location data and assist in determining the relationship between the minerals and geology of the rock that is driving the measured geophysical response.

The collection of destructive data acquired from small rock specimens requires that specific attention be paid to the execution of the test themselves. As it is impossible to crush the same rock twice, the quality control measures are centred on repeatability of the testing procedure. Indications are that the introduction of geophysical measurements of core just before it is destructively tested would improve laboratory quality control. This would also help to develop understanding of the relationship, at core scale, between the geophysical responses and the measured destructive response.

Several multivariate techniques can be used to identify relationships between the properties of the rock and the responses that are measured. PCA and PLS regression models demonstrated here, are used to augment the destructive data with geophysical responses. Acoustic velocity measurements show a correlation with the

elastic moduli of the rock. These in turn have been shown to be correlated with the destructive t_{10} data.

The massive differences in the scale of laboratory test work and operations require that existing approaches to up-scaling be carefully evaluated. The impact of the size of specimens used in destructive rock property tests on the data dispersion and variogram range requires further investigation. Larger specimens may reduce the error in block scale estimates of rock property.

Response variables, such as throughput, can be calculated and estimated in different ways. It has been demonstrated that the choice of the pathway has an impact on the resulting block scale estimate. It is recommended that where possible the most primary version of the data that are gathered at small scale be used in the estimation process.

In the next chapter, the use of spatial rock characteristic estimates in process simulations will be explored.

6 PROCESS SIMULATION AND ROCK CHARACTERISTICS

6.1 Introduction

The methodology suggested here to evaluate the metallurgical recovery factor requires a 'value chain simulation' that comprises multiple realisations of the orebody and a framework that can be used to evaluate the impact of variable kimberlite characteristics on diamond recovery. This processing framework requires unit process models that can be used to simulate the mining and treatment processes that respond to the variable and uncertain kimberlite characteristics.

The chapter begins with a review of open pit mine models and a discussion of their limits and constraints is discussed. A method to model and simulate the process of ore extraction is provided. A description of the outputs of the mining model, and its use in the unit process models in the treatment plant simulation is given.

The remainder of the chapter describes a methodology for formulating an integrated model that can be used to evaluate how uncertain and variable rock properties impact on the performance of the treatment process. The application of the model is described in the subsequent chapters, where the integrated model is used and demonstrated in two case studies that analyse a number of operational configurations, assess diamond recovery uncertainty and improve the definition of the range of the expected metallurgical recovery factor.

Three, increasingly complex, diamond recovery models can be used to estimate the metallurgical recovery factor. The approaches are depicted in Figure 50 and include:

a) A model based on the extension of micro and macro diamond size distributions to determine total diamond content and size distribution;
b) A model based on the relationship between total kimberlite grind, diamond liberation and lockup; and
c) A model based on a plant process simulation that incorporates a calibrated processing model of the diamond recovery plant.

The micro-macro diamond model approach is suited to early stage projects where little is known about the deposit. In such a model only a few macro diamond samples are available but the relatively large number of micro diamonds (of the order of 100's of stones per kg) that occur in small samples of diamond bearing ore can be used to model the in situ diamond distribution (Chapman and Boxer, 2003; Caers and Rombouts, 1996). This modelled in situ size distribution can be used to predict the abundance of coarse diamonds and in some cases the expected macro diamond recovery. This requires the use of relatively broad assumptions about mining and treatment efficiencies to predict the expected diamond recovery at a specified top and bottom size cut off.

The granulometry based liberation and lock-up model is suited to projects that have a well-conceived overall process design and treatment flowsheet, but where there is limited information on unit process efficiency and the impact of mining methods or the ore properties on process rate, efficiency and cost. Several parameters of this model are usually inferred from other operations. The 'granulometry liberation loss model' relates the size distribution of the recovered diamonds to the discarded kimberlite particles to estimate the 'locked' diamonds; i.e., those that are not sufficiently freed from the host ore and are unrecovered or lost. The model provides sufficient insight to begin trade-off studies between different flowsheet options.

A more detailed approach that uses calibrated population balance models can only be taken when sufficient inputs are available to calibrate accurately the unit process models. The population balance models can be adapted to include several unit processes that are all impacted by the variable and uncertain properties of the treated rock.

In most diamond operations a mass balance model that has several unit processes, including at least a comminution circuit, a dense media separation circuit and a final recovery plant, is required. With this model it is possible to estimate how the changes in the feed characteristics impact on the recovered diamond grade and size distribution.

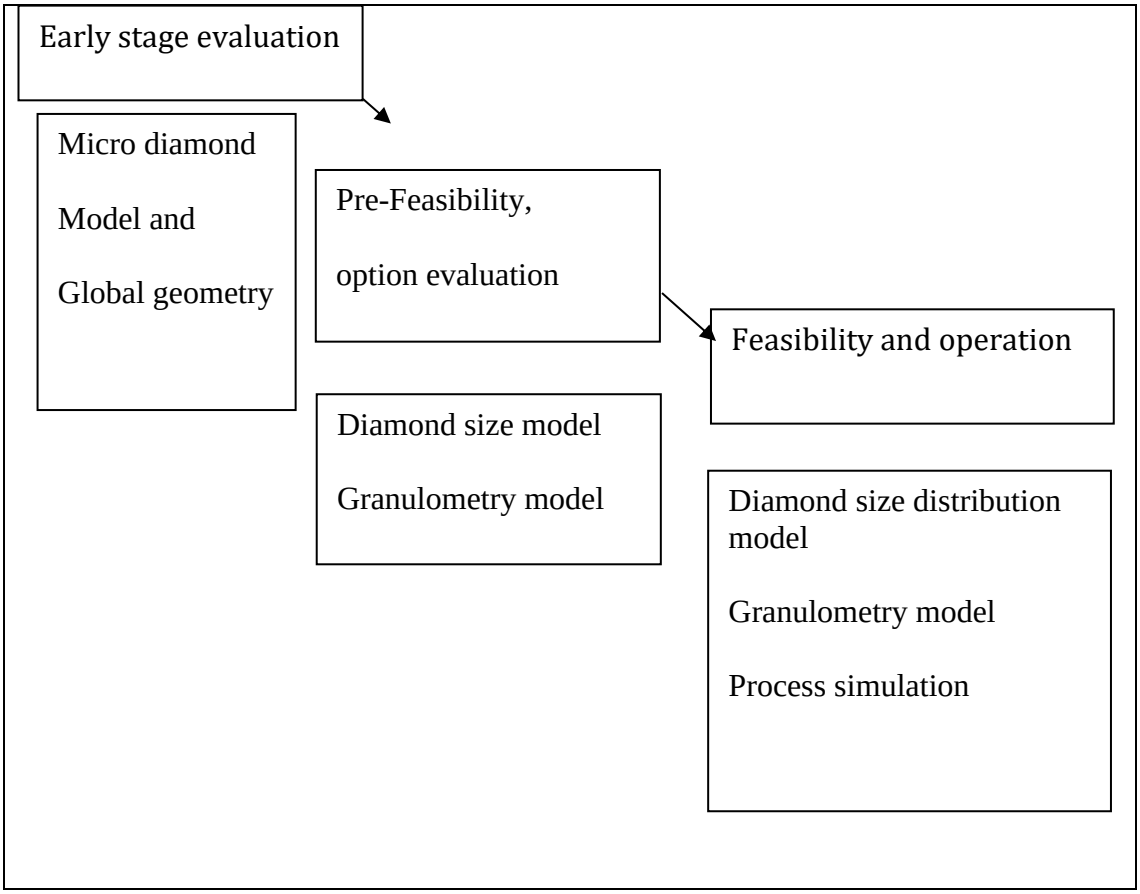

Figure 50: A schematic depiction of approaches to estimating the recovery factor for different project maturities.

Approaches used to determine block sequencing and characteristic alteration during mining

The design and selection of a mining process determines the sequence in which the ore arrives at the process plant and the extraction methods that are used to fracture the ore and transport it either directly to the plant, or to a stockpile or to dump as waste. Design and optimisation of the ultimate pit, the mining sequence execution process methods used to plan the schedule and sequence of blocks to be mined, and model the impact that drilling, blasting and haulage have on the physical rock characteristics (Dowd, 1976; Lane, 1998)

These usually aim first to determine an ultimate pit shell which contains the ore that is profitable given the economic constraints of the project (Lerchs Grossman, 1965) and expected contents and value of each mining block. This ultimate maximum size excavation is then 'optimised' in terms of the sequence of push-backs or cuts to excavate the ultimate pit. The schedule is then derived by determining the fleet size and targeted treatment tonnage over relatively long periods. The result of the mine

design work is to assign a sequence to each of the selective mining units (SMU) in the block model. This is discussed in more detail later in this chapter.

Approaches to liberation modelling in the minerals industry

The modelling of crushing processes is required to predict comminution outcomes (the size distribution of the rock product, the throughput rate, diamonds liberated, and potential for diamond damage) for several feed types and process configurations.

Initial models considered, that have been developed in the mining industry, require the following assumptions for their predictions to be valid:

- Limited or very little mineral grain fracture;
- Breakage rates and selection criteria are independent of rock texture;
- Liberation is related to mineral grain size; and
- Liberation and comminution can be considered to be independent processes.

Several liberation models have been developed, and according to Munn *et al*. (Napier-Munn *et al*, 1999) two primary approaches can be distinguished.

The first approach is to evaluate the rock texture and then to develop predictive models based on a mathematical description of the texture to relate the change in the size of the rock to the change in liberation. These models include work by Gaudin (1939), Weigel and Li (1967) and King (Beniscelli *et al*., 2000). They provide an estimation of the possibility that fractures will intersect a diamond for a given stone density and fracture size.

The second approach is to gather feed and progeny data from a crushing process and analyse the degree to which valuable minerals have been liberated. Weedon (1992) carried out several tests on crushed rock particles and reviewed the degree to which the mineral of interest had been liberated. This data was then used to establish characteristic curves that described the relationship between final rock size and the expected liberation. Morell *et al*. (Box and Draper, 1987) demonstrated that the liberation was largely independent of the process used to achieve comminution. As a result, liberation could be predicted by a measure of the size distribution of the contained mineral and the size distribution for the crushed ore. Using this finding they could model and predict the liberation of sphalerite using a three stream, two process population balance model. The three streams that were modelled were the gangue, the locked valuable component and liberated valuable component. The gangue and the liberated valuable component are processed

through conventional population balance model crushers (Box and Draper, 1987). The locked valuable component stream is also processed through a conventional crusher model and its products, locked and liberated mineral streams and gangue, are added to the other products emerging from the other crusher models. Gay (2002) has also produced similar models that reconstruct the parent composition from the progeny that is observed in both valuable and discard streams.

In the sampling of diamonds, the micro-diamond recovery process recovers most of the diamonds in a sample by dissolving the host rock. This suggests that very high recoveries can be obtained and that the size distribution of the diamonds is not materially changed during the recovery process. This contrasts markedly with the bulk sampling of kimberlite for diamonds where the recovered, or observed, distribution is compromised by the impact of losses in the process of sample treatment. These losses include diamond damage, destruction of diamonds above the top process size, loss of diamonds below the bottom cut-off size and lock up of diamonds in the discarded coarse kimberlite. The micro-diamond distribution, however, under-represents the coarse diamonds and can be viewed as giving a truncated distribution. Despite this, the recovered micro diamond distribution gives an indication of the size distribution of the valuable coarser component of in situ diamonds. It is possible to establish a relationship between these micro and macro distributions to model the liberation that is likely for a given size distribution of processed kimberlite. This in situ size distribution is the main 'texture' feature that is required for modelling liberation in the context of estimating the metallurgical recovery factor.

Approaches to modelling diamond recovery at different project stages

The objective of modelling the treatment processes is to create a relationship between:

- the estimated kimberlite properties;
- the contained diamond distribution; and
- the expected recovery efficiency measured in grade recovery and stone size distribution recovery.

This model can be used to determine the quantity and size distribution of diamonds that will be recovered from each estimated unit of ore in each period of mining.

As diamond projects move from prefeasibility to the feasibility study stage more sampling of the orebody is carried out, to provide additional information on the diamond grade, size distribution and value as well as the spatial nature of waste and kimberlite characteristics. This information typically includes several

measurements of the rock characteristics (measures of strength, fracture properties, density etc) that facilitate the use of models to select critical items of equipment, e.g. crushers, and estimate the relationship between the rock properties and the unit expected average performance. The population balance modelling approach is widely used in the industry for the design and configuration of process plants and can be adapted specifically to estimate diamond recovery plant efficiencies. In this more detailed approach to the modelling, the relationship between diamond size, rock density and fracture properties becomes a vital component in both estimating liberation and tracking the degree of diamond release through the process.

The unit process models for comminution and DMS separation are data dependant and require the fitting of model parameters are consistent with the observed data. The fitting process is iterative and is assumed to be valid when the errors between the observed data and the model are minimised. In brownfield situations this can be time consuming but is generally achievable with well-considered and executed process surveys. In greenfield situations it is necessary to rely on several diverse sources of data to estimate process model parameters and to create a feasible process simulation (i.e. one that converges to a stable solution.).

The primary focus of this research is to model the impact of variable and uncertain rock strength on comminution, liberation and recovery of diamonds. There is a tacit assumption that the equipment is well maintained and effectively operated. It is however possible that operational personnel can at times have an influence on process performance by adjusting process parameters (e.g., crusher gap setting). Changes to the operating parameters of crushers, screens and dense media separation units can either increase or decrease recoveries but will increase the variability of the process output (Demming, 1986). These impacts have not been explicitly considered in this research work, though some of these impacts may contribute to the overall variance of the data that are obtained from operating mines and is an area for further research.

6.2 Modelling of mining processes

Mining processes include drilling, blasting, material handling mixing and transportation of the ore to the processing plant. The main implications of mining processes that are considered in this research are:

- The impact of mining on the sequence and rate of mining; and
- The impact that the mining processes have on rock properties that are considered to influence diamond recovery.

Usually, in the case of open pit mining of kimberlite pipes, all the kimberlite material is mined and so the mined excavation extends to the boundary of the kimberlite .The decision to leave sub-economic material in the pit is usually constrained by the low structural strength of kimberlite and the need to ensure access to payable kimberlite. In some cases where the pit is large enough (e.g. Williamsons mine) areas of sub-economic kimberlite can be mined around, although this is not common. In mines that contain relatively small un-payable material volumes (e.g. Ellendale) a variety of ore/waste selection and rejection (grade control) practices are used to determine the ideal destination for mined material i.e. waste or sub-grade or plant feed. Given the difficulty and cost of sampling for grade these practices are often based on a combination of the assigned grade in the resource/reserve model, a visual assessment of the kimberlite as it is exposed, and ease with which the location of the pipe contact with waste rock can be defined.

In the 'Integrated Evaluation Model' a method to replicate the block selection and destination assignment has been developed. Each block in the grade model is assigned a planned sequence number that is derived from the long-term mine plan that is derived using conventional pit optimisation algorithms. The resulting schedule is derived from the integrated model that responds to the interaction of the orebody properties and the constraints of the mining method.

The mining process will impact on the rock strength properties, requiring some modifier to the primary properties that have been spatially estimated or simulated into the block model. The relationship between blasting parameters and diamond distribution has been investigated by Guest *et al*. who found that within four blast hole diameters most of the contained diamonds would be destroyed. (Guest, 1997)

Impacts of drilling and blasting on ore characteristics

To extract material from the mined pit, many operations use a drilling and blasting method. Increasing the efficiency and reducing the cost of this operation has been the focus of considerable research (Wilmott 2004, McGee 1995) The blasting will produce a range of sizes of rock and the impact that this has on the process will include the total power required as well as the mass flow in the primary section of the comminution circuit. The impact on total grind will, however, primarily be related to the total energy used in the blast, commonly referred to as the powder factor measured in kg of explosives used per tonne of ore mined.

It is also important to consider the residence time of the ore post blasting in the pit or on stockpiles where it is exposed to the atmosphere and will degrade to some extent. In Kimberley in the late 1800's this process of natural weathering was used to limit the energy required to crush the kimberlite. At some sites the total content

of clay and the clay species can be used to build a relationship between proportion of the feed that has been exposed to rain and the overall comminution achieved

Materials handling stockpiling and storage

There is invariably some form of stockpiling on diamond mines, ranging from small surge capacity bins (e.g., Snap Lake) to large +100,000 tonne stacker reclaiming systems (Premier Mine). The impacts of blending and weathering need to be correctly considered in any model of the operation as this process can, if correctly operated, reduce the variability of grade and other important ore characteristics such as waste rock content, UCS etc. (Robinson, 2004; Everett, 2001) This can be relatively simplistically modelled in extreme cases by either not adapting block characteristics which implies no blending or, for each characteristic of interest, the entire load in the stockpile is averaged at each time increment in the simulation. More realistic approaches include creating sub-parcels of several blocks that are deemed to be co-located and the degree of mixing is controlled by some function of both residence time and sequence of loading and withdrawal.

6.3 Modelling of diamond treatment plant process

Integration and adaption of population balance process models with an ore stream that has multivariate characteristics is required to estimate the recovery factor. Particular attention is given to the derivation of the parameters of the unit process models, and how these are influenced by rock properties, and how they can be perturbed realistically to quantify the range and variability of the process response to changing rock properties.

Population balance modelling is used extensively in the minerals processing industry and can be carried out on several software platforms but is typically used on relatively advanced projects as the unit process models require calibration of their parameters that are usually best derived from operating units that are operating on the ore in question. In the absence of full-scale operational data, it is however, possible to use small-scale pilot studies to derive the relationships between ore characteristics and process responses.

Population balance models work by creating several ‘bins’ or “intervals’ for each rock characteristic (e.g. size intervals, density intervals, grade intervals etc) that are carried through the flowsheet and the masses entering and leaving each interval at each stage of the flowsheet are required to balance. The balancing is achieved through a set of iterative calculations and mathematical models that are required to converge to some pre-set error tolerance. Using this approach for diamond processing it is possible to model both the ore size distribution, the ore density

distribution as well as the diamond size distribution and to carry these through the flowsheet.

A survey of De Beers' operations provides an insight into the ranges associated with the parameters that can be input into unit processes. The rock properties used include the expected head feed size distribution, the strength of the rock expressed by an energy size relationship using sampled t_{10} and a fitted breakage function, and a distribution of density per size class.

Theoretical underpinnings of population balance models

Population balance model methodology

The aim of this approach is to simplify the quantitative description of particle characteristics yet retain sufficient detail to enable process modelling and simulation. A useful distinction can be made between internal and external particle coordinates and distribution densities (King, 2001). The properties that describe the individual particle properties are considered 'internal coordinates of the particle phase space,' and the external coordinates are those that describe 'location' of the particle in the process in terms of the energy, stress, strain etc. to which the particle will be subjected.

The internal coordinates should be sufficient to describe all significant characteristics of the particle. These may include some characteristics that are primary and some that are response. Even when considering primary properties (e.g., particle density) these may have to be inferred or derived from the mineral composition of the material that has entered a specific unit.

The external coordinates and their changes impact on the internal coordinates. This relationship can be modelled in several ways and sets up a formalised framework for developing and testing simulation of mineral processing flow sheets.

Notation conventions used by King (2001) to describe population model method include:

$\psi(x)dx$ is the number fraction of particles per unit volume of phase space;

x is the coordinate point in phase space $x\varepsilon\mathbb{R}^N$;

μ is a vector of velocities at which particles change their phase space;

$\mathcal{R}(x)$ is the rate at which particles at coordinate position x are destroyed, this rate is specified as mass per unit volume of phase space per unit time;

W_{in} is the mass rate at which solid particles enter the system;

W_{in} is the mass rate at which solid particles leave the system;

$\bar{m}$ is the average mass of a particle at point x in the phase space;

N is the total number of particles in the system;

A, B, D are the rates of addition, birth and destruction of particles; and

Q is the rate of removal of material through product streams.

$B(x; x')$ is a distribution function that describes how particles move discrete distances in the internal phase space following breakage. It is the mass fraction of material that has phase co-ordinate less than x after a destructive event of particles originally located at x'. This suggests that every phase co-ordinate of the particle is now less than the corresponding element of x. The associated density function for breakage is defined as b$(x; x')$ and

a$(x; x')$ is the distribution density function for particles produced by attrition and wear of particles at x'

It is possible, as described by King (2001) to define a region R_c of the particle phase space enclosed by a surface S_c and then develop a model that accounts for all particles arriving and leaving this area.

$$\frac{\partial}{\partial t}\int_{R_c} N\psi(x)dx = -\int_{S_c} N\psi(x)u.ndσ - D + B - Q + A \qquad \textbf{Equation 14}$$

where $\boldsymbol{N}$ is the 'outward pointing' normal vector to the phase space S_c at point x.

The destruction, birth, material removal and arrival terms are described below.

The destruction processes are represented by:

$$\boldsymbol{D} = \int_{\boldsymbol{R_c}} \frac{\boldsymbol{\mathcal{R}}(\boldsymbol{\psi}(\boldsymbol{x}), \boldsymbol{x}, \boldsymbol{F}[\boldsymbol{\psi}(\boldsymbol{x})]}{\bar{\boldsymbol{m}}(\boldsymbol{x})} \boldsymbol{dx} \qquad \textbf{Equation 15}$$

Where D is the number of particles broken per unit time in the control volume R_c. The rate of breakage is a function of the number distribution of both the particles in the control volume and of the entire distribution function.

The birth processes are given by:

$$\begin{aligned} &\boldsymbol{B} \\ &= \int_{\boldsymbol{R_c}} \frac{\mathbf{1}}{\bar{\boldsymbol{m}}(\boldsymbol{x})} \int_{\boldsymbol{R'(x)}} \boldsymbol{\mathcal{R}}(\boldsymbol{\psi}(\boldsymbol{x'}), \boldsymbol{x'}, \boldsymbol{F}[\boldsymbol{\psi}(\boldsymbol{x})])\mathbf{b}(\boldsymbol{x}; \boldsymbol{x'})\boldsymbol{dx'dx} \\ &- \int_{\boldsymbol{R_c}} \frac{\boldsymbol{N}}{\bar{\boldsymbol{m}}(\boldsymbol{x})} \int_{\boldsymbol{R''(x)}} \boldsymbol{\psi}(\boldsymbol{x'}), \boldsymbol{\mu}(\boldsymbol{x'}), \boldsymbol{F}[\boldsymbol{\psi}(\boldsymbol{x})])\mathbf{a}(\boldsymbol{x}; \boldsymbol{x'})\boldsymbol{dx'dx} \end{aligned} \qquad \textbf{Equation 16}$$

In Equation 16 $R'(x)$ and $R''(x)$ are the regions of phase space where particles that have changed their size either by breakage or attrition and can enter the phase volume dx around the point x.

The addition of material in this phase space can be described as:

$$\boldsymbol{A} = \boldsymbol{W_{in}} \int_{\boldsymbol{R_c}} \left(\frac{\boldsymbol{N}}{\boldsymbol{M}}\right) \boldsymbol{\psi_{in}}(\boldsymbol{x})\boldsymbol{dx} \qquad \textbf{Equation 17}$$

And the removal rate as:

$$\boldsymbol{Q} = \sum_{\boldsymbol{j}} \boldsymbol{W_{out\,j}} \int_{\boldsymbol{R_c}} \left(\frac{\boldsymbol{N}}{\boldsymbol{M}}\right) \boldsymbol{\psi_{out\,j}}(\boldsymbol{x})\boldsymbol{dx} \qquad \textbf{Equation 18}$$

The above equations can be integrated over the surface of the reference region. King (2001) however suggests that the application of the divergence theorem, which equates the integral of the phase space volume R_c.with that of the enclosing space surface S_c leads to a more tractable form for the steady state operation.

$$\int_{R_c} N \vee \psi(x) dx = \int_{S_c} N \psi(x) u.n d\sigma \qquad \textbf{Equation 19}$$

which, when expanded, gives the working equation for the steady state operation as:

$$N \int_{R_c} \vee \psi(x) dx + D + B = -Q + A$$

$$\begin{aligned} & N \int_{R_c} \vee \psi(x) dx + \int_{R_c} \frac{\mathcal{R}(\psi(x), x, F[\psi(x)])}{\overline{m}(x)} dx \\ & + \int_{R_c} \frac{1}{\overline{m}(x)} \int_{R'(x)} \mathcal{R}(\psi(x'), x', F[\psi(x)]) \mathbf{b}(x; x') dx' dx \\ & - \int_{R_c} \frac{N}{\overline{m}(x)} \int_{R''(x)} \psi(x'), \mu(x'), F[\psi(x)]) \mathbf{a}(x; x') dx' dx \\ & = - \sum_j W_{out\,j} \int_{R_c} \left(\frac{N}{M}\right) \psi_{out\,j}(x) dx \\ & + W_{in} \int_{R_c} \left(\frac{N}{M}\right) \psi_{in}(x) dx \end{aligned} \qquad \textbf{Equation 20}$$

The form of Equation 20 can be simplified as a 'integro-differential equation' for analytical purposes.

$$\begin{aligned} & N \vee \psi(x) dx + \int_{R_c} \frac{\mathcal{R}(\psi(x), x, F[\psi(x)])}{\overline{m}(x)} dx \\ & + \int_{R_c} \frac{1}{\overline{m}(x)} \int_{R'(x)} \mathcal{R}(\psi(x'), x', F[\psi(x)]) \mathbf{b}(x; x') dx' dx \\ & - \int_{R_c} \frac{N}{\overline{m}(x)} \int_{R''(x)} \psi(x'), \mu(x'), F[\psi(x)]) \mathbf{a}(x; x') dx' dx \\ & = - \sum_j W_{out\,j} \int_{R_c} \left(\frac{N}{M}\right) \psi_{out\,j}(x) dx \\ & + W_{in} \int_{R_c} \left(\frac{N}{M}\right) \psi_{in}(x) dx \end{aligned} \qquad \textbf{Equation 21}$$

In the preceding section the fundamental population balance model has been reduced to an appropriate discrete form with the region R_c representing an appropriate particle class, and the material entering and leaving each size class is calibrated using data acquired from existing processes.

6.4 Unit process models

The unit processes that have a material impact on estimating the release, recovery and loss of diamonds in the processes of comminution, separation and recovery have been adapted for use in the integrated evaluation model.

There are three main processes in the diamond process flow sheet: size reduction achieved in several steps, a density separation and final diamond recovery using a combination of x-ray and magnetic recovery. Models used to simulate or emulate these processes are described briefly below.

Crushing models

There are several types of crushers that are used in the diamond industry, including jaw, gyratory, short-head and high-pressure roll crushers. In each part of the flowsheet different modes of crushing are used. The key to understanding the overall liberation is however the sequence of size distributions that are achieved.

Rocks do not generally fracture by breaking of atomic bonds, King (2001) demonstrates that rocks that have measured hardness of ~50mpa would exhibit a fracture strength of over 6000mpa if this were the case. It is suggested in the Griffith theory of breakage (Griffith, 1921) that when a rock is exposed to rapid impact stress it initially deforms elastically and absorbs the applied energy as elastic strain. The strain grows until the stress intensity at the most sensitive flaw exceeds the Griffith criterion for crack growth. The crack then propagates very rapidly and may bifurcate several times being driven by the release of the stored strain energy, until it meets an edge of the particle, and the original particle splits apart. The origin, growth and the pattern/directions of crack propagation are a function of rock characteristics (e.g., the contents and texture of the rock) and the nature of the energy that is imparted (speed of loading, magnitude of stress, difference in primary and secondary stresses) on the rock. King (2001) also suggests that the term ‘hardness’ be used to describe a rock’s resistance to indentation and that fracture toughness be used to refer to a rocks resistance to the propagation of fracture for a given set of stress or strain conditions.

Measuring and describing the relationship between energy input and the degree of fracture produced is not trivial. Some of the challenges include:

- Accurate measurement of the energy used to generate breakage;
- Quantitative description of the breakage produced;
- Description of the limits of the relationships measured.

Depending on how these problems are addressed will, by and large, dictate the limits and usefulness of any subsequent process modelling framework.

The earliest references reviewed show that initial work was aimed at developing a relationship between energy input and fracture achieved. The difficulty in describing these relationships lies in the complex non-linear relationship between energy input into the crushing device and in some way measuring and quantifying 'breakage' and 'fracture' as the reduction ratio.

As described by Holmes (1957) the earliest breakage models include those by Rittinger (1867), Kick (1885) and Bond (1943) (see Equation 22 to Equation 25) and Whitten (1972). The forms of these models are extensions of the earlier approaches and their formulation is described below. Holmes (1957) carried out an analysis of data from several deposits and suggested that the relationship needed to be defined in a way that would include different behaviours and interactions that were exhibited by different machines and different rock types.

Rittinger:

$$\boldsymbol{W = K_1\left[1 - \frac{1}{R}\right].\frac{1}{a^3}} \qquad \textbf{Equation 22}$$

Kick:

$$\boldsymbol{W = K_2\left[\frac{logR}{log2}\right]} \qquad \textbf{Equation 23}$$

Bond:

$$\boldsymbol{W = K_3\left[1 - \left(\frac{1}{R}\right)^{\frac{1}{2}}\right].\frac{1}{a^{\frac{1}{2}}}} \qquad \textbf{Equation 24}$$

Holmes:

$$\boldsymbol{W = K_4\left[1 - \left(\frac{1}{R}\right)^r\right].\frac{1}{a^r}} \qquad \textbf{Equation 25}$$

Where:

$W = 100^r . W_i$ is a constant for one material and one machine.

R is the particle size reduction ratio, usually expressed as the median size of the feed to the crusher and divided by the median size of the product.

r is a variable parameter that is related to the material's reluctance to grind as a function of the material's size. Holmes (1957) refers to this parameter as the "Kicks law deviation exponent, since it is a measure of the departure of the crushing system from ideal Kicks law behaviour".

a is a product grind size usually represented by the single side dimension measure of the square aperture that 80% of the product post crushing would pass.

Rittinger's theory suggested that the energy necessary to reduce particle size is proportional to the increase in specific surface area. It is focused on modelling the rupture of chemical and physical bonds in the material.

In 1880 Kick suggested an energy fracture relationship. It was translated from the original by Stadler to suggest "the energy required for producing analogous changes in configuration in geometrically similar bodies of equal technological state varies as the volumes of these bodies." Kicks law centred on the energy required to deform the particle to its elastic limit. In 1957 Holmes came to the forefront of the discussion where up until then the 'laws' of Kick, Bond and Rittinger were in use.

Holmes' model begins with the consideration of the failure of a cube of rock of dimension **D**. Using Hooke's law and three assumptions Holmes demonstrated that by expansion of multiple failure events it can be shown that the energy required to reduce a unit weight of cubes of side **D** can be formulated as in Equation 26:

$$\boldsymbol{E_w = \frac{3k\,D^{-r}(R^r - 1)}{\rho.(2^r - 1)}} \qquad \textbf{Equation 26}$$

Where:

ρ is the material density.

D is the dimension of one side of the starting cube.

r is the variable parameter of the rock type considered referred to by Holmes as the "Kicks law deviation exponent."

k is another parameter of the model that is used to describe the failure boundary conditions.

Holmes used an additional fourth assumption to derive a more generic form as shown in Equation 27. The first assumption is that the model is independent of shape changes. The second is that it is possible to represent the progeny distribution through a single number (not withstanding prior comments about bimodality) in this case the representation is given by the P80 of the distribution in the form stated in Equation 27.

$$\boldsymbol{Y = 80(X/a)^m} \qquad \textbf{Equation 27}$$

Where:

Y is the cumulative percentage passing at size X.

X is the size for which the percentage passing is to be calculated.

a is the size at which 80% passes.

m is a parameter which varies to some extent with a, normally it is taken as $1/\sqrt{2}$.

The third assumption is that the effects of boundary conditions should be considered. This includes the size and shape of the particles entering the system and the machine that is used to perform size reduction.

The fourth assumption implies that there will have to be some consideration of the proportion of energy that is used to propagate factures vs the energy that is input into the device. This should take the form of an efficiency factor η and will be different for different sizes of material broken.

With these four assumptions it is possible to reduce Equation 27 to Equation 28:

$$\boldsymbol{W = K\left(\frac{R^r - 1}{R^r}\right).\frac{1}{a^r}} \qquad \textbf{Equation 28}$$

Where:

W is the work input into a comminution machine in KWh/tonne to a crushing machine reducing the feed size F to a product size a.

$R = F/A$ is a parameter which varies to some extent with a is the size at which 80% passes.

$K = \eta.\frac{240k'}{\rho}\frac{m(1.25)^{(m-r)/m}(R^r-1)}{(m-r).(2^r-1)}$ where k' includes constants that enable the implementation to account for the units of measure of particle size and of power input.

r is a variable parameter that is related to the material's reluctance to grind as a function of the material's size

m is a parameter which varies to some extent with a, normally it is taken as $1/\sqrt{2}$.

Holmes then suggests that the parameters in the model should be considered as 'engineering measures' rather than laws. He also suggests that the constants used in the models are as much a function of the rock properties as the machine properties. This substantiates the requirement for a framework to formalise the relationships between primary, response and process properties of any comminution system. The main shortcomings of direct explicit rock fracture models include the inability to directly access, measure and hence model the internal so-called 'co-ordinate shifts,' and that these internal shifts are the result of an interdependent, potentially non-linear function of the material properties, the machine properties and operating characteristics of the comminution device. A further challenge to the explicit modelling framework, as discussed by King (2001), is that the energy will propagate into the progeny in several ways and differently into different factions of the progeny as it evolves through the comminution device.

Repeating breakage events using a controlled apparatus that loads the particle in some way to failure of single particles of a single mineral of a selected size can however give some indication of the overall relationship between input energy, probability of failure at differing energy levels and final progeny distribution (this of course has to assume that the nature of flaws in the parent particles are randomly distributed and is very similar between the particles tested, and that sufficient particles of a given size can be tested to demonstrate the 'average' energy fracture

response). Tavares and King (1998) conducted such tests on several Taconite Quartz, Sphalerite and Galena particles and demonstrate that the cumulative distribution of energies required to cause fracture can be represented using a log normal distribution and have represented this relationship as per Equation 29.

$$P(E; d_p) = G\left(\frac{ln(E/E_{50})}{\sigma_E}\right) \qquad \textbf{Equation 29}$$

With G being the cumulative Gaussian distribution and E_{50} being the median fracture energy which can be said to vary with size as per the relationship described in Equation 30:

$$E_{50} = E_{\bowtie}\left(1 + \frac{d_0}{d_p - d_{pmin}}\right)^{\varphi} \qquad \textbf{Equation 30}$$

The values of d_0 and φ are material specific and have been measured for several common minerals. d_{pmin} is the size of particles produced and below this size particles absorb energy but do not fracture. $E_{\bowtie}$ is the median fracture energy for large particles. In this study 'large' was deemed to be above 1cm. Using the models provided by King (2001). it is possible to plot the relationship between the energy input and the probability of failure shown in Figure 51.

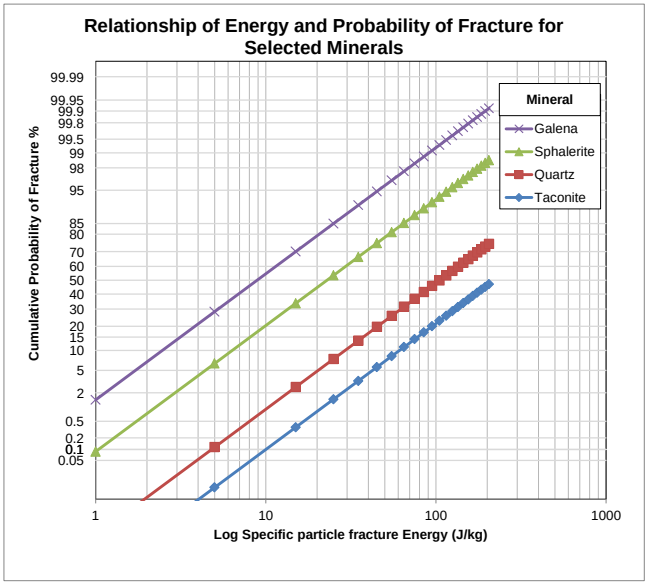

Figure 51: A plot of the specific input energy and cumulative probability of failure for a few selected minerals, size parameter set to 5mm (Adapted after King 2001).

The impact of the size selected also exhibits an exponential form, this is shown in the plot in Figure 52. This clearly demonstrates that the measurement and estimation of the energy required to fracture smaller particles is not trivial and

especially as the material is ground ever finer the distribution of particle fracture toughness will also expand dramatically.

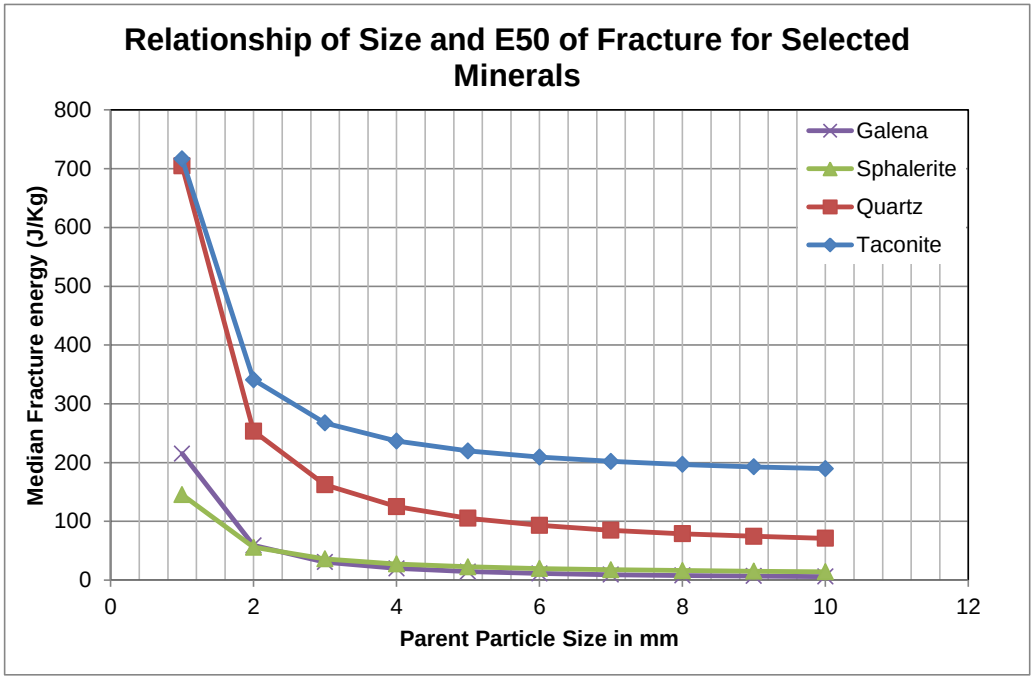

Figure 52: A plot of the median fracture energy for mineral particles of different sizes.

Given the distributions shown in Figure 51 and Figure 52 it is evident that even for a mineral with a defined composition the range of energy required to achieve the same degree of breakage varies substantially. This suggests that it would be limiting to consider a single value for rock toughness per lithology when modelling the operation of process plant equipment. Rather it is proposed that a variable that describes the range of 'resistance to breakage' or so-called 'toughness', should be spatially estimated into the block model. This would describe the rock properties in a block to be mined and become a variable that can be used as an input into the process model. This requires a review of approaches to population balance modelling to determine how the variability and uncertainty in rock toughness can be realistically incorporated into these models.

The general equation, according to King (2001), for the population balance model can be written for comminution machines as follows:

$$N\frac{d}{dx}(u(x)\psi(x)) + \frac{\mathcal{R}(\psi(x), x, F[\psi(x)])}{\beta x^3} + \frac{1}{\beta x^3}\int_{R'(x)} \mathcal{R}(\psi(x'), x', F[\psi(x)])\mathbf{b}(x; x')dx'dx - \frac{N}{\beta x^3}\int_{R''(x)} \psi(x'), \mu(x'), \frac{d\beta x'^3}{dx}\mathbf{a}(x; x')dx'dx = -\sum_j W_{out\,j}\int_{R_c}\left(\frac{N}{M}\right)\psi_{out\,j}(x)dx + W_{in}\int_{R_c}\left(\frac{N}{M}\right)\psi_{in}(x)dx \quad \textbf{Equation 31}$$

In Equation 31 the scalar x represents the particle size d_p measured in linear mm and the average mass of the particle can be related to size by Equation 32:

$$\bar{m}(x) = \beta x^3 \quad \textbf{Equation 32}$$

A commonly used mode for abrasion rates is to assume that it is proportional to the surface area. It is then possible to relate the change in the proportion of material in size d_p per unit time as some function of the area of the particle (Equation 33).

$$\pi\frac{\pi}{6}\frac{dx^3}{dt} = -\frac{k'\pi x^2}{2} \quad \textbf{Equation 33}$$

This suggests that the rate at which particles move in phase space is considered constant and can be given by (Equation 34):

$$u(x) = \frac{dx}{dt} = -k' \quad \textbf{Equation 34}$$

And hence more generally as in Equation 35:

$$\frac{dx}{dt} = -k(x) = -kx^{\Delta} \quad \textbf{Equation 35}$$

If delta is a constant varying between 0 and 1 then the rate of change of mass with respect to time is given by:

$$\frac{dm}{dt} = -k\frac{\pi\rho_s x^{2+\Delta}}{2} \qquad \textbf{Equation 36}$$

It is then possible to convert Equation 31 above using the relationship to derive Equation 37:

$$\psi(x) = \frac{M}{N}\frac{p(x)}{\beta x^3} \qquad \textbf{Equation 37}$$

And so, the population balance equation can be converted to (Equation 38):

$$\begin{aligned} &-\frac{M}{b}\frac{d(k(x)p(x)/x^3}{dx} + \frac{\mathcal{R}(p(x), x, F[p(x)])}{\beta x^3} \\ &+\frac{1}{\beta x^3}\int_{R\prime(x)} \mathcal{R}(p(x'), x', F[p(x')])\mathrm{b}(x; x')dx'dx \\ &-\frac{M}{\beta x^3}\int_{R\prime\prime(x)} \frac{p(x')}{x'^3}3k(x')x'^2, \mathrm{a}(x; x')dx' \\ &= -W_{out\,j}\frac{p_{out}(x)}{\beta x^3} + W_{in}\frac{p_{in}(x)}{\beta x^3} \end{aligned} \qquad \textbf{Equation 38}$$

There are several unit process models in use in the industry that are based on the principles described above; these include models by Whitten (1972) and Andersen(1988).

The Whitten breakage and selection functions (Napier-Munn, 1999) can be described as a combination of models for selection and fracture. In each size class the number of particles leaving and entering the size class is defined for each breakage 'event.' The selection and breakage functions can be calibrated for each ore type. Equation 39 presents a formulation of this approach:

$$P_i = f_i + \tau\sum_{i=1}^{n}\sum_{j=1}^{n} b_{ij}.C_j.P_j - \tau S_i P_i \qquad \textbf{Equation 39}$$

Where P_i is the mass proportion of material in class i

f_i is the feed to class i

b_{ij} is the fraction of material reporting to size class j when material in size class i is comminuted

τ is the time step

C_j is the composition class *j*

P_j is the proportion of particles of size *i* in composition class *j*

S_i is the selection rate for breakage of particles in class *i*

This can be rearranged as follows in Equation 40**:**

$$\boldsymbol{P_i(1-\tau S_i) = f_i + \tau \sum_{i=1}^{n}\sum_{j=1}^{n} b_{ij}.C_j.P_j - \tau\, S_i} \qquad \textbf{Equation 40}$$

And thus, the proportion within each class can be determined using Equation 41:

$$\boldsymbol{P_i = \frac{f_i + \tau \sum_{i=1}^{n}\sum_{j=1}^{n} b_{ij}.C_j.P_j - \tau\, S_i}{(1-\tau S_i)}} \qquad \textbf{Equation 41}$$

The formulae are, however, not in a closed form and must be solved iteratively across all sizes and for each class within each size fraction. The factors that are used to define the parameters for breakage rate and selection function are often derived through experimentation. Often a statistic, commonly the means, of values derived from an assessment of comminution performance of several batch tests on small samples are used in the calibration. This approach requires an assumption that the samples are representative of the material that is to be treated in production, and that the change in scale between laboratory scale machines to full scale operational machines will not result in a substantial bias.

To use this function in the 'Integrated Evaluation Model' the breakage and selection functions need to be fitted to each comminution device in the process flowsheet and must also be calibrated for material domains in the kimberlite pipe.

An Application of the Whitten Crusher model

A feed with a distribution as described in column f_i of Table 23 is sent to a comminution device. The selection function is described by column S_i and the time

adjustment factor (T) is derived for each size fraction, to determine the percentage of each size fraction that will be selected for breakage. The blue block in this table is the breakage matrix or breakage function. It describes the post-crushing distribution of material selected and crushed from each size fraction. The distributions in the breakage matrix can be multiplied by the proportional fraction of each size that is selected for breakage to determine the combined size distribution of material that is selected and broken. This distribution can be added to the material that was not selected for breakage and passed through the unit unscathed. In this way the crushed distribution can be determined, shown in the last row of the table.

		Mins	Frac of Hour
	Residence time	30	0.5

						Destination Sizes - breakage matrix						
Class midpoint	Size Class	% per class in the feed	Selection function	Time Adustment	Actually selected per class	100	10	3.16	1.78	1.33	1.15	1.07
mm	Num	fi	Si	T	%	mm	mm	mm	mm	mm	mm	mm
100.00	1	10	0.5	0.5	2.00		0.1	0.1	0.1	0.1	0.3	0.3
10.00	2	15	0.3	0.5	1.96			0.1	0.1	0.2	0.3	0.3
3.16	3	25	0.2	0.5	2.27				0.1	0.2	0.3	0.4
1.78	4	12	0.4	0.5	2.00					0.1	0.5	0.4
1.33	5	16	0.7	0.5	4.15						0.5	0.5
1.15	6	12	1	0.5	4.00							1
1.07	7	10	0	0.5	0.00							1
	Total	100		Total	16.38		0.1	0.2	0.3	0.6	1.9	3.9

								Total
Distribution of material selected and crushed	0.0	0.2	0.4	0.6	1.2	4.9	9.0	16.4
Unselected in each class	8.0	13.0	22.7	10.0	11.9	8.0	10.0	83.6
New Distribution	8.0	13.2	23.1	10.6	13.1	12.9	19.0	100.0

Table 23: A tabular demonstration of a Whitten selection and breakage model.

The calibration of this model requires several inputs to determine the functions that underpin selection and breakage. As the material or the unit operating parameters change, these functions will require recalibration. The model does not have a direct link to material properties but does provide a large degree of flexibility to model a range of comminution devices. The derivation of the different breakage functions for each size has been the focus of a large body of work. More recent work carried out at the JKMRC has described a form of energy breakage modelling that is based on measurements made on single particle fracture tests (Napier-Munn *et al.*, 1999). The framework for this is expanded below, as it provides a way to relate material properties to expected size distribution of the rock and hence to the diamonds that will be liberated.

Energy Fracture modelling

One useful form of the comminution model is based on the idea that the progeny of breakage events can be based on a mixture of two separate populations and that each cumulative population can be modelled in the form depicted in Equation 42.

$$\boldsymbol{B(x;y) \propto \left(\frac{x}{y}\right)^{n}} \qquad \textbf{Equation 42}$$

where:

$B(x;y)$ is the breakage function

$\frac{x}{y}$ is the ratio of the size of the progeny to the size of the original particle

n is used to describe different distributions of particles produced from tensile stress and particles produced by compressive stress at the points of contact in the comminution device. These two distributions are added using a suitable weighting scheme.

$$\boldsymbol{B(x;y) = K\left(\frac{x}{y}\right)^{n} + (1-K)\left(\frac{x}{y}\right)^{n_2}} \qquad \textbf{Equation 43}$$

The first term in Equation 43 describes the distribution of particles generated by compressive stress at the point of contact, and the second term describes the progeny of tensile stress fracture. It is possible to determine the constants *K*, n and n_2 experimentally for a given rock type and fracture mechanism.

The data gathered from drop weight tests in which a single particle is subject to a known input energy can be used to determine the size distribution of fine and coarse particles. These can be plotted on log-log plot of the size of progeny vs the breakage function value. King (2001) suggests that if d_r is a representative size for a distribution, say the size for which 80 per cent of the particles are smaller than, then a change in the breakage energy depends inversely on the initial particle size.

It is possible to describe a generic form of relationships demonstrated by Kick (1883), Rittinger (1857) and Bond (1943) as shown in Equation 44 :

$$\boldsymbol{f(d_r) = -Kd_r^{-n}} \qquad \textbf{Equation 44}$$

Where

K is a constant

n is a constant for which a value above 1 reflects an increase in energy per unit mass as the particle size decreases.

It is possible to integrate Equation 44 to determine the energy that will be required to change the representative size. Starting with the assumption that $E = 0$ for the initial distribution described by d_{ri}, this derivation is shown in Equation 45

$$\boldsymbol{f(d_r) = -K d_r^{-n}}$$

$$\boldsymbol{E = -\frac{K}{1-n} d_r^{1-n} + C \quad n \neq 1}$$

Equation 45

$$\boldsymbol{0 = -\frac{K}{1-n} d_r^{1-n} + C}$$

$$\boldsymbol{E = \frac{K}{1-n}\left(\frac{1}{d_r^{(n-1)}} - \frac{1}{d_r^{(n-1)}}\right)}$$

This form can be used to show how the equation changes for values used by Kick where *n*=1, Bond where *n* = 1.5, and Rittinger where *n*=2 (Daniel, Lane and McLean, 2010). Single impact tests can be used to determine the progeny distribution that is achieved for a given energy input. The data produced can then be plotted as the cumulative percentage passing a given size on a relative size scale.

The distribution of the progeny can be characterised by the percentage passing one-tenth of its original size (t_{10}). This is another form of the representative size d_r referred to above. In the prior work this size was defined as the P_{80}. It is suggested that given t_{10} it is possible to define a relationship that will describe the other points on the distribution (t_n) . The value for the t_{10} is determined experimentally and is derived from Equation 46:

$$t_{10} = t_{10}max\ (1 - e^{-\beta E/E_{50}}) \qquad \textbf{Equation 46}$$

Where

$t_{10}max$ is a material specific breakage function;

β is a material specific breakage parameter;

E_{50} is the median fracture energy.

Once the value of t_{10} has been derived then the rest of the expected progeny size distribution for a specific energy input to a specific material can be determined. This is often done with truncated distribution functions such as the Rosin-Rammler described in Equation 47.

$$t_n = 1 - (1 - t_{10})^{\left(\frac{10-1}{n-1}\right)^{\alpha}} \qquad \textbf{Equation 47}$$

Where

t_n is the cumulative percentage of progeny passing a proportional size;

t_{10} is material specific breakage parameter;

α is material specific constant; and

n is the fractional size number.

It is possible to plot the expected size distribution for a range of progeny sizes using the above relationships. A worked example from King (2001) is depicted in Figure 53.

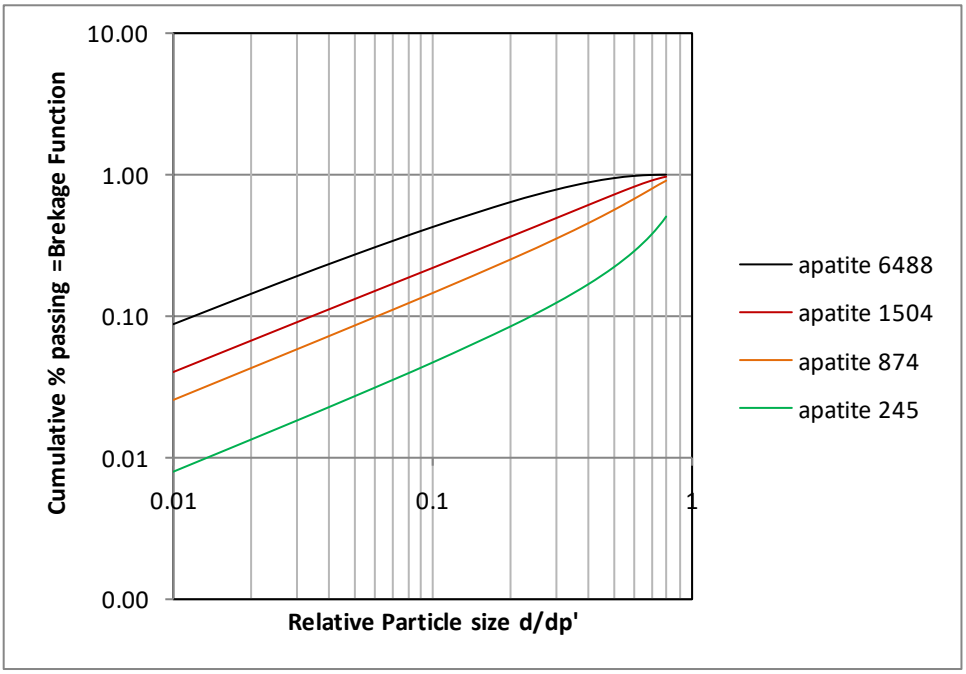

Figure 53: A plot of energy input vs product size using the t_{10} approach and a Rosin Rammler breakage function modified after King (2001).

Screen models

These models are used to determine the split of material through a screening device and have an impact on the ultimate size distribution of material that either leaves the circuit or that is fed to the next crushing or comminution unit process.

There are several versions of the model, but all are based on determining the probability of particles of a given size being presented to an aperture and passing the given screen aperture. The model calibration varies depending on the shape of the aperture, the loading of the screen and the screen deck inclination.

$$\boldsymbol{P = K[(n-1)/n]^2} \qquad \textbf{Equation 48}$$

In Equation 49 the probability P of a particle of dimension l/n passing through a square aperture of dimension l is described by the squared ratio of $(n-1)/n$ where n is any number greater than 1. K is a process-specific parameter used to adjust for operational inefficiency and calibrated by direct experimentation (Taggart, 1964).

DMS Models

Estimating separation efficiency and forecasting the yield tonnage is a very important component of the flowsheet simulation. The DMS process is responsible for the highest proportion of material mass reduction and hence errors in this process model will have a marked impact on the overall recovery model accuracy. In its simplest form the yield can be predicted by taking a sample from the orebody and determining the proportion of material that will be in each density class and multiplying this by the probability of material in a density class reporting to the sink or recovered fraction stream. This curve is commonly referred to as a partition curve. The parameters of this curve are usually determined experimentally, and these data are used to derive the Ep value as described in Equation 49:

$$\boldsymbol{E_p = \frac{D_{75} - D_{25}}{D_{50}}} \qquad \textbf{Equation 49}$$

Where:

E_p is the probability of separation.

D_{75} is the density at which 75% of the material reports to the sink fraction.

D_{50} is the density at which 50% of the material reports to the sink fraction.

D_{25} are the densities at which 25% of the material reports to the sink fraction.

There is also an option to include a constant *K* value in the estimation of separation efficiency that reflects the proportion of material that is misplaced due to its shape or other inefficiencies. To determine the proportion of material that will report from any given density fraction to the sinks, the formula above is rearranged to give the following Equation 50:

$$\boldsymbol{P_s = \frac{E_p}{1 - e^{K \times (D_c - D_{50})}}} \qquad \textbf{Equation 50}$$

Where:

P_s is the probability of sink.

E_p is the probability of separation.

Dc is the density of the class being considered.

K is a separation efficiency factor.

Estimating the proportion per density class per size fraction for a given kimberlite size distribution is not trivial. The laboratory process for densiometric determination typically consumes about 70kg of core that is crushed in a jaw crusher to produce a given size distribution, and then the product is screened into several size fractions. Each size fraction is then split into density classes using liquids of ascending density. The products from each sink float split are weighed and documented. This produces data that can be represented in a table such as in Figure 54**.**

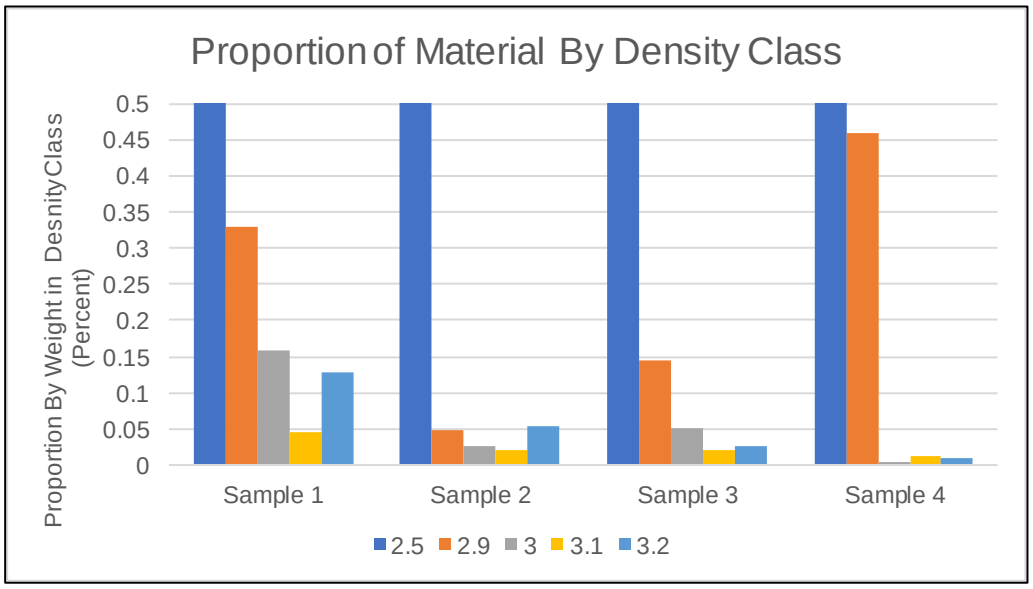

Figure 54: A Densimetric distribution plotted for four samples derived from kimberlite, crushed to 100% passing 12mm and grouped by density classes.

- It is, however, evident that as the size distribution changes the distribution of density within each size class will change. The adaption of the density distribution for changing size distribution requires a function that relates the change in size distribution to the change in density distributions in each size class. If one were to consider five density classes and 13 size classes one would end up with 75 'density by size' classes, so material breaking out of one of the larger size classes will produce progeny that has some undefined

probability of ending up in several of the smaller density classes. To do this mapping requires staged comminution and density test work for each material type considered. The number of tests and stages of crushing required to facilitate this multidimensional mapping depend to a large degree on:

- the density distribution of the components that make up the rock;
- size distribution of different components; and
- the affinity or adherence between the different components in the rock under investigation that will give rise to the composites at different levels of fracture

This approach can to some extent be informed by the texture of the kimberlite rock type and will also provide a quantitative approach to classification of textures that result in distinctly different response variables.

6.5 Establishing relationships between comminution and diamond recovery

Once it is possible to relate rock property to process performance, and especially total comminution that will be achieved at a block scale, a model of diamond liberation and lock up is required to enable the estimation of a diamond recovery factor. The next section describes in some detail how the particulate nature, and size distribution relationships that have been shown to exist in kimberlitic diamond deposits can be used to relate overall comminution and DMS efficiency to diamond recovery.

The macro micro diamond recovery model

In the earliest phases of a diamond project the grade is estimated using microdiamonds, recovered from small samples(~100-400kg) that generally include diamonds smaller than ~ 0.7mm. These are recovered from core in a process of thermochemical dissolution and evaluated by taking microscopic measurements of each diamond. The estimate is achieved by determining the abundance of small diamonds in several size classes, and then modelling the diamond size frequency in the form of a quadratic equation as depicted in Equation 51.

$$y_i = ax^2 + bx + c \qquad \textbf{Equation 51}$$

This curve model can then be extrapolated into the larger diamond size classes. This is commonly referred to as a total content curve (see Figure 55 below).

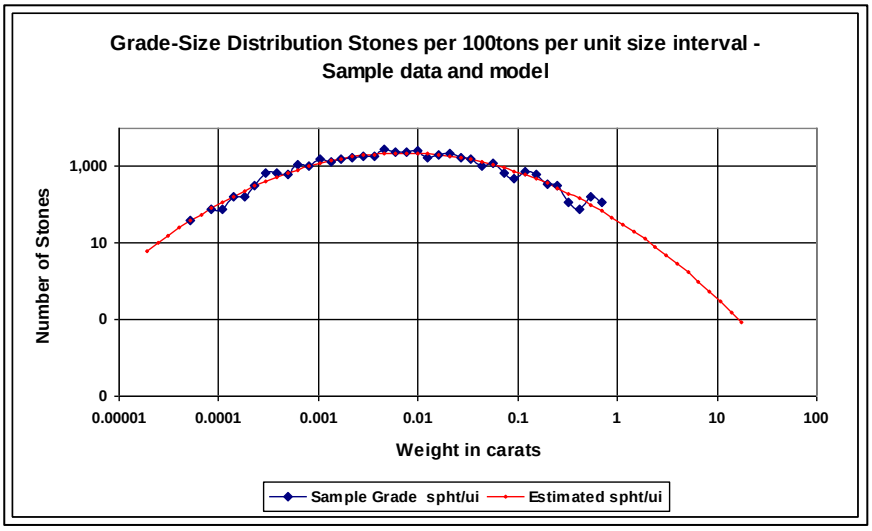

Figure 55: A plot of the log of diamond weight vs log of the number of stones in each class per hundred tonnes per unit interval.

The total stone content can be derived by integrating this function across all size fractions (Equation 52). This can be used to determine the grade between an upper and lower cut off size by converting the stones frequency to a mass.

$$\boldsymbol{total\ contained\ stones} = \int_{\boldsymbol{d_i}}^{\boldsymbol{d_n}} (\boldsymbol{y})\boldsymbol{dx} \qquad \textbf{Equation 52}$$

Process plants however usually operate in the size range of 1mm to 32mm although some plants operate beyond this size range (Technical and Financial Report, 2001). To adapt this curve to estimate recoverable grade there is a requirement to trim the upper and lower ends of the curve. This is done by fitting a third-order polynomial to the total content curve at both the top and bottom end of the planned recovery size envelope. The shape and sharpness of the top and bottom size cut-off curves is usually determined by the modeller and is based on experience of curves achieved at several existing operations.

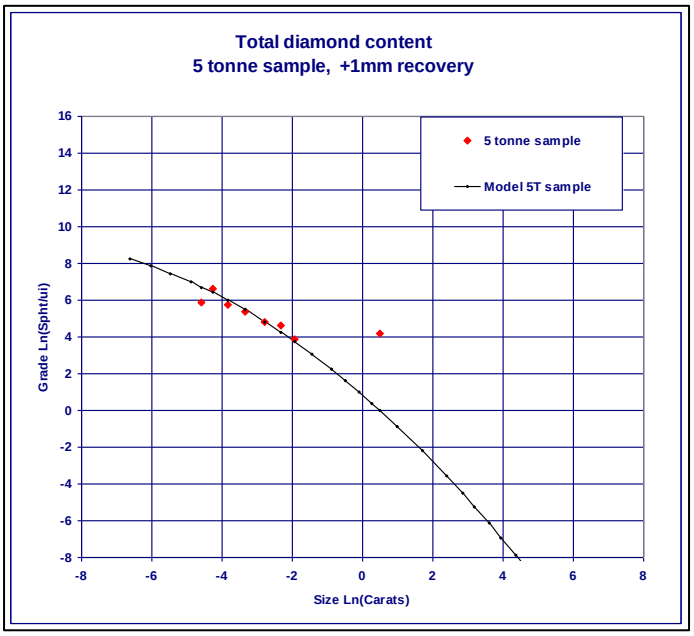

Figure 56: A plot of the logarithm of diamond size vs stone frequency in stones per hundred tonnes per unit interval.

This trimming can then be used to determine the resource grade and size distribution that is reported at a bottom size cut-off of 1mm. In cases where economics suggest that the lower cut-off should be higher than 1mm the curve is adjusted to the recommended cut-off in a similar way to that shown in Figure 56

Benefits and limitations of the micro - macro modelling approach

The sampling for microdiamonds requires of the order of 50 to 400kg of material that is digested in a sequence of chemical treatments that do not require any crushing and do not leave any residue larger than several microns. This process does not damage the contained diamonds and does not leave any diamonds locked in the kimberlite. With sufficient samples it is possible to distinguish size distributions within internal lithology types in kimberlite deposits. The method, however, relies on extrapolating from the microdiamond size range to the macro-diamond size range. This extrapolation becomes subjective in the absence of an abundance of macro-diamonds that can be obtained from bulk sample treatment.

Samples that provide macro-diamonds need to be in the order of tens to hundreds of tonnes and may, or may not, be representative of the diamond population in each of the lithologies in the deposit. Also, the recoveries from bulk sampling are subject to loss and lock up that is a function of the total grind achieved and the efficiency of the diamond processing equipment.

The trimming of the ends of the curves is also subjective in this method in the absence of operating plant data, and small increments in the larger sizes have a relatively low impact on the carat recovery but can have a substantial impact on the revenue recovery. The benefits of having an underlying diamond size frequency model when sampling for grade are described in Coward and Ferreira (2004)

The granulometry liberation and lock-up model

Once the in situ total content has been estimated and relatively strict cut-off sizes applied, the process of diamond recovery and loss can be modelled in more detail. As diamonds are particulate in nature, having a large range of size distributions, one of the ways in which the estimated diamond recovery can be modelled is to relate the comminution of rock to the expected proportion of diamonds that will be released or liberated from the kimberlite.

The model was originally conceived and applied to operating facilities on the west coast of Namibia with the aim of trying to calculate the loss of diamonds that arises from the inability to crush all the material to lower than the smallest contained diamond (Kleingeld, 1982). Diamonds lost in this way are deemed to be "locked". The model is centred on an assumption that it is possible to build a relationship between the recovered size distribution of diamonds and the grind size of the ore achieved to estimate the diamonds that are still not liberated, and hence discarded in the tailings. The model was subsequently applied by Ferreira to a number of kimberlitic deposits. During this time a collaboration with Lantuéjoul(1998) saw several improvements in the formulation of the model. This author worked with Ferreira from 1998 to 2008 to improve various aspects of sampling, data collection and its use in implementing the model at several of De Beer's operating mines. Ferreira (2013) gives a brief description of the model, however a more detailed description is presented here due to its importance in this research. The model can then be used in a variety of ways with total content curves to estimate the expected recovered diamond distribution.

Model description

The model begins with an assumption that the diamonds that have been recovered represent only a portion of the total population of diamonds. The total population of diamonds is deemed to be the sum of the diamonds recovered and the diamonds that are still ‘locked’ in the discarded tailings. The model assumes that there is a relationship between the proportion of recovered diamonds within a size class and the proportion of the discarder kimberlite in an equivalent size class. An additional assumption of the model is that the that the diamonds are not damaged in the rock crushing process.

A very simple conception of the model can be applied to a process that only includes crushing of the rock and handpicking out the diamonds. Assume that prior to crushing all the rock particles were in one size class, say 5mm to 4mm and that the deposit only contains diamonds in the 5mm to 4mm fraction. If we do not crush the ore any further and carry out a hand sorting , i.e. there are no ore particles less than the 5-4mm size class, it can be reasonably assumed there is 0% liberation. If, however the grind achieved meant that there was still 50% of the material in this fraction, and the other 50% was less than 4mm it would be possible that only half of the diamonds were liberated. By extension if the grind achieved ensured that there was no material larger than 4mm, and none of the diamonds were damaged in the kimberlite size reduction process, then all the diamonds would be liberated.

The range of sizes of diamonds recovered and the range of size of ore particles (grind) produced can be obtained by sampling and screening the discarded ore, and screening and recording the mass size distribution of the diamonds recovered. The relationship between the size distribution of the recovered and the kimberlite discarded can be used to develop an estimate of the diamonds that are still contained in the discarded kimberlite stream.

There are several sampling and data assumptions required by the model:

- It is possible to define the relationship between diamond size classes and ore size classes;
- It is possible sample for, and reconstitute the total grind of the diamond bearing ore;
- The diamond concentration is relatively low and hence the crushed size distribution of the rock is independent of the size distribution of the diamonds;
- Diamonds are randomly distributed in the ore blocks; and
- There is no relationship between the diamonds size and its location in broken particles.

Several ore sizes are tabulated in Table 24. From the recovery process the total grind of the ore fed to the plant is recorded. This size distribution is reflected in the third column of this table. The recovered diamonds could be sieved, and the size distribution represented in the fourth column as the percentage of stones per class. By summing the classes from the smallest to the largest it is possible to express the proportion of the distribution that could still be “locked” within each ore size class.

		Measured Data			Model Calculation	
Class Number	Class bottom Size	% of Ore in Size Class	% of Diamonds in Size Class	Cumulative % of Diamonds Less than Size Class	% of Diamond Distribution Possibly Locked in Class	Cts Locked per 100cts Recovered
1	15	10	0	100	100	10
2	10	20	15	85	85	17
3	8	50	35	50	50	25
4	4	15	45	5	5	0.75
5	2	5	5	0	0	0
Totals		100	100			52.75

Table 24: Calculation of locked diamond content.

It is then possible to calculate the proportion of carats that can be locked in each size fraction by multiplying the proportion of the ore that is in each size class and the proportion of the diamond size distribution that could be contained in the ore particle. As depicted in Table 24 the second class (10mm) of ore particles make up 20% of the material discarded. 15% of the total diamonds recovered lie in this class, and 85% of the diamonds recovered are below 10mm. This suggests that 85% of the diamond population can be locked, and by multiplying the ore proportion by the proportion of the diamond distribution that can be locked we calculate that the lock up in this size class can be 17 cts. By summing the locked content estimated for each size fraction we see that for every 100cts recovered 52.75 cts could be locked. This implies that the liberation efficiency can be estimated to be:

$$\%\boldsymbol{Liberation} = \frac{\mathbf{100}}{\mathbf{100} + \boldsymbol{locked\ estimated}} \boldsymbol{X}\mathbf{100} \qquad \textbf{Equation 53}$$

So, in this case the liberation would be expected to be 65%.

The process, however, also includes a float and sink separation process, and for a kimberlite particle to sink and be recovered in the final process, the density of the particle must exceed that of the effective cut point in the dense media separation process. This means that is possible to calculate the maximum size of diamond that can be floated out of the dense media separation process given the ore density, diamond density and the density cut point in the plant. This change in the lock up calculation by limiting the maximum size of diamond that can be recovered to below the ore size is depicted in table 25.

		Measured Data			Model Calculation		
Class Number	Class bottom Size	% of Ore in Size Class	% of Diamonds in Size Class	Cumulative % of Diamonds Less than Size Class	Maximum Size of Diamond in this Class	% of Diamond Distribution Possibly Locked in Class	Cts Locked per 100cts Recovered
1	15	10	0	100	10	85	8.5
2	10	20	15	85	8	50	10
3	8	50	35	50	4	5	2.5
4	4	15	45	5	2	0	0
5	2	5	5	105	1	0	0
Totals		100	100				21

Table 25: Calculation of lock up with constraint placed on the maximum size of contained diamond.

In this adapted calculation, the class 2 (10mm) ore particles can only lock up diamonds up to 8mm. There are only 50 % of diamonds below this size limit that can potentially be locked. The same calculations are carried out. The estimated locked content has dropped to 21cts for every 100cts recovered, equating to a liberation of 83%.

To generate a model requires a realistic method for determining the limiting mass of diamond that can be contained in a particle and for that particle to be recovered by the process. One approach to derive this limit is to consider the physical nature of the process used to separate diamonds from kimberlite post the crushing stage. In this process the density differences between diamonds (specific gravity of 3.52 g/cm^3) and most kimberlites (specific gravity of 2.7 g/cm^3) is exploited to generate a diamond rich concentrate. The maximum volume of diamond contained in a particle of kimberlite that could be floated out of the dense media separation process is a function of the density of media that is used to separate the diamonds from the kimberlite, the density of the kimberlite, the density of the diamond and the relative volume of the diamond and kimberlite in the particle. A critical particle can be defined as one where the forces of buoyancy and the sinking force are equal. The mass of displaced medium will equal the mass of the particle, and the mass of the particle is the combined mass of the contained diamond and the enclosing kimberlite.

Model assumptions

The main underlying assumptions of the liberation model include:

- Total diamond content is the sum of the recovered and locked diamonds;
- The density of kimberlite particles is homogenous across a range of sizes and particle shapes;
- The diamonds exist in very low concentrations and thus have little influence on the location and orientation of fractures in the rock;

- All diamonds that report to the sink stream, including those in composite diamond and kimberlite particles, will be recovered;
- The recovered diamond size distribution and the in situ size distribution do not differ markedly; and
- The diamond size distribution can be reliably modelled as a log normal distribution.

Model formulation

The general formulation of the liberation model will be described in this section and is broadly based on the work of Kleingeld (1982) and Ferreira (2013) and unpublished work by Lantuéjoul(1998).

The notation used is described in King (2000). The particle size distribution function $P(d_p)$ is the mass fraction of that portion of the size fraction that consists of particles of a size less than or equal to d_p where d_p is the size of the particle. This function has the properties:

P (0) =0
P (∞) =1
P(d_p) increases monotonically from 0 to 1 as d_p increases from 0 to ∞

By differentiating the distribution function, it is possible to work out proportions of particles that are less than or equal to a given size threshold x. The distribution density function $p(x)$ can be defined by Equation 54:

$$\boldsymbol{p(x) = \frac{dP(x)}{dx}} \qquad \textbf{Equation 54}$$

And likewise, the discrete density distribution can be related to its density function in a similar way (Equation 55):

$$\boldsymbol{p_i = \sum_{D_i}^{D_{1-1}} p(x)dx} \qquad \textbf{Equation 55}$$

The usefulness of this approach for describing particle size distributions is that it facilitates the assumption that it is possible to work with the size class rather than the individual particles. To do this requires the definition of the 'average' particle in a size class, and the allocation of several empirical distribution functions to the particle populations.

In reality the distribution for a sample of ore or diamond particles is truncated at both the upper end, due to the maximum size of rock that is considered, and at the lower end by the minimum size of particle that is sampled or diamond that is recovered. The continuous distribution could be obtained for a parcel of diamonds by weighing each stone. It is, however, normal practice for the particles to be sieved on a set of screens and for the mass of particles in each size class to be measured. This then gives rise to the discrete particle size density function (Equation 56):

$$\mathbf{P_i(d_p)} = \int_{\mathbf{D_i}}^{\mathbf{D_{i-1}}} \mathbf{dP(d_p)} = \mathbf{P(D_{i-1})}\,\mathbf{P(D_i)} = \Delta\mathbf{P_i} \qquad \textbf{Equation 56}$$

$\mathbf{P_i}$ is the mass fraction of the particle population that consists of particles between size D_i and D_{i-1}.

$\Delta d_p = D_{i-1} - D_i$ is known as the size class width, with the upper and lower-class size boundaries given by D_i and D_{i-1} respectively. The representative size in this class is required so that the 'average' characteristic in this class can be used in modelling the behaviour of all particles within this class. One method proposed by King (2001) is to develop the number density distribution function (as opposed to a mass distribution considered above). The number distribution function for any characteristic can be defined as$\varphi(x)$, which is the faction by number of particles in the population having size equal to x or less. The number density function can be defined as in Equation 57:

$$\boldsymbol{\varphi} = \frac{\boldsymbol{d\varphi(x)}}{\boldsymbol{dx}} \qquad \textbf{Equation 57}$$

and the discrete number density function is given by Equation 58:

$$\boldsymbol{\varphi_i} = \boldsymbol{\varphi(X_{i-1})} - \boldsymbol{\varphi(X_i)} = \Delta\boldsymbol{\varphi_i} \qquad \textbf{Equation 58}$$

Here the upper-case letters represent the class boundaries. The number distribution facilitates the calculation of the average properties of the particles either in the total population or in each size interval. This can be calculated as follows in Equation 59:

$$\overline{\boldsymbol{x}}_{\boldsymbol{N}} = \frac{\mathbf{1}}{\boldsymbol{N_T}} \sum_{\boldsymbol{j=1}}^{\boldsymbol{N_T}} \boldsymbol{x_{(j)}} \qquad \textbf{Equation 59}$$

Here $x_{(j)}$ is the value of the characteristic for particle j and N_T is the total number of particles in the population. Grouping the particles, in this case diamonds, into

classes of particles having the same or similar characteristics allows the summation of the characteristics of the properties of each class. It is then possible to calculate the average property *x* in the whole population using Equation 60 as follows:

$$\bar{x}_N = \frac{1}{N_T}\sum_{i=1}^{N} n_{(i)} x_{(i)} \qquad \textbf{Equation 60}$$

In this case *N* is the number of classes or groups that have been formed, $n_{(i)}$ is the count of the number of particles in each group *i* and $x_{(i)}$ is the characteristic defining each group. If the groups have different sizes or densities for example it is possible to weight this calculation by mass per group (Equation 61):

$$\bar{x}_N = \frac{1}{M_T}\sum_{i=1}^{N} m_{(i)} x_{(i)} \qquad \textbf{Equation 61}$$

where M_T represents the total mass of the population being considered.

To describe the behaviour of particles within a size class a representative size is required for each class. The objective is to define a single size that will adequately represent the behaviour of all the particles in this class. One derivation for this representative size is described by King (2001) as in Equation 62:

$$d_{pi}^3 = \frac{1}{\varphi_i(d_p)}\int_{D_i}^{D_{i-1}} d_p^3\, \varphi(d_p)\, dd_p \qquad \textbf{Equation 62}$$

Where $\varphi(d_p)$ is the number distribution density function, and $\varphi_i(d_p)$ is the number fraction of the population in a size class.

For most ore streams, the sieving is conducted with a variety of screen sequences. This process provides data where the size class width is not constant and thus a factor needs to be used to convert the stone count frequencies or masses observed in each class by the relative width (a measure of 'distance' in size space) of the classes. For the diamond size distribution this factor, known as the unit interval, is derived by taking the difference of the logarithms of the critical carat mass between the upper and lower-class boundaries (Equation 63)

$$U_i = \frac{1}{log(CritSz_i) - log(CritSz_{i+1})} \qquad \textbf{Equation 63}$$

where $CritSz_i$ is the critical size in cts/stone of the screen on which the diamonds have been retained, and;

$CritSz_{i+1}$ is the critical size in cts/stone of the screen above the retaining screen.

The critical carat mass for a given screen size is defined as that size of diamond that will have a 50% probability of being passed or retained on a given sieve. These factors are usually derived empirically for each diamond deposit or groups of similar deposits. Likewise, the average representative size of the diamonds retained on each screen size is also derived empirically. Table 26 gives the critical sizes and average stone masses for several diamond deposits for a standard set of diamond sized sieves.

Sieve Class Number	Diamond Sieve name	Square Aperture mm	Average Size Carats	Critical size Cts/stone
1	200+	30.05	213.31	199.80
2	150+	27.05	160.74	149.80
3	100+	23.33	107.86	99.80
4	75+	21.01	81.25	74.80
5	60+	19.36	65.21	59.80
6	45+	17.43	49.1	44.80
7	30+	15.02	32.9	29.80
8	25+	14.07	27.58	24.80
9	20+	12.95	22.02	19.80
10	15+	11.64	16.54	14.80
11	+23	8.04	8.04	7.94
12	+21	7.09	3.69	3.79
13	+19	5.56	1.92	1.95
14	+17	4.93	1.42	1.40
15	+15	4.62	1.20	1.17
16	+13	3.85	0.70	0.71
17	+12	3.42	0.52	0.51
18	+11	2.86	0.32	0.31
19	+9	2.35	0.18	0.18
20	+7	2.00	0.12	0.12
21	+6	1.72	0.08	0.08
22	+5	1.47	0.05	0.05
23	+3	1.15	0.03	0.03
24	+2	1.03	0.02	0.19
25	+1	0.82	0.01	0.01
26	-1	0.01	0.00	0.00

Table 26: Listing of Diamond screen sieve classes and associated sieve apertures, average stone size per class and critical stone size per class.

In diamond process modelling the diamond particles are considered to have a log normal distribution (Rombouts, 1995). This distribution can be defined as per Equation 64:

$$\boldsymbol{P(D) = G\left(\frac{ln(D/D_{50})}{\sigma}\right)} \qquad \textbf{Equation 64}$$

Where G(x) is the function presented in Equation 65:

$$\boldsymbol{G(x) = \frac{1}{\sqrt{2\pi}}\int_{-\infty}^{x} e^{-t^2/2}dt} \qquad \textbf{Equation 65}$$

$$\boldsymbol{= \frac{1}{2}\left[1 + erf\left(\frac{x}{\sqrt{2}}\right)\right]}$$

and where:

$$\boldsymbol{\sigma = \frac{1}{2}(lnD_{84} - lnD_{16})} \qquad \textbf{Equation 66}$$

D_{50} is the particle size at which P (D_{50}) = 0.5, this is called the median size.

The log normal distribution has theoretical significance in that it is the distribution that results when a particle is crushed using several fracture events (Kolmogrov 1941). Its usefulness partly lies in the fact that this its properties suitably reflect the diamond mass size distribution variable and it can be modelled using two parameters (Aitchison and Brown, 1957). In the case of the granulometry model a two-part fit is used. This requirement arises most likely from the incomplete liberation of finer stones in the distribution, and or the loss and destruction of diamonds from the coarser side of the distribution (Ferreira, 2013).

The graphic in Figure 57 shows the fitting of the curve to the recovered diamond distribution.

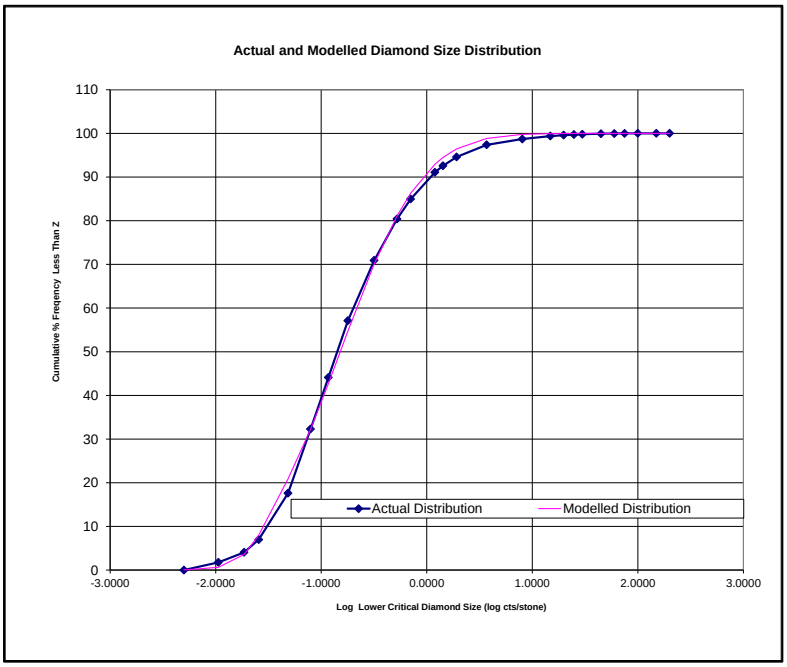

Figure 57: Plot showing the actual and modelled log normal diamond size distribution.

If all the particles of kimberlite remain larger than the largest diamond, then each of the kimberlite particles can feasibly contain a diamond of any size from the full range of recovered diamond sizes. Once there are kimberlite particles that are smaller than the largest diamond, the kimberlite particles can only feasibly contain diamonds from a selected, or trimmed range of the recovered diamond size distribution. Hence as the kimberlite ore is crushed, and the liberated diamonds recovered, then the estimated probability of diamonds being locked in single size fraction of discarded kimberlite is given by:

$$\boldsymbol{p_L(C_i) = \sum_{i=1}^{i} \left[Md_i \Big/ \sum_{i=1}^{i=n} Md_i \right] \times \left[Mk_i \Big/ \sum_{i=1}^{i=n} Mk_i \right]} \qquad \textbf{Equation 67}$$

Where :

n is the number of size classes

$p_L(C_i)$ is the probability of diamonds being locked in kimberlite in size class i

Md_i is the mass of diamond recovered in size class i

Mk_i is the mass of kimberlite in size class i

Further if one assumes the relationship shown in Equation 68:

$$\boldsymbol{total\ recoverable\ diamond\ content = liberated\ diamonds + locked\ diamonds} \quad \textbf{Equation 68}$$

Then by rearrangement for every 100cts recovered the liberated carats can be expressed as in Equation 69 :

$$\%\boldsymbol{Liberation} = \frac{\boldsymbol{100}}{\boldsymbol{100 + locked\ estimated}}\boldsymbol{X100} \quad \textbf{Equation 69}$$

This assumption allows us to convert the locked potential calculated to an estimated locked carat number for every 100 cts that are recovered.

The maximum diamond size that can possibly be found in a kimberlite particle that has been discarded is, however, not only a function of the ore and diamond particle size but must also have floated out of the dense media separation process. For this to have happened the apparent weight of the particle must have been less than the force of buoyancy to which the particle was exposed. A critical particle can be defined as a particle that neither sinks nor floats, and hence the force of buoyancy (F_b) is equivalent to the sinking force (F_s). By equating these two forces it is possible to derive the volume and hence maximum size of diamond that can be locked in a tailings particle for a given set of input parameters. (Equation 70)

$$F_b = F_s$$

$$\boldsymbol{V_P \times \rho_M = V_k \times \rho_k + V_d \times \rho_d} \quad \textbf{Equation 70}$$

Equation 71 shows the result of solving for V_d

$$\boldsymbol{V_d = \frac{V_p(\rho_M - \rho_k)}{(\rho_d - \rho_k)}} \quad \textbf{Equation 71}$$

Where:

V_d: Maximum volume of diamond that can be contained in the particle and still float

V_P: Volume of particle

ρ_M: The density of the cut-point that the particle is exposed to in the dense media separation process

ρ_k: The density of the host kimberlite

ρ_d: The density of the contained diamond

Thus it is likely for most operations that the formulation in Equation 67 will be optimistic as it assumes that a diamond of the same size as the particle can be locked in the discarded rock. As shown in Equation 71**,** the probability of being locked can be reduced to equate to cumulative proportion of the diamond size distribution that lies below the maximum size of diamond ($D_{vmax)}$ that can be locked in a kimberlite particle of size class i. To find this class the maximum volume is converted to a mass of diamond and then the class that this diamond of this mass would be classified into is chosen as the "*Max-i'*. This leads to the probability of lockup in class i being reformulated as in Equation 74.

$$\boldsymbol{p_L(C_i) = \sum_{i=1}^{i=Max\ i} \left[Md_i \Big/ \sum_{i=1}^{i=n} Md_i \right] \times \left[Mk_i \Big/ \sum_{i=1}^{i=n} Mk_i \right]} \quad \textbf{Equation 72}$$

This model provides the maximum size of diamond that can potentially be locked in each size particle. Also having knowledge of the size distribution of diamonds recovered, it is possible to calculate the possible locked distribution in each ore particle size class and summing across all ore sizes it is then possible to construct an estimate of the discarded diamond size distribution.

This in turn can be used to determine the maximum potential value of the discarded stream of kimberlite particles, by multiplying the $/ct value for each size of diamond by the estimate of locked diamond potential (see Table 33)

Application of the model

In this section the application of the granulometry model to the Venetia diamond size frequency and a sample of two weeks production will be described.

The first part of the process is to derive the degree to which the kimberlite was crushed, the total grind, or resulting size distribution of all the processed kimberlite is required. This is achieved by sampling at various points in the process and determining the relative mass flows in each stream to reconstruct the size

distribution of the processed kimberlite. The sampling collects a representative size distribution of the mass of coarse discarded material over a two-week period and this material is sieved into sizes. Each size fraction is then sorted into kimberlite and non-kimberlitic particles. Once this information is available the true size distribution can be calculated.

1	2	3	4	5	8	9	10	11
Sieve Size mm	*Mass retained (kg)*	*% retained in class %*	*cumulative passing %*	*% kimberlite in class %*	*Mass Kimberlite kg*	*Mass per size Fed to DMS tonnes*	*Mass Kimberlite tonnes*	*Total Kimberlite % per class %*
12.00	0.00	0.00	100.00	83.72	0.000	0	0	0.0
8.00	0.04	0.59	99.41	83.72	0.033	40	40	0.5
5.60	0.80	11.76	87.65	52.63	0.421	505	505	6.3
4.00	1.29	18.97	68.68	75.00	0.968	1160	1160	14.5
3.35	0.63	9.26	59.41	75.00	0.473	566	566	7.1
2.80	0.64	9.41	50.00	73.91	0.473	567	567	7.1
2.00	1.16	17.06	32.94	72.41	0.840	1007	1007	12.6
1.40	1.15	16.91	16.03	75.76	0.871	1044	1044	13.1
1.00	0.78	11.47	4.56	79.17	0.618	740	740	9.3
-1.00	0.31	4.56	0.00	100.00	0.310	372	2372	29.6
	6.80			Totals	5.006	6000	8000	100

Table 27: Description of method used to convert the sampled tailings distribution to a total kimberlitic distribution.

In the first column of Table 27 the aperture of the sieves used to size the sampled material is recorded. The mass retained and the % kimberlite in each size class is given in columns 2 and 5 respectively. This information is used to calculate the mass of kimberlite in each size class which is shown in column 8. The size distribution is converted to tonnes of kimberlite in each size class that will have been processed in the period being considered by multiplying the percentage in each class by the dense media feed tonnes for the period (6000 in this example). As there is material that is below the bottom screen size (i.e-1mm) that will not have been sampled in the discard material, the size distribution must be adjusted to include this material. In this example two thousand tonnes of undersize material (also commonly referred to as slimes) was discarded in the underflow. It is assumed that this material is all kimberlite, which is a reasonable assumption given that most waste rock components are usually harder than the kimberlite. This mass is added into the size distribution in the second last row of column 10. This tonnage size distribution can then be converted to a cumulative % retained size distribution of the processed kimberlite for use in the model. To map the ore sizes to diamond sizes a linear interpolation is used.

The diamonds recovered over the period are sieved and the size distribution is modelled using a two-part log normal model.

1	2	3	4	5	6	7	8	9
Diamond	Critical	Log Critical	Actual %	Fitting of Size Distribution			Cumulative	Error
Sieve	Size	Size	Passing	Gauss1	Gauss2	Fit	Retained	on model
	cts/stone	log cts/stone	%	%	%	%	%	%
200+	199.80	2.30	100.00	100.00	100.00	100.00	0.00	0.00
150+	149.80	2.18	100.00	100.00	100.00	100.00	0.00	0.00
100+	99.80	2.00	100.00	100.00	100.00	100.00	0.00	0.00
75+	74.80	1.87	99.99	100.00	100.00	100.00	0.00	0.00
60+	59.80	1.78	99.96	100.00	100.00	100.00	0.00	0.00
45+	44.80	1.65	99.92	100.00	100.00	100.00	0.00	0.01
30+	29.80	1.47	99.80	99.99	100.00	99.99	0.01	0.04
25+	24.80	1.39	99.72	99.99	100.00	99.99	0.01	0.07
20+	19.80	1.30	99.60	99.97	100.00	99.97	0.03	0.14
15+	14.80	1.17	99.38	99.94	100.00	99.94	0.06	0.31
+23	8.04	0.91	98.71	99.77	100.00	99.77	0.23	1.11
+21	3.69	0.57	97.38	98.85	100.00	98.85	1.15	2.18
+19	1.92	0.28	94.61	96.47	100.00	96.47	3.53	3.47
+17	1.42	0.15	92.58	94.47	99.98	94.47	5.53	3.56
+15	1.20	0.08	91.10	92.94	99.96	92.94	7.06	3.38
+13	0.70	-0.15	84.97	86.29	99.66	86.29	13.71	1.75
+12	0.52	-0.28	80.40	81.13	99.03	81.13	18.87	0.54
+11	0.32	-0.50	70.89	70.07	95.70	70.07	29.93	0.68
+9	0.18	-0.75	57.12	54.75	84.33	54.75	45.25	5.61
+7	0.12	-0.93	44.11	42.73	68.46	42.73	57.27	1.92
+6	0.08	-1.10	32.29	32.24	49.85	32.24	67.76	0.00
+5	0.05	-1.31	17.60	20.89	27.02	20.89	79.11	10.80
+3	0.03	-1.59	6.99	10.29	8.00	8.00	92.00	1.03
+2	0.02	-1.73	4.06	6.78	3.58	3.58	96.42	0.23
+1	0.01	-1.97	1.76	2.92	0.62	0.62	99.38	1.30
-1	0.01	-2.30	0.00	0.76	0.03	0.03	99.97	0.00

Table 28: Fitting of the lognormal model to the recovered size distribution.

Table 28 shows the resulting fit and the squared error in each of the size classes. The graph of the actual and fitted distribution is shown in Figure 57. Although some classes show some deviation between the actual and the model fit, in general the form of the model and actual recovery correspond reasonably well.

The parameters of the process that has been used to separate the kimberlite is also recorded and is given in Table 29.

For each composite particle size, Equation 60 can be used to calculate the maximum size of diamond that can be locked in a ‘critical’ class particle. Once this has been done for each size class considered it is possible to calculate what proportion of the diamond distribution can be locked in this particle.

Plant Operating Parameters		
Diamond Density	3.515	g/cm^3
Kimberlite Density	2.5	g/cm^3
Operating density	3	g/cm^3
Actual Cut Point	2.7	g/cm^3
Headfeed	8000	dry tonnes per day
Tonnes to oversize discard	0	dry tonnes per day
Tonnes feed to fines DMS	6000	dry tonnes per day
Tonnes to undersize	2000	dry tonnes per day

Table 29: Process parameters required for the granulometry model.

This diamond mass will most likely have a distribution that is equivalent to the recovered distribution truncated by the maximum locked diamond particle size. The result of these calculations is shown in Table 30.

Sieve Parameters		Kimberlitic Breakdown		Kimberlite Distribution		Particle Size			Maximum Locked diamond		
Diamond	Square	Average	Critical	Cum %	Class	log Square	Spherical	Factored vol	Volume	Size	Size
Sieve	mesh	Size	size	tonnes	tonnes	Mesh	Volume	0.9	diamond	carats	mm
name	mm	cts/stone	cts/stone	%	%	log mm	cm^3	cm^3	cm3	cts	mm
	32			0.00		1.51	17.16	15.44	2.45	43.04	18.58
200+	30.05	213.31	199.80	0.00	0.00	1.48	14.21	12.79	2.03	35.64	17.45
150+	27.05	160.74	149.80	0.00	0.00	1.43	10.36	9.33	1.48	26.00	15.71
100+	23.33	107.86	99.80	0.00	0.00	1.37	6.65	5.98	0.95	16.68	13.55
75+	21.01	81.25	74.80	0.00	0.00	1.32	4.86	4.37	0.69	12.18	12.20
60+	19.36	65.21	59.80	0.00	0.00	1.29	3.80	3.42	0.54	9.53	11.24
45+	17.43	49.1	44.80	0.00	0.00	1.24	2.77	2.50	0.40	6.96	10.12
30+	15.02	32.9	29.80	0.00	0.00	1.18	1.77	1.60	0.25	4.45	8.72
25+	14.07	27.58	24.80	0.00	0.00	1.15	1.46	1.31	0.21	3.66	8.17
20+	12.95	22.02	19.80	0.00	0.00	1.11	1.14	1.02	0.16	2.85	7.52
15+	11.64	16.54	14.80	0.05	0.05	1.07	0.83	0.74	0.12	2.07	6.76
+23	9.28	8.04	7.94	0.34	0.30	0.97	0.42	0.38	0.06	1.05	5.39
+21	7.09	3.69	3.79	2.85	2.51	0.85	0.19	0.17	0.03	0.47	4.12
+19	5.56	1.92	1.95	6.81	3.96	0.75	0.09	0.08	0.01	0.23	3.23
+17	4.93	1.42	1.40	12.66	5.85	0.69	0.06	0.06	0.01	0.16	2.86
+15	4.62	1.20	1.17	15.54	2.88	0.66	0.05	0.05	0.01	0.13	2.68
+13	3.85	0.70	0.71	22.94	7.39	0.59	0.03	0.03	0.00	0.07	2.24
+12	3.42	0.52	0.51	27.62	4.68	0.53	0.02	0.02	0.00	0.05	1.99
+11	2.86	0.32	0.31	34.70	7.08	0.46	0.01	0.01	0.00	0.03	1.66
+9	2.35	0.18	0.18	44.95	10.25	0.37	0.01	0.01	0.00	0.02	1.36
+7	2.00	0.12	0.12	48.05	3.11	0.30	0.00	0.00	0.00	0.01	1.16
+6	1.72	0.08	0.08	54.14	6.09	0.24	0.00	0.00	0.00	0.01	1.00
+5	1.47	0.05	0.05	59.58	5.44	0.17	0.00	0.00	0.00	0.00	0.85
+3	1.15	0.03	0.03	66.89	7.30	0.06	0.00	0.00	0.00	0.00	0.67
+2	1.03	0.02	0.19	69.66	2.78	0.01	0.00	0.00	0.00	0.00	0.60
+1	0.82	0.01	0.01	75.70	6.04	-0.09	0.00	0.00	0.00	0.00	0.48
-1	**0.01**	0.00	0.00	100.00	24.30	-2.00	0.00	0.00	0.00	0.00	0.01
					100.00						

Table 30: Calculation of the maximum locked diamond size in kimberlite particles in each sieve class.

While particles are assumed to have a spherical shape, their volume, expressed in cm3, is based on the square mesh size, d_i, specified in mm (Equation 73).

$$Vi = \frac{4}{3} \times \pi \times \left(\frac{d_i}{2}\right)^3 \times 1000 \qquad \textbf{Equation 73}$$

This volume must be factorised to some volume lower than a sphere. In the model presented a value of 0.9 is used. This value can be calibrated for various ore types and crushing methods, by direct measurement of the volume of particle volumes in each sieve class. Once the representative volume of each sieve class has been calculated it is possible, using the parameters given in Table 29 and Equation 71, to calculate the maximum volume (in cm^3) and mass of diamond that can be locked up in this particle size class.

It is now possible to work out the proportion of the size distribution of diamonds that can be locked in each size class. This calculation is demonstrated in Table 32. The parameters used to fit a log normal distribution to the recovered diamond size distribution (Table 28) are used to determine this percentage given the maximum locked diamond size. However, this percentage of the distribution represents a number of carats locked for every 100 carats recovered and will most likely occur in the same size distribution as that of the recovered diamonds. The single rider is that if the carats locked in any given size is smaller than the lower critical size of that sieve class, the locked carat potential is moved down to the next smallest size class. This calculation is show in Table 31.

Sieve Parameters		Allocation of Locked potential in each size class using the recovered diamond distribution														
Diamond Sieve name	Square mesh mm	+19	+17	+15	+13	+12	+11	+9	+7	+6	+5	+3	+2	+1	-1	Reallocated Cts/class cts
	32															
+19	5.56	0.13														0.13
+17	4.93	0.09	0.06													0.16
+15	4.62	0.07	0.05	0.02												0.14
+13	3.85	0.28	0.19	0.09	0.15											0.71
+12	3.42	0.21	0.14	0.06	0.11	0.06										0.59
+11	2.86	0.43	0.30	0.13	0.24	0.12	0.10									1.32
+9	2.35	0.62	0.44	0.20	0.34	0.17	0.14	0.11								2.02
+7	2.00	0.59	0.41	0.18	0.33	0.16	0.14	0.10	0.00							1.91
+6	1.72	0.53	0.37	0.17	0.30	0.15	0.12	0.09	0.00	0.00						1.74
+5	1.47	0.66	0.46	0.21	0.37	0.18	0.15	0.12	0.00	0.00	0.00					2.16
+3	1.15	0.48	0.34	0.15	0.27	0.13	0.11	0.08	0.00	0.00	0.00	0.03				1.59
+2	1.03	0.13	0.09	0.04	0.07	0.04	0.03	0.02	0.00	0.00	0.00	0.01	0.01			0.44
+1	0.82	0.10	0.07	0.03	0.06	0.03	0.02	0.02	0.00	0.00	0.00	0.01	0.01	0.00		0.35
-1	**0.01**	0.08	0.06	0.03	0.04	0.02	0.02	0.01	0.00	0.00	0.00	0.00	0.00	0.00	0.01	0.27
	Total locked per class	4.40	2.99	1.31	2.28	1.06	0.84	0.56	0.00	0.00	0.00	0.04	0.02	0.00	0.01	13.52

Table 31: Allocation of the locked potential in each size class according to the probabilities derived from the recovered diamond size distribution.

The re-assigned locked potential is shown in Table 32 in the column titled 'Re-distributed per class cts'.

Sieve Parameters		Determination of Locked Diamond Distribution					Total Estimated Distribution	
Diamond Sieve name	Square mesh mm	% of Diam. Distribution < crit size	max locked Cts in class cts/100 rec	Re-Distributed per class cts	% per Clss Locked %	Locked Stones number	Recovered Distribution cts	Total distribtuion cts
	32	100.00						
200+	30.05	99.99	0.00	0.0000	0.0000	**0.00**	0.00	0.00
150+	27.05	99.99	0.00	0.00	0.00	**0.00**	0.00	0.00
100+	23.33	99.96	0.00	0.00	0.00	**0.00**	0.00	0.00
75+	21.01	99.91	0.00	0.00	0.00	**0.00**	0.01	0.01
60+	19.36	99.84	0.00	0.00	0.00	**0.00**	0.03	0.03
45+	17.43	99.68	0.00	0.00	0.00	**0.00**	0.04	0.05
30+	15.02	99.20	0.00	0.00	0.00	**0.00**	0.12	0.14
25+	14.07	98.83	0.00	0.00	0.00	**0.00**	0.08	0.09
20+	12.95	98.17	0.00	0.00	0.00	**0.00**	0.12	0.14
15+	11.64	96.87	0.04	0.00	0.00	**0.00**	0.21	0.24
+23	9.28	91.60	0.27	0.00	0.00	**0.00**	0.67	0.76
+21	7.09	78.93	1.98	0.00	0.00	**0.00**	1.34	1.52
+19	5.56	61.20	2.42	0.13	0.93	**0.07**	2.77	3.14
+17	4.93	51.11	2.99	0.16	1.15	**0.11**	2.03	2.30
+15	4.62	45.58	1.31	0.14	1.00	**0.11**	1.48	1.69
+13	3.85	30.84	2.28	0.71	5.26	**1.01**	6.13	6.96
+12	3.42	22.56	1.06	0.59	4.34	**1.12**	4.57	5.19
+11	2.86	11.93	0.84	1.32	9.77	**4.17**	9.51	10.79
+9	2.35	2.81	0.29	2.02	14.96	**11.30**	13.77	15.63
+7	2.00	0.60	0.02	1.91	14.14	**16.33**	13.01	14.77
+6	1.72	0.11	0.01	1.74	12.84	**21.92**	11.82	13.42
+5	1.47	0.01	0.00	2.16	15.96	**44.49**	14.69	16.68
+3	1.15	0.00	0.00	1.59	11.73	**61.95**	10.62	12.05
+2	1.03	0.00	0.00	0.44	3.29	**23.92**	2.93	3.32
+1	0.82	0.00	0.00	0.35	2.58	**33.05**	2.30	2.61
-1	**0.01**	0.00	0.00	0.27	2.03	**108.09**	1.76	2.00
			13.52	13.52	100.00	327.64	100.00	113.52

Table 32: Calculation of the locked carat potential per diamond sieve class.

In the example presented here approximately 13.5 carats are locked for every 100 hundred recovered. The liberation derived for this period would be calculated as per Equation 69, and result in estimated carat liberation of 88%. Knowing the recovered size distribution and the locked potential facilitates the calculation of the locked and liberated revenue. This is essentially a weighting of the distribution by the revenue obtained for each size of diamond. This calculation is summarised in Table 33.

Sieve Parameters		Recovered	locked	Estimated Total Distribution			Revenue Distribution Caclulation			Cumulative% of Revenue	
Diamond	Square	Carats per	Redistributed	Total	Total	Cumulative	Revenue	Revenue	Revenue		
Sieve	mesh	Class	locked	Contained	Contained	% retained	per class	Free	Locked	Free	Locked
name	mm	Cts	Cts	Cts per class	% per class	%	$/ct	$/100cts	$/100cts	%	%
	31.5										
200+	30.05	0.00	0.00	0.00	0.00	0.00	100.00	0.00	0.00	0.00	0.00
150+	27.05	0.00	0.00	0.00	0.00	0.00	100.00	0.00	0.00	0.00	0.00
100+	23.33	0.00	0.00	0.00	0.00	0.00	100.00	0.00	0.00	0.00	0.00
75+	21.01	0.01	0.00	0.01	0.01	0.01	100.00	1.01	0.00	0.06	0.00
60+	19.36	0.03	0.00	0.03	0.02	0.03	100.00	2.65	0.00	0.20	0.00
45+	17.43	0.04	0.00	0.04	0.04	0.07	100.00	4.03	0.00	0.43	0.00
30+	15.02	0.12	0.00	0.12	0.11	0.18	100.00	12.41	0.00	1.12	0.00
25+	14.07	0.08	0.00	0.08	0.07	0.25	100.00	7.76	0.00	1.55	0.00
20+	12.95	0.12	0.00	0.12	0.11	0.35	100.00	12.31	0.00	2.24	0.00
15+	11.64	0.21	0.00	0.21	0.19	0.54	100.00	21.40	0.00	3.44	0.00
+23	9.28	0.67	0.00	0.67	0.59	1.13	75.00	50.43	0.00	6.25	0.00
+21	7.09	1.34	0.00	1.34	1.18	2.31	70.00	93.53	0.00	11.47	0.00
+19	5.56	2.77	0.13	2.89	2.55	4.86	65.00	179.94	8.14	21.51	0.45
+17	4.93	2.03	0.16	2.18	1.92	6.78	40.00	81.02	6.23	26.03	0.80
+15	4.62	1.48	0.14	1.62	1.43	8.21	35.00	51.96	4.73	28.93	1.07
+13	3.85	6.13	0.71	6.84	6.03	14.24	30.00	183.94	21.35	39.19	2.26
+12	3.42	4.57	0.59	5.16	4.54	18.78	26.00	118.78	15.26	45.82	3.11
+11	2.86	9.51	1.32	10.83	9.54	28.32	15.00	142.59	19.82	53.77	4.21
+9	2.35	13.77	2.02	15.79	13.91	42.23	12.00	165.23	24.27	62.99	5.57
+7	2.00	13.01	1.91	14.92	13.14	55.37	11.00	143.10	21.02	70.97	6.74
+6	1.72	11.82	1.74	13.55	11.94	67.31	10.00	118.19	17.36	77.57	7.71
+5	1.47	14.69	2.16	16.85	14.84	82.15	8.00	117.53	17.26	84.13	8.67
+3	1.15	10.62	1.59	12.20	10.75	92.90	7.00	74.32	11.10	88.27	9.29
+2	1.03	2.93	0.44	3.37	2.97	95.87	6.00	17.55	2.67	89.25	9.44
+1	0.82	2.30	0.35	2.65	2.33	98.21	5.00	11.49	1.75	89.89	9.54
-1	0.01	1.76	0.27	2.04	1.79	100.00	5.00	8.81	1.37	90.39	9.61
TOTAL		100.00	13.52	113.52	100.00		1420.00	1620.00	172.33		

Table 33: Calculation of the liberated and locked potential revenue.

Using the same form of calculation as in Equation 74 we can derive an estimate of the liberated revenue as follows:

$$\%\ \boldsymbol{Revenue\ Liberation} = \frac{\mathbf{100}}{\mathbf{100} + \boldsymbol{locked\ revenue}} \boldsymbol{X}\mathbf{100} \qquad \textbf{Equation 74}$$

In this case the revenue liberation would be estimated to be in the vicinity of 90%, suggesting that there remains an additional 11% of current revenue to be recovered if the crushing circuit was modified to release all of the contained diamonds.

Using this approach to determine liberation allows for the identification of which size fractions are most important in terms of locking up carats and which will have the largest impact on the variation in liberated revenue. In this way it is possible to carry out trade-off studies to determine steps to find the best balance between process cost and revenue.

Generating a flowsheet using calibrated process models

It is possible, using a platform such as Microsoft Excel, to combine the unit process models to create a model of a diamond liberation and dense media separation plant. An example is provided in the appendix and has been created using the add-in package "Limn" developed, and kindly sponsored for this research, by Dave Wiseman. Using this model, it is possible to determine the total grind, estimate DMS separation efficiency and estimate the recovery and loss of diamonds that will be achieved for each given set of rock properties when the plant is in a stable state.

The output of this model can be stored in a matrix that can be used in an integrated way to interact with the block model containing spatially varying rock properties.

Use of the liberation model to derive a metallurgical recovery factor

In cases where this model is shown to be a robust estimator of the diamonds that are liberated and locked for a given size distribution of ore particles, the process simulation that is required will consist of a comminution model that produces an estimate of the final grind size distribution. The comminution model can be integrated with a spatial model of the properties of the rocks that govern the final grind, then a methodology can be devised that will facilitate the relationship between ore properties and diamond recovery.

6.6 Process simulation and sensitivity testing

Dynamic process simulation modelling introduces a time dimension to the processes of modelling diamond recovery. Using this approach, it is possible to stress the various settings in the process model and to determine how the steady state operation will change if several of the parameters of the process can oscillate through a realistic range with some predetermined probability distribution of that range.

6.7 Limitations of processing models

There are several limits to both the granulometry model and the process simulations model and their use in integrated models. These include:

- Difficulty of defining the relationships between individual rock properties and the impact of rock mixes on unit process models;

- Stress testing the process responses when the material changes and the process responds in different ways; and
- Time that the process takes to reach steady state and its incorporation into process models.

Each of these difficulties has implications for the reliability of the estimation of the recovery factor these will be explained in some detail in this section.

6.8 Conclusion

It is possible to estimate the expected total grind that will be achieved for a given process flowsheet and ore type characteristic given sufficient data. Ideally for existing processes the experiments can be designed to define relationships between operating parameters, ore types and the resulting diamond recovery. For new deposits without this information it is possible to generate some understanding of the range of expected recoveries and to determine which processes are likely to constrain impact on recovery.

Process models can be used in integrated evaluation processes provided a matrix of inputs, parameters and outputs can be created for the range of rock types that are to be expected. This does, however, mean that it is very difficult to test the sensitivity of diamond recovery to changes in process parameters or uncertainty in rock properties as there is a distinctly non-linear relationship between changes to rock types and the outcomes of the process.

In the subsequent chapters the methods developed here are integrated with orebody sampling, simulation and estimation approaches suggested in the prior chapters to develop an integrated value chain model that simulates the interaction of variable ore characteristics with the mining and processing models to produce period by period production outputs.

7 VALUE CHAIN MODELS - CASE STUDY 1

7.1 Introduction

This case study demonstrates an integrated value chain model that comprises multiple orebody realisations with mining and treatment process models. The value chain model is used to simulate the mine operation and generate daily production summaries. This output is used to quantify the impact that the rock characteristics have on the range and variability of the metallurgical recovery factor.

The case study was published as "Integrated Mine Evaluation – Implications for Mine Management" in the proceedings of the AusIMM Mine Managers Conference (Nicholas et al., 2007). The author of this thesis presented this paper at this conference held in Melbourne, Australia in 2007, and was responsible for developing the orebody models, the VBA coding, execution of mining and process simulations and providing links into the financial model. The work was completed in collaboration with Grant Nicholas, Kurt Petersen, Alain Galli and Margaret Armstrong.

In this case study the in situ diamond grade and revenue were relatively well constrained. However uncertain orebody geometry and the impact that the complex geometry would have on mining rate and recovery, were not.

The case study demonstrates how it is possible to acquire data from the orebody to spatially simulate the vertical displacement, the thickness of the dyke and the grade using conventional geostatistical techniques. These characteristics of the orebody are used in a mining simulation to generate a variable mining rate and feed characteristics for the process plant. The process plant model was configured to respond to the feed ore characteristics and predict throughput, comminution and diamond recovery.

Using the novel approach developed during this research it was possible to model and simulate the key aspects of this project including:

- Generating a synthetic version of the orebody that was simulated at a small block size that resembled the orebody geometry, variable thickness and grade;

- Developing a method to sample the synthetic orebody at different drill hole spacings to generate multiple estimates and simulations of the orebody and hence incorporate sampling uncertainty in the model;

- Developing a method to assign a feasible block sequence to each ore block used in a mining simulation;

- Simulating mining that adheres to the planned sequence of mining with the rate of mining each block being determined by the interaction of the morphology of the dyke and mining equipment used;

- Determination of dilution incurred when mining blocks as a function of dyke thickness, planned mining height and vertical displacement of dyke location; and

- Using dilution as an input into the process model to calculate throughput, liberation and recovery.

The simulated production outputs were used as inputs into a financial model to calculate the value of each of the alternatives considered, defined by the Net Present Value. The benefit of using a "Master Synthetic Orebody model" or so-called "V-Bod" model to represent reality is that it is possible to compare and then track the differences between the processing of the Master model (simulated reality at small scale) and the models generated from the sampling of the Master model and using these sample values to generate estimated resource models.

Project Background

The orebody is a kimberlite dyke that dips at 15 degrees towards the north east and is on average 2.8m thick. Most of the kimberlite dyke is hosted within an Archean multiphase suite of intrusive granitoids, with a minor portion of the kimberlite dyke emplaced within overlying metavolcanics and metasediments of the Archean greenstone belts.

The geometry of the dyke is variable. On the regional scale (100's of metres) the Snap Lake dyke appears to be a 'simple' continuous, gently dipping sheet, although three areas of offset have been identified by surface seismic imaging' (McBean et al., 2001). At a more local scale (10-100m), orientation changes and splits and large

splays have been observed. These are thought to be structurally controlled. On a small scale (0-10m), the dyke is typically controlled by two different host rock features. Within the strongly foliated metavolcanics, the kimberlite appears to roll and undulate on a small scale matching the foliation, while in the granitic host rocks, local variations occur along a primary set of joints that are flat lying but affected by secondary jointing at approximately 35° dip resulting in an angular step-like nature of the dyke (McBean et al., 2001).

This variability in the geometry of the deposit has several implications for grade estimation, mine design and plant operation, including but not limited to:

- Uncertainty in the volume of the dyke volume in each block;
- The rate at which development and mining can be achieved;
- Dilution that will be incurred when mining;
- Waste ore mix that will be fed to the process; and
- Impact of dilution on recovery efficiency.

The mine plan was based on kriged estimates of the grades, volumes and other variables and is assumed, on average, to provide a way to develop an unbiased prediction of the annual production. In the derivation of the plan no allowance was made for the short impact of short-scale variability (in both the spatial and temporal sense) on the rate and efficiency (ore recovery, ore loss, diamond recovery) of the mining and treatment processes.

Orebody model data and model preparation

Sampling data that is used in any evaluation play a fundamental part in producing estimates that aim to reflect an unknowable reality. Although the inclusion of more samples reduces uncertainty associated with both the mean and variance of resource estimates, it does not alter the true "natural" variability within the deposit. It does however alter out quantification of it which can only be estimated from the results of the samples.

The limitations of designing a sampling campaign for multiple variables have been discussed by Kleingeld and Nicholas (2004). In this case study three orebody variables were considered in the evaluation model:

- The geometrical variability of the top surface of the dyke (v1);
- Thickness, which can be used to determine the volume of the dyke; and
- Grade (in carats per hundred tonnes)

Synthetic core drilling was used to delineate geological variability on three different grid densities; 50 by 50m, 25m by 25m and 10m by 10m, creating scenarios one, two and three. These were designed to sample within the expected variogram ranges of 75m for thickness and 50m for v1. Sampling campaigns set beyond the range would return the variable's average value and would not detect the short-scale variability. A 50m by 50m drilling grid was used to sample for grade, using large diameter drilling (LDD). Grade was not deemed to have any significant variability between scenarios and therefore, a single sampling campaign was deemed sufficient.

Table 1 describes the design of the simulated sampling campaigns on the virtual orebody (V-bod); sampling occurred at point support and simulation grid nodes were 4m by 4m in dimension.

	V-bod	**Scenario 1**	**Scenario 2**	**Scenario 3**
Description	Assumed Reality	Wide spaced samples	Moderate spaced samples	Close Spaced Samples
Grid Dimensions	4m x 4m	50m x 50m	25m x 25m	10m x 10m
No of Samples	45 000	288	1152	7200
Samples as a % of the V-bod Blocks	-	0.64	2.56	16

Table 34: Summary of the characteristics of three sampling campaigns and that used to define the 'Virtual Orebody(V-bod)

The V-bod was created using a non-conditional geostatistical simulation based on data gathered from a combination of drilling information, bulk-samples and face mapping from an exposed part of the dyke. It is assumed to be the 'reality' on which the various sampling campaigns were simulated to generate virtual sample data. These sample data were used to generate kriged estimates and resource simulations of grade, dyke thickness and geometric surface undulations of the dyke. A mine plan was overlain onto each estimate and the complete simulation to determine the reserves. All production output was fed into the financial model.

The graphic base maps of the V-bod and each sampling campaign are shown in Figure 58 (warmer colours represent higher values while darker colours are low values).

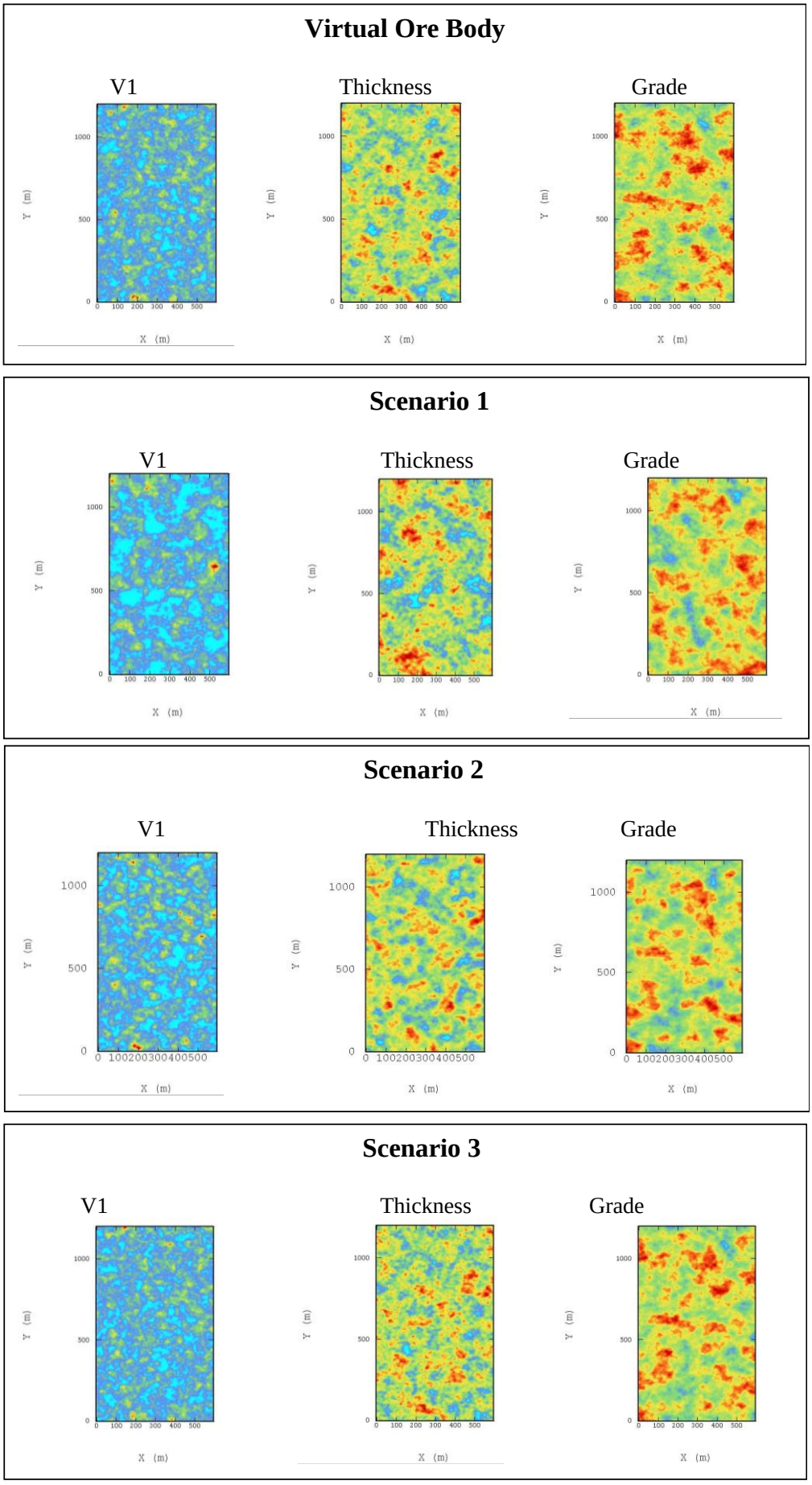

Figure 58: Comparison of the thickness and v1 base maps for the kriged and simulated outputs of each scenario with that of the V-bod. Grade was held constant for each scenario.

Table 2 - Resource Simulation Output

	V-bod	Scenario 1	Scenario 2	Scenario 3
Mean Thickness	1.67	1.62	1.64	1.65
Std dev Thickness	0.43	0.52	0.45	0.45
Mean v1	1.88	1.79	1.85	1.87
Std dev v1	0.34	0.40	0.39	0.35
Mean Grade	196.50	197.30	196.10	197.00
Std dev Grade	35.51	38.08	34.41	35.43

Table 35: The descriptive statistics for the V-bod and each scenario for grade, dyke thickness and the geometrical variability of the dyke surface (v1).

Processing system model

The block model data for each realisation (the kriged model is one realisation, and the 25 simulated realisations constituted the remainder) were exported from the Isatis software into a text file containing the information associated with each block in individual rows. These files can then be processed individually through the system. The model is built in an Excel VBA framework, and consists of several modules that represent the functions for mining, stockpiling, crushing and dense media separation processes.

Mining parameters and constraints

The mine simulation presented an opportunity to evaluate the impact of the dyke geometry on mining selectivity and rate.

The proposed mining method utilised a mixed fleet of trackless vehicles to mine in a stope and pillar configuration. The designed mine plan targeted an average extraction rate of 75 percent of in situ kimberlite at average daily delivery of 3150 tonnes of kimberlite with minimal dilution . Each mining panel, approximately 250 m by 250 m was mined in a sequence that required the establishment of rim tunnels, then stope tunnels and finally excavations to facilitate stope slashing or drifting.

The model operated as the scale of the smallest mining unit (SMU) with each block having planar dimensions of 4 m by 4 m, but with variable heights. The rate, and hence time, to mine each SMU was determined at run time as a function of the machine used to carry out the mining and the height that was mined. The mined height, (and hence mined volume, tonnage, dilution and grade) was determined by the tunnel type, a set of mining height constraints for each tunnel type were selected as follows :

• rim tunnels maximum of 3.5 m (height)

• stope tunnels minimum 2.0 m (height), and

• stope blocks minimum 1.0 m (height), for small machines and 1.5m (height) for large machines.

Pillar dimensions varied depending on the support required as a function of fracture frequency/ground conditions but a maximum span limit of 8 m was imposed in all tunnel configurations. The change in vertical location of the footwall in rim and stope tunnels was constrained to an angle that would not exceed the safe incline/decline on which the mining machines could operate. This constraint lead to loss of kimberlite in the hanging wall in some cases. The implementation of these constraints is depicted in the diagram in Figure 59.

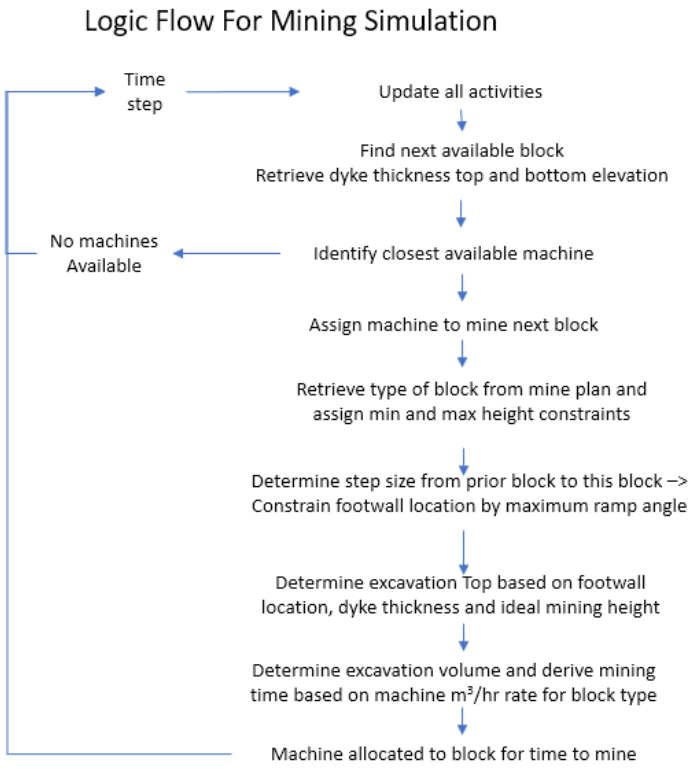

Figure 59: A diagram depicting the implementation of the mining constraint logic.

Processing parameters

The system has several constraints that can be modified. A set of constraints that is used in processing was referred to in this case as a scenario. Note that in later models, and publications, this term has been specifically reserved for future operating contexts.

When processing the orebody models through the value chain the variability of the orebody geometry impacts on the mining rate and the relative proportion of kimberlite and waste rock mined. This mix of kimberlite and waste contained in the material processed impacts on the plant throughput rate, the degree of comminution and the recovery efficiency of the DMS.

To determine the relationship between the dilution and process efficiency, data were acquired from the sample plant that had been treating samples from the deposit. A process simulation model was developed using Limn software in collaboration with Dr. K. Petersen (Petersen, 2005) . The simulation represented the planned full-scale process plant using the sample plant data to calibrate both expected size reduction and recovery. The model was run for several different combinations of granitoid waste, metavolcanic waste and kimberlite. The resulting data was used to investigate the relationship between the proportion of dilution and comminution and DMS performance. It was observed that the comminution and DMS responses could be simplified and represented by a least squares linear fit to the simulation outputs. This approach allow content range of responses for differing proportions of waste and kimberlite vs diamond recovery were plotted and a least squares linear model was fitted.

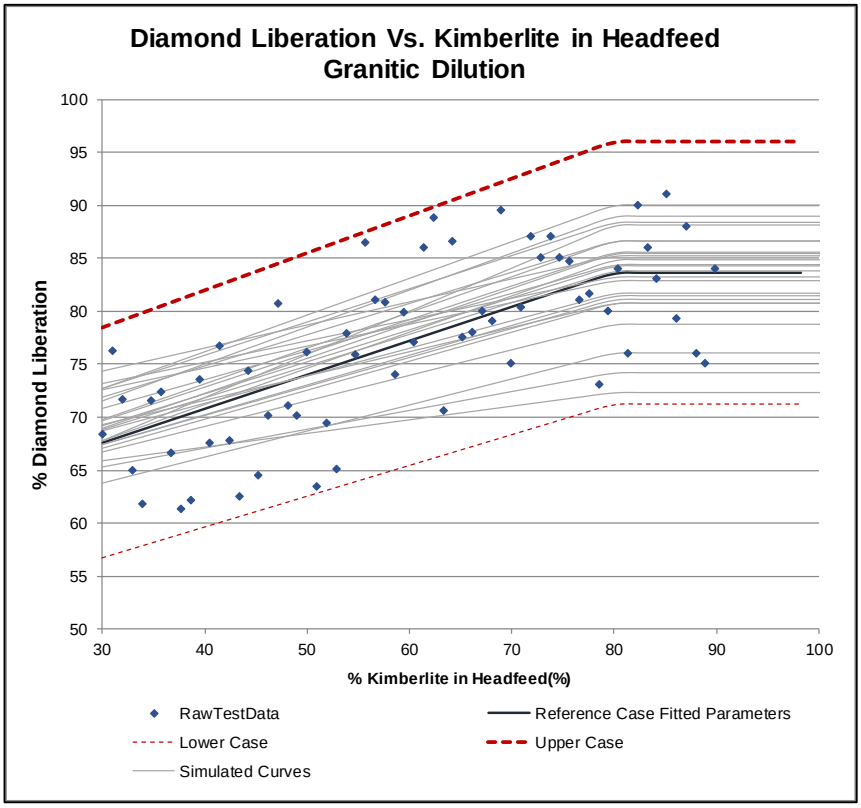

Figure 60: A depiction of liberation as a function of the concentration of kimberlite in the headfeed.

Once relationship was established it was possible to use the standard error of the regression line to determine the uncertainty in the parameters of the fit and use this

to seed a simulation of the value for these parameters (Figure 60). The parameters, in this case M and C for the regression line can be randomly drawn from a calibrated normal distribution to generate a set that can be used in the value chain model. Simulated parameters that produce a line that falls outside the limits found at other similar operations are rejected from the set of feasible parameters. In this way it is possible to introduce a range of uncertainty that is constrained by prior observation and gives a realistic model to the variability in recovery that the changing ore properties will drive.

The use of these simplified functions facilitates simulation of the entire life of mine at a block scale and to reflect the interactions of the ore characteristics with the process. This would not currently be possible in realistic timeframes suing a full population balance model.

Interpretation and use of outputs from the value chain model

The processing of the mineral resource block models generates comprehensive production data that are evaluated using a comprehensive financial model. This approach allowed technical range analysis to be converted into meaningful and comparative financial terms. The outputs can be used to rank and thus identify the mining and processing constraints that impact most on the range of output. Consequently, the value chain model can be used iteratively in a structured way to search for so-called ‘plateaus of value’ where the trade-off between an overall maximum value (using a financial indicator such as NPV) and a value that is relatively robust in the face of uncertain operational outcomes is revealed.

7.2 Benefits and limitations of the methodology

The model as conceived and represented in this research paper demonstrates an implementation of the methodology that can be used to define confidence levels around the expected metallurgical recovery factor and the project value for various configurations. The validity of the findings requires that several assumptions about the uncertainty in the orebody and the interaction of this uncertainty with constraints in the value chain hold true for the duration of the operation. These assumptions and the implications they have for the design and management of this mine are briefly discussed below.

The model can be used to demonstrate how changes in dyke footwall location will impact on both development and mining rates. When there were changes in footwall location that resulted in mining roadway slopes that are too steep to be safely used by the mining equipment, the mining teams would have to retreat and redevelop ramps and roadways. The additional activity would reduce production output. The

model also shows how it is possible to evaluate impact of this constraint in areas of high dyke variability in which small machines with less tolerance for steep roadways are typically allocated. This unexpected result suggests that more cover drilling may be required to inform roadway design and machine allocation planning.

The model can be used to show how the impact of reduced mining rates can to some extent be managed by additional advance development to create flexibility to mine ore from several operating areas simultaneously. It can be shown that adopting this strategy will increase the dilution of ore fed to the process plant whilst setting up panels to mine, but the average dilution in the later years of operation would be able to be brought inline with initial expectations.

Establishing a relationship between the rock mix fed to the plant, the comminution, liberation and hence recovery, required a combination of sample plant processing and process modelling to predict the nature of the relationship. The assumption that the impact of diluting waste on comminution that was observed at sample plant scale (Samples comprising ~80 tonnes each) will be observed at production scale appears reasonable but will have to be verified during commissioning of the full-scale plant. This relationship does, however, highlight that evaluation of the impact of dilution without using a block-by-block evaluation model (as opposed for instance with doing a sensitivity analysis in the financial model) will most likely underestimate the impact that dilution will have on the operation.

This model has assumed that the 3000-tonne storage to buffer surges between the mine and the plant is a fixed maximum. The model can be used to demonstrate how increasing this capacity constraint will have a material impact on the value of the operation. The flexibility that additional surge capacity will provide can be valued and hence the capital that is allocated to this part of the operation can be justified. If a smoothed model of the orebody, or a smoothed feed rate was assumed the value of storage would be materially underestimated.

The value chain modelling approach can accommodate not only unsystematic risk (risks associated with the specifics of the envisaged project) but can also be used simultaneously to evaluate the impact of systematic risk, i.e. risks that are independent of the project configuration, such as exchange rate and diamond sales price. In this holistic approach it is possible to contrast and compare the relative merits of technical risk mitigation and mitigating project risk through various financial engineering measures.

8 VALUE CHAIN MODEL - CASE STUDY 2

8.1 Introduction

This case study demonstrates an integrated value chain model that comprises multiple orebody realisations with several alternative mining and treatment process options. The value chain model is used to simulate the mine operation and generate daily production summaries. This output is used to quantify the impact that the rock characteristics have on the range and variability of the metallurgical recovery factor.

The main source of uncertainty in this project was the impact that hard and dense kimberlite breccias would have on diamond recovery and process performance. The hardness of the kimberlite was expected to compromise liberation, and the zones of higher density were expected to compromise the DMS operation. The yields expected in some parts of the orebody were higher than average, and if this coincided with poor comminution and poor separation the throughput would be severely limited by the capacity in the final recovery process. In addition to the orebody grade, diamond assortment data had also been collected. These data were used to fit a model to the revenue distribution within each size class that results from the mix of diamond colour, clarity and shape within each size class. This assortment model was used to quantify the influence of the range of the diamond selling price on project cashflows.

The integrated evaluation model can test the impact of uncertainty related to the orebody, the engineering design decisions (e.g. plant capacity) and future outcomes (diamond selling price) and then combine the outputs in several different ways. To clarify the use and operation of the model the terminology used is given in Table 36.

Alternative	Realisations	1 2 … 25	Spatial realisations of the Orebody
	Mine Plans	1 2	Several Mine Plans
	Iterations	1 2 3 4 5	Several versions of process performance
	Scenarios	1 2 3	Versions of future outcomes

Table 36: Schematic depiction of terminology used to describe aspects of the Integrated Evaluation Model.

Alternative - this term refers to the combination of inputs, processes and outputs that are considered in the model. At this level it is possible to compare and contrast very different approaches to operating strategy for a mining project.

Realisation - refers to one image of the orebody that honours the sampling data. Typically, all realisations are processed through the model at a block-by-block scale.

Mine plans- there may be typically one to five mine plans that are developed based on different assumptions including ground conditions, capacity, fleet size, angle of repose etc.

Iterations - these refer to different operating conditions or efficiencies in the mining and metallurgical processes.

Scenarios – Typically, three to five scenarios are developed to provide coherent internally consistent futures that the project will possibly operate in. In each scenario the trajectories of values that have a material impact on the project (e.g. cost of capital, diamond selling price) are described, as are the relationships among these inputs. These are most often financial inputs to the model but may also include various environmental variables that have an impact on project performance e.g. higher and lower rainfall impacting on mining rate.

Alternative - This represents a collection of plausible realisations, mine plans, Iterations and scenarios. Each alternative would arise from a materially different strategy of how the entire project is to be conceptualised and operated (e.g. large-scale vs small scale, open pit vs combined underground and open pit)

The author was responsible for generating a number of orebody simulations, incorporation of the mine plan, and development of VBA code to run the simulated orebody models through the value chain. Grant Nicholas and Johan Ferreira collaborated on this project which resulted in a conference publication (Nicholas, 2008). This project led to the development of a methodology to generate individual diamond $/ct values by sampling from the modelled diamond value distribution.

Project background

The orebody is a kimberlite pipe located in Botswana. The tri-lobate pipe-like orebody has intruded through the basement granites and is variably contaminated by diluting basalt. This dilution is variable with maximum measured values of 45% measured at 900m amsl in the north lobe and 25% measured in core retrieved from the south lobe at 800m amsl.

The following sources of variability were considered to have important implications in this project:

- The variability of the mined grade that would be achieved;
- Magnitude and type of internal dilution that will be encountered when mining;
- The impact of hard waste and hard kimberlite on comminution circuit and liberation performance;
- Impact of low comminution and dense minerals on DMS yield and DMS separation efficiency;
- Capacity limitation in the final recovery; and
- Uncertain and variable diamond assortment impact on diamond selling price

A number of mitigating steps were taken during the design phase to provide sufficient flexibility in the process plant to cope with anticipated comminution and yield challenges. Some of these design features included:

- Stockpile capacity ahead of the process plant, as well as a 150t surge bin ahead of the recovery plant which would allow mining to change zones should high yield be experienced;
- Optimisation of cyclone configuration to allow for higher spigot loadings without compromising efficiency;
- Inclusion of capability to adapt the HPGR crushing circuit to cope with harder material;
- Elimination of recycle of final concentrate by including grease belts and mills in the final recovery flowsheet; and

- Creation of flexibility in the layout of the final recovery to allow for inclusion of additional units as technology and needs change - e.g. inclusion of rare earth drum separators to deal with increased DMS yield.

Each of these risk mitigation features were designed to deal with the advent of one of the risk factors and almost all the existing models were based on annual averages. This meant that the existing project evaluation methods were unable to quantify how well the project would respond to a combined synchronous 'onslaught' of all the modelled uncertainty.

After consultation with the project team an integrated model was developed to quantify the impact of various sources of uncertainty on project performance. The next section describes the components of this model.

8.2 The value chain components

The capital for this project was limited and hence the project was based on a two-phase operation, with the first phase of low throughput lasting approximately three years, followed by a substantial expansion to increase throughput in phase two. This would allow the project to acquire more information on the grade of the orebody and to use the initial commissioning to gain greater insights into rock characteristics and their impact on liberation and DMS separation. This approach to capital rationing required a model that would be able to be adapted over time to reflect the planned increase in mining rate and plant throughput.

The orebody models:

The surfaces of the orebody, consisting of three pipe-like bodies, were modelled using conventional geological techniques (Figure 61). These surfaces were used to constrain several simulations of the grade and density of the orebody. The turning bands method of geostatistical simulation was used to generate 25 realisations of the orebody.

The mining model

The mining sequence was designed to reduce capital expenditure and was split into two phases. The first phase was planned to be a relatively small pit (down to 70m) that would operate for the first three years and was expressed as pushback surfaces per quarter.

The second phase targeted the southern lobe and was designed to extend down to 390m. This phase was based on annual surfaces that used tag blocks that were to be mined in any period. A simplified sequence was derived based on reasonable

assumptions about directions and geometric constraints on the advance of the excavation.

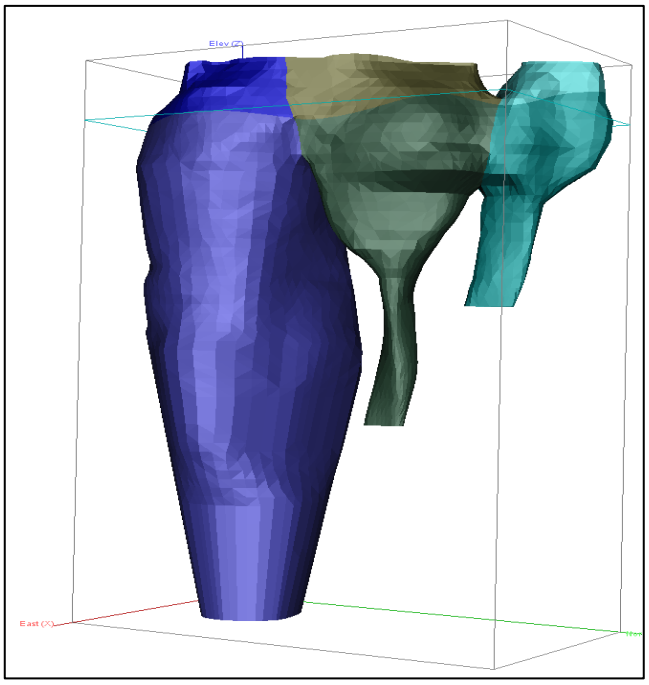

Figure 61: A view of the three lobes of the deposit looking from the west to the east (South Lobe in Dark Blue) adapted after Campbell (2009).

The processing models

The phased approach to mining suggested that the initial plant design would be required to treat 400tph. During years three and four the process plant capacity would be expanded to 630tph and be adapted to improve the capability of handling high yield kimberlitic material. Although the project team considered several options during the feasibility study the process plant configurations remained consistent Figure 62. The main flexibility in the design was the inclusion of the civil infrastructure for additional streams required in phase 2, but the timing of acquisition of the main capital items for these additional streams would depend on the information acquired during phase one of the operation.

Capital Item	Number for phase 1	Number for Phase 2
Scrubbing and screening	2	4
Secondary Crushing	1	2
Fines DMS	1	3
Coarse DMS	1	2
Reconcentration DMS	1	2
Pneumatic drier	1	2
X-ray machines	4	8
Single Particle Sorters	0	1

Table 37: Summary of major capital items planned for each phase.

The design criteria for the sizing of these units was based on extensive studies of core samples that were treated to determine the yield from dense media separation that could be expected from various depths in the orebody (Table 38)

Depth	Fines Module	Coarse Module
0-70m	4%	2%
70-390m	37%	39%

Table 38: Average expected DMS yields for each phase.

Although these average yields were problematic the design team felt that it would be uneconomic to design the plant in the early phase to cope with this high level of yield. It was also important to consider that this yield was based on small samples and the project required an understanding of the sequence of high yielding blocks to evaluate the effect that stockpiling, and blending might have on ameliorating the negative impacts of designing for high instantaneous yield.

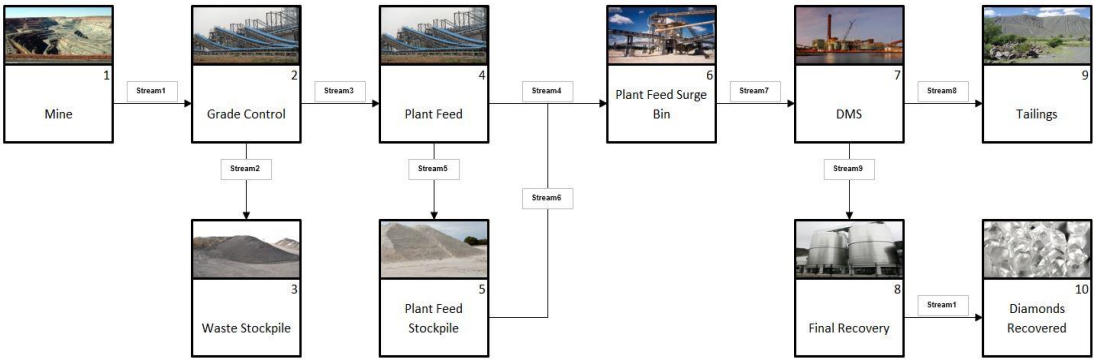

Figure 62: Schematic of process flows used for process model.

The diamond assortment model

Given the relatively few numbers of stones that were used in the evaluation of the expected diamond price that would be achieved, a model was developed to draw the value from each stone from a calibrated distribution for value in each size class.

For every block in the mine plan, the grade and average stone size was used to calculate the number of stones in each block. The mass of each stone was then determined by drawing at random from a modelled cumulative stone size distribution. In each mass class a cumulative distribution of the revenue in that size class was used to draw a value at random for each stone. In this way the value for the diamonds in each block could be cumulated to derive the realised value that could be expressed as either the $/ct for diamonds in each block, or the $/tonne of that block (Figure 63).

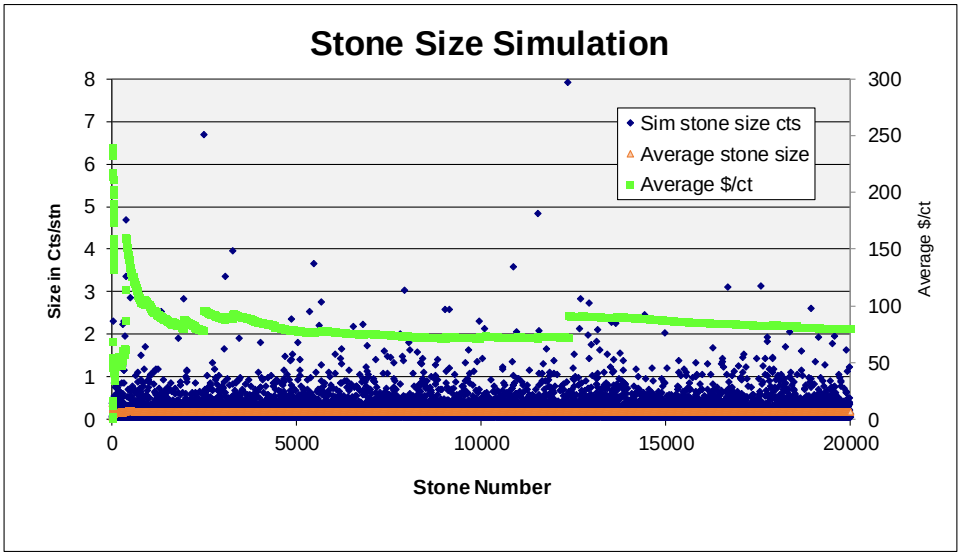

Figure 63: Plot showing a simulation of the size of 20 000 diamonds drawn.

The financial model

A conventional discounted financial model was built to value the project. The model was set up in an excel spreadsheet and was run using VBA scripts. The model has several variables that can be set prior to running the model. An example of the settings used for the base case model is given in Table 39.

Model Asumptions	Unit	Value
Life of mine	Years	14
North lobe Diamond Price Growth	Annual Factor	1.03
Central lobe Diamond Price Growth	Annual Factor	1.03
South lobe Diamond Price Growth	Annual Factor	1.03

Costs	Unit	Base	Annual Escalation factor
Ore Mining cost	US$/tonne	3.02	1.1
Waste Mining Cost	US$/tonne Waste	2.97	1.1
Ore Processing cost	US$/Tonne	8.62	1
Ore Treatment Cost	US$/tonne	27.32	1
Carat Recovery Cost	US$/ct	188.69	1

Royalties	Unit	Value
Administration Overheads	Percent of Revenue	2.5

Process Recovery Modifier	Unit	Value
North lobe	Unitless	1
Central Lobe	Unitless	1
South Lobe	Unitless	1

Table 39: List of model settings used for the financial model.

These settings can be varied individually or as a group. The scenario approach to evaluation provides a basis for qualitative correlation between the settings, i.e. if the selling price is high and growing it is likely that the input costs would also be rising. This approach can be used to limit the number of times that the simulation model must be run.

8.3 Considerations for development and simulation of integrated value chain models

The development and implementation of a dynamic and robust value chain simulation requires a flexible and rapidly configurable modelling environment. There is also a requirement to provide users with the ability to re-run the model with a variety of adapted settings and save the associated results in a structured and sequential framework. This system was thus designed using the concepts that underpin the model view controller architecture (MVC) as depicted in Figure 64.

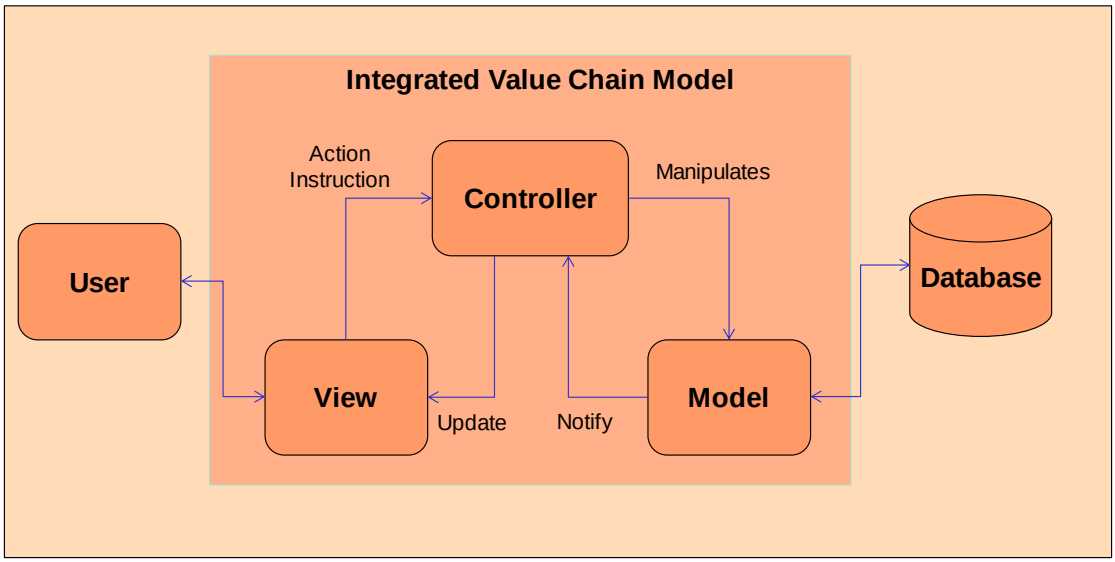

Figure 64: Schematic of the Integrated Evaluation Model Architecture (adapted after Burbeck, 1992) .

In this architecture the interaction of the user with the application is separated from the control of the model and access to the data by a so-called "View" object. The "controller" object interprets user instructions that are sent from the view to the controller. These instructions are then routed to the "Model" object. This model object is the heart of the simulation and is capable of sending multiple structured requests to the database, as-well as sending outputs to the database. When the model has completed an instruction, it notifies the "controller" object. Depending on the logic embedded in the controller it may then either re-manipulate the "model" or send an update to the view or do both.

There are several benefits of this approach to development including:

- This view object can be readily changed and adapted as the application evolves and acquires additional functionality. It is also possible to obscure functionality from the user until it is ready to be included;
- Ability to separate the development of the individual components, so that each component can be developed and tested separately. At the point where the model is to be integrated, the logic that controls the interaction between the components can be designed, tested and implemented. This sequence reduces the complexity of detecting and eliminating errors from the system; and
- Development of parallel processing architecture, in the IEM case each combination of orebody and value chain can be separated and run simultaneously by the "model object" which is far quicker than running each of these sequentially.

The "view" was developed in Microsoft Excel as it provided a familiar and readily customisable user interface. The "controller" was written in Visual Basic for Applications in Excel. Several commercial applications were used to support the sub-models that underpin the IEM framework e.g. Isatis for spatial simulation, Statistica for generation of stone distributions, Datamine for mine plan sequencing. Microsoft SQl express was used as a database for storing input data, processing parameters and result data.

The orebody models can be quite large and exist in a multitude of formats in the software that is used to generate them. They were thus exported from their source software and stored as flat text files. These files were in turn read into the database with a table for each realisation. Likewise, the mine plans were contained in separate text files, with each block having been assigned an ideal year for extraction, which was brought into the database. Lists of blocks to be processed in each year were generated by executing a dynamic query that was triggered by the process model. The process model used the simulated block properties to determine the treatment time and the liberation that would be achieved on a block-by-block basis. In each year the treatment ceased when the allocated hours available in a year had been consumed. The production outputs were written back to the database and the next year's list of available blocks were retrieved. The production consumption data and diamonds produced were carried forward to the financial model to determine the costs and revenue in each year.

The use of an integrated system meant that post initial configuration and testing, a standard i7 processor desktop computer was able to process a set of five alternatives (each alternative consisting of 25 realisations, four iterations and three scenarios) in just over eight hours.

8.4 Case study findings

In this case study the block models contained more than just grade information. Each block also contained variables that could be used to determine the comminution, liberation and DMS efficiency and the results of spatial simulations of diamond size distribution and value within each size class. The project also required differing treatment rates to be achieved over the life of the operation.

The aim of this case study was specifically to identify processing challenges and how these could be addressed through pre-emptive risk mitigation that would not compromise the capital constraints placed on the project.

The summary statistics of the simulated variables in the mined blocks are presented in Table 40.

	Grade	Density	Yield
Count	62975	62975	62975
Minimum	0.00	1.80	0.06
Average	0.51	2.59	4.63
Maximum	6.42	3.17	48.00
Stdev	0.342	0.311	5.830
Coeff Var %	67.6	12.0	125.9

Table 40: Summary statistics of spatially simulated Grade, Density and DMS yield values.

The yield value has the highest coefficient of variation followed by the grade and then the density. This suggests that the uncertainty in the yield is higher than that for grade. The apparent low range in density values is partly a result of inserting a background value of 2.90 for blocks to be estimated that were further away from samples than the range of the variogram.

Throughput

The throughput model planned for an annual mined capacity of 600kt per quarter and a process plant or mil capacity of 525 Kt per quarter. A summary of the tonnage treated is given in .

In the initial period the ramp up for mining and plant increases markedly from year one to year two. The plant capacity is satisfied from the middle of the project onwards. During the ramp-up period however the cash flows derived from production fall short of the plan. This is primarily an impact of the slower rates achieved due to the processing of harder ore.

Figure 65: Summary of tonnage treated

In the initial period the ramp up for mining and plant increases markedly from year one to year two. The plant capacity is satisfied from the middle of the project onwards. During the ramp-up period however the cash flows derived from production fall short of the plan. This is primarily an impact of the slower rates achieved due to the processing of harder ore.

Revenue from diamonds recovered

The simulation of stone sizes and values generated a total of just over 600 M stones for the life of the mine and took approximately four hours to generate these stones. The stones were seeded back into the orebody to produce a range of $/tonne values for each block as it was mined. The summary statistics for these data are given in Table 41.

Lobe	Minimum	Average	Maximim	Stdev	Coeff. Var. %
N	11.32	36.39	87.83	16.00	43.96
C	11.22	32.24	52.84	8.42	26.13
S	2.51	18.70	53.01	6.11	32.66

Table 41: Summary Statistics of $/tonne depleted by lobe based on simulated stone values.

The highest $/tonne value, on a mining block scale, was 87.83 $/tonne in the North lobe which also showed the highest coefficient of variation. This was to a large degree driven by the coarser stone size distribution in this lobe and the contribution of larger stones in the assortment.

Project Valuation

The initial modelling identified that using a 10% discounted cashflow model the Net Present Value(NPV) ranged from BWP -262 million (P10) to BWP +1 million(P90) with a P50 NPV of BWP -156 (Figure 66) .

The model identified that the cashflows in the plan for 2010 and 2012 had the highest uncertainty, and that the project team needed to review mining and process flexibility in these periods. A shortfall of the order of 10% of tonnes treated in this period of the project would translate to close to a 10% change in project value.

8.5 Generic findings from the IEM relevant to the derivation of the metallurgical recovery factor

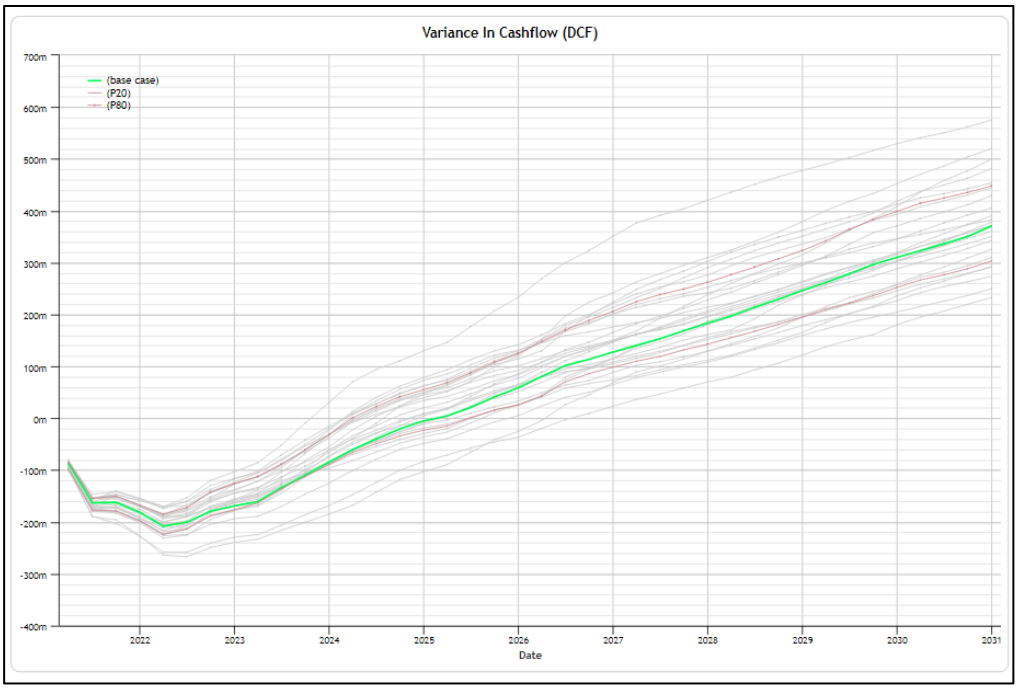

Figure 66: Summary Plot of Cumulative Discounted Cashflow for the Ak project, P50 case shown in green,P80 and P20 case shown in red, individual cases shown in grey.

The traditional approaches to deriving project value using single smoothed orebody models are likely to under-estimate the impact of orebody variability on project value. The integrated modelling approach facilitates a far richer exploration of the impact that orebody uncertainty will have on project performance. The same potentially biased estimation of recovery factors can also result from the use of single averaged assumptions about process performance.

It is possible to arrive at an expected recoverable diamond distribution using a truncated average total diamond content curve. The truncation is achieved by applying a fractional factor to stones that are expected to be recovered below the lower cut of screen size. This modified diamond stone size distribution can then be used to represent the expected recovered diamond distribution and concentration for the life of the operation. Figure 67 shows how it is possible to truncate the total content curve to represent the impact of changes in bottom cut-off size used in the process plant on the expected size distribution of recovered distributions.

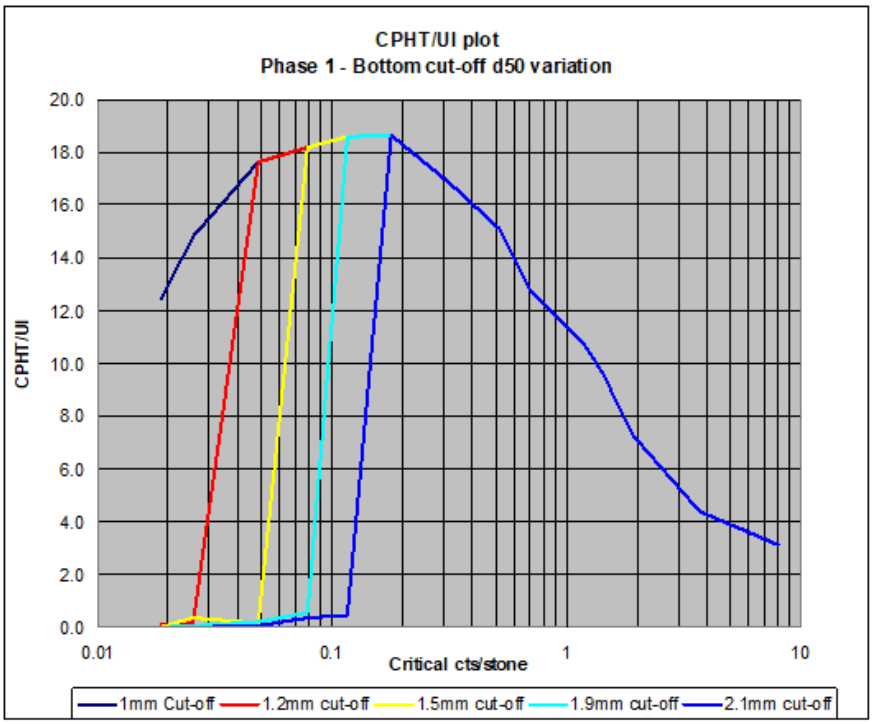

Figure 67: Grade size plot showing the impact of applying a strict size cut-off to a total content curve.

In this particular case a combination of bulk sample and microdiamond results were used. This approach applied to this project gives a range of total content carat recovery ranging from 0.84 at 1mm down to 0.51 at 2mm bottom cut-off size. Using the average grade of the resource and its average distribution this would translate to a revenue recovery range of just over 3 $/tonne. This clearly underestimates the variability that is likely to be experienced during the life of the operation as shown using the integrated model.

Using this approach it is possible to define the recovery factor in several alternative forms, working back from the bulk sample recovery factor (Equation 75)to the intended main treatment plant recovery factor(Equation 76) . The ratio of the intended plant recovery factor to the bulk sample plant recovery factor is then used to determine the resource to reserve factor that is used to account for metallurgical efficiency (Equation 77).

$$BSP_{Rec\ Fac} = BSP_{Lib\ Fac} \times BSP_{Free\ Diamond\ Rec} \quad \textbf{Equation 75}$$

$$MTP_{Rec\ Fac} = MTP_{Lib\ Fac} \times MTP_{Free\ Diamond\ Rec} \quad \textbf{Equation 76}$$

$$Met\ Rec\ Fac_{RsctoRsve} = MTP_{Rec\ fac}/BSP_{Rec\ Fac} \qquad \textbf{Equation 77}$$

Using this approach with average bulk sample plant recovery as the input, the range of the metallurgical (resource to reserve) recovery factor was calculated to range from 0.97 to 1.08. When using the integrated evaluation model approach, it became apparent that the variability due to processing constraints was far higher. The variability produced by the IEM correctly reflects the combined impact of the variable grade of the ore being treated and the variable efficiency of the process that results from the changing characteristics of the rock treated. This approach also allows a much finer temporal scale evaluation of variability in throughput, total carat production and hence project value. Using the IEM approach, it is also possible to assign a localised ore recovery factor and in doing so identify where in the orebody the recovery is likely to vary most, and why it will vary.

The rock characteristics developed here were mainly content variables, however their impact on liberation of dense species within the ore also impacts on throughput and recovery quality.

The use of a log normal stone characteristic simulation allowed the model to incorporate the uncertainty of diamond assortment on the expected recovered revenue. Even with a small number of parcels of stones it is possible to demonstrate the range of expected revenue that extends several orders of magnitude beyond that achieved with a simple static cut-off analysis.

This case study has demonstrated that it is important to consider variable small-scale (mining block scale) impacts of rock properties, rather than the average impact of average kimberlite characteristics, to determine correctly the range of metallurgical recovery that will be experienced over the life of the operation. This requires multiple images of the orebody to be processed at a block scale through a dynamic integrated value chain model. This method is feasible and relatively straight forward to implement.

The final chapter concludes with a summary of the developments that this research has provided in the derivation and use of metallurgical recovery factors for project evaluation.

9 DISCUSSION

9.1 Introduction

This thesis describes current practices used to derive and evaluate metallurgical recovery factors for kimberlitic diamond mines. The recovery factors are used to account for the discrepancy between in situ values of variables that drive project value (diamond stone concentration (stones/ht), diamond grade (Ct/ht), diamond size (Cts/stone), diamond value($/ct), and ore value ($/tonne)), and the expected 'recovered value' of these variables. The literature reviewed shows that predictions of recovery that are based on assumptions of average rock characteristics acquired from a few spatially dispersed samples can be biased.

Several significant improvements to the current approaches have been presented in this thesis and they have been demonstrated to give better recovery factors. These include:

- Clarifying the variable taxonomy using the primary response framework;
- A methodology to develop proxy measurements to augment costly time-consuming destructive rock characterisation testing;
- The use of multiple data sources to generate combinations of estimated and simulated orebody models of rock characteristics;
- The development and use an integrated evaluation framework to model and simulate process performance;
- The application of uncertainty and range analysis techniques to demonstrate how the range of expected recovery factors can be used to mitigate project risks.

The application and benefits of each of these improvements are briefly described below.

9.2 A taxonomy for variables used in recovery factor determination

The building of spatial models of orebody characteristics that can be used to derive recovery factors requires data with sufficient spatial intensity and appropriate support to characterise their spatial behaviour. Historically, sampling for rock

characteristic variables that can be used to predict recovery has often been limited to a few large 'representative' samples that do not capture the range or the spatial variability of the characteristics of interest.

To overcome some of the physical and financial constraints of sampling, several innovative technologies and approaches have emerged. These include the augmentation of high-cost large support samples with smaller, less costly samples or measurements that can be taken from more places in the orebody. These so-called 'proxy' tests or measurements are typically slightly less accurate than the full-scale representative sample and require the building of some form of mathematical model to enable the proxy data to be used in the generation of the spatial models.

There is a requirement for a taxonomy to classify the numerous tests, data sources used to quantify the variables used in recovery factor evaluation. An ideal taxonomic framework will guide the selection of samples and the tests that they are subjected to so that the data sets generated can be effectively used. The suggested taxonomy provides a useful framework for design and implementation of the approached described here. Variables used in recovery factor evaluation range from diamond content variables to characteristics that describe the primary properties and responses of treated rocks to some energy input (Figure 68). The use of two such approaches (Coward et al, 2003) and (Keeney and Walters, 2008) are described to demonstrate how they can be used to balance the rationalisation of sampling with the need for sufficient data of appropriate support to facilitate spatial estimation and simulation of the characteristics of interest.

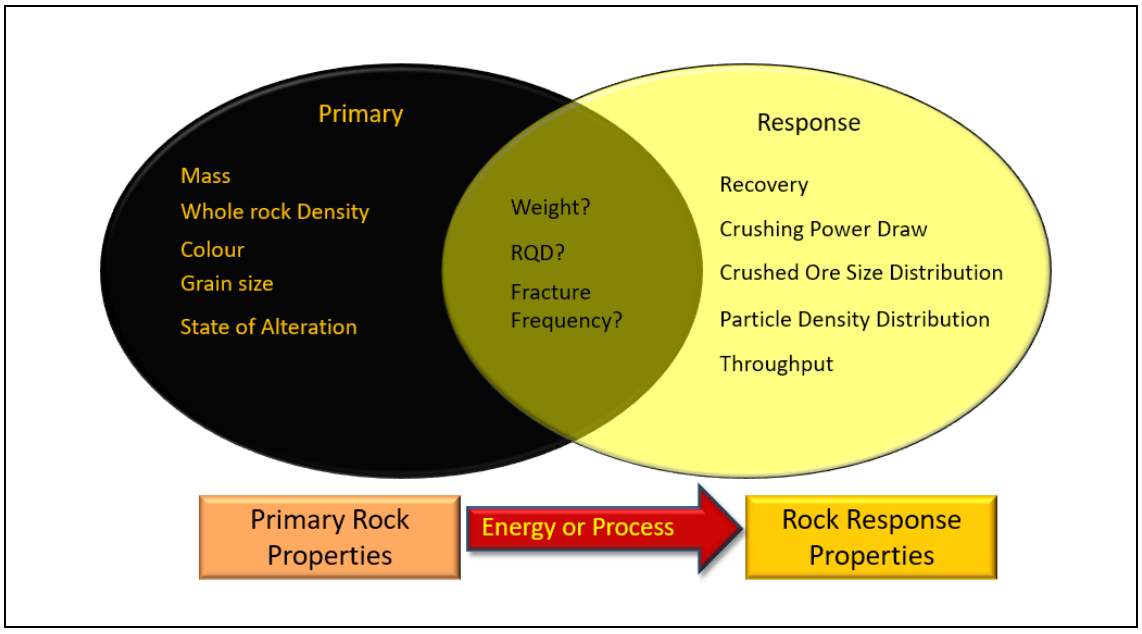

Figure 68: A schematic representing the primary response framework for geometallurgical variables.

The primary response framework for geometallurgical variables provides a useful distinction between variables that are closely associated with the in situ rock characteristics and variables that are associated with the response of the rock to some process. Primary variables typically are easier to estimate but require more spatially intense sampling. Response properties are often characterised by nonlinear relationships which make them harder to estimate and require larger samples with larger support. The third dimension in this classification - 'energy and process' - gives an indication of the meta data that should be collected when carrying out measurements and tests on rock samples.

A taxonomy developed by Keeny and Walters (2008) suggests there are four levels of data (Figure 69), with level one being geologically focussed and spatially representative and level four data being typically acquired from large composite samples that have a metallurgical focus. This suggests that Level 1, 2 and 3 data are derived from drill core, and in some cases from large diameter drilling (LDD) that produces rock chips. On operating mines it is possible to gather additional level 1-3 data from in situ samples taken from the pit, or from post production blasting and during mineral processing.

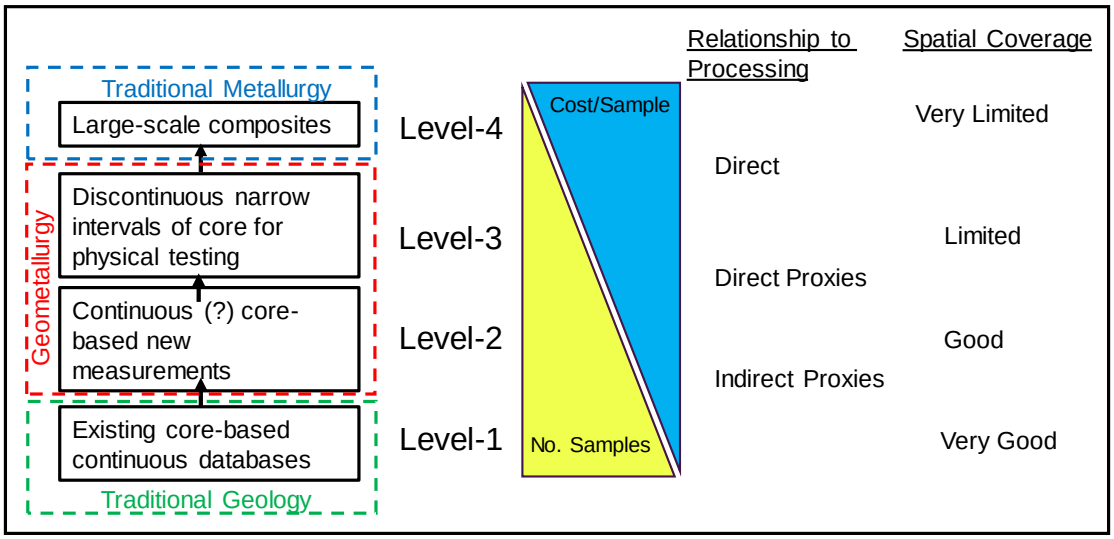

Figure 69: A data typology adapted after Keeney and Walters (2008).

In the case of sampling to measure the characteristics of kimberlites and their diamond content, their particulate nature and the low concentration of the mineralisation generates some data types that do not quite fit into this taxonomy. For instance, large samples of several thousand tonnes are occasionally collected and treated at operating mines (and in some cases from trenches made across orebodies in early project phases) to obtain a sample large enough to represent the contained diamond footprint (ranges of colours, shapes and qualities). In this case the sample has very limited spatial coverage, is discontinuous, and the main

objective of collecting the data is focussed on a content variable that is arguably geological in nature.

Although the classification has some limitations in kimberlites, it is, however, relatively simple and provides a useful framework for developing a sampling programme that aims to achieve a balance between the high-cost per sample and low coverage of level 4 data, with the lower cost per sample and higher coverage that is associated with collection of level 1 data. This type of trade-off is often confronted by mining project evaluation programs. The 'optimal' sampling programme depends on a number of factors that are specific to the characteristics of the kimberlite to be mined and the mining and process configuration. The best, or optimal, combinations of number of samples, sample support and tests carried out on each sample will differ from mine to mine, deposit to deposit and lithology to lithology and will be specific to the variables required to inform the project as-well as the phase that the project is in.

By ranking and mapping the planned tests and sampling on an independent classification for sample methods based on their level (Keeney et al., 2008) of coverage and the degree to which the sample and tests are used to derive data that reflect a primary or response property of the variables it is possible to evaluate which trade-off will make most sense in terms of time, cost and the ability to generate models and reconcile the model to make useful value adding decisions in both the tactical and strategic aspects of the mining business.

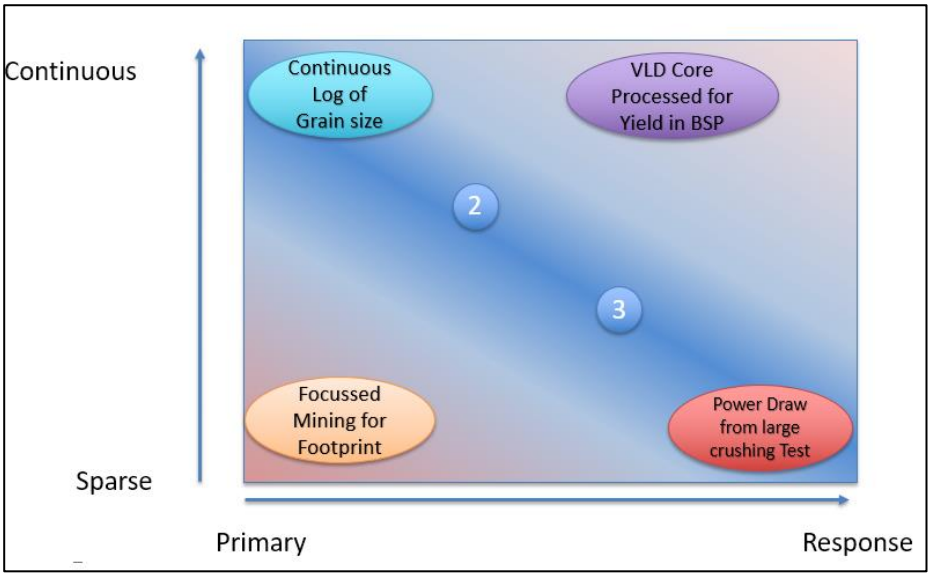

Figure 70: A landscape for sample type classification in terms of both spatial continuity and primary response dimensions.

In Figure 70, a landscape for classification of tests is presented - the scales on the X and Y axes are broken down into two regions - giving four quadrants into which each sample type can be placed.

These taxonomies suggest that there is substantial benefit in applying several generic principles when designing and implementing a sampling programme that aims to acquire data that will support the estimation of metallurgical recovery factors. Table 42 Presents a potential list of such guidelines that will be very useful in defining the parameters for designing sampling experiments and subsequent workflows for the purpose of providing sufficient information to facilitate the evaluation of a project or mine metallurgical recovery factors.

Principles	Explanation
Spatial coverage	The data used for geometallurgical modelling should be spatially distributed and on an appropriate support to permit reasonable estimation of the chosen variables, including domaining and selection of estimation techniques.
Primary Response Variable Classification	Rock characteristic variables can be usefully classified as either primary attributes that are closely associated with in situ rock characteristics and response variables that are closely related to the response of the process to rock characteristics. The relationship between primary and response variables is also a function of the process used to generate the response.
Sample rationalisation	Sample selection and analysis are rationalised to meet the demands of being both adequately representative of geology and processing responses. For example, fewer samples will be required for early exploration of a kimberlite to inform the decision to continue sampling, than the number of samples required to develop a model that can be used for resource classification.
Co-location	As far as practically possible, samples chosen for analysis should be co-located in space and at a scale that is appropriate and relevant to the model that is being built and the intended use of that model. Isotopic data, i.e. having as many of the same measures on samples at all sampled locations, have value in their potential to be used for development of proxy measures.
Calibration and new technology	Where response variable proxies are being proposed to predict primary rock characteristic variables, calibration of the relationship between the proxy variable to primary characteristics must be undertaken at an appropriate scale. This requirement is applicable to both existing and new technology.
Business case	An appropriate business case should be made for any sampling campaign with respect to the tactical and/or strategic model that is to be designed and created and used to support decision making.
Generic vs specific	Generic guidelines are considered useful for sampling problem framing and sample to model planning and development at a strategic level. It is important that specific site, domain and variable specific sampling experiments should be designed given the heterogeneity of kimberlitic deposits.
Objectives and measurements	The objectives of each sampling campaign should be clearly articulated, and measurement criteria defined to assess the success or failure of each campaign
Principles of correct sampling	Correct sampling practices should lead to unbiased results. Design and execution of any sampling experiment must consider good sampling science (Gy, 2004) and be designed to minimise sampling bias.
Building on existing data	Where possible, new sampling campaigns must allow existing data to remain valid so that the database grows organically, and that no repeat sampling is required; e.g., consistent use of a set grind size for slime content analysis.

Table 42: A list of guiding principles for rock characteristic sampling.

These guiding principles provide a useful framework to plan and execute a sampling programme that will produce a data set of sufficient quality for the purposes of spatially estimating rock characteristics that can be used to evaluate metallurgical recovery factors.

9.3 Increasing the quality of spatial estimates -using proxy measurements, scale-up and testing for additivity or non-linearity

Prior work on increasing spatial coverage of rock characteristic data (Dowd, 1997) has shown that it is possible to infer rock characteristics at unsampled locations using a combination of direct and indirect data. This research has extended this concept and presented an experiment to demonstrate how a similar approach can be used in Kimberlitic rocks. The experiment has shown how it is possible to acquire data sets from a combination of in-hole measurements, measurements on core and regional geophysical measurements. These data make it possible to improve the qualitative understanding of geological domain boundaries and create a framework for finding proxy measurements for difficult and costly destructive rock tests.

The collection of the data requires attention to be paid to descriptions of the core and careful colocation of the measurements made down the hole and on the core. It was found in this specific data set (i.e. a southern African volcaniclastic kimberlite and kimberlite breccia) that averaging to approximately 70cm increased correlations between various measurements. This result suggests that the scale of geophysical response and errors in location are minimised at this level of support - for the rock types tested here. In applications to other deposits a similar approach will be required to improve the correlations between the response measures made. The methodology of finding the minimum point of the summed within-sample variance and between sample variance can be applied to several variable pairs and could produce different ideal support sizes.

Work described here has identified that scale-up is not complex where variables exhibit linear relationships and can be considered to have additive behaviour. The approach required for variables that exhibit non-linear relationships, of which there are many in this field (e.g., bond work index, abrasion index), are likely to require more considered, and potentially far more complex approaches (Carrasco, 2014). A pathway for developing suitable approaches for spatial modelling of a variety of rock characteristic variables is discussed in chapter 6. This approach suggests that the parameters used to generate the spatial model are not independent of the use for which the model is intended. For example, in some cases the when generating a kriged grade estimate, the modeller may choose a set of kriging parameters that will be better suited to providing an estimate that is more suited to a global or local

estimate. The methods used to generate spatial simulated models of rock characteristics can also be tailored to the intended use of the spatial simulations (for example by choosing appropriate block sizes and setting up of domains that reflect the spatial nature of the physical rock characteristic being simulated). Block to block variability of the rock characteristics may be important when the spatial models are used in highly granular dynamic simulations to predict rates and efficiencies of mining and metallurgical recovery processes.

9.4 Diamond metallurgical recovery factors – exploring uncertainty and variability by effective use of value chain models

The linking of populated multivariate models of the orebody with process models that respond at an appropriate scale opens several avenues to derive and evaluate the Metallurgical Recovery Factor for Diamonds recovered from Kimberlitic Deposits.

In early stage projects where there is little information on the orebody, and still significant flexibility in design criteria selection, it is still useful to have a quantitative model that links the orebody characteristics to the expected recovered diamond population. Although the expected value for total recovered diamond mass, size distribution and revenue distribution are important, it is perhaps more important to be able to develop and apply a methodology to quantify the ranges of these values.

The published literature has demonstrated that it is common practice to use the average rock properties either at a global scale or at a domain scale to predict the fracture and process rates of rocks through a given process (Farrow, 2019). This limited approach is, in some cases, justified by the limited availability of rock characteristic data and the inability of traditional approaches to incorporate this information effectively in the derivation of recovery factors.

System theory (Boulding, 1956) suggests that dynamic effects that arise from the interaction of constraints with variability will not be correctly reflected in models that are based on long-term averages. This same effect is referred to in the theory of constraints (Goldratt, 1990). In this theory, the average of the throughput of several interdependent processes will not equal the average throughput. This also known as the 'flaw of averages' (Savage, 2008) and although it seems that these biasing effects would be explicitly addressed in mining project evaluations, it is evident that several projects are evaluated on data that are summarised on an annual scale for inclusion in financial models. The biases that arise from this shortcoming are difficult to detect and may be very complex. It is for these reasons that a highly

granular interdependent system model of the mining and treatment process should be used to evaluate the expected range and variability of performance of the diamond recovery processes.

9.5 Conclusion

This research aimed to investigate ways to identify and measure the rock characteristics that have an impact on the metallurgical recovery factor. A case study has shown it is possible to sample for several response characteristics and then estimate these effectively using a so-called proxy framework to augment response property data with non-destructive measurements in the hole and on core. These data also facilitate the generation of several spatial simulations of these characteristics. The development of a way to process these multivariate models of the orebody at a fine scale (block scale resolution) enables the assessment of the impact of these rock characteristics on diamond recovery on widely varying time scales. The output data can be analysed in many varied ways to quantify the mean and the range of recovery factors for diamonds recovered from kimberlitic deposits.

Data processing speed has increased exponentially for several decades (Moore, 1965). Effective access to this increasing rate of processing has to some extent been limited. Recent developments in arbitraging rates for excess server capacity by some of the broadcast networks, via various service providers, including Amazon Web Services and Oracle, suggests that the constraint on processing large and previously unwieldly data sets is becoming affordable to mid-tier mining companies. This suggests that the cost of providing platforms for processing large multivariate orebody models will reduce and their use in the mining industry will become more common. These developments mean that the methodology presented here is not only valid but can now be practically implemented at a cost that is of a similar scale to those traditionally associated with resource estimation and project evaluation.

A large non-technical challenge to the adoption of this methodology has been the ability to convey the outputs of the range analysis in a way that is embraced by senior stakeholders in the mining industry. Although the concept of issuing "Guidance Ranges" for critical performance targets is being more widely adopted (e.g. Newmont annual report, 2015) it's use in corporate decision-making requires more work but is gaining acceptability. Cyclicity, decreasing margins, lower average grades and increasing competition for fewer resources are hall marks of the mining industry. The development of methods that can validly assess, and respond to, the impacts of uncertainty and variability of project value will confer special competitive advantages on the companies that embrace it. The methodologies presented here, when used as part of a strategy for improved decision-making, will add substantial value to the mining industry.

10 SUMMARY AND CONCLUSIONS

10.1 Introduction

The specific limitations of traditional recovery factor evaluation that have been addressed in this thesis are those associated with the difficulty of incorporating variable and uncertain rock properties in the derivation of the metallurgical recovery factors.

Metallurgical recovery factors are required to account for the difference between the estimated in situ diamond content and expected diamond recovery. These factors are used to modify the stone concentration, the mass concentration and diamond size frequency so that the expected recovered $/tonne can be predicted. Failure to explicitly include the impacts of rock properties in traditional project valuation can result in sub-optimal mine design, incorrect processing configuration (design, operating strategy) and potentially biased production and cashflow forecasts. Not only are there vast differences between the scale of measurement and the scale of estimation of these properties but the data acquired from tests and measurements on small samples may not directly correlate with the rock-process relationship that will eventuate at full-scale operation. The consequences of potential biases are amplified when global estimates of rock and diamond characteristics, based on few and spatially sparse data, are used for planning and designing the entire life of the project.

The problem statement is described as:

- Current known estimation techniques for recovery factors of kimberlite diamond deposits are based on global assumptions and average values and do not explicitly incorporate the spatial variation of rock properties. The problem stems from the following inadequacies:
  - No existing method to measure and estimate the physical spatial characteristics of kimberlite.
  - Mine production and metallurgical process modelling is insensitive to spatial estimates of physical character.

- Project decision making/valuation frameworks do not incorporate the change in project value that can be attributed to responses to the recovery factor uncertainty.

A research framework was developed to address the problem statement that focussed on three areas of research. The first area required a combination of in-field sampling experimentation, and considerable work to develop a model to generate multiple spatial realisations of orebody characteristics. The approach explored methods to use multiple sources of data to create rock characteristic estimates.

The second area of successful research identified aspects of current practice in process plant simulation that could be used to process the multiple realisations of the orebody and predict process outcomes. Several methods were developed and demonstrated in two case studies; one for an underground mine and a second for an open-pit operation.

The third area of research was focused on a means to evaluate the range and uncertainty of the derived forecasts for metallurgical recovery. This required the development of an integrated value chain model that could be used to translate the technical uncertainty into financial metrics. This approach allows for comparisons to be made between various project risk mitigation strategies.

The remainder of this chapter highlights areas of successful developments, reviews some of the limitations of this research and concludes with a brief discussion of areas for further research.

10.2 Concluding Themes

This research has demonstrated that several current reviewed methods of evaluating the metallurgical recovery factor for diamonds recovered from kimberlite deposits have limitations. Improvements in several areas can now be made as a direct result of the work reported here. These are briefly discussed below.

Variable selection and identification

The primary response framework (Coward et al., 2009) was developed to clarify the taxonomy for variables that are used in this research. This conceptual framework provides a basis for developing quantitative models of the relationships between variables that drive uncertainty in the recovery of diamonds. The benefit of this framework is that it provides guidance in the use, and limits to some extent potential misuses, of methods for generating spatial models of rock characteristics.

A study of several existing plant processes has identified important metallurgical response areas and developed relationships between rock properties and the performance of those processes. These can broadly be divided into characteristics of the rock that impact on comminution, dense media separation, final diamond recovery, water management and materials handling. The study also identified several diamond properties that impact on their likelihood of being recovered. These include diamond geometries, surface characteristics and luminescent properties.

These insights have facilitated the development of an approach to improving the design of sampling campaigns so that they provide enough data of sufficient quality to facilitate rock characteristic estimation.

Sampling for rock characteristics

As a result of historical constraints placed on the acquisition and treatment of samples to provide data to model unit process performance, the models have in several cases evolved to consider so-called 'average rock characteristics' as their inputs. This has in turn led to the use of so-called composite representative samples that aim to emulate the average characteristics that will be encountered in the treatment process. This approach has been shown to have several limitations that can be overcome by developing sampling campaigns that acquire samples from several locations with sufficient support to facilitate spatial estimation of the characteristics of interest at unsampled locations. Where this can be achieved, the selection and definition of geometrically constrained domains, so-called "processing" or "geometallurgical" domains, becomes an important step in being able to estimate these characteristics with any confidence. The requirement for spatial stationarity becomes even more onerous when spatially simulating these characteristics.

The benefits of this approach to establishing the spatial nature of rock characteristics is that the estimated models will provide an unbiased estimate of the expected characteristic at all estimated locations, and the spatial simulation approach provides a pathway to explore and define the range of rock characteristics that will be encountered when mining the deposit. As a suite, the simulations provide a probabilistic expression of the range of outcomes that could be encountered.

Sampling for rock characteristics requires a rigorous approach to sampling to eliminate a host of biases that can arise – an approach has been demonstrated here using an experiment carried out on an operating kimberlite mine.

Kimberlites comprise a complex suite of rock types that exhibit a wide range of physical characteristics. These arise from a combination of differences in composition, texture and weathering or alteration state. Accounting for these three aspects of the rock require suitable adjustments in the acquisition of samples and the testing of characteristics of those samples. This is especially true for coarse textured breccias that require a larger sample support. To mitigate some of the risks associated with the constraints on the number and spatial coverage of physical samples it is possible to use more cost effective, and potentially less accurate, proxy measurements to enhance the estimation of values at unsampled locations (e.g., using acoustic velocity to augment various measures of rock strength that are used to predict fracture.)

Spatial estimation and simulation

Spatial estimation and simulation are different methods that both produce spatial models but that have differing characteristics that are useful in certain circumstances. Both approaches require attention to spatial coverage, support and scale-up, and provide different benefits to the evaluation process.

When sufficient data have been acquired it is possible to derive parameters for the spatial estimation and spatial simulation of the rock characteristics of interest. Best linear unbiased estimation methods such as ordinary kriging provide models that are unbiased but potentially smoother than the reality that will be encountered when mining. Conditional spatial simulation methods provide a means to replicate the in situ variability of the characteristics of interest. As a suite, the realisations can be used to determine the uncertainty of these characteristics. This is important and there are often constraints in the mining and processing of these rocks that respond to extreme values rather than the average characteristics.

Mining and treatment process simulation

Process simulation can be used in combination with spatial rock characteristic models to quantify the impact of rock variability on diamond liberation and recovery. A model to do this has been developed and implemented in this research.

Conventional unit process models have traditionally been limited by both speed of processing and the limited availability of valid spatial models of characteristics that could be used as inputs for dynamic process simulation. The evolution of a methodology for using spatially estimated (and spatially simulated) rock characteristics to simulate total comminution and link total comminution to diamond liberation and diamond recovery provides a quantitative way to forecast

the mean and expected range of metallurgical recovery for a given process flowsheet.

A linked value chain model is an appropriate way of evaluating the impact of rock and diamond variability on the expected value and range of the metallurgical recovery factor. The benefits of an integrated value chain model include:

1. A quantified approach to estimating the range and uncertainty in the metallurgical recovery factor will improve the identification and selection of strategies to optimise kimberlite mine operation.
2. As the model uses multiple spatial realisations of the orebody characteristics it is possible to identify periods when the recovery factor is most uncertain and hence identify which actions (e.g. additional sampling, or additional crushing capacity) will have the biggest impact on metallurgical recovery.
3. The process model is calibrated to a specific flowsheet and can thus be adapted and rerun to determine how changes in design and operation will impact on the metallurgical recovery. This allows for iterative optimisation that targets robust recovery rather than a vulnerable 'optimum' design that does not explicitly consider uncertainty.

10.3 Specific contributions of this research

This research has specifically addressed the following areas:

- Development and demonstration of an approach to extend the spatial coverage of data that is acquired from costly destructive rock testing methods;
- Investigation and demonstration of viable methods to estimate and simulate rock properties into block models at an appropriate scale;
- Development of an integrated value chain model that facilitates analysis of the impact that variable and uncertain rock properties have on mining and treatment efficiency; and
- Use of an integrated evaluation model to calculate the metallurgical recovery factor for the life of diamond mining projects at different resolutions, and to generate confidence limits around the estimate of the metallurgical recovery factor.

10.4 The limits of this research

Uncertainty and variability are two very distinct characteristics of a variable. Unfortunately, the variability of any variable, as described by its values, is a composite of several potential sources of variability. The spatial models and simulations of the values of these variables at unsampled locations will produce realisations with variability that is a function of both the true spatial variability and the variability that is introduced by other sources of variability from the measuring and testing processes. Understanding the relative magnitude of the variability that is intrinsic to the deposit and the variability that arises from the uncertainty due to the inability to measure accurately at all locations will require further work.

The fitting of functions to data imposes the modellers will, not only on the parameters that are used to control the location and shape of the function used, but in the selection of the form of the equation that is used to resemble a real-world phenomenon. Some of the functions that are used in mineral processing models have been validated by comparing their predictions, on average, with the averages of observations of real-world process plant responses (e.g., exponential comminution models). The approach developed and demonstrated in this thesis uses errors, or residuals, of model fitting to generate a feasible range of the parameters for the models used. One such approach used here allows the inclusion of the standard error to induce a measure of uncertainty for both linear and curvilinear equations has specific merit as it can be readily used in the value chain models.

There are limits to this approach of incorporating uncertainty in process modelling, especially where the response is a function of more than one input variable. Reducing the dimensionality of relationships between primary and response variables using multiple or partial regression models (e.g., Nipals algorithm (Esbensen, 2002)) is one alternative solution. Another approach does not reduce the input data dimensionality but aims to model the response variable using multiple multidimensional response surfaces. This requires that sampling experiments be designed to collect multivariate test data that are isotopic (i.e. the same data types collected for all samples from all locations) is collected at the right scale. This data makes it possible to generate response surfaces using some interpolation method - such as kriging or radial basis functions. These modelled surfaces can then be perturbed using the error of the fit to represent uncertainty and then be applied to the value chain model. This development is currently being embedded in the value chain system that has resulted from this research and is a far more rapid method of deriving multiple responses from estimated block characteristics.

The data acquisition experiment required several different types of data to be acquired from several different laboratories. The co-ordination of the sample movements was not trivial and is perhaps one of the major hurdles that can be overcome in acquiring valid and reliable rock characteristic data. Where practical it is recommended that part of the trade-off studies that should be carried out when planning sampling designed to acquire data for recovery factor estimation includes the accessibility of more than one type of measurement at each laboratory. This aids substantially in tracking the sample and data. The information acquired from downhole geophysics has shown itself to be of substantial use not only for estimating physical rock characteristics, but also for providing a basis for improving the location of the acquired core.

10.5 Recommended areas for additional research

Several of the findings of this research have resulting in suggestions for either a deeper investigation or additional experimentation to validate and expand specific findings.

In tandem with this research, the author has been responsible for adapting the methodology developed here to quantify recovery in various operations and some of these models have been reported in the literature. This has resulted in the identification of areas which required additional work to enable value chain models to be applied to projects for other mined commodities including iron ore, uranium and gold projects.

Evolution of access to less costly computing power continues to enable a far greater range of more complex unit process models. This includes access to online cloud infrastructure that allows access to multiple configurable servers for limited time at almost no cost. The value chain approach lends itself to parallel computing. A single orebody, single mine plan, single process configuration and associated financial model constitutes a single yet complete value chain model, and so it is possible to distribute each value chain model to disparate servers for processing. Work is continuing in this area and is likely to lead to a reduction of several orders of magnitude in processing speed.

Several of the non- destructive geophysical tools were identified as having some weak yet discernible correlation with the destructive measures. As these tools improve and the ratios of the signal strength to noise increases the use for this additional, relatively cheap, data will increase. This will require specific calibration of the tools to the environments and mineralogy of the rocks in which they are to be used.

Value chain model validation can be improved by using this approach on existing operations in a predictive way. Ensuring that the value chain model that includes orebody characteristics and a suitable process model is up to date can provide several benefits to these operations. This includes being able to create a production performance forecast, and to identifying periods in which the metallurgical recovery factor will be compromised because of variable rock characteristics. This approach will allow mine decision-makers to take pre-emptive action to mitigate recovery risk and harness opportunities for increasing recovery and process performance.

11 REFERENCES

Agricola, G., 1556. De Re Metallica. 1950 ed., New York: Dover Publications.

Aitchison, J. & Brown, J.A.C., 1957. *The Lognormal Distribution*, Cambridge, England: Cambridge University Press.

Anglo American, 2018. Anglo American Ore Reserves and Mineral Resources Report 2018., p.53.

Ameluxen, P. 2003. The application of the SAG Power Index to orebody hardness characterization for the design and optimization of comminution circuits. McGill University, Montreal, Canada.

American Society for Testing and Materials,1988: Standard Method for Splitting Tensile Strength of Intact Rock Core Specimens D 3967-86. 1988 Annual Book of ASTM Standards, Vol. 04.08, Soil and Rock; Building Stones; Geotextiles, 471–475.

American Society for Testing and Materials 1998: D7012 - 14e1 Standard Test Methods for Compressive Strength and Elastic Moduli of Intact Rock Core Specimens under Varying States of Stress and Temperatures.

Andersen, J.S. 1988. Development of a cone crusher model. M.Eng.Sc Thesis, University of Queensland, Brisbane.

Appleyard, G.R. ,2001. An Overview and Outline, in Mineral resource and Ore Reserve estimation- The AusIMM guide to good practice', in Edwards, A. . (ed.). Melbourne: The Australasian Institute of Mining and Metallurgy, pp. 3–12.

Armstrong, M. 1988. Geostatistics volume 1 and 2, 268 p (Kluwer Academic publishers' group: Amsterdam, The Netherlands).

Ashley, K.J. and Callow, M.I. 2000. Variability: Exercises in Geometallurgy [online], Available from: <http://e-j.com/ar/mining_ore_variability_exercises/; > [Accessed: 10 March 2004].

Aspinall, W.P., 2018. Structured Elicitation of Expert Judgment for Probabilistic Hazard and Risk Assessment in Volcanic Eruptions. In Statistics in Volcanology. The

Geological Society of London on behalf of The International Association of Volcanology and Chemistry of the Earth's Interior, pp. 15–30.

American Society for Testing and Materials, 1998. ASTM Standards on Environmental Sampling.

Bagnell, W., Bedell, P., Bertrand, V., Brummer, R., Farrow, D., Gagnon, C.L.G., Gormely, L., Magnan, M. and St-Onge, J. 2013. NI 43-101 Technical Report for The Renard Diamond Project, Québec, Canada, Stornoway Diamond Corporation, Québec, Canada.

Bearman, R.A., Pine, R.J., and Wills, B.A. 1989. Use of Fracture Toughness Testing in Characterizing the Comminution Potential of Rock, Proceedings of MMIJ/IMM Joint Symposium, Kyoto pp161-170

Beniscelli, J., Carrasco, P., Dowd, P.A. Ferguson, G. and Tulcanaza, E. 2000. Estimation of Resources and Conversion to Reserves - Protocols for the Assessment, Reduction and Management of Risk, paper presented to Mass Min 2000, Brisbane, Australia.

Bojcevski, D., Vink, L., Johnson, N.W., Landmark, V., Johnston, M., Mackenzie, J. and Young, M. F. 1998. Metallurgical characterisation of George Fisher Ore Textures and Implications for Ore Processing, paper presented to Mine to Mill conference, Brisbane Australia.

Boulding, K.E., 1956. General Systems Theory - The Skeleton of Science. Management Science, 2(3), pp.197-208

Box, G. E. P. and Draper, N. R. 1987. Empirical Model-Building and Response Surfaces John Wiley & Sons, Inc.

Boychuk, K.G., Garcia, D. H., Sharp, A.W., Vincent, J.D. and Yeomans, T. J., 2012. NI 43-101 Technical Report on the Pitarrilla Project, Durango State, Mexico, Silver Standard Resources.

Bradfield, R., Wright, G., Burt, G., Cairns, G., Van Der Heijden, K., 2005. The origins and evolution of scenario techniques in long range business planning. *Futures*, 37(8), pp.795–812.

Bratvold, B. and Begg, S. 2002. Would You Know a Good Decision if You Saw One, paper presented to SPE Annual Technical Conference, San Antonio, Texas.

Brennan, M.J. and Schwartz, E.S. 1985. Evaluating Natural Resource Investments, Journal of Business, 58(2).

Brown, R., Tait, M., Field, M., Sparks, R.S.J. 2008. Geology of a complex kimberlite pipe (K2 pipe, Venetia Mine, South Africa): Insights into conduit processes during explosive ultrabasic eruptions. Bulletin of Volcanology, 71, pp.95–112.

Burbeck, S. 1992. Applications Programming, how to use Model-View-Controller (MVC). *Applications Programming in Smalltalk-80*, p.3. Available at: https://web.archive.org/web/20120729161926/http://st-www.cs.illinois.edu/users/smarch/st-docs/mvc.html [Accessed September 14, 2011].

Bush, E.D. 2010. An overview of the estimation of kimberlite diamond deposits. *Southern African Institute of Mining and Metallurgy: Diamonds - Source to Use 2010*, pp.73–84.

Bye, A.R. 2011. Case Studies Demonstrating Value from Geometallurgy Initiatives. In *Geomet 2011*. pp. 5–7.

Caers, J. and Rombouts, L. 1996. Valuation of Primary Diamond Deposits by Extreme Vale Statistics, Economic Geology 91( ):841-854.

Campbell, J.A.H. 2009. THE DEVELOPMENT OF AK6. In *Diamonds Source to Use 2009*. Gaberone: The Southern African Institute of Mining and Metallurgy, pp. 1–20.

Carrasco, P., Chiles, J. P., Séguret, S.A. 2008. Additivity, Metallurgical Recovery, and Grade, in Geostats 2008: VIII International Geostatistics Congress (eds: J Ortiz and X Emery), Santiago, December, pp 465-476.

Chapman, J. G. and Boxer, G. L. 2003. Size distribution analyses for estimating diamond grade and value, paper presented to 8th International Kimberlite Conference, Victoria.

Cookenboo, H.O. & Grutter, H.S. 2010. Mantle-derived indicator mineral compositions as applied to diamond exploration. Geochemistry: Exploration, Environment, Analysis, 10, pp.81–95.

Copur, H., Billgin, N., Tuncdemir, H. and Balci, C. 2003. A set of indices based on indentation tests for assessment of rock cutting performance and rock properties, South African Institute of Mining and Metallurgy.

Cornah, A., Vann, J., & Driver, I. 2013. Comparison of three geostatistical approaches to quantify the impact of drill spacing on resource confidence for a coal seam (with a case example from Moranbah North, Queensland, Australia). International Journal of Coal Geology, 112, 114-124. DOI: 10.1016/j.coal.2012.11.00

Coward, S.J. and Ferreira, J. 2005. Development and conceptual evaluation of a methodology for sampling for diamonds in broken ore. In *EMMES Conference*. p. 149.

Coward, S.J., Vann, J., Dunham. S., Stewart, M. 2009. The Primary-Response Framework for Geometallurgical Variables. In Seventh International Mining Geology Conference. pp. 109–113.

Daniel, M., Lane, G. and McLean, E. 2010. Efficiency, economics, energy and emissions – Emerging criteria for comminution circuit decision making., paper presented to XXV International Mineral Processing Congress (IMPC) Brisbane, Qld, Australia, 6 - 10 September 2010.

Davis, G.A. 1995. An Investigation of the Under Pricing Inherent in DCF Valuation Techniques, paper presented to SME Annual Meeting, Denver, Colorado, 6-9th March 1995.

De Beers Group Services, 2017. De Beers Annual Finance Seminar, London UK.

De Beers Mineral Resource Intelligence Unit, 2005. Estimates of Global Diamond Production.

Demming, W.E. 1986. Out of the Crisis, Massachusetts Institute of Technology, Centre for Advanced Engineering Study.

Dimitrakopoulos, R. and Ramazan, S. 2004. Uncertainty Based Production Scheduling in Open-Pit Mining, SME Transaction, 316(03-151): pp 1-9.

Lamghari, A. & Dimitrakopoulos, R., 2016. Network-flow based algorithms for scheduling production in multi-processor open-pit mines accounting for metal uncertainty. European Journal of Operational Research, 250(1).

Dowd, P.A. 1978. Advances in Geostatistics: Numerical Methods and their Application. Ph.D. Thesis, University of Leeds, UK

Dowd, P. A. 1992. A review of recent developments in Geostatistics. Computers and Geosciences, 17(10): pp. 1481-1500.

Dowd, P. A. 1994, 2004. Geostatistical Simulation Course Notes.

Dowd, P.A. 1997. Geostatistical Characterisation of Three-Dimensional Spatial Heterogeneity of Rock Properties at Sellafield. Transactions of the Institution of Mining and Metallurgy, 106, A133-197. London, United Kingdom.

Dowd, P.A. and Dare-Bryan, P.C, 2004. Planning Designing and Optimising Production Using Geostatistical Simulation. Proceedings of the International

Symposium on *Orebody Modelling and Strategic Mine Planning*. Pub AusIMM (Melbourne). ISBN 1 920806 22 9; 321-338.

Dowd, P.A. and Pardo-Igúzquiza, E., 2006. Core-log integration: optimal geostatistical signal reconstruction from secondary information, Transactions of the Institution of Mining and Metallurgy, Section B, 115(2):12.

Esbensen, K. 2002. Multivariate Data Analysis - In Practice, 5th ed, 598 p (Camo Process AS: Oslo).

Esbensen, K. 2004. 50 Years of Pierre Gy's "Theory of Sampling", Chemometrics and Intelligent Laboratory systems, 74(1): pp3-6.

Farrow, D.J. 2015. 2015 Mineral Resource Update for the Renard Diamond Project - Ni 43-101 Technical Report, Vancouver.

Ferreira, J.J., 2013. Sampling and estimation of diamond content in kimberlite based on microdiamonds. PhD thesis, l'École nationale supérieure des mines de Paris, Paris.

Field, M., Stiefenhofer, J., Robey, J. and Kurszlaukis, S. 2008. Kimberlite-hosted diamond deposits of southern Africa: A review., Ore Geology Reviews, 34:33-75.

Field, M. and Scott Smith, B.H. 1999, 'Contrasting geology and near-surface emplacement of kimberlite pipes in Southern Africa and Canada', The J. B. Dawson Volume, pp. 214–237.

Fullagar, P.K. and Fallon, G.N. 1997. Orebody Delineation and Rock Mass Characterisation, paper presented to Explor97, Toronto, Canada, 14-18 September 1997.

Garman, M.B. and Kohlhagen, S.W. 1983. Foreign currency option values, International Money Finance, Vol 2: p231-237.

Goldratt, E.M. 1990. Theory of Constraints. Great Barrington: North River Press, pp.1–159.

Griffith, A.A. 1921. The Phenomenon of Rupture and Flow in Solids, Philosophical Transactions of the Royal Physical Society, Vol. 221, pp. 163-198.

Gy, P. 2004. Sampling of Discrete Materials - A New Introduction to the Theory of Sampling, Chemometrics and Intelligent Laboratory Systems, 74(1): pp 7-24.

Hawthorne, J.B. 1975. Model of a kimberlite pipe. In First International Kimberlite Conference. Physics and Chemistry of the Earth, v. 9, pp. 1–16.

Holmes, J.A. 1957. Contribution to study of comminution -- Modified form of Kick's law. Institution of Chemical Engineers -- Transactions, 35(2): 125-141.

ISRM, 1972. Suggested Methods for Determining the Uniaxial Compressive Strength and Deformability of Rock Materials.

ISRM, 1994. Suggested Methods for Determining Mode 1 Fracture Toughness Using Cracked Chevron Notched Brazilian Disc.

Johnson, D., Meikle, K., Pilotto, D. and Lone, K. 2014. NI 43-101 Technical Report for the Gahcho Kué Project 2014 Feasibility Study Mountain Province Diamonds Inc., Montréal.

JORC, 2012. Australasian Code for Reporting of Exploration Results, Mineral Resources and Ore Reserves (The JORC Code)) [online]. Available from: <http://www.jorc.org> (The Joint Ore Reserves Committee of The Australasian Institute of Mining and Metallurgy, Australian Institute of Geoscientists and Minerals Council of Australia).

Journel, A.G. 1974. Simulations Conditionnelles - Theorie et Practique, Centre de Geostatistique, Fontainebleau, France.

Journel, A.G. and Huijbrechts, C. 1978. Mining Geostatistics, 600 p (Academic Press: London).

Kahneman, D., 2011. *Thinking fast, thinking slow* 1st ed., New York: Farrar, Straus and Giroux.

Keeney, L. and Walters, S. 2008. Geometallurgical modelling. GeMIII (Amira P843) Technical Report I, p 16.1 – 16.24.

King, R.P. 2001. Modelling and Simulation of Mineral Processing Systems, (Butterworth-Heinemann.: Oxford).

Kjaarsgaard, B.A. 1995. Geological of Canadian Mineral Deposit types, p560 p (Geological Survey of Canada: Ottawa).

Kleingeld, W.J. 1976. Reconciliation of Ore Reserves in the Number One Diamond Mining Area.

Kleingeld, W. 1982. A reconciliation of diamond losses at CDM, Internal Report, De Beers Consolidated Mines, South Africa.

Kleingeld, W. J., Lantuéjoul, C., Prins, C. F. and Thurston, M.L. 1996. The Conditional Simulation of a Cox Process with Application to Diamond Deposits and Discrete Particles, paper presented to Geostatistics Congress, Wollongong, Australia.

Kleingeld, W.J. and Nicholas, G.D. 2004. Diamond Resources and Reserves - Technical Uncertainties affecting their Estimation, Classification and Evaluation. Proceedings of the International Symposium on *Orebody Modelling and Strategic Mine Planning*. Pub AusIMM (Melbourne). ISBN 1 920806 22 9;

Kolmogorov, A.N. 1941. Uber das logarithmisch normale Verteilungsgesetz der Dimensionen der Teilchen bei Zerst¨uckelung. Dokl. Akad. Nauk. SSSR 31, 99–101.Translated as "The logarithmically normal law of distribution of dimensions of particles when broken into small parts", NASA technical translation NASA TTF–12,287, NASA, Washington, D. C., June 1969

Krige, D.G., Guarascio, M. & Camisani-Calzolari, F.A. 1988. Early South African Geostatistical Techniques in Todays's Perspective. In M. Armstrong, ED. Geostatistics: Proceedings of the Third International Geostatistics Congress. Avignon, p. 1027.

Lane, K.F. 1988. *The economic definition of ore: cut-off grades in theory and practice*, London: Mining Journal Books.

Lantuéjoul, C. 1990. The Benefit Function, Internal Report, De Beers Consolidated Mines Pty Ltd., Johannesburg, South Africa.

Lantuéjoul, C. 1998. On liberation and breakage, Internal Report, De Beers Consolidated Mines Pty Ltd., Johannesburg, South Africa.

Lerchs, H. and Grossman, I.F., 1965. Optimum Design of Open Pit Mines, Transactions CIM, 68(633): pp17-24.

Lewis, P. J., 2001. Metallurgical Evaluation Leading to the Determination of Ore Reserves, in Mineral Resource and Ore Reserve Estimation, pp359–368 p (The Australasian Institute of Mining and Metallurgy: Melbourne).

Lilford, B. 2003. Design Criteria for Voorspoed, De Beers, Johannesburg, South Africa.1

Lilford, E.V. & Minnitt, R.C.A. 2005. A comparative study of valuation methodologies for mineral developments. Southern African Institute of Mining and Metallurgy, pp.p29-41.

Lynn, M., Nowicki, T., Valenta, M., Robinson, B., Gallagher, M., Bolton, R. and Sexton, J. 2014. Karowe Diamond Mine, Botswana, NI 43-101 Independent Technical Report Lucara Diamond Corp., Vancouver, BC, Canada.

Mackey, P.J. and Nesset, J.E. 2003. The impact of commissioning and start-up performance on a mining/metallurgical project, paper presented to Proceedings of the 35th Annual Meeting of the Canadian Mineral Processors.

Macnae, J. 1995. Applications of geophysics for the detection and exploration of kimberlites and lamproites. Journal of Geochemical Exploration, 53(1-3), pp.213-243.

Markowitz, H. M. 1952. Portfolio Selection, Journal of Finance, Vol. 7: p77-91.

Matheron, G. 1963. Principles of Geostatistics. *Economic Geology*, 58(8), pp.1246–1266.

Matheron, G. 1973. The Intrinsic Random Functions and their Application, Advances in Applied Probability, 5: pp 439-468.

McKee, D.J., Chitombo, G.P., & Morrell, S. 1995. The relationship between fragmentation in mining and comminution circuit throughput. Minerals Engineering, 8(11), 1265–1274. https://doi.org/10.1016/0892-6875(95)00094-7

McBean, D., Kirkley, M. and Revering, C. 2001. Structural controls on the morphology of the Snap Lake Dyke. 8th International Kimberlite Conference.

Moore, G.E. 1965. Cramming More Components onto Integrated Circuits, Electronics, April 19, 1965. Electronics, 38(8), pp.82–85.

Momayez, M., Sadri, A. & Hassani, F.P. 1995. MSR: A technique for determining the mechanical properties of rocks. In 35th US Rock Mechanics Symposium. Lake Tahoe, Nevada, pp. 843–848.

Morrell, S., Dunne, R. C. and Finch, W. 1993. The liberation of a grinding circuit treating gold bearing ore, paper presented to XVIII Int. Min Proc Cong, Sydney.

Morell, S. 2003. Predicting the Specific Energy of Autogenous and Semi Autogenous Mills from Small Diameter Drill Core Samples Minerals Engineering, 17: pp 447-451.

Morkel, J. 2006. Kimberlite weathering: mineralogy and mechanism, University of Pretoria, Pretoria.

Napier-Munn, T., Morell, S., Morison, R. and Kojovic, T. 1999. Mineral Comminution Circuits, Their Operation and Optimisation, 2nd ed, 413 p (JKMRC, University of Queensland: Indooroopilly).

NI43-101, 2001. National Instrument 43-101, Standards of Disclosure for Mineral Projects, Canadian Institute of Mining, 21.

Nicholas, G., Coward, S., Armstrong, M. and Galli, A. 2006. Integrated Mine Evaluation - Implications for Mine Management. In: AUSIMM. ed. International Mine Management Conference. Melbourne. Australia.

Nicholas, G.D., Coward, S. J., Rendall, M., and Thurston, M.L. 2007. Decision-Making Using an Integrated Evaluation Model Versus Sensitivity Analysis and Monte Carlo Simulation. In *Canadian Institute of Mining and Metallurgy International conference*. Montreal, Canada.

Nicholas, G., Coward, S. & Ferreira, J. 2008. Financial Risk Assessment Using Conditional Simulations in an Integrated Evaluation Model. In *the Eighth International Geostatistics Congress*. Santiago, Chile, p. 10.

Olea, R.A. 1991. Geostatistical Glossary and Multilingual Dictionary, Oxford University Press, New York.

Olsson, W. 1974. Grain Size Dependence of Yield Stress in Marble, Journal of Geophysical Research, (November 1974): pp 4859-4862.

Ozturk, C. N. E., Bilgin, N. 2004. The assessment of Rock cut ability, and physical and mechanical rock properties from a texture coefficient, Journal of the South African Institute of Mining and Metallurgy.

Parker, H. 1997. Applications of Geostatistical Methods in Exploration Programme Design., National Council for United States - China Trade Technical Exchange, Peking.

Petersen, K., 2005. Development of a Flowsheet Model for the Snap Lake Mine. Unpublished Report.

Petra Diamonds, 2019. *Petra Diamonds Limited Annual Report 2019*, London UK.

Plitt, L. R. 1976. A Mathematical Modelling of the Hydro cyclone Classifier, CIM Bulletin 69(776):114-123.

Rappaport, 2009. Rapaport price list - July-03., available at http://store.rapaport.com, accessed 2009/03/07.

Richmond, A.J. 2003. Multi-Scale Ore Texture Modelling for Mining Applications, University of Brisbane, Brisbane.

Rittinger, Peter Ritter von. 1867. Lehrbuch der Aufbereitungskunde, Berlin: Verlag von Ernst & Korn.

Robinson, G.K. 2004. Managing variation of bulk materials in stockpiles and mineral processing plants. Chemometrics and Intelligent Laboratory Systems, 74, pp.121–133.

Rombouts, L. 1995. Sampling and statistical evaluation of diamond deposits, Journal of Geochemical Exploration, 53:351-367.

Royle, A.G. 1986. Alluvial Sampling Formula and Recent Advances in Alluvial Deposit Evaluation, Transactions of The Institution of Mining and Metallurgy: pp B179-B182.

Samis, M., Laughton, D., and Davis, G.A. 2006. Valuing uncertain asset cash flows when there are no options: A real options approach, Resources Policy, 30: p285-298.

SAMREC, 2016. The South African Code for the Reporting of Exploration Results, Mineral Resources, and Mineral Reserves (the SAMREC code).

SAMREC, 2017. SAMREC Guideline Document for the Reporting of Diamond Exploration Results, Diamond Resources and Diamond Reserves.

Shipiki-Kali, M. 2000. A Comparative analysis of Operational Costs - 2000. Internal Report, De Beers, Johannesburg, South Africa.

Silva, D.S.F. & Boisvert, J.B. 2014. Mineral resource classification: a comparison of new and existing techniques. Journal of the Southern African Institute of Mining and Metallurgy, 114, pp.265–273. Available at: http://www.scielo.org.za/scielo.php?script=sci_arttext&pid=S2225-62532014000300017&nrm=iso.

Skinner, E.M.W. and Clement, C.R. 1979. Mineralogical classification of southern African kimberlites. In F. R. Meyer & H. O. A. Boyd, EDS. Proceedings of 2nd International Kimberlite Conference. Washington, pp. 129–139.

Sothcott, J., Hennah, S.J., Mc Cann, C., Black, S and Stevenson, I. 2005. Measurement of the Broadband Acoustic Properties of Kimberlite: A Feasibility Study, De Beers Consolidated Mines South Africa, Johannesburg.

South African Institute for Mining and Metallurgy, 2002. The SAMVAL code, Draft Standards and guidelines for valuation of mineral projects, properties and assets in the mining industry of South Africa.

Sparks, R.S.J. 2006. Dynamical constraints on kimberlite volcanism. Journal of Volcanology and Geothermal Research, 155(1–2), pp.18–48.

Sparks, R.S.J., Brooker, R., Field, M. 2009. The nature of erupting kimberlite melts. Lithos, 112, pp.429–438.

Sperra, F.J. 2000. Encyclopaedia of Volcanoes, London: Academic Press.

Taggart, A.F. 1964. Handbook of Mineral Dressing, 8th ed (John Wiley and Sons: London).

Tavares, L. & King, R.P. 1998. Single-particle fracture under impact loading. International Journal of Mineral Processing, 54, pp.1–28.

De Beers Consolidated Mines Limited , 2001., Technical and Financial Report, 149 p.

Thurston, M.L. 1998. The quantification of uncertainty attached to selected sampling protocols in a kimberlite using a discrete simulation method, University of the Witwatersrand, Johannesburg.

Vose, D. 2002. Risk Analysis, a Quantitative Guide (John Wiley and Sons Ltd: London).

Wackernagel, H. 1995. Multivariate Geostatistics, 256 p (Springer-Verlag: Berlin).

Whiten, W.J. 1972. Simulation and Model Building for Mineral Processing, PhD dissertation - University of Queensland, Australia.

12 APPENDICES

The appendices provided here are to give the interested reader more technical substantiation of aspects of metallurgical recovery estimation that are addressed by this research.

APPENDIX 1 -EXPERIMENTAL DESIGN AND DATA FROM OREBODY SAMPLING

Brief depiction of the layout, the types of samples collected and the raw data that were generated from this experiment. In Figure 71 a surface schematic is shown depicting the area in which the sample holes were located.

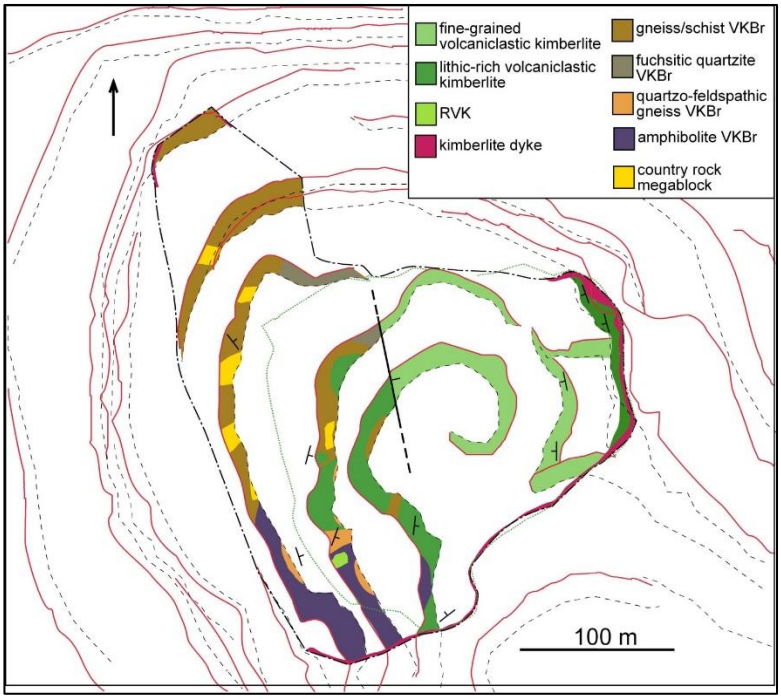

Figure 71: Schematic showing the location of samples from K2 pipe.

Two categories of drill holes were defined. The first comprises holes where all the material was sampled, and the second where only portions were sampled. In Figure 72 the layout of the holes is shown with the different coloured banding representing the type and location of samples. The white areas of cores were not sampled. The full details of the sampling are contained in Figure 73 and in Figure 74

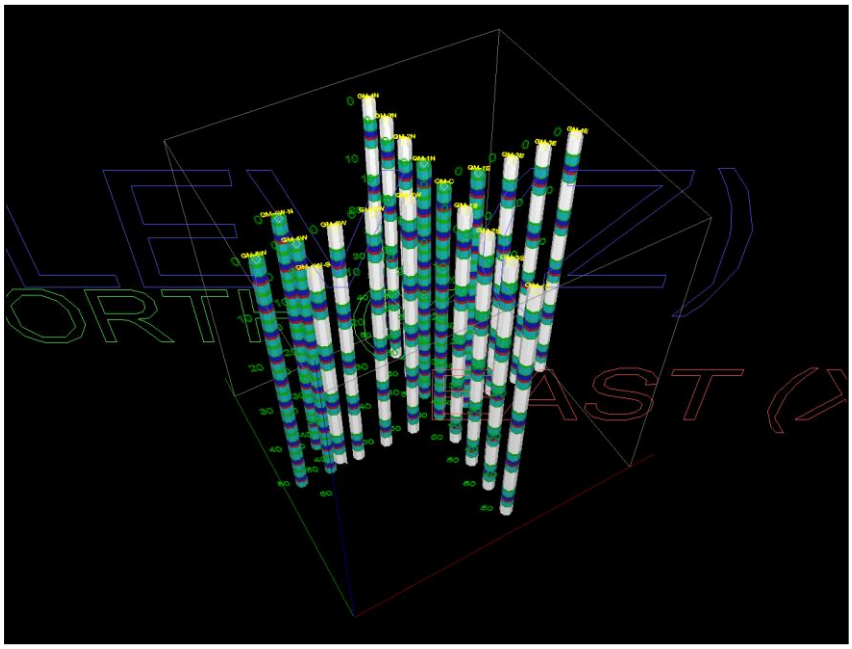

Figure 72: A view of the layout of the core holes depicting the location of the subsamples

The sampling layout of the cores extracted is depicted in Figure 72.White intersections were not sampled but retained; all other coloured intersections were sampled. Details are of the subsamples are shown in Figure 73 and Figure 74.

TO (M)	A_CODE	TO (M)	ANALYSIS	SAMPNO	DMT	SPECTRAL	GEOPHYSI
		0.0	Pet	GM-1E/0m/Pet			
		0.5	Mida	GM-1E/0.5m/Mida			
		1.8	Pet	GM-1E/1.75m/Pet			
		2.0	Geomet	GM-1E/2m/Geomet			
		3.0	Geotech	GM-1E/3m/Geotech			
		3.5	Mida	GM-1E/3.5m/Mida			
5.0		4.8	Pet	GM-1E/4.75m/Pet			
		5.0		GM-1E/5m/Pet			
		5.5	Mida	GM-1E/5.5m/Mida			
		6.8	Pet	GM-1E/6.75m/Pet			
		7.0	Geomet	GM-1E/7m/Geomet			
		8.0	Geotech	GM-1E/8m/Geotech			
		8.5	Mida	GM-1E/8.5m/Mida			
10.0		9.8	Pet	GM-1E/9.75m/Pet			
		10.0		GM-1E/10m/Pet			
		10.5	Mida	GM-1E/10.5m/Mida			
		11.8	Pet	GM-1E/11.75m/Pet			
		12.0	Geomet	GM-1E/12m/Geomet			
		13.0	Geotech	GM-1E/13m/Geotech			
		13.5	Mida	GM-1E/13.5m/Mida			
15.0		14.8	Pet	GM-1E/14.75m/Pet			
		15.0		GM-1E/15m/Pet			
		15.5	Mida	GM-1E/15.5m/Mida			
		16.8	Pet	GM-1E/16.75m/Pet			
		17.0	Geomet	GM-1E/17m/Geomet			
		18.0	Geotech	GM-1E/18m/Geotech			
		18.5	Mida	GM-1E/18.5m/Mida			
20.0		19.8	Pet	GM-1E/19.75m/Pet			
		20.0		GM-1E/20m/Pet			
		20.5	Mida	GM-1E/20.5m/Mida			
		21.8	Pet	GM-1E/21.75m/Pet			
		22.0	Geomet	GM-1E/22m/Geomet			
		23.0	Geotech	GM-1E/23m/Geotech			
		23.5	Mida	GM-1E/23.5m/Mida			
25.0		24.8	Pet	GM-1E/24.75m/Pet			
		25.0		GM-1E/25m/Pet			
		25.5	Mida	GM-1E/25.5m/Mida			
		26.8	Pet	GM-1E/26.75m/Pet			
		27.0	Geomet	GM-1E/27m/Geomet			
		28.0	Geotech	GM-1E/28m/Geotech			
		28.5	Mida	GM-1E/28.5m/Mida			
30.0		29.8	Pet	GM-1E/29.75m/Pet			
		30.0		GM-1E/30m/Pet			
		30.5	Mida	GM-1E/30.5m/Mida			
		31.8	Pet	GM-1E/31.75m/Pet			
		32.0	Geomet	GM-1E/32m/Geomet			
		33.0	Geotech	GM-1E/33m/Geotech			
		33.5	Mida	GM-1E/33.5m/Mida			
35.0		34.8	Pet	GM-1E/34.75m/Pet			
		35.0		GM-1E/35m/Pet			
		35.5	Mida	GM-1E/35.5m/Mida			
		36.8	Pet	GM-1E/36.75m/Pet			
		37.0	Geomet	GM-1E/37m/Geomet			
		38.0	Geotech	GM-1E/38m/Geotech			
		38.5	Mida	GM-1E/38.5m/Mida			
40.0		39.8	Pet	GM-1E/39.75m/Pet			
		40.0		GM-1E/40m/Pet			
		40.5	Mida	GM-1E/40.5m/Mida			
		41.8	Pet	GM-1E/41.75m/Pet			
		42.0	Geomet	GM-1E/42m/Geomet			
		43.0	Geotech	GM-1E/43m/Geotech			
		43.5	Mida	GM-1E/43.5m/Mida			
45.0		44.8	Pet	GM-1E/44.75m/Pet			
		45.0		GM-1E/45m/Pet			
		45.5	Mida	GM-1E/45.5m/Mida			
		46.8	Pet	GM-1E/46.75m/Pet			
		47.0	Geomet	GM-1E/47m/Geomet			
		48.0	Geotech	GM-1E/48m/Geotech			
		48.5	Mida	GM-1E/48.5m/Mida			
50.0		49.8	Pet	GM-1E/49.75m/Pet			

Figure 73:Listing of subsamples taken from cores that were fully sampled

Figure 74: Depiction of the subsamples taken from cores that were partially sampled.

APPENDIX 2 -OREBODY CHARACTERISTIC ESTIMATES

The data gathered during the orebody sampling experiment were used in several ways to generate spatial estimates of the primary and response characteristics of the orebody. This Appendix presents images of the data obtained from the Venetia K2 orebody.

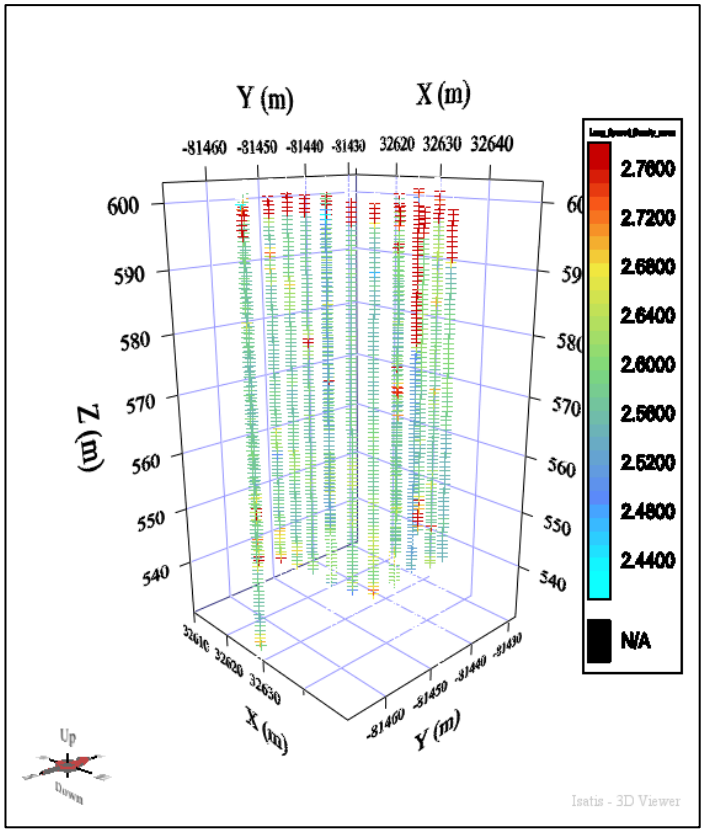

Figure 75:A view from the south-west of Venetia K2 sampled area - showing downhole density.

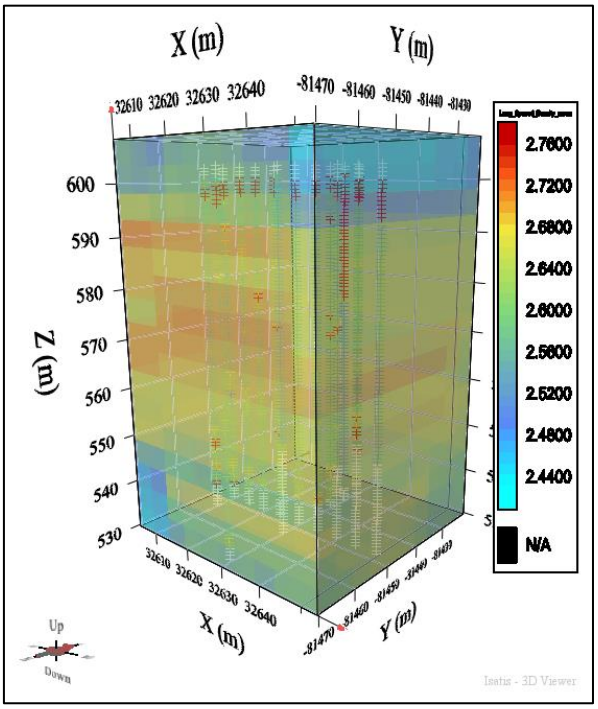

Figure 76:A view from the south-west of Venetia K2 sampled area - showing downhole density and P wave velocity.

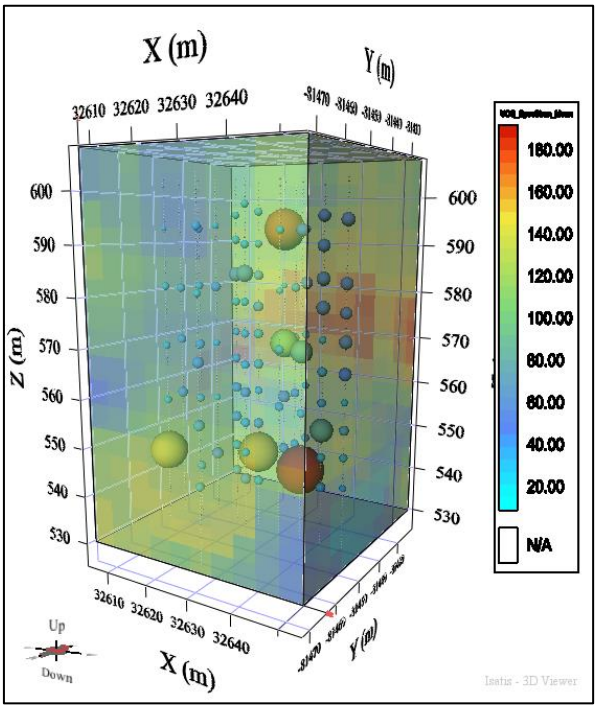

Figure 77:A view from the south-west of Venetia K2 sampled area - UCS sample values as scaled spheres and estimated block density in transparent blocks.

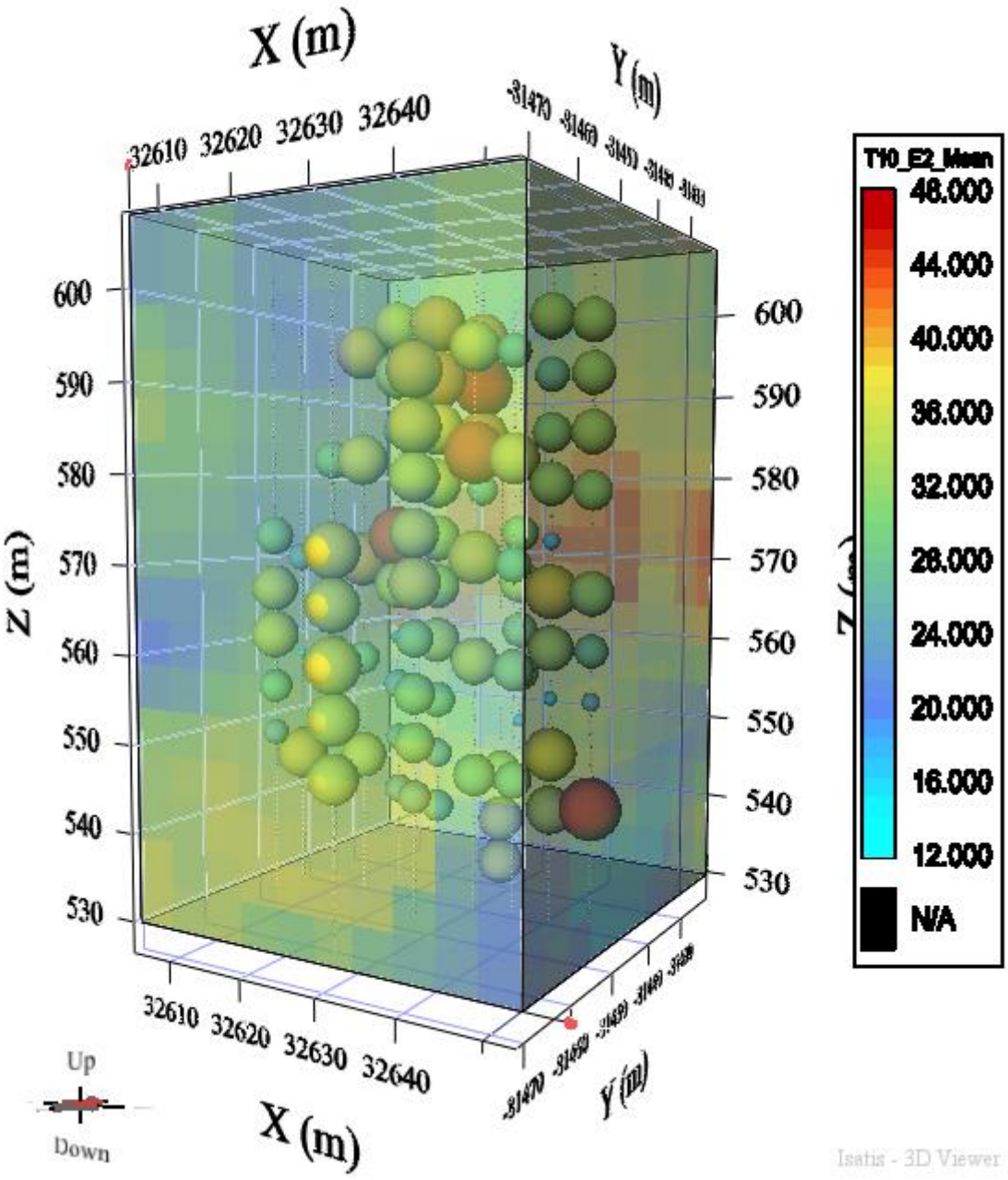

Figure 78:A view from the south-west of Venetia K2 sampled area - t_{10} sample values as spheres and estimated t_{10} in transparent blocks.